

Self-Folding of Single Chain Polymers: Towards Synthetic Biomacromolecule Design

Zur Erlangung des akademischen Grades eines

DOKTORS DER NATURWISSENSCHAFTEN

(Dr. rer. nat.)

Fakultät für Chemie und Biowissenschaften

Karlsruher Institut für Technologie (KIT) – Universitätsbereich

Genehmigte

DISSERTATION

von

Özcan Altintas

aus

Sindirgi, Türkei

Dekan: Prof. Dr. Martin Bastmeyer

Referent: Prof. Dr. Christopher Barner-Kowollik

Korreferent: Prof. Dr. Michael A. R. Meier

Tag der mündlichen Prüfung: 20.07.2012

Die vorliegende Arbeit wurde von Juli 2009 bis Juli 2012 unter Anleitung von Prof. Dr. Christopher Barner-Kowollik am Karlsruher Institut für Technologie (KIT) Universitätsbereich angefertigt.

Declaration

I hereby declare that the thesis entitled 'Self-Folding of Single Chain Polymers: Towards Synthetic Biomacromolecules Design' is my original work and has not been submitted to any other institute or university for award of any degree. Where other people's work has been used (*via* any source), this has been properly acknowledged.

Özcan Altintas

23.07.2012

*For my family
Halime and Mehmet Selim*

Abstract

Single Chain Folding of Synthetic Polymers via Covalent and Non-Covalent Interactions: State of the Art

The exquisite design of well-defined polymer chains – that can subsequently undergo single chain folding driven by covalent and non-covalent interactions – has been made possible by the control over the composition, molecular weight and molecular weight distribution of synthetic macromolecules offered by several controlled/living radical polymerization (CLRP) techniques including atom transfer radical polymerization (ATRP), nitroxide mediated polymerization (NMP), reversible addition-fragmentation chain transfer (RAFT) polymerization, single electron transfer living radical polymerizations (SET-LRP), activators generated by electron transfer ATRP (AGET-ATRP) or activators regenerated by electron transfer ATRP (ARGET-ATRP). Modular ligation chemistries combine particularly well with these polymerization techniques reactions. The initiators utilized for these polymerizations provide functional groups that are readily converted to the desired functionality for modular ligation chemistries. The preparation and characterization of synthetic polymers mimicking folding elements occurring in natural macromolecules as well as polymeric nanoparticles via single chain folding methods using intramolecular covalent and non-covalent interactions are critically reviewed. The current state of the art in the field of single chain folding indicates that covalent bond driven nanoparticle preparation is well-advanced, while the first encouraging steps towards building reversible single chain folding systems via the use of the mutually orthogonal hydrogen bonding motifs have been made.

Single Chain Self-folding of Well-Defined α,ω -Functional Linear Polymers Generated by ATRP and Modular Ligation Chemistry

Well-defined α,ω -functional linear poly(styrene) carrying thymine (thy) / diaminopyridine (DAP) ($M_{n,GPC} = 9300$, $PDI = 1.04$) and Hamilton wedge (HW) / cyanuric acid (CA) ($M_{n,GPC} = 8200$, $PDI = 1.04$) bonding motifs are prepared via a combination of controlled/living radical polymerization and copper catalyzed azide alkyne cycloaddition and are subsequently self-assembled as single chains to emulate – on a simple level – the self-folding behavior of natural biomacromolecules. Hydrogen nuclear magnetic resonance (^1H NMR) in deuterated dichloromethane and dynamic light scattering (DLS) analyses provide evidence for the hydrogen-bonding interactions between the α -thymine and ω -diaminopyridine as well as α -cyanuric acid and ω -Hamilton wedge chain ends of the heterotelechelic polymers leading to circular entropy driven single chain self-assembly. The study demonstrates that the choice of NMR solvent is important for obtaining well-resolved NMR spectra of the self-assembled structures. In addition, steric effects on the Hamilton wedge can affect the efficiency of the self-assembly process.

Bioinspired Dual Self-Folding of Single Polymer Chains via Reversible Hydrogen Bonding

With the aim of preparing synthetic macromolecules that mimic the folding action of natural biomacromolecules, a single synthetic polymer chain containing two distinct and orthogonal hydrogen bonding recognition motifs has been synthesized using an atom transfer radical polymerization and orthogonal ligation strategy. The hydrogen bonding recognition units based on both three-point thymine (Thy) – diaminopyridine (DAP) and six-point cyanuric acid

(CA) – Hamilton wedge (HW) interactions, induced – at low concentrations – a single chain self-folding process. The self-assembly process was monitored – initially between small molecule models – by proton nuclear magnetic resonance (^1H NMR) spectroscopy, revealing full orthogonality of the two recognition pairs, HW-CA and Thy-DAP. ^1H -NMR spectroscopy in deuterated dichloromethane and dynamic as well as static light scattering (DLS and SLS) analyses of the macromolecular self-assembly systems provide unambiguous evidence for the hydrogen-bonding interactions between both the Thy-DAP and CA-HW leading to well-defined dual point single chain self-folding, indicating that more complex single chain self-assemblies based on synthetic polymers should be able to mimic – on a simplified level – the folding actions of natural biomacromolecules. The reversibility of the self-folding action depends on temperature as confirmed via ^1H -NMR spectroscopy in $[\text{D}_2]$ tetrachloroethane.

Star and Miktoarm Star Block (Co)polymers via Self-Assembly of ATRP Generated Polymer Segments Featuring Hamilton Wedge and Cyanuric Acid Binding Motifs

Hamilton Wedge (HW) end-functionalized poly(styrene) (PS-HW, $M_n = 5400 \text{ g mol}^{-1}$, $PDI = 1.06$), HW mid-chain functionalized poly(styrene) (PS-HW-PS, $M_n = 4600 \text{ g mol}^{-1}$, $PDI = 1.04$), cyanuric acid (CA) end-functionalized poly(styrene) (PS-CA, $M_n = 3700 \text{ g mol}^{-1}$, $PDI = 1.04$) and CA end-functionalized poly(methyl methacrylate) (PMMA-CA, $M_n = 8500 \text{ g mol}^{-1}$, $PDI = 1.13$) precursors were successfully synthesized via a combination of atom transfer radical polymerization (ATRP) and copper catalyzed azide–alkyne cycloaddition (CuAAC). The precursor polymers were characterized via size exclusion chromatography (SEC) and ^1H -NMR with respect to both molecular weight and structure. Supramolecular homopolymer (PS-HW•PS-CA), block copolymer (PS-HW•PMMA-CA), star polymer (PS-HW-PS•PS-CA) as well as

miktoarm star polymer (PS-HW-PS•PMMA-CA) was formed in solution in high yields at ambient temperature (association close to 89% for PS-HW•PS-CA, 90% for PS-HW-PS•PS-CA and 98% for PS-HW-PS•PMMA-CA) via H-bonding between the orthogonal recognition units, HW and CA. The formation of supramolecular polymers was confirmed via ^1H NMR at ambient temperature in deuterated methylene chloride (CD_2Cl_2) solution.

Combining Modular Ligation and Supramolecular Self-Assembly for the Construction of Star-Shaped Macromolecules

A well-defined random copolymer of styrene (S) and chloromethylstyrene (CMS) featuring lateral chlorine moieties (on 6% of all repeat units) with an alkyne terminal group is prepared by the nitroxide-mediated radical polymerization (NMP) process (P(S-*co*-CMS), $M_n = 5500$ Da, $PDI = 1.13$). The chloromethyl groups of CMS are subsequently converted to Hamilton wedge (HW) entities via an etherification with hydroxyl functional HW (P(S-*co*-HWS), $M_n = 6200$ Da, $PDI = 1.13$). The P(S-*co*-HWS) precursor polymer is subsequently ligated with tetrakis(4-azidophenyl)methane to give HW-functional star-shaped macromolecules via copper catalyzed azide-alkyne cycloaddition (CuAAC) ((PS-*co*-HWS) $_4$, $M_n = 25100$ Da, $PDI = 1.08$). Supramolecular grafted star-shaped copolymers have then been prepared through self-assembly between the HW functionalized 4-arm star macromolecules (PS-*co*-HW) $_4$ and cyanuric acid (CA) end-functionalized poly(styrene) (PS-CA, $M_n = 3700$ Da, $PDI = 1.04$), CA end-functionalized poly(methyl methacrylate) (PMMA-CA, $M_n = 8500$ Da, $PDI = 1.13$) and CA end-functionalized polyethylene glycol (PEG-CA, $M_n = 1700$ Da, $PDI = 1.05$). The star self-assembly in solution is monitored by proton nuclear magnetic resonance (^1H NMR) spectroscopy

as well as dynamic and static light scattering (DLS and SLS) analyses, demonstrating an efficient formation of self-assembled star-shaped polymers.

Table of Contents

1 Motivation and Goals	1
1.1 Motivation	3
1.2 Research Goals	4
1.3. Reference	6
2 Theoretical Background and – A Literature Review	8
2.1 Controlled/Living Polymerization Techniques	10
2.1.1 Atom Transfer Radical Polymerization (ATRP)	10
2.1.1.1 Lowering the Concentration of Copper-Catalyst in ATRP	13
2.1.1.1.1 Activators Generated by Electron Transfer ATRP	13
2.1.1.1.2 Activators Regenerated by Electron Transfer ATRP	14
2.1.1.1.3 Initiators for Continuous Activator Regeneration ATRP	15
2.1.1.1.4 Single Electron Transfer Living Radical Polymerization	16
2.1.1.2 Functional Initiators	17
2.1.1.2 Chain-End Functionality	19
2.1.2 Nitroxide-Mediated Radical Polymerization (NMP)	21
2.1.3 Ring-Opening Polymerization (ROP)	22
2.1.4 Reversible Addition-Fragmentation Chain Transfer (RAFT) Polymerization	23
2.2 Click Chemistry	25
2.2.1 Modular Ligation Reactions	26
2.2.1.1 Cu(I) Catalyzed Azide-Alkyne Cycloaddition (CuAAC)	26
2.2.1.2 Diels-Alder (DA) and Hetero Diels-Alder (HDA) Reactions	27
2.2.1.3 Thiol-ene and Thiol-yne Reactions	28
2.2.1.4 Nitroxide Radical Coupling (NRC) Reaction	29
2.3 Syntheses of Star Polymers	29
2.4 Supramolecular Chemistry	31
2.4.1 Hydrogen Bonds	32
2.4.1.1 Trivalent Hydrogen Bonds	33
2.4.1.2 Quadruple Hydrogen Bonds	33
2.4.1.3 Multiple Hydrogen Bonds	33

2.5 Protein Structures.....	34
2.6 Folding of Single Polymer Chains via Intramolecular Covalent Bonds	36
2.7 Self-Folding of Single Polymer Chains via Non-Covalent Interactions	49
2.8 References	56
3 Single Chain Self-Folding of α,ω-Functional Linear Polymers.....	65
3.1 Introduction	67
3.2 Preparation of α -CA and ω -HW Functionalized Polystyrene	70
3.2.1 Synthesis	70
3.2.1.1 Synthesis of N^1, N^3 -bis(6-pivalamidopyridin-2-yl)-5-(prop-2-ynyloxy) isophthalamide	70
3.2.1.2 Synthesis of 1-(6-hydroxyhexyl)-1,3,5-triazinane-2,4,6-trione	72
3.2.1.3 Synthesis of 6-(2,4,6-trioxo-1,3,5-triazinan-1-yl)hexyl 2-bromo-2-methyl propanoate	72
3.2.1.4 Synthesis of α -Cyanuric Acid Functional Polystyrene.....	73
3.2.1.5 Synthesis of α -Cyanuric Acid Functional Polystyrene with Azide	73
3.2.1.6 Synthesis of α,ω -Donor-Acceptor Single Chain Polystyrene	74
3.2.1.7 Self-Assembly Studies between 3 and 6	74
3.2.1.8 Single Chain Self-Assembly Studies of Polymer 8 with ^1H NMR	74
3.2.1.9 Single Chain Self-Assembly Studies of Polymer 8 via DLS.....	75
3.2.1.10 Preparation of Compound and Polymers that are Described in Scheme 3.3	75
3.2.1.11 Self-Assembly Studies between Polymer 12 and Compound 3 or 10	76
3.2.1.12 Single Chain Self-Assembly Studies of Polymer 13 and 14	76
3.2.2 Results and Discussion of Synthesis α CA and ω HW Functionalized Polystyrene ...	77
3.3 Preparation of α -Thy and ω -DAP Functionalized Polystyrene.....	91
3.3.1 Synthesis	92
3.3.1.1 Synthesis of 11-bromoundecanoylchloride.....	92
3.3.1.2 Synthesis of 11-bromo- N -(6-(3,3-dimethylbutanamido)pyridin-2-yl)undecanamide	92
3.3.1.3 Synthesis of Methyl 4-(11-(6-(3,3-dimethylbutanamido)pyridin-2-ylamino)-11-oxoundecyloxy) benzoate	94

3.3.1.4 Synthesis of 4-(11-(6-(3,3-dimethylbutanamido)pyridin-2-ylamino)-11-oxoundecyloxy) benzoic acid	94
3.3.1.5 Synthesis of Prop-2-ynyl 4-(11-(6-(3,3-dimethylbutanamido)pyridin-2-ylamino)-11-oxoundecyloxy) benzoate	95
3.3.1.6 Synthesis of α -Thymine Functional Poly(styrene)	96
3.3.1.7 Synthesis of α -Thymine Functional Poly(styrene) with Azide.....	96
3.3.1.8 Synthesis of α -Thymine ω -Diaminopyridine Functional Poly(styrene)	97
3.3.1.9 Self-Assembly Studies between Compound 17 and Polymer 21	97
3.3.1.10 Single Chain Self-Assembly Studies of Polymer 23	97
3.3.2 Results and Discussion of α -Thy and ω -DAP Functionalized Polystyrene	98
3.4 Conclusions.....	109
3.5 References	110
4 Dual Self-Folding of Single Polymer Chains via Reversible Hydrogen Bonding	112
4.1 Introduction.....	114
4.2 Synthesis	116
4.2.1 Synthesis of 2-((2-bromo-2-methylpropanoyloxy)methyl)-2-methyl-3-oxo-3-(prop-2-ynyloxy)propyl 4-(11-oxo-11-(6-pivalamidopyridin-2-ylamino)undecyloxy)benzoate.....	116
4.2.2 Synthesis of 11-(5-methyl-2,4-dioxo-3,4-dihydropyrimidin-1(2H)-yl)undecanoic acid.....	117
4.2.3 Synthesis of 2-((2-bromo-2-methylpropanoyloxy)methyl)-2-methyl-3-oxo-3-(prop-2-ynyloxy) propyl 11-(5-methyl-2,4-dioxo-3,4-dihydropyrimidin-1(2H)-yl)undecanoate	117
4.2.4 Synthesis of α CA and ω Br Functional Polystyrene.....	118
4.2.5 Synthesis of α CA and ω Thy Functional Polystyrene	118
4.2.6 Synthesis of CA-PS-Thy-PS-Br	119
4.2.7 Synthesis of CA-PS-Thy-PS-DAP.....	119
4.2.8 Synthesis of CA-PS-Thy-PS-DAP-PS-Br	119
4.2.9 Synthesis of CA-PS-Thy-PS-DAP-PS-HW.....	120
4.3 Result and Discussion.....	120
4.3.1 Synthesis of the Dual Self-Folding System and Orthogonality Assessment	120

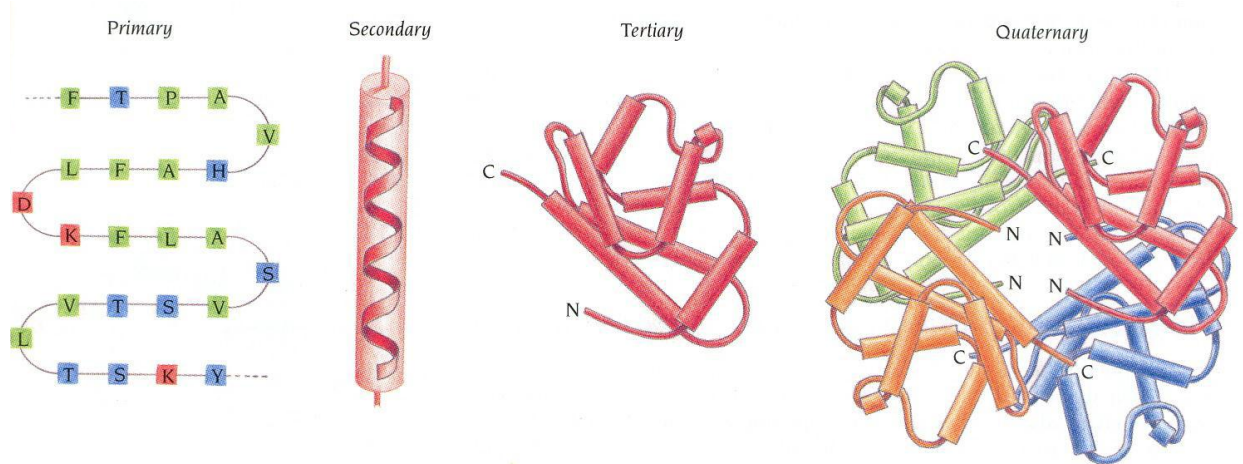
4.3.2 Single Chain Self-Folding of Dual Hydrogen Bonding Macromolecules	137
4.4 Conclusions.....	151
4.5 References.....	152
5 Complex Macromolecules Architectures via Multiple Hydrogen Bonding	155
5.1 Introduction.....	157
5.2 Preparation of Supramolecular Block, Star and Miktoarm Star Polymers through Multiple Hydrogen Bonding.....	163
5.2.1 Synthesis	163
5.2.1.1 Synthesis of 11-bromoundecyl 2,2,5-trimethyl-1,3-dioxane-5-carboxylate.	163
5.2.1.2 Synthesis of 11-bromoundecyl 3-hydroxy-2-(hydroxymethyl)-2-methylpropanoate.....	164
5.2.1.3 Synthesis of 11-azidoundecyl 3-hydroxy-2-(hydroxymethyl)-2-methylpropanoate.....	165
5.2.1.4 Synthesis of Azide-Functionalized ATRP initiator..	165
5.2.1.5 Synthesis of Azide mid-Functionalized Poly(styrene)..	166
5.2.1.6 Synthesis of Hamilton Wedge (HW) mid-Functionalized Poly(styrene).. ...	166
5.2.1.7 Synthesis of CA end-Functionalized Poly(styrene).....	167
5.2.1.8 Synthesis of CA end-Functionalized Poly(methyl methacrylate).....	168
5.2.1.9 Synthesis of HW end-Functionalized Poly(styrene).....	168
5.2.1.10 Self-Assembly Study between PS-HW and PS-CA.....	169
5.2.1.11 Self-Assembly Study between PS-HW-PS and PS-CA.....	169
5.2.1.12 Self-Assembly Study between PS-HW and PMMA-CA.....	169
5.2.1.13 Self-Assembly Study between PS-HW-PS and PMMA-CA.....	169
5.2.2 Results and Discussion of Supramolecular Block, Star and Miktoarm Star polymers through Multiple Hydrogen Bonding	170
5.3 Construction of Star-shaped Macromolecules through Multiple Hydrogen Bonding	188
5.3.1 Synthesis	189
5.3.1.1 Synthesis of Prop-2-yn-1-yl 4-chloro-4-oxobutanoate	189
5.3.1.2 Synthesis of 2-Phenyl-2-((2,2,6,6-tetramethylpiperidin-1-yl)oxy)ethyl prop-2-yn-1-yl succinate	189
5.3.1.3 Synthesis of 3,5-bis(chlorocarbonyl)phenyl benzoate	192

5.3.1.4 Synthesis of 3,5-Bis((6-(3,3-dimethylbutanamido)pyridin-2-yl)carbamoyl)phenyl benzoate	192
5.3.1.5 Synthesis of N^1, N^3 -Bis(6-(3,3-dimethylbutanamido)pyridin-2-yl)-5-hydroxy isophthalamide	192
5.3.1.6 Synthesis of Methyl 11-(2,4,6-trioxo-1,3,5-triazinan-1-yl)undecanoate	194
5.3.1.7 Synthesis of 11-(2,4,6-Trioxo-1,3,5-triazinan-1-yl)undecanoic acid	195
5.3.1.8 Synthesis of Cyanuric Acid Functional Poly(ethylene glycol)	196
5.3.1.9 Synthesis of Alkyne end-Functionalized P(S-co-CMS) Copolymer	198
5.3.1.10 Synthesis of Alkyne end-Functionalized P(S-co-HWS) Copolymer	198
5.3.1.11 Synthesis of Hamilton Wedge Functionalized Star-Shaped Macromolecules	198
5.3.2 Results and Discussion of Construction of Star-shaped Macromolecules through Multiple Hydrogen Bonding	199
5.3.2.1 Preparation of Hamilton Wedge Functionalized Star-Shaped Macromolecules	199
5.3.2.2 Supramolecular Construction of Star-Shaped Macromolecules	204
5.4 Conclusions	211
5.5 References	212
6 Concluding Remarks and Outlook	217
6.1 Concluding Remarks	219
6.2 Outlook	220
7 Materials and Characterization Techniques	222
7.1 Materials	224
7.2 Characterization Techniques	225
7.2.1 Nuclear Magnetic Resonance Spectroscopy	225
7.2.2 Static and Dynamic Light Scattering	226
7.2.3 Size Exclusion Chromatography	227
7.2.4 Electrospray Ionization-Mass Spectrometry	227
7.2.5 Attenuated Total Reflectance-Infra Red Spectroscopy	228
7.3 References	228

List of Abbreviations	229
Curriculum Vitae	231
List of Publications	231
Patents	233
Conference Contributions	233
Acknowledgements	235

Motivation and Goals

Chapter 1



A specific three-dimensional structure from a single linear polypeptide chain can be generated by folding of the protein with a specific sequence of amino acids.

1. 1 Motivation

The emulation of natural processes and the design of chemical reaction sequences inspired by nature is one of the most important driving forces for synthetic macromolecular design. Undoubtedly, reversible self-folding processes are nature's approach to control the conformation of biological polymers. The synthesis of highly defined and functional three dimensional structures with a uniform polydispersity – such as proteins – remains still beyond the reach of current materials science.^[1] Many biomolecules undergo folding in solution to yield delicate molecular assemblies stabilized by non-covalent or – in some cases – covalent interactions.^[2-4] Folding of proteins, for instance, leads to complex secondary, tertiary and quaternary structures, which determine their properties and functions.

Well-defined synthetic single polymer chains with a functionality that can enable a folding process may be generated by combining controlled/living radical polymerization (CLRP) techniques^[5] with recent advances in modular and orthogonal polymer ligation protocols.^[6] Such single chain synthetic polymers – when carrying specific functionalities – may be reversibly folded into well-defined unimolecular structures akin to folded biomacromolecules.^[7] Related to the synthesis of reversibly folding single chain entities, the synthesis of well-defined static polymeric nanoparticles via folding of single chains driven by covalent interactions has drawn significant attention in the last decade with potential applications in e.g. nano-medicine.

The exquisite design of well-defined polymer chains – that can subsequently undergo single chain folding driven by covalent and non-covalent interactions – has been made possible by the control over the composition, molecular weight and molecular weight distribution of synthetic macromolecules offered by several CLP techniques including atom transfer radical polymerization^[8] (ATRP), nitroxide mediated polymerization^[9] (NMP), reversible addition-

fragmentation chain transfer (RAFT)^[10] polymerization and ring-opening polymerization^[11] (ROP).

Supramolecular chemistry is characterized by non-covalent interactions, which play a key role in the assembly, conformation, and/or behavior of supramolecular systems.¹² These reversible non-covalent interactions mainly include H-bonding,¹³ metal ligand coordination,¹⁴ π - π stacking¹⁵ and ion-dipole interactions.¹⁶ In a similar fashion, supramolecular polymers can be classified as polymeric systems that utilize these reversible non-covalent interactions to define their assembly, conformation, and/or behavior.^{17,18,19} Thus, supramolecular polymers can be generated by a single or a combinations of these non-covalent interactions described above. H-bonding has proved to be one of the most prominent supramolecular motifs, due to its ease of accessibility and high binding constants.

1. 2 Research Goals

The aim of the thesis is the preparation and characterization of synthetic polymers bearing donor-acceptor groups at pre-selected positions on the polymer backbone via a combination of CLP techniques and modular conjugation chemistry to understand the single-chain self-folding behavior of well-defined functional polymers in solution. The prepared macromolecules mimic folding elements occurring in natural biomacromolecules via single chain folding methods using intramolecular non-covalent interactions.

The long term aim – with the current thesis representing a first step – is the generation of well-defined macromolecules having non-identical hydrogen donor/acceptor entities at well-defined points within their backbone, allowing for a geometrically defined folding/unfolding action into a defined geometry similar to a natural protein. Thus, the key idea behind the current

initial attempts is to evaluate the possibility of employing single polymer chains in self-assembly procedures that are inspired by those of natural proteins. The field of single macromolecule folding is of substantial interest in both academia and industry for several applications ranging from the potential design of synthetic macromolecular proteins to bio-delivery systems.

In addition to the above aims, new complex macromolecular architectures were synthesized combining modular conjugation chemistry, CLP techniques and supramolecular chemistry. Supramolecular miktoarm star polymers and grafted star-shaped macromolecules have been prepared through self-assembly between complementary recognition motifs, to aid in the general understanding of complex macromolecular architecture design via H-bonding driven self-assembly.

The self-assembly processes presented in the present thesis in solution have been monitored by proton nuclear magnetic resonance (^1H NMR) spectroscopy as well as dynamic and static light scattering (DLS and SLS) analyses.

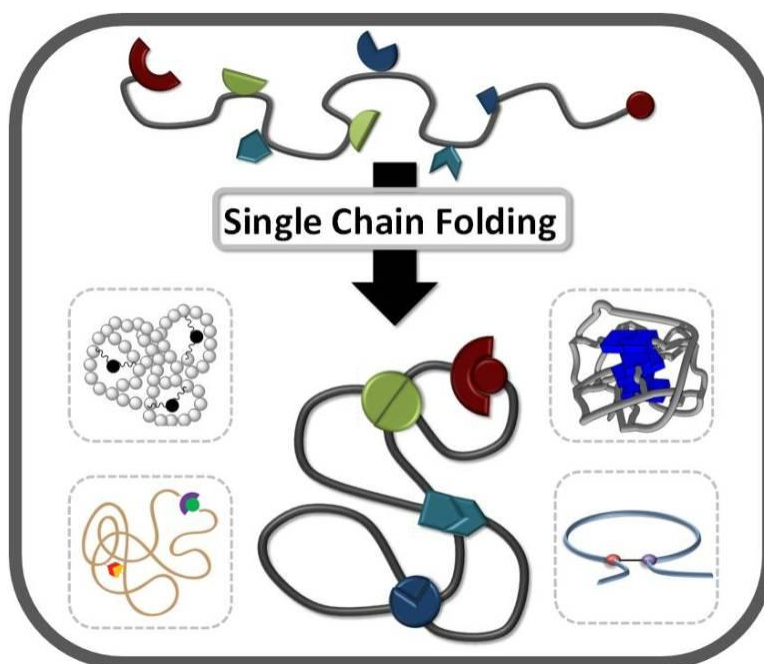
1.3 References

- [1] S. Perrier, *Nat. Chem.*, **2011**, *3*, 194.
- [2] C. B. Anfinsen, *Science*, **1973**, *181*, 223.
- [3] C. M. Dobson, *Nature*, **2003**, *426*, 884.
- [4] D. J. Hill, M. J. Mio, R. B. Prince, T. S. Hughes, J. S. Moore, *Chem. Rev.*, **2001**, *101*, 3893.
- [5] W. A. Braunecker, K. Matyjaszewski, *Prog. Polym. Sci.*, **2007**, *32*, 93.
- [6] O. Altintas, A. P. Vogt, C. Barner-Kowollik, U. Tunca, *Poly. Chem.*, **2012**, *3*, 34.
- [7] M. Ouchi, N. Badi, J.-F. Lutz, M. Sawamoto, *Nat. Chem.*, **2011**, *3*, 917.
- [8] K. Matyjaszewski, J. Xia, *Chem. Rev.*, **2001**, *101*, 2921.
- [9] C. J. Hawker, A. W. Bosman, E. Harth, *Chem. Rev.*, **2001**, *101*, 3661.
- [10] a) J. Chiefari, Y. K. Chong, F. Ercole, J. Krstina, J. Jeffery, T. P. T. Le, R. T. A. Mayadunne, G. F. Meijs, C. L. Moad, G. Moad, E. Rizzardo, S. H. Thang, *Macromolecules*, **1998**, *31*, 5559. b) C. Barner-Kowollik, S. Perrier, *J. Polym. Sci. Part A: Polym. Chem.*, **2008**, *46*, 5715.
- [11] N. E. Kamber, W. Jeong, R. M. Waymouth, R. C. Pratt, B. G. G. Lohmeijer, J. L. Hedrick, *Chem. Rev.*, **2007**, *107*, 5813.
- [12] J.-M. Lehn, *Chem. Soc. Rev.*, **2007**, *36*, 151.
- [13] F. H. Beijer, H. Kooijman, A. L. Spek, R. P. Sijbesma, E. W. Meijer, *Angew. Chem. Int. Ed.*, **1998**, *37*, 75.
- [14] M. Chipper, M. A. R Meier, D. Wouters, S. Hoeppener, C.-A. Fustin, J.-F. Gohy, U. S. Schubert, *Macromolecules*, **2008**, *41*, 2771.
- [15] L. Brunsveld, E. W. Meijer, R. B. Prince, J. S. Moore, *J. Am. Chem. Soc.*, **2001**, *123*, 7978.
- [16] P. R. Ashton, P. J. Campbell, E. J. T. Chrystal, P. T. Glink, S. Menzer, D. Philp, N. Spencer, J. F. Stoddart, P. A. Tasker, D. J. Williams, *Angew. Chem. Int. Ed.*, **1995**, *34*, 1865.
- [17] J. D. Fox, S. J. Rowan, *Macromolecules*, **2009**, *42*, 6823.
- [18] L. Brunsveld, B. J. B. Folmer, E. W. Meijer, R. P. Sijbesma, *Chem. Rev.*, **2001**, *101*, 4071.

- [19] T. F. A. De Greef, M. M. J. Smulders, M. Wolffs, A. P. H. J. Schenning, R. P. Sijbesma, E. W. Meijer, *Chem. Rev.*, **2009**, *109*, 5687.

Theoretical Background – A Literature Review

Chapter 2



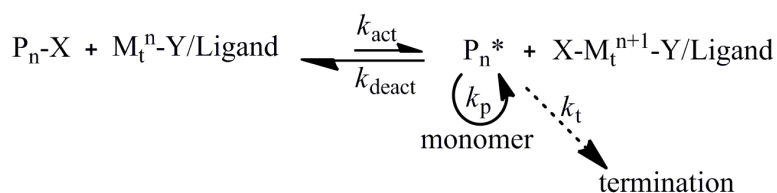
The synthetic routes for preparation synthetic macromolecules are described. Synthesis and characterizations of polymeric nanoparticles and initial attempts towards mimicking the structure of natural biomacromolecules via single chain folding of well-defined functional linear synthetic macromolecules are summarized.

2.1 Controlled/Living Polymerization Techniques

In the last decade, based on significant advances in controlled/living polymerization (CLP) techniques¹⁻¹² such as atom transfer radical polymerization (ATRP), nitroxide mediated radical polymerization (NMP), ring-opening polymerization (ROP) and reversible addition fragmentation chain transfer (RAFT) polymerization, the synthesis of polymers with complex architectures and predetermined chemical composition was significantly simplified and has received increased attention due to the exceptional variety of applicable monomers and significant tolerance to experimental conditions in comparison with living an ionic polymerization techniques.¹³

2.1.1 Atom Transfer Radical Polymerization (ATRP)

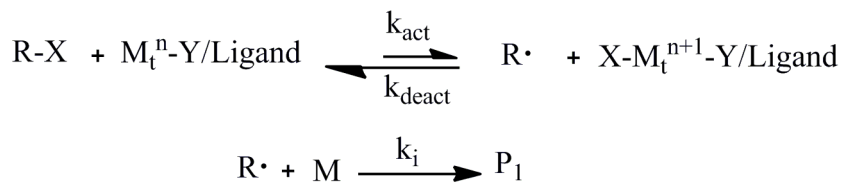
Matyjaszewski,¹⁴ Sawamoto¹⁵ and Percec¹⁶ independently reported transition-metal mediated controlled/living radical polymerization in 1995. ATRP is one of the most powerful techniques to obtain polymers with high control over compositions, architectures, and functionalities. The polymerization, which is mechanistically similar to atom transfer radical addition (ATRA), therefore, is often termed as ATRP. ATRP was developed by designing a metal catalyst utilizing an alkyl halide as an initiator with an appropriate structure and adjusting the polymerization conditions. The molecular weights increasing linearly with conversion and associated low polydispersities are typical for a living process.



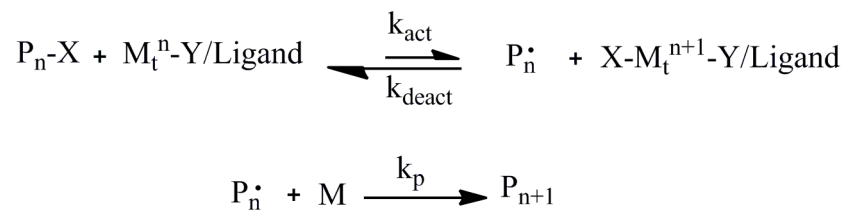
Scheme 2.1 General mechanism of ATRP.

The general mechanism of ATRP is shown in Scheme 2.1. The radicals (the propagating species P_n^*) are generated through a reversible redox process catalyzed by a transition metal complex (activator, $M_t^n - Y / \text{ligand}$) which undergoes a one-electron oxidation with concomitant abstraction of a (pseudo) halogen atom, X, from a dormant species, P_n-X . Radicals react reversibly with the oxidized metal complexes (the deactivator, $X-M_t^{n+1} / \text{ligand}$) to reform the dormant species and the activator. These processes are rapid and the dynamic equilibrium, which is established, favors the dormant species. All chains begin to grow at the same time. The concentration of the free radicals is relatively low, resulting in a reduced amount of irreversible radical-radical termination.

Initiation



Propagation



Termination



Scheme 2.2 Fundamental mechanism of ATRP, embedded in a free radical polymerization process.

The position of the equilibrium governed by the rate coefficient of activation, k_{act} , and deactivation k_{deact} , respectively determines the amount of available radicals. Polymer chains grow by the addition of monomers to the free radicals in a manner similar to a conventional radical polymerization with the rate coefficient of propagation, k_p . Bimolecular termination reactions, governed by the chain length dependent termination rate coefficient (k_t), also occur in ATRP, mainly through radical coupling and disproportionation; however, in a well-controlled ATRP, no more than a few percent of the polymer chains undergo termination. The initiation, propagation, and termination processes are illustrated in Scheme 2.2.¹⁷

A successful ATRP will not only feature small contributions of terminated chains but also uniform growth of all chains; this is accomplished through fast initiation and rapid reversible deactivation. The rates of polymerization and polydispersity in ATRP, assuming steady-state kinetics, are given in the equations 2.1 and 2.2, respectively.¹⁸⁻²⁰

$$R_p = k_p \cdot K_{\text{eq}} \frac{[\text{R-X}][\text{Mt}^n]}{[\text{Mt}^{n+1}]} [\text{M}] \quad \text{or} \quad \ln \left(\frac{[\text{M}_0]}{[\text{M}]} \right) = \frac{k_p \cdot k_{\text{act}} [\text{R-X}][\text{Mt}^n]}{k_{\text{deact}} [\text{Mt}^{n+1}]} t = k_{\text{app}} t \quad (\text{Eq. 2.1})$$

$$\frac{M_w}{M_n} = 1 + \left(\frac{k_p [\text{R-X}]}{k_{\text{deact}} [\text{Mt}^{n+1}]} \right) \left(\frac{2}{p} - 1 \right) = 1 + \frac{2}{k_{\text{act}} [\text{Mt}^n] t} \quad (\text{Eq. 2.2})$$

From eq. 2.1, the rate of polymerization, R_p , is directly proportional to the equilibrium constant K_{eq} , and the propagation rate coefficient k_p . The proper selection of the reaction components of an ATRP process leads to the establishment of an appropriate equilibrium between activation and deactivation processes. The equilibrium constant ($K_{\text{eq}} = k_{\text{act}}/k_{\text{deact}}$) plays the key role in the performance of ATRP because it determines the concentration of radicals, the rates of

polymerization and the termination frequencies. K_{eq} must be small to maintain a low stationary concentration of radicals; thus, termination reactions are minimized. For the ATRP system, the rate of polymerization, R_p , is first order with respect to the monomer $[M]$ and the activator $[Mt^n]$ concentrations and increases with the concentrations of activator, monomer, and initiator $[R-X]$ and decreases with the increasing deactivator $[Mt^{n+1}]$ concentration. Equation 2.2 suggests that lower polydispersities are obtained at higher conversion, higher k_{deact} relative to k_p , higher concentration of deactivator, and higher monomer to initiator ratio, $[M]_0/[I]_0$.

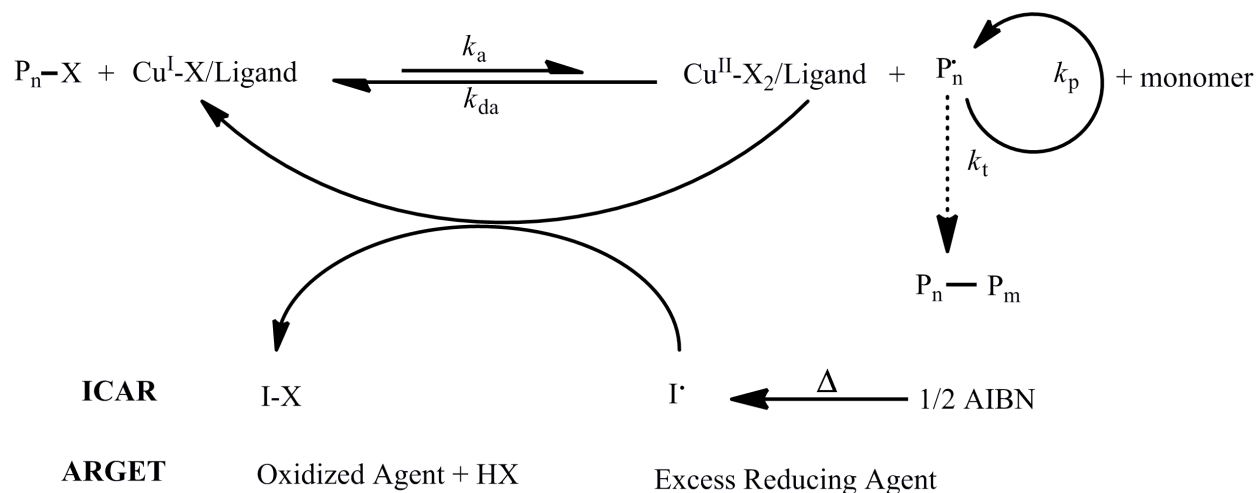
2.1.1.1 Lowering the Concentration of Copper-Catalyst in ATRP

The several modified ATRP techniques have been developed to overcome its main drawback, i.e. the amount of catalyst present in a traditional ATRP system.^{21,22} These techniques include activators generated by electron transfer (AGET) ATRP, initiators for continuous activator regeneration (ICAR) ATRP and activator regenerated by electron transfer (ARGET) ATRP. In these systems, oxidatively stable Cu^{II} complexes are reduced to the Cu^I complexes at the beginning of the reaction with various reducing agents. Single electron transfer living radical polymerization (SET-LRP) is prominent in that it uses metallic copper as the catalyst.

2.1.1.1.1 Activators Generated by Electron Transfer (AGET) ATRP

Preparation of pure block copolymers has some limitations with both simultaneous reverse and normal initiation in ATRP. In AGET ATRP, the addition of stoichiometric amounts of reducing agents to the reaction mixture containing alkyl halide, monomer and the air-stable deactivator ($X-Cu^{II}$) can regenerate the activator (Cu^I) during polymerization. The polymerization kinetics of AGET ATRP are similar to the kinetics of traditional ATRP after reproduction of the activator

(Cu^I). Tin^{II} 2-ethylhexanoate,²³ ascorbic acid,²⁴ and triethylamine²⁵ can be used as the reducing agents which react with the deactivator to generate the activator. Well-defined block copolymers can be produced with this technique with limited homopolymer formation. The technique can be utilized in aqueous and miniemulsion systems.^{26,27,28,29}



Scheme 2.3 Proposed mechanism for the regeneration of copper (I) complex in ARGET and ICAR ATRP.

2.1.1.1.2 Activators Regenerated by Electron Transfer (ARGET) ATRP

There is a small difference between ARGET ATRP and AGET ATRP: ARGET ATRP uses much smaller concentrations of the activator (Cu^I) and a large excess of the reducing agent.^{30,31,32}

A copper (I) complex is required to homolytically cleave the initiator. In ARGET ATRP, the polymerization can be conducted with very small amounts of a copper catalyst using a large amount of a reducing agent (see Scheme 2.3). Reducing agents are used in AGET ATRP and can be also utilized in ARGET ATRP of methyl acrylate, *n*-butyl acrylate, methyl methacrylate and styrene.³² Moreover, an excess amount of the reducing agent can also be utilized to consume

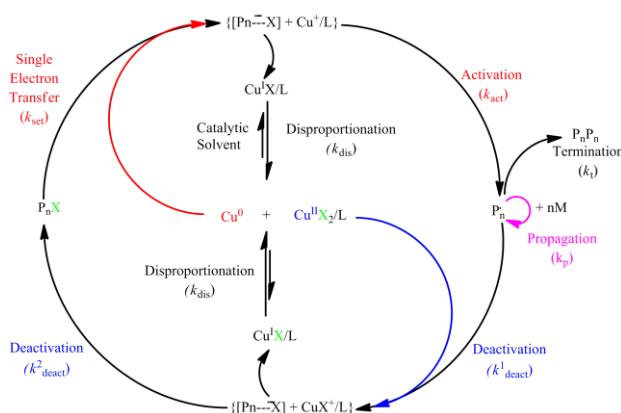
dissolved oxygen and other inhibitors from the polymerization system. Herein, the preparation of block copolymers via ARGET ATRP is described as an example. Poly(*n*-butyl acrylate)-*b*-poly(styrene) and poly(styrene)-*b*-poly(*n*-butyl acrylate) were successfully prepared by ARGET ATRP.³¹ Initially, poly(*n*-butyl acrylate) was synthesized via ARGET ATRP of *n*-butyl acrylate with 50 ppm of copper complex ($M_{n, \text{GPC}} = 19\,400 \text{ g mol}^{-1}$ and $M_{n, \text{theo}} = 18\,100 \text{ g mol}^{-1}$) and subsequently the polymer was utilized as a macroinitiator. A block copolymer was prepared using the macroinitiator by ARGET ATRP of styrene with 15 ppm of copper-catalyst ($M_{n, \text{GPC}} = 34\,900 \text{ g mol}^{-1}$, $M_{n, \text{theo}} = 37\,000 \text{ g mol}^{-1}$ and $M_w/M_n = 1.18$).

2.1.1.1.3 Initiators for Continuous Activator Regeneration (ICAR) ATRP

Irreversible accumulation of persistent radicals or deactivator (X-Cu^{II} complex) in typical ATRP conditions occur due to radical-radical termination where the initial catalyst concentration is too low or all of the activator is used as a persistent radical. Oxidants are consumed and also the amount of catalyst is reduced by ICAR in ATRP. The free radicals are slowly and continuously produced by conventional radical initiators such as AIBN during a polymerization and subsequently reduce and regenerate Cu as a persistent radical. By means of this technique, the amount of a Cu catalyst can be reduced from several thousand ppm to < reduction of 50 ppm for industrial applications while still allowing for excellent control over molecular weights and molecular weight distribution. The kinetics of ICAR are very similar to RAFT as suggested by recent mechanistic studies.³³

2.1.1.1.4 Single Electron Transfer Living Radical Polymerization (SET-LRP)

Percec and co-workers³⁴ introduced SET-LRP as new metal-catalyzed CRP method in 2002, which is slightly different than the radical polymerization techniques that are discussed above in terms of Cu sources. The SET-LRP process is catalyzed by Cu(0) powder or wire and provides for rapid synthesis of poly(acrylates)³⁵ and poly(methacrylates)³⁶ at ambient temperature or poly(vinyl chloride).³⁷ A more active Cu(0) catalyst in the SET-LRP is generated by the disproportionation of Cu(I)X to obtain a self-regulated mechanism that provides controlled architecture, narrow molecular weight distributions, as well as excellent chain-end fidelity.^{38,39} The key point of the proposed mechanism (see Scheme 2.4)⁴⁰ of SET-LRP is the formation of Cu(I) species and the active polymeric radical (P) via an outer-sphere electron transfer process where Cu(0) can donate an electron through space to a dormant polymer with a halide end group (P_n-X) to form a radical anion. On the other hand, the SET-LRP has demonstrated some advantages over other CRP techniques such as ambient temperature polymerization, ultra high polymerization rate, easily removal of catalyst and decreasing chance of side reactions.⁴¹



Scheme 2.4 Proposal mechanism of SET-LRP.³⁴

2.1.1.2 Functional Initiators

Telechelic polymers¹³ can be readily prepared via ATRP using functional initiators that can be synthesized in various ways. These initiators can be utilized in ATRP, as long as the functional group does not interfere with the mechanism of ATRP. A polymer prepared by ATRP contains a halogen atom at its terminus and can subsequently be used to generate a block copolymer via a chain extension process.⁴² For example, poly(*tert*-butyl acrylate) homopolymers were synthesized via ATRP of *t*BA. The polymerization was catalyzed by the CuBr/PMDETA system that led the formation of bromine-terminated P*t*BA macroinitiator with a narrow polydispersity ($M_{n,\text{GPC}} = 18\,200 \text{ g mol}^{-1}$, $M_{n,\text{theo}} = 19\,400 \text{ g mol}^{-1}$ and $M_w/M_n = 1.10$). Diblock copolymers including of *t*BA and MMA segments were prepared by polymerizing MMA with CuCl/PMDETA using P*t*BA macroinitiator through chain extension process ($M_{n,\text{GPC}} = 68\,000 \text{ g mol}^{-1}$, $M_{n,\text{theo}} = 72\,200 \text{ g mol}^{-1}$ and $M_w/M_n = 1.13$). Tri- and other multi-block copolymers have been synthesized via difunctional ATRP initiators.⁴³ For example, an asymmetric difunctional initiator containing a 2,2,6,6-tetramethylpiperidinyl-1-oxy (TEMPO) and a 2-bromo-2-methyl propionate group was synthesized and subsequently employed for the preparation of block copolymers via a combination of ATRP-NMP.⁴⁴ As a further example, a linear homopolymer of MMA was synthesized by ATRP using the functional initiator and catalyzed by CuBr/PMDETA with TEMPO moiety at the chain end ($M_{n,\text{GPC}} = 7\,500 \text{ g mol}^{-1}$, $M_{n,\text{theo}} = 6\,000 \text{ g mol}^{-1}$ and $M_w/M_n = 1.13$). The polymer was used as macroinitiator for NMP of styrene to generate poly(styrene)-*b*-poly(methyl methacrylate) with controlled molecular weight and narrow polydispersity. A polymer containing a halogen atom at its terminus which was prepared by ATRP and can subsequently be used to generate a block copolymer ($M_{n,\text{GPC}} = 18\,000 \text{ g mol}^{-1}$, $M_{n,\text{theo}} = 14\,900 \text{ g$

mol^{-1} and $M_w/M_n = 1.30$). Initiators can also contain multiple initiating sites. Multifunctional ATRP initiators can be used to synthesize star copolymers and other hyperbranched materials as well.⁴⁵ An ABC miktoarm star terpolymer⁴⁶ was first achieved via the core-first method using a combination of modular ligation chemistry, ATRP and NMP (see Figure 2.1). In this study, a trifunctional miktoinitiator with bromide, TEMPO and alkyne moieties was synthesized and successively used as an initiator in the ATRP of MMA ($M_{n,\text{GPC}} = 6200$ g/mol, $M_w/M_n = 1.2$) and consequently NMP of styrene. Finally, the CuAAC click reaction was accomplished between alkyne mid-functional copolymer (PMMA-PS-alkyne) and PtBA- N_3 ($M_{n,\text{GPC}} = 6000$ g/mol, $M_w/M_n = 1.28$) or PEG- N_3 ($M_n = 2000$ g/mol) to yield PMMA-PS-PtBA or PMMA-PS-PEG miktoarm star terpolymers.

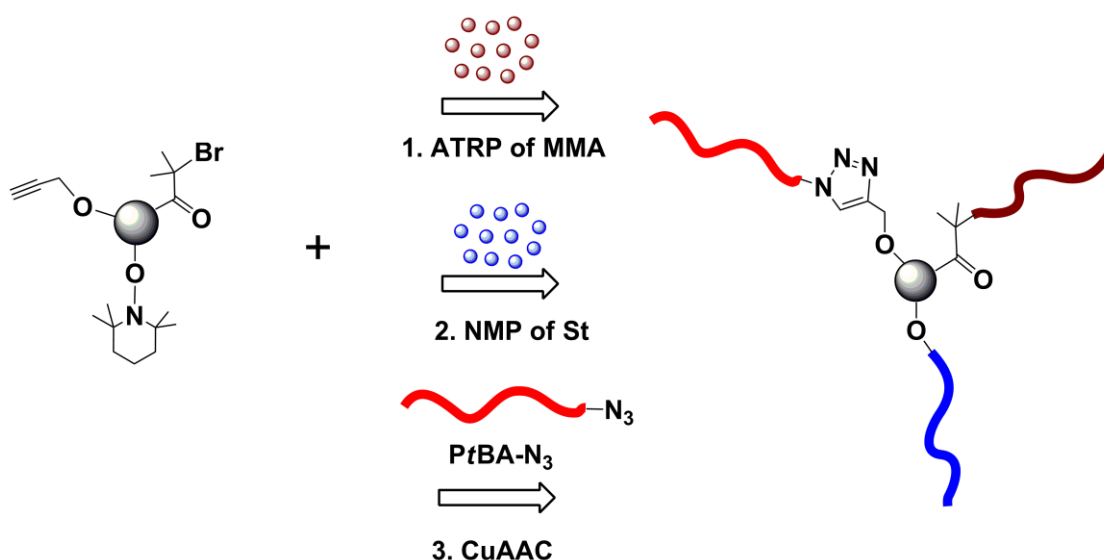


Figure 2.1 ABC miktoarm star terpolymer obtained from sequential atom transfer radical polymerization (ATRP), nitroxide mediated radical polymerization (NMP) and CuAAC.

2.1.1.3 Chain-End Functionality

End group functional polymers can be prepared via ATRP, as the halogen atom located at the end of the polymer chain can be readily converted into various other functionalities. For example, an azide functional polymer can be synthesized by nucleophilic substitution reaction of bromide functional polymer in the presence of NaN_3 . For example, a variety of block copolymers could be prepared using azido- and diazido-terminated polystyrene (PS-N_3 and $\text{N}_3\text{-PS-N}_3$), alkyne-terminated poly(methyl methacrylate) (PMMA-alkyne) as well as azide- and alkyne-terminated poly(ethylene glycol) (PEG- N_3 and PEG-alkyne) in the CuAAC click reaction.⁴⁷ Moreover, ABC type triblock terpolymers were also prepared through ATRP and modular ligation chemistry.⁴⁸ In that case, poly(methyl acrylate) (PMA)-*b*-PS-*b*-poly(*tert*-butyl acrylate) (PtBA) triblock terpolymer was successfully prepared with catalysis CuBr/ tris(2-(dimethylamino)ethyl)amine (Me_6TREN) in DMF at 50 °C in a modular fashion by performing two sequential CuAAC click reactions of polymeric precursors, both ATRP generated PMA- N_3 ($M_n = 7150$ g/mol, $M_w/M_n = 1.18$) and PtBA-alkyne ($M_n = 3560$ g/mol, $M_w/M_n = 1.24$), onto an alkyne-PS-alkyne central block ($M_n = 5800\text{-}6980$ g/mol, $M_w/M_n = 1.13\text{-}1.15$) (see Figure 2.2).

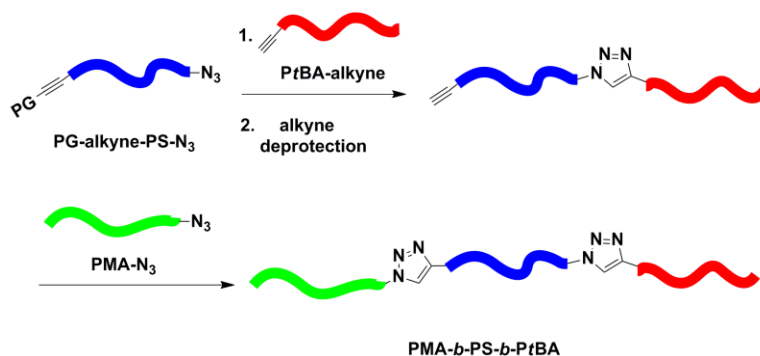


Figure 2.2 Synthesis of linear ABC triblock terpolymer via sequential copper catalyzed azide-alkyne cycloaddition (CuAAC) click reactions.

Additionally, the bromide end group of ATRP made polymers can be also transformed into a double bond employable as a macromonomer, which can be incorporated as an initiating site for another polymerization.⁴⁹ Furthermore, the most popular Cu(I) catalyzed azide–alkyne cycloaddition has been combined with ATRP to generate pedant-functionalized polymers,⁵⁰ end-functionalized polymer,^{51,52} multisegmented block copolymers,⁵³ stars,⁵⁴ brushes,⁵⁵ and H-shaped polymers.⁵⁶ The synthesis of star block copolymers via a modular ligation strategy was reported by Matyjaszewski and coworkers,⁵⁷ in which they accomplished the synthesis of a 3-arm star block copolymer $(AB)_3$ by sequential core-first and CuAAC (coupling-onto) methods. In this strategy, 3-arm star PS $(PS-Br)_3$ with highly functionalized bromine chain-ends were first synthesized by ATRP using the ‘core-first’ method (see Figure 2.3). After complete conversion of the bromo-terminated polymers into azido-terminated polymers by nucleophilic substitution with sodium azide, the product $(PS-N_3)_3$ ($M_{n, GPC} = 3300 \text{ g}\cdot\text{mol}^{-1}$, $M_w/M_n = 1.07$) was further conjugated with alkyne-terminated PEG (PEG-alkyne) ($M_{n, GPC} = 2100 \text{ g}\cdot\text{mol}^{-1}$, $M_w/M_n = 1.05$) yielding 3-arm star block copolymers $(PS-b-PEG)_3$ via the CuAAC (‘coupling-onto’) method with high coupling efficiencies. The weight fraction of the $(PS-b-PEG)_3$ star block copolymer was 85% in the final conjugated product between $(PS-N_3)_3$ and PEG-alkyne.

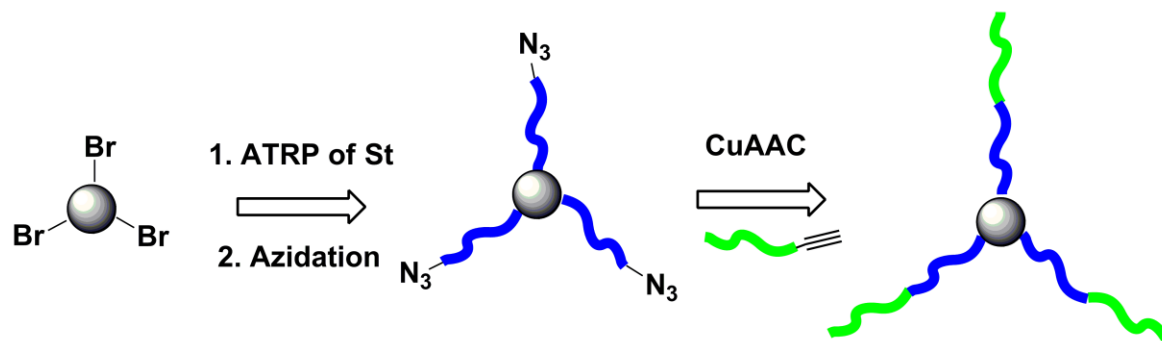
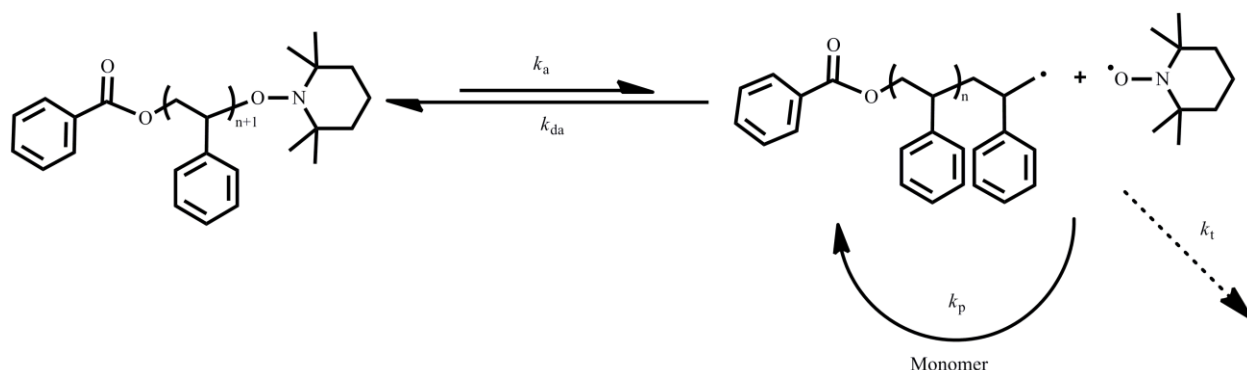


Figure 2.3 Synthesis of 3-arm star block copolymer $(PS-b-PEG)_3$ using ATRP and CuAAC reaction sequence.

2.1.2 Nitroxide-Mediated Radical Polymerization (NMP)

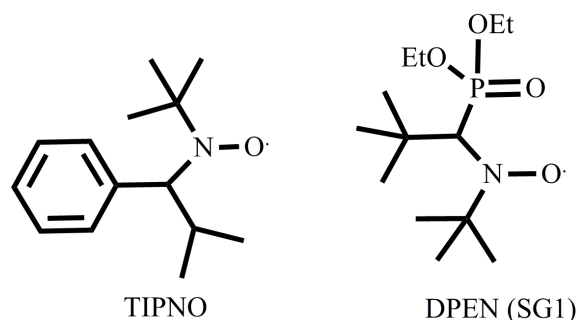
NMP has become popular as a method for preparing living polymers with good control over both the polydispersity and molecular weight. NMP relies on the reversible homolytic cleavage of a relatively weak bond in a covalent species to generate a growing radical and a less reactive radical. The stable free radicals do not react with themselves or with monomer to initiate the growth of new chains; they only react reversibly with growing radicals. The best known and most investigated stable radicals have been nitroxides, especially 2,2,6,6-tetramethylpiperidinyloxy (TEMPO). Georges and co-workers⁵⁸ described – for the first time – that the polymerization of styrene using various ratios of benzoyl peroxide (BPO) and TEMPO as an initiating system. The polymers are obtained in the above study with narrow polydispersity and good control over the molecular weight ($M_{n,GPC} = 18\,200\text{ g}\cdot\text{mol}^{-1}$, $M_w/M_n = 1.19$). The equilibrium reaction between activation and deactivation for the polymerization of styrene using TEMPO is shown in Scheme 2.5.



Scheme 2.5 Deactivation and activation step for the polymerization of styrene using TEMPO.

Subsequently, the living character of this novel procedure has been evidenced in several studies.^{59,60,61,62} NMP was utilized within combination with other CRP techniques for the

preparation of a variety of well-defined and complex macromolecular architectures (see Figure 2.1). Preparation of polymers based on acrylic monomers with TEMPO mediated NMP was difficult and resulted in products with broad molecular weight.⁶³ To overcome these problems, alternative nitroxide mediators have been investigated by several researchers in order to extend the range of monomers for NMP.⁶⁴ Di-*tert*-butyl nitroxide (DBN) and the novel *N-tert*-butyl-*N*-[1-diethylphosphono-(2,2-dimethylpropyl)] nitroxide (DEPN) depicted in Scheme 2.6 were discovered and utilized for the synthesis of complex macromolecular architecture.⁶⁵ For example, three-arm star polymers of styrene and *n*-butyl acrylate were readily prepared with relatively narrow molecular weight distributions ranging from 1.09 to 1.40 using DEPN mediating group. The polymerization of styrene with TEMPO and some of the acrylic monomer with TIPNO and DPEN was well-established with NMP; however, extension of the technique to other monomer families requires further manipulation of the reaction conditions or structure of the nitroxide.



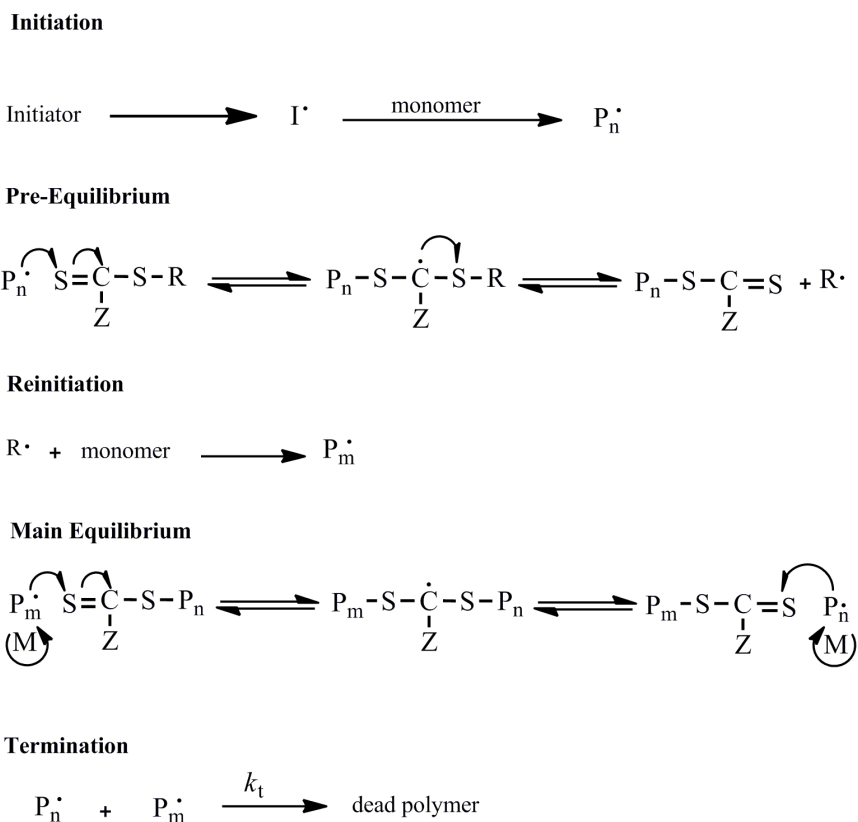
Scheme 2.6 Structures of the nitroxides TIPNO and DEPN (SG1).

2.1.3 Ring-Opening Polymerization (ROP)

ROP is a unique polymerization process^{66,67} where a cyclic monomer is opened to generate a linear polymer. It is fundamentally different from a condensation polymerization in

that there is no small molecule byproduct during the polymerization. Polymers with a wide variety of functional groups can be produced by ring-opening polymerizations. Examples of industrially important polymers made by ring-opening polymerizations are Nylon 6, polysiloxane, polycaprolactone and epoxy resin. The poly(ϵ -caprolactone) (PCL) family of polyesters is synthesized by ROP of ϵ -caprolactone (ϵ -CL). Nowadays, increasing attention is paid to biodegradable and biocompatible polymers for applications in the biomedical and pharmaceutical fields.

2.1.4 Reversible Addition-Fragmentation Chain Transfer (RAFT) Polymerization



Scheme 2.7 Simplified general mechanism of the RAFT process.

One of the most extensively studied CLP methods is RAFT polymerization.⁶⁸ This method has some crucial advantages over ATRP and NMP in terms of a wide range of accessible functionalities, monomers and solvents.⁶⁹ Well-defined polymers with complex macromolecular structure can be readily generated via RAFT technique that has more tolerance to monomers choice and functional groups. Moreover, free radical polymerizations can be readily converted into a RAFT process by adding an appropriate RAFT agent while other reaction parameters can be kept unchanged. The RAFT polymerization is composed of a small amount of RAFT agent, monomer and a radical initiator. The molecular weight distribution of the polymer and the rate of polymerization depend on the free radical concentration.⁷⁰ The mechanism of RAFT polymerization with the thiocarbonylthio-based RAFT agents involves a series of addition–fragmentation steps as depicted below. Initiation and radical–radical termination occur as in conventional radical polymerization. Initiation starts with the decomposition of the initiator leading to the formation of propagating chains. In the early stages of the polymerization, addition of a propagating radical ($P_n\cdot$) to the thiocarbonylthio compound $[S=C(Z)SR]$ is followed by fragmentation of the intermediate radical, giving rise to a polymeric RAFT agent and a new radical ($R\cdot$). The radical $R\cdot$ reinitiates the polymerization by reaction with monomer to form a new propagating radical ($P_m\cdot$). In the presence of a monomer, the equilibrium between the active propagating species ($P_n\cdot$ and $P_m\cdot$) with the dormant polymeric RAFT compound provides an equal probability for all chains to grow (see Scheme 2.7). This feature of the RAFT process offers the production of narrow polydispersity polymers. When the polymerization is complete, most of the chains retain the thiocarbonylthio end-group.⁷¹ In RAFT polymerization, radicals may be generated by decomposition of organic initiators, the use of an external source (UV–vis

or γ -ray) or thermal initiation. The polymerization temperature is usually in the range of 60–80 °C, which corresponds to the optimum decomposition temperature interval of the well-known initiator azobis(isobutyronitrile) (AIBN). However, even ambient temperature and high temperature conditions can also be applied.^{72,73} Generally, a RAFT agent/free-radical ratio of 1:1 to 10:1 yields polymers with narrow molecular weight distributions.

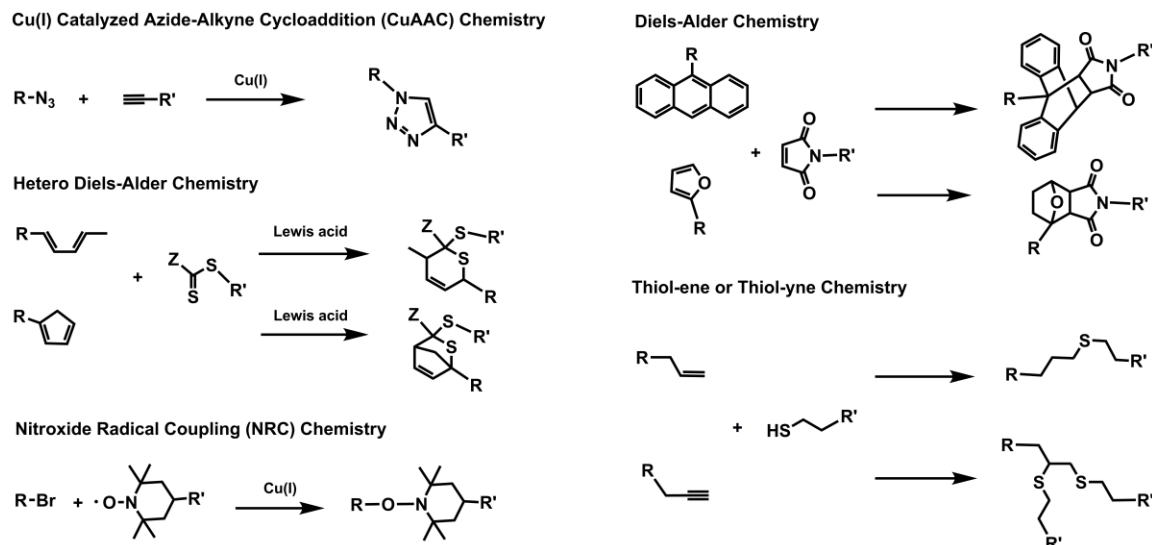
2.2 Click Chemistry

The click chemistry philosophy – introduced by Sharpless and coworkers in 2001 – comprises chemical reactions which display high stereo- and regio-selectivity, high yields, simple recovery of the main product, mild reaction conditions, compatibility in a wide range of solvents and a tolerance to a wide range of functional groups.⁷⁴ This conjugation chemistry concept has been adapted to a vast variety of applications⁷⁵⁻⁸³ and has possibly led to a ‘paradigm shift’⁸⁴ toward the modular construction approach within polymer chemistry. This ‘paradigm shift’ is due in part to the applicability of the click chemistry concept to prepare macromolecular structures that would have otherwise not been achievable by such simple quantitative methods, and has opened up a particularly rapid and efficient synthetic route to functional materials with predefined polymeric architectures.⁸⁴ Recently, Barner-Kowollik et al. refined the requirements that a click reaction should fulfill within synthetic polymer chemistry in adaptation of the original definitions by Sharpless and co-workers.⁸⁵ These refined requirements include the use of equimolar amounts of the polymeric building blocks, a simple large-scale purification process, high yields, reasonable time scales and mild reaction conditions.⁸⁵ It is important to note that the term ‘click chemistry’ has been employed in the literature in an inflationary fashion and reactions have been included under the click definition, which definitely do not fall under its

strict criteria. Thus, we will adapt a cautious approach herein when denoting a reaction as of the click-type.

2.2.1 Modular Ligation Reactions

The most prominent modular ligation reactions are shown in Scheme 2.3 which widely adaptable to polymer chemistry include the Cu(I) catalyzed azide-alkyne cycloaddition (CuAAC), Diels-Alder, hetero Diels-Alder, thiol-ene, thiol-yne, and the nitroxide radical coupling (NRC) reactions.



Scheme 2.8 Schematic representation of modular ligation reactions.

2.2.1.1 Cu (I) Catalyzed Azide-Alkyne Cycloaddition (CuAAC)

The CuAAC reaction is a modified Huisgen 1,3-dipolar [3+2] cycloaddition, where the presence of a copper catalyst affords a quantitative 1,4 triazole product which proceeds at non-demanding reaction conditions.^{86,87} Here, the [3+2] notation describes the number of atoms in the two components involved in the 1,3-dipolar cycloaddition. Huisgen type reactions are exergonic

processes, which combine two (e.g. azide and alkyne) unsaturated reactants and produces a racemic mixture of 1,4- and 1,5-disubstituted 1,2,3-triazoles, whereas the CuAAC reaction is highly regioselective and yields only a 1,4-disubstituted 1,2,3-triazole. The CuAAC reaction was first adapted⁸⁸ to the field of polymer chemistry due of its often quantitative yields, mild reaction condition, tolerance to a wide range of functional groups, and harmony with the CLP techniques.⁷⁵ In many circumstances, the CuAAC process fulfills the click criteria. Among the CLP techniques utilized in conjunction with the CuAAC, ATRP shares a number of important features with the CuAAC reaction including robustness, tolerance to many functional groups, and the same catalytic system. Most significantly, however, ATRP and the CuAAC constitute a beneficial combined/tandem synthetic route due in part to ATRP offering well-defined polymer chains with chlorine or bromine end-groups which may consequently be converted efficiently to an azide using a classic substitution reaction.⁷⁵

2.2.1.2 Diels-Alder (DA) and Hetero Diels-Alder (HDA) Reactions

The Diels-Alder [4+2] cycloaddition involves the reaction of a conjugated diene (4π) with a dienophile (2π) to yield a 6-membered ring, where the [4+2] denotes the number of π -electrons that are involved in the cycloaddition process.⁸⁹ The most encountered diene/dienophile functionalities extensively employed in synthetic polymer chemistry are anthracene/maleimide, butadiene or cyclopentadiene/electron deficient dithioesters, and furan/maleimide. The anthracene-maleimide cycloaddition reactions are conducted at high temperatures, commonly 125 °C. Additionally, furan must be used as a protecting agent for the maleimide to avoid a possible radical polymerization during the preparation of maleimide end-functionalized

polymeric precursors when used in conjunction with LRP techniques.⁹⁰ A more attractive cycloaddition occurs with a diene and dithioester in a hetero Diels-Alder (HDA) process,⁹¹ which is carried out at relatively lower temperatures of 50 °C for butadiene or ambient temperature for cyclopentadiene.⁹² Compared to the anthracene-maleimide Diels-Alder cycloaddition, the dithioester end-functionality may be introduced into the polymer backbone via the RAFT process. The obtained adducts are not thermally stable over 80 °C for cyclopentadiene/dithioester and over 120 °C for furan/maleimide, limiting the applicability of the resulting polymers at high temperatures.⁹³ However, the same instability conversely enables the design of macromolecular structures with reversible thermoresponsive properties.^{94,95} Just as with the CuAAC process, some of the above noted (H)DA systems only fulfil the click ligation criteria under certain reaction conditions.^{96,97}

2.2.1.3 Thiol-ene and Thiol-yne Reactions

Thiol-ene or thiol-yne radical addition reactions are based on the free radical reaction between a thiol and an alkene or an alkyne by using a thermal or photochemical process resulting in thioether products with high degree of anti-Markovnikov selectivity.⁹⁸⁻¹⁰⁰ Additionally, it has been shown that the thiol-ene reaction can be catalyzed by employing a primary amine¹⁰¹ which is advantageous when used in conjunction with a RAFT precursor as the primary amine both aminolyzes the RAFT agent and catalyzes the thiolene-Michael type reaction. Commonly, the thiolene-Michael addition is used to conjugate thiols to an acrylate or a maleimide, yielding thioether-ester or -imide functionalized adducts, respectively.¹⁰² In a thiol-yne reaction the alkyne reacts first with a thiol to result in a vinyl sulfide followed by a subsequent reaction of the vinyl sulfide with another thiol to yield the 1,2-disubstituted thioether adduct.^{98,99} However, the

thiol-ene and thiol-yne reactions have some limitations for polymer-polymer conjugation due to disulfide coupling, which has resulted in research exhibiting a higher efficiency for thiol-ene reactions ligating small organic molecules to polymers.¹⁰³ Importantly, there exists significant doubt whether the radical version of thiol-ene reaction can be classified as a click reaction, due to the occurrence of radical-radical coupling reactions during the ligation process.¹⁰³

2.2.1.4 Nitroxide Radical Coupling (NRC) Reaction

The NRC reaction proceeds between a halide- and 2,2,6,6-tetramethylpiperidine-1-oxyl (TEMPO)-terminated polymers in the presence of a CuBr/ligand complex at elevated temperatures based on an ATRP type mechanism.¹⁰⁴ Huang and coworkers first applied the NRC reaction for the preparation of linear triblock terpolymers together with the CuAAC reaction.¹⁰⁴ Later, the NRC process was carried out – according to the authors – under single electron transfer living radical polymerization (SET-LRP) conditions.¹⁰⁵ In the SET process, Cu(0) (equimolar) transfers an electron to a halogen-terminated polymer to provide a macroradical and Cu(I) at ambient temperature via a SET-LRP mechanism, in which the macroradical is then efficiently trapped by a TEMPO-terminated polymer. The modular nature of the NRC reaction was proven in the preparation of well-defined polymers with different topologies such as block, star, and graft copolymers.^{106,48,58}

2.3 Syntheses of Star Polymers

Star polymers may be classified into two categories based on the chemical composition of the arm species, being a homoarm (regular) star polymer or miktoarm (heteroarm) star polymer (Figure 2.4).¹⁰⁷⁻¹⁰⁹ Homoarm star polymers consist of a symmetric structure comprising radiating arms with similar molecular weight and identical chemical composition. Within this

classification, star block copolymers may be defined as homoarm star polymers, in which each is constituted of identical copolymers (diblock, triblock, etc.). In contrast, a miktoarm star polymer contains two or more arm species with different chemical compositions and/or molecular weights.¹¹⁰

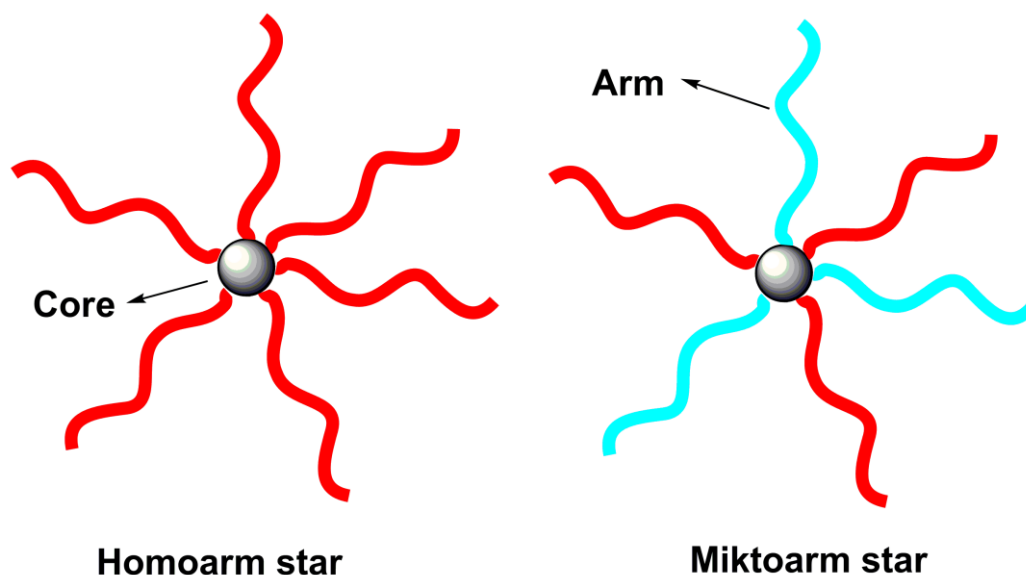


Figure 2.4 Schematic representation of star polymer structures

Star polymers are usually synthesized via one of three common methodologies, i.e. core-first, arm-first, and coupling-onto.¹¹¹ These three synthetic methods differ from each other based on the sequence employed for the formation of the core and the arms. In the “core-first” approach (divergent), multifunctional initiators are used to grow arms via living polymerization techniques. The “arm-first” approach (convergent) is carried out by linking telechelic preformed linear arm precursors commonly using a divinyl compound to form the final star polymer with a highly cross-linked core. In the “coupling-onto” methodology, linear arm precursors with reactive functional end-groups are attached via ligation reactions onto a multifunctional core to

create a star polymer. Although these methodologies provide a powerful tool to produce star polymers, a number of challenges remain regarding the structural homogeneity, purity, and molecular weight distribution of star molecules. Star-star coupling is the main reason for broad molecular weight distribution in the “core-first” method due to the high number of initiating sites with propensity for radical-radical recombination, therefore “core-first” star polymerizations are usually limited to low monomer conversion (< 20 %) to avoid star-star radical coupling. Moreover, in the “arm-first” approach, poor structural homogeneity and broad molecular weight distribution arises from the result of a random distribution of arms per molecule during the cross-linking reaction of the core. The main problem encountered in the “coupling-onto” methodology is commonly inefficient coupling reactions between the polymer chains and the multifunctional core. Fortunately, the developed modular ligation strategies have emerged as a powerful tool to solve the problem of inefficient coupling. Despite the increasing attention paid to the construction of complex macromolecular architecture via covalent bonds, the development of well-defined supramolecular block copolymers or supramolecular stars from self-assembly of tailor-made hydrogen-bonding macromolecules remains in its infancy in comparison with covalent analogues.¹¹²

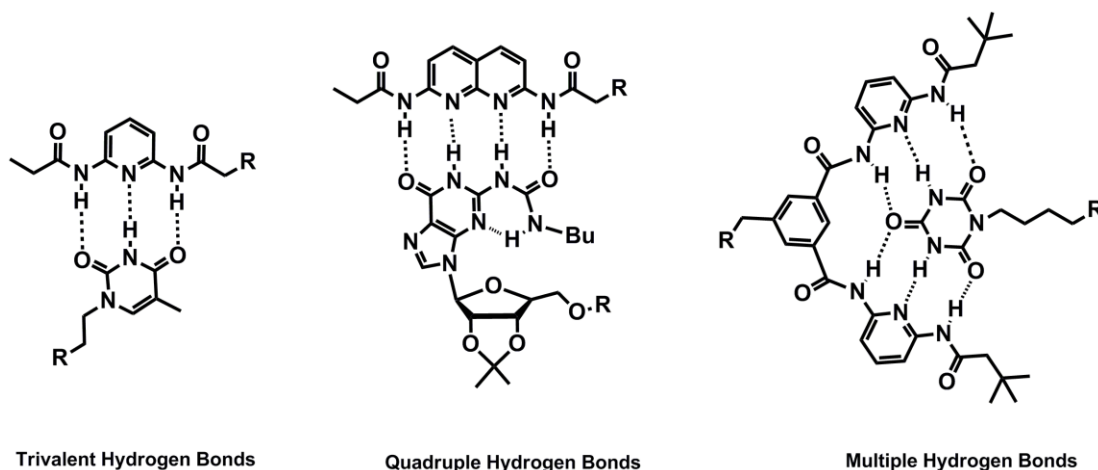
2.4 Supramolecular Chemistry

In diverse areas such as physics, chemistry and biology – as well as their interdisciplinary interactions – supramolecular chemistry has become an integral tool due to its ability to generate highly complex structures. Supramolecular chemistry exceeds its study area of molecules and points its focus on chemical systems containing a distinct number of assembled

molecular subunits or constituents.^{113,114} Traditional chemistry studies covalent bonds whereas supramolecular chemistry investigates the reversible non-covalent interactions between molecules. Supramolecular polymers exhibit a very important class in polymer science where well-defined intramolecular interactions permit a precise tuning of the polymer properties.¹¹⁵ The construction of these polymers is achieved by reversible and highly directional secondary interactions that are non-covalent bonds. Hydrogen bonding is more effective when compared with other intermolecular forces employed in studies of non-covalent interactions. Hydrogen bonds make it possible to tune the binding constants between several M^{-1} up to $10^7 M^{-1}$ with the help of a specific hydrogen-bond matching pair.¹¹⁵

2.4.1 Hydrogen Bonds

Hydrogen bonds are reported as the most beneficial interactions that fortify the molecules to self-assemble into well-defined objects.¹¹⁶ A hydrogen bond can be defined as the attractive interaction between a hydrogen atom and an electronegative atom such as nitrogen, oxygen or fluorine that belongs to another molecule or chemical group.¹¹⁵ To construct the hydrogen bond, the hydrogen atom must have a covalent bond formed with another electronegative atom (Scheme 2.9). These bonds can be formed between molecules or between the different sides of a particular molecule. The strength of the hydrogen bond is higher than a van der Waals interaction and lower than ionic bonds and covalent bonds. The strength and selectivity of the hydrogen bonds can be improved with the help of the arrays of the donor (D) and the acceptor (A) sites.



Scheme 2.9 Trivalent, quadruple and multiple hydrogen-bonding systems that can be employed in supramolecular chemistry of polymers.

2.4.1.1 Trivalent Hydrogen Bonds

Trivalent hydrogen-bonding systems have been employed for the formation of supramolecular polymers. The most critical triple-hydrogen bonds arise from 2,6-diaminopyridines, 2,6-diamino-1,3,5-triazines and their complexes with flavine- and thymine/uracil.¹¹⁵ Lehn and co-workers^{117,118} made use of the significance of the 2,6-diaminopyridine/uracil interaction.

2.4.1.2 Quadruple Hydrogen Bonds

Quadruple hydrogen bonds have been constructed to improve the effects investigated and known from triple hydrogen bonds. Meijer and co-workers^{119,120} have reported the use of small molecules containing quadruple hydrogen bonding motifs for the formation of supramolecular polymers with high molecular weights. The arrangement of these small components to form materials with polymeric properties in solution is limited by the strength of the binding constant that was calculated by Meijer and colleagues. A concentration of the monomeric units with

recognition motifs at 1 M leads to the formation supramolecular polymers with 100 repeating units and binding constant at 10^4 M^{-1} .

2.4.1.3 Multiple Hydrogen Bonds

Multiple hydrogen bonds are a continuation of the concept to bring more connecting sites within a hydrogen bonding system. There are reasons for the exploration of the higher-order systems for the formation of new polymeric architectures and structures: stability enhancement by accumulating more hydrogen bonds into the binding systems and the requirement to prevent ureidopyrimidones considering their self-complementary structure.¹¹⁵ One example is a hexapolar hydrogen-bonding moiety [DAD–DAD] named after Hamilton and co-workers¹²¹ with either barbituric acid or N-alkyl-cyanurate. These hydrogen bonding systems can be used as alternative system to the ureidopyrimidones.

2.5 Protein Structures¹

Proteins are made up of amino acids that is to say that proteins are the polymers of amino acids. Therefore, a polypeptide can be defined as a single linear chain of amino acids that are bonded by peptide bonds among amino and carboxyl groups. It is important that proteins fold into one or more particular conformations to achieve their biological properties by means of non-covalent interactions such as hydrogen bonding, ionic interactions, van der Waals forces, and hydrophobic packing.¹²² There are four specific levels of protein structure¹²³ that are demonstrated in Figure 2.5.

¹ The information included in section 2.5 has been adopted from reference 123 and 124.

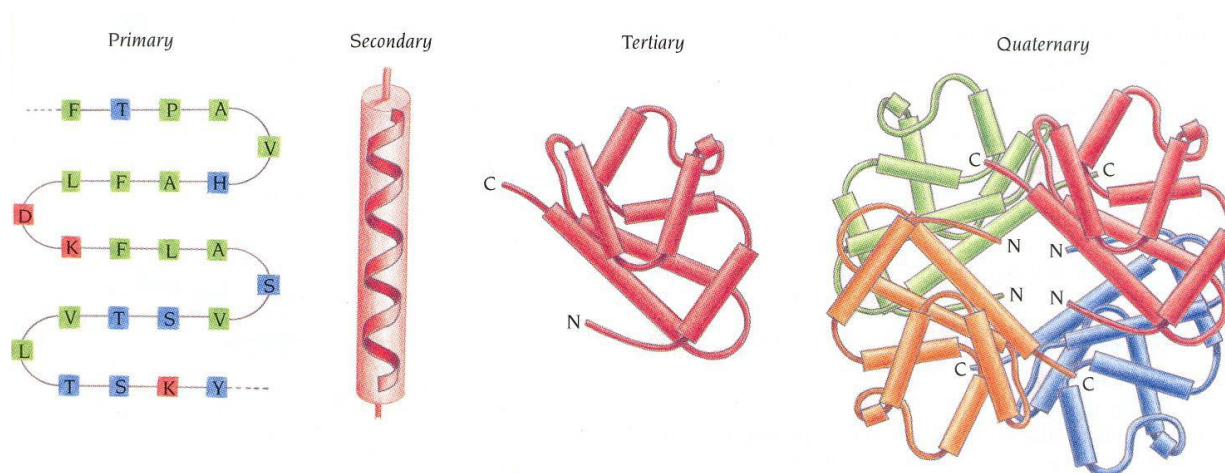


Figure 2.5 Schematic representation of the protein structures.¹²³ Copyright 1999, Introduction to Protein Structure by Branden and Tooze. Reproduced with kind permission from Garland Science/Taylor & Francis Books, LLC.

The primary structure is formed by the sequence of amino acids and the location of disulfide bridges. The covalent connections of the proteins can be described by the primary structure. The steric relationship of amino acid residues that are near to each other in the linear sequence is important for the formation of the secondary structure of the proteins. The examples of the secondary structure can be the α -helix and the β -pleated sheet. The definitions of these secondary structures are defined by the patterns of the hydrogen bonds among the main-chain peptide groups. The α -helix and the β -pleated sheet structures of the proteins are constructed through the hydrogen bonds among the NH and CO groups that are located in the peptide main chain. The distinction between a β -pleated sheet and an α -helix is as follows: The peptide chain in the α -helix is firmly coiled whereas the peptide chain in the β -pleated sheet is almost fully elongated. Additionally, the β -pleated sheet is stabilized by intermolecular hydrogen bonds between NH and CO groups, yet the α -helix structure is formed by intramolecular hydrogen

bonds between NH and CO groups. A three-dimensional tertiary structure is configured via the α -helix and the β -pleated sheet that are folded into a compact globule. The stabilization of the quaternary structure is achieved by the same non-covalent interactions and additionally disulfide bonds as in the tertiary structure.

A protein folds into one or more domains such the α -helix, the β -pleated sheet and additionally loops. Protein folding is the process of a polypeptide chain acquiring its correct three-dimensional structure to accomplish the biologically active native state.¹²⁴ A specific three-dimensional structure from a linear polypeptide chain can be generated by folding of the protein with a specific sequence of amino acid residues. The secondary structural elements of the domains and the whole domains steadily undergo small movements in space.¹²⁵ The process of a protein acquiring its functional shape and conformation is termed protein folding.

2.6 Folding of Single Polymer Chains via Intramolecular Covalent Bonds

Folding of well-defined linear single polymer chains via intramolecular covalent bonds both mimicking structures of biomacromolecules and/or nanoparticles will be discussed in the current chapter. It has to be noted that the covalent fixation of the polymer geometry removes the dynamic nature of the single chain folded entity and does thus limit their application in biomimetic systems that rely on dynamic configuration process, such as the folding / unfolding action that determines the functions of certain proteins.

Mecerreyes, Miller and co-workers¹²⁶ reported the preparation of polymeric nanoparticles between 3 and 15 nm in diameter by intramolecular self-crosslinking of functional polymers via covalent bonds in ultradilute solution. In their study, linear polyesters carrying methacryloyl groups are synthesized by ROP of either ϵ -caprolactone or L,L-lactide. The nanoparticles are

subsequently formed by self-crosslinking in dilute solution using a radical initiator such as 2,2-azobisisobutyronitrile (AIBN). The polymeric nanoparticles are characterized by infrared (IR), NMR, DLS and SEC. For instance, SEC demonstrates that the hydrodynamic volumes of the nanoparticles are significantly smaller than the starting linear macromolecules at low concentrations resulting in the formation of new internal covalent bonds. The utilization of these nanoparticles has been also demonstrated as sacrificial porogens for the generation of nanoporous thin films.

In related work, Hawker and co-workers¹²⁷ prepared well-defined nanoparticles through intramolecular reactions of benzocyclobutene (BCB) groups at high temperatures. In their study, the BCB-functionalized polystyrene derivatives were synthesized via NMP and subsequently the BCB-functionalized linear polymer was added dropwise via a peristaltic pump at approximately $12.8 \text{ mL}\cdot\text{h}^{-1}$ to a benzyl ether solution at $250 \text{ }^\circ\text{C}$ under vigorous stirring in an argon atmosphere. The resulting well-defined single-chain nanoparticles were readily characterized by the standard techniques such as SEC, DLS, ^1H NMR, and DSC. For example, the starting linear polymer features a number average molecular weight, M_n , of 84 800 Da; however, upon intramolecular reaction the hydrodynamic volume of the macromolecule decreases to an apparent M_n of 59 000 Da to yield a nanoparticle. DLS was additionally applied to follow the decrease in size from 8.7 to 6.6 nm that was following the intramolecular collapse.

In a related work, Hawker, Fréchet and co-workers¹²⁸ described the preparation of hybrid block copolymers composed of polymeric nanoparticles and linear polymers using controlled radical polymerization, convergent dendrimer synthesis as well as benzocyclobutene (BCB) cross-linking chemistry. Herein, a novel Fréchet-type dendritic initiator was prepared employing

a convergent approach containing peripheral tetrahydropyranyl (THP) protected phenolic groups. The dendritic initiator was utilized for the sequential polymerization of *n*-butyl acrylate followed by the polymerization of styrene/BCB via NMP and ATRP, respectively, affording well-defined asymmetric star-coil block copolymers. The intramolecular cross-linking reaction of the BCB unit was carried out to form hybrid nanoparticle-coil copolymer by the slow addition of the star copolymer structure to a benzyl ether solution at 250 °C. The formation of the nanoparticle-copolymer was confirmed by ¹H NMR spectroscopy. The disappearance of the BCB peaks in the ¹H NMR spectrum and the decreased molecular weight and hydrodynamic volume in the SEC traces indicate the formation of the hybrid nanostructure.

Frank and co-workers¹²⁹ reported the formation of linear-nanoparticle block copolymers resulting from selective intramolecular cross-linking of the BCB units and the effect of architecture on the surface aggregation. In this work, the linear block copolymer precursors were prepared by NMP starting from an alkoxyamine-substituted polyethylene glycol (PEG) macroinitiator. The tadpole shaped single chain linear-nanoparticle was prepared without any intermolecular cross-linking reaction by continuous addition of the precursor polymer solution to hot benzyl ether at 250 °C, thus achieving a low concentration of the linear precursor in the solution. The formation of a linear nanoparticle structure was confirmed by ¹H NMR and SEC upon the thermal cross-linking of the BCB units. The hydrodynamic volume of the nanoparticle block is decreased by up to 80% due to the intramolecular cross-linking of the linear chain. The AFM studies of the Langmuir-Blodgett (LB) transferred films indicated that disk-like aggregates are detected for the linear block copolymers, while worm-like aggregates are observed for the linear-nanoparticle block copolymers.

Thayumanavan and co-worker¹³⁰ described the preparation of polystyrene-based functional nanoparticles with amino moieties. In their study, the protected amino group monomer (4-*N*-Boc-aminostyrene) and chloromethylstyrene were copolymerized via RAFT using AIBN as the initiator. Two compositions of the molecular weight of poly(4-*N*-Boc-aminostyrene)-*co*-(chloromethylstyrene) were prepared using various feed ratios of the monomers. The copolymers were reacted with 4-[(3-hydroxyphenoxy)methyl]styrene to afford the corresponding vinyl-functionalized cross-linkable polymers ($M_n = 21\ 000$ Da, $PDI = 1.66$) and ($M_n = 19\ 000$ Da, $PDI = 1.50$). Subsequently, an intramolecular cross-linking reaction of these polymers was performed under high dilution conditions via radical polymerization conditions using AIBN as the initiator in refluxing THF to yield polymeric nanoparticles. The characterization of the nanoparticles was achieved by SEC, DLS and ¹H NMR. The (apparent) number-average molecular weight of the polymeric nanoparticles was shifted to lower molecular weight. The decrease in hydrodynamic volume is assigned to a change in the architecture of the macromolecules from a random coil to a nanoparticle (from $M_n = 21000$ Da to $M_n = 12000$). Similarly, DLS measurements also evidenced a decrease in the hydrodynamic radius (R_h) of the polymers due to the intramolecular cross-linking in the architecture of the polymer (from $R_h = 26.1$ nm to $R_h = 16.9$ nm). The ¹H NMR spectrum demonstrated that the peaks of the double bond of the pendant styrene at 5.25 and 5.72 ppm almost disappeared upon cross-linking to form polymeric nanoparticles. The above mentioned characterizations using NMR, SEC and DLS clearly evidence that intramolecularly cross-linked polymer nanoparticles were achieved. The nanoparticles were subsequently reacted with acetyl chloride in methanol to remove the *tert*-butyl carbonate moiety yielding the

functional nanoparticles containing amino functionalities that can be used for further transformations.

In an interesting study, Harth and co-workers¹³¹ emphasized an easy and elegant way inspired by BCB chemistry employing a novel vinylbenzosulfone (VBS) cross-linking unit for the preparation of the well-defined nanoparticles. In their communication, the authors synthesized cross-linking units at entailing a five-step pathway which requires only two purification steps. The monomers containing cross-linkable units can be polymerized with NMP procedures. Random copolymers with various feeding ratio of styrene and the VBS were prepared with high control over molecular weight and low polydispersity in the presence of α -hydrido alkoxyamine as an initiator ($M_n = 25\ 500$ Da, $PDI = 1.20$). The intramolecular chain collapse process was carried out in dibenzyl ether to form *o*-quinodimethane intermediates leading to well-defined monodisperse nanoparticles in the 5-10 nm size dimensions at temperatures close to 250 °C. SEC results revealed that the formation of polymeric nanoparticles from random linear polymers can be observed by following a decrease in the apparent number-average molecular weight from 30 600 Da to 19 000 Da. Furthermore, ¹H NMR studies indicated that the aliphatic protons of the incorporated benzosulfone ring observed at 4.0-4.3 ppm vanish after collapse, while a broad resonance structure at 2.6-3.1 ppm appears, which is associated with cross-linked unit. In order to achieve a hydrophilic nanoparticle with carboxylic acid groups, benzyl acrylate monomers with benzosulfone cross-linking units were polymerized followed by removing the benzyl protecting groups yielding hydrophilic nanoparticles soluble under physiological conditions. The resulting purified nanoparticles were analyzed with SEC and ¹H NMR as described above.

The preparation of vinyl-containing polycarbonate and the formation of nanoparticles by intramolecular cross-linking using Grubbs' catalyst followed by SEC, DSC and AFM was carried out by Coates and co-workers.^[132] Herein, polycarbonates containing vinyl functionality were prepared through the terpolymerization of vinylcyclohexene oxide (VCHO), cyclohexene oxide (CHO) and CO₂ with a β -diiminate zinc(II) acetate catalyst ([BDI]ZnOAc)₂. The polymer featured a high molecular weight ($M_n = 54100$ Da) and low polydispersity molecular weight distribution ($PDI = 1.20$). Well-defined linear polymer with pendant vinyl groups was effectively cross-metathesized using Grubbs' catalyst chain in diluted polymer solutions. As a result of the formation of the polymeric nanoparticles, the apparent molecular weight of the polymer decreased from 54100 Da to 31500 Da, indicating a decrease of the hydrodynamic volume. In addition, a glass transition temperature (T_g) increase from an initial value of 114 to 194 °C was observed due to decreasing chain mobility when the linear polymer chains collapse into nanoparticles. The formation of macromolecular nanoparticles was also confirmed by AFM, providing further support – along with the SEC – for intramolecular cross-linking under dilute conditions.

In the field of *click* chemistry,¹³³⁻¹³⁴ Loinaz and co-workers¹³⁵ employed copper-catalyzed azide alkyne cycloaddition for the preparation of polymeric nanoparticles for bioconjugation based on single-chain intramolecular cross-linking reaction at ambient temperature (see Figure 2.6). The linear terpolymer based on poly(methyl methacrylate) chains containing azide and protected alkyne functionalities were prepared via RAFT polymerization in the presence of an excess of azide moieties at various concentrations. Subsequently, the alkyne group in the well-defined linear terpolymer was deprotected, followed by a single-chain

intramolecular copper catalyzed azide alkyne cycloaddition at ambient temperature using a continuous addition technique of Cu^{I} salt leading to azide functional polymeric nanoparticles. SEC revealed that a significant reduction of the hydrodynamic volume and the apparent molecular weight result in the formation of the individual nanoparticles. The formation of well-defined spherical nanoparticles was additionally confirmed by TEM. Modular conjugation was performed on the free azide groups of the nanoparticles by reacting them with propargyl glycine biomolecules. The amino acid-substituted polymeric nanoparticles were characterized by FT-IR and ^1H NMR spectroscopy.

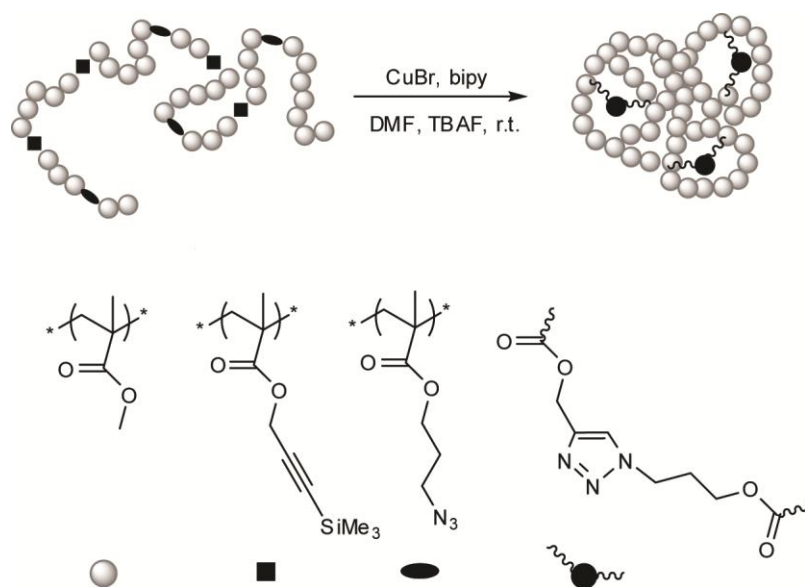


Figure 2.6 Schematic illustration of the preparation of single-chain cross-linked polymeric nanoparticles by the intramolecular modular conjugation of poly[(methyl methacrylate)-*co*-(3-azidopropyl methacrylate)-*co*-(3-trimethylsilyl-propyn-1-yl methacrylate)] from the work of Loinaz and colleagues.¹³⁵ Reproduced with kind permission from Wiley-VCH.

Hawker and co-workers¹³⁶ introduced a new synthetic approach for the preparation of intramolecularly collapsed nanoparticles under mild and ambient temperature conditions based

on commercially available vinyl monomers bearing isocyanate functionalities coupled to a secondary component in the form of a diamine to affect cross-linking. In their study, the RAFT mediated free-radical polymerization of methacrylate comonomers was performed employing a chain transfer agent to afford well-defined linear polymers featuring lateral isocyanate moieties. A solution of the copolymer was added to the diamine containing solution in high dilution; the reactive units were subsequently able to undergo cross-linking reactions leading to the formation of polymeric nanoparticles at ambient temperature. The resulting single chain nanoparticles were successfully characterized via SEC, DLS, viscosity measurements, ^1H NMR and Fourier transform infrared (FT-IR) comparing them with the linear copolymers precursors.

The synthesis of polymeric nanoparticles from single ABA type block copolymers in an intramolecular cross-linking process by means of the benzosulfone ring was reported by Harth and co-workers.¹³⁷ In this strategy, α,ω -alkoxyamine functionalized linear polymers were prepared via Yamamoto polymerization using dibromo fluorene and dibromo thiophene derivatives. Styrene and vinylbenzosulfone were polymerized via NMP utilizing the macroinitiators to form ABA triblock copolymers that contain a semiconducting polymer block as a central segment in linear styrene copolymer blocks. The formation of the nanoparticles via an intramolecular chain collapse process is achieved in a similar fashion as reported in ref [131] (see Figure 2.7). Intramolecular chain collapse process was confirmed by ^1H NMR spectroscopy with the consumption of the characteristic protons of the benzosulfone ring at 4.0-4.3 ppm in the linear precursor and appearance of protons at 2.6-3.1 ppm belonging to BCB units in the polymeric nanoparticle. SEC traces also verified the folding of the linear triblock copolymers into polymeric nanostructure with a change in the hydrodynamic volume that reveals a decreased

(apparent) molecular weight of the nanoparticle. Furthermore, the quantum efficiency of formed polymeric nanoparticles (6%) was three times higher as compared to the linear precursor (2%). Moreover, AFM and DLS studies confirmed the formation of nanoparticles through the chain collapse process of individual ABA triblock copolymer chains.

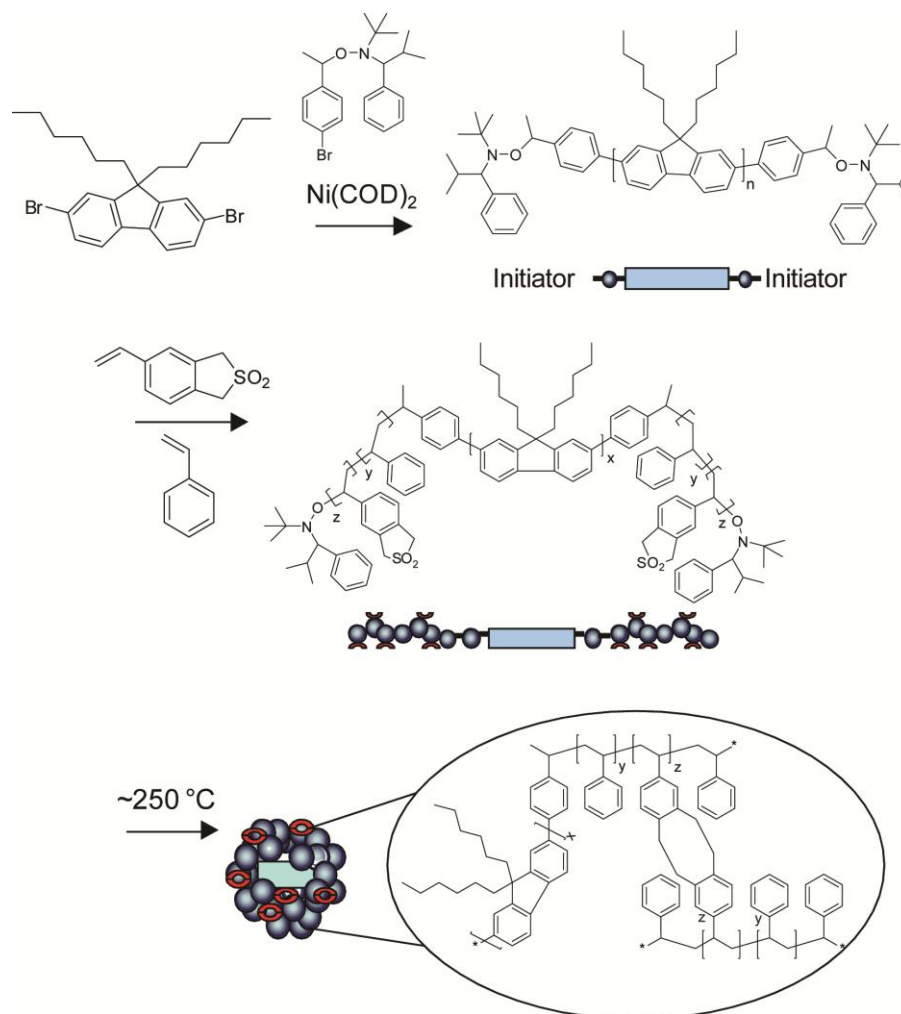


Figure 2.7 Preparation of single chain nanoparticles from ABA block copolymers that contain a semiconducting polymer block as a central segment within linear styrene block from the work of Harth and colleagues¹³⁷ Reproduced with kind permission from the American Chemical Society.

The modular conjugation chemistry was employed by Pomposo and co-workers¹³⁸ for the generation of polymeric nanoparticles based on precursors of functional polystyrene nanoparticles prepared by the use of both RAFT copolymerization and a subsequent very efficient functionalization step. Well-defined statistical copolymers with similar reactivity ratios of monomers were generated via RAFT copolymerization of 4-chloromethyl styrene (CMS) and a protected alkyne-containing methacrylate monomer (2-methyl-acrylic acid 3-trimethylsilyl-prop-2-ynyl ester, TSPMA). After appropriate functionalization of the linear copolymers via converting chlorine groups to azide moieties with NaN_3 and removal of the trimethylsilyl group, modular ligation chemistry was employed to generate functional nanoparticles with diameters of close to 4.2 nm as determined by DLS. The obtained functional nanoparticles were further characterized by AFM, ^1H NMR and FT-IR. The remaining chloro-functional groups permit a surface decoration of the polymeric nanoparticle using ATRP or other modification technique.

Fulton and co-worker¹³⁹ described the cross-linking of single polymer chains through dynamic covalent acylhydrazone bonds to obtain polymer nanoparticles. In their work, 4-vinylbenzaldehyde and styrene were polymerized under RAFT conditions in the presence of a chain transfer agent and a radical initiator to yield linear polymers with aldehyde functionalities along the backbone. The functional polymeric nanoparticles were prepared through single chain folding of the well-defined linear polymers by dropwise addition of a cross-linker (bis-hydrazide) in THF followed by addition of a catalytic amount of trifluoroacetic acid (TFA). The remaining aldehyde groups of the nanostructures can be utilized by reacting monoacyl hydrazides or alkoxyamines for further functionalization that provide potential applications for

the nanoparticle. The functional polymeric nanoparticles were characterized by SEC, ^1H NMR and DLS. The SEC trace of the linear polymers symmetrically shifted to low molecular weight regions indicating the folding of the single polymer chain by a reduction in its hydrodynamic volume. For instance, the (apparent) number average molecular weight of the polymer was reduced from $M_n = 8400$ Da to $M_n = 6950$ Da due to intramolecular cross-linking evidencing that intramolecular cross-linking reactions occurred in highly diluted condition. ^1H NMR spectroscopy and dynamic light scattering (DLS) analysis were employed to further characterize of the cross-linked nanoparticles.

In an interesting approach, Hu and co-workers^{140,141} applied thermal Bergman cyclization and photo-induced Bergman cyclization at ambient temperature mediating intramolecular chain collapse to generate polymeric nanoparticles. 2-hydroxyethylmethacrylate (HEMA) and MMA were polymerized via living/controlled radical polymerization to afford the corresponding copolymers followed by the modification of the pendant hydroxyl groups into enediyne moieties. Bergman cyclization was applied to the copolymers containing enediyne moieties for the intramolecular chain collapse under ultra-dilute conditions via a continuous addition technique. Polymeric nanoparticles with variable sizes were generated in a facile fashion. The SEC results indicate that the apparent molecular weight of the copolymer decreases depending on the enediyne content due to the intramolecular cross-linking reaction. Differential scanning calorimetry (DSC) and AFM techniques were employed for the further characterization of the single chain nanoparticles. The DSC measurements revealed that there is no glass transition temperature for the polymeric nanoparticle indicating that more compact nanostructures are

formed and that the enediyne groups are completely consumed during the Bergman cyclization process.

The preparation of polymer nanoparticles via intramolecular crosslinking of sulfonyl azide functionalized polymers was reported by Pu and co-workers.^[142] In this study, a RAFT-polymerization was carried out for the preparation of copolymers from cross-linkable sulfonyl azide functionalized styrene and MMA in the presence of a chain transfer agent and an initiator. Nitrenes are formed by sulfonyl azide losing nitrogen at high temperature that can subsequently react with a C-H bond.¹⁴² Single chain polymeric nanoparticles are prepared through the intramolecular collapse of the appropriate functionalized copolymer via a continuous addition strategy in ultra-dilute solution. SEC traces evidenced that the structural change from the random coil of the linear copolymer to the polymeric nanoparticle was obtained via intramolecular crosslinking of the single chain that results in a decrease of the apparent molecular weight of the copolymer. Data from DLS also confirm the results of the SEC experiments. The formation of polymeric nanoparticles was further verified by FT-IR measurements via the disappearance of the azide signal and the formation of the C-N bonds. The diameter of the nanoparticles was determined to being close to 14 nm by AFM and 15 nm by TEM.

The same team described the preparation of single-chain nanoparticles with a well-defined structure via intramolecular crosslinking of linear polymers with pendant benzoxazine groups.¹⁴³ Here, RAFT polymerization was performed for the preparation the copolymers of the P(S-*co*-CMS) with chloromethylstyrene (CMS) and styrene (S) in the presence of a chain transfer agent and thermal initiator. The chloromethyl groups of the copolymers were converted into azide functionalities. The alkyne functionalized benzoxazines were subsequently ligated

with the lateral azide functionalized copolymers to afford cross-linkable linear polymers. The linear polymers collapsed into polymeric nanoparticles via intramolecular reaction of the benzoxazine groups using the continuous addition technique at high temperature. The structural change from the random coils of the linear polymers to intramolecular collapsed nanoparticles was followed by ^1H NMR, FT-IR and SEC. The hydrodynamic radius (R_h) of the nanoparticles was determined by TEM, AFM, and DLS. Clearly, the TEM confirms the controlled crosslinking process of the linear precursors into nanostructures with a mean diameter of 8.7 nm.

An interesting photo-induced single chain collapse was applied by Zhao and colleagues¹⁴⁴ who reported the preparation of polymeric nanoparticles via the intramolecular photodimerization of coumarin. A random copolymer of *N,N*-dimethylaminoethyl methacrylate (DMAEMA) and 4-methyl-[7-(methacryloyl)oxy-ethyl-oxy]coumarin (CMA) was prepared via RAFT polymerization. Single chain polymeric nanoparticles were achieved via the intramolecular photodimerization of the coumarin moieties of the well-defined linear polymers by UV irradiation at $\lambda > 310$ nm at a very low concentration. The recorded SEC traces revealed that the photodimerization takes place intramolecularly under these conditions. The prepared polymeric nanoparticles were further characterized by means of the solution viscosity, DSC, TEM and ^1H NMR. Gold nanoparticles (AuNPs) were prepared utilizing the polymeric nanoparticles as a nanoreactor.

Not connected to the realm polymeric nanoparticle formation, Lutz and co-workers¹⁴⁵ introduced a versatile strategy for preparing foldable linear polymer chains. Therein, ATRP was utilized to generate macromolecules featuring functional groups at pre-selected positions of the single polymer chain that induce the folding process by forming covalent bonds. The well-

defined and functional polymers were folded into variable macromolecular geometries – via copper-catalyzed azide–alkyne cycloaddition (CuAAC) – such as tadpole (P-shaped), pseudocyclic (Q-shaped), bicyclic (8-shaped), and knotted (α -shaped) shapes, which were characterized by SEC and FT-IR measurements. For example, to prepare an 8-shaped species, the polymerization with styrene and triisopropylsilyl-protected *N*-propargyl maleimide was performed using a difunctional ATRP initiator followed by the transformation of the bromine groups into an azide functionality. After deprotection of the alkyne moieties, the CuAAC cyclization of the precursor material was carried out to form single chain folded structure at high dilutions. FT-IR and SEC data evidence that the two azide chain-ends of the polymer reacted intramolecularly with the alkyne group, thus generating the targeted 8-shaped folded structure.

The same team also very recently reported¹⁴⁶ a new strategy for preparing α -shaped polymers via single chain folding technology. Here, well-defined linear polystyrene precursors containing triisopropylsilyl-protected *N*-propargyl maleimide (TIPS-PMI) and pentafluorophenyl 4-maleimidobenzoate (PFP-MI) units at a pre-selected position were prepared by sequence-controlled NMP. An azide functionality was incorporated into the polymer chain via the reaction between the PFP activated ester and 11-azido-3,6,9-trioxaundecan-1-amine. After removal of the triisopropylsilyl-protected group, the alkyne and azide moieties within the polymer chains reacted intramolecularly in dilute DMF solutions and in the presence of a copper-based catalyst leading to folded α -shaped polymers. SEC traces of the single chain folded structures evidenced that the hydrodynamic volumes of the folded macromolecular origamis, measured by the elution time, are significantly smaller than those of the linear polymer precursors. All polymer samples were additionally characterized by SEC, ¹H NMR and FT-IR spectroscopy. Furthermore, ¹H

NMR spectra indicated in most cases the formation of a triazole group. Moreover, azide and alkyne signals at 2102 cm^{-1} and 3297 cm^{-1} disappeared from the FT-IR spectra after reaction, thus evidencing significant consumption of these reactive groups.

2.7 Self-Folding of Single Polymer Chains via Non-Covalent Interactions

The field of single chain self-folding based on non-covalent and covalent interactions has recently experienced substantial growth and is often intertwined with the question of sequence control in synthetic macromolecules.^{152,146}

In an early study in the field, Hawker, Kim and co-workers¹⁴⁷ reported that random poly(methyl methacrylate) (PMMA) copolymers carrying dendritic hydrogen-bonding units can be prepared via RAFT polymerization; their subsequent supramolecular single chain self-assembly was studied in various solvents. In the above study, the copolymerization of methyl methacrylate (MMA) and MMA containing a benzamide-dendron with hydrogen-bonding units was performed in *N,N*-dimethylformamide (DMF) employing a chain-transfer agent and a thermal initiator. The isolated copolymers formed polymeric nanoparticles when dissolving the polymer in a mixture of tetrahydrofuran (THF) and toluene followed by evaporation of the THF. Scanning force microscopy (SFM) clearly evidenced that the copolymer was well dispersed, forming spherical and uniform nanoparticles. The formation of nanoparticles was additionally followed by dynamic light scattering (DLS) measurements evidencing a mean diameter of 24 nm. The diameter of the particles is stable after two days indicating the intramolecular nature of the hydrogen bonds and suggesting that the intermolecular interactions have not taken place under the given conditions. Moreover, concentration studies to assess the viscosity properties of

the polymer solutions were performed in variable solvents including toluene. In contrast, viscosity properties similar to non-folded chains have been evidenced for the copolymer in THF due to the lack of supramolecular interactions in this solvent. However, the viscosity of the solutions was observed to increase sharply with changing concentrations in toluene, suggesting strong intermolecular hydrogen bonding interactions. These results imply that intramolecular hydrogen bonding was promoted in low concentration regimes in toluene allowing for the formation of well-defined and stable nanoparticles.

Similarly Meijer and co-workers¹⁴⁸ employed a facile way to well-defined metastable polymer particles via the supramolecular intramolecular crosslinking of single polymer chains. In this study, poly(norbornenes) containing protected 2-ureido-pyrimidinone (UPy) urea or UPy urethane pendants bearing alkyl substituents to overcome solubility problems were synthesized at concentrations of $\sim 5 \text{ mg}\cdot\text{mL}^{-1}$ of monomer in CH_2Cl_2 by ROMP using a second generation Grubbs' catalyst. The terminal carbonyl moiety of the UPy group is protected with *o*-nitrobenzyl chloride circumventing UPy dimerization in concentrated solutions; the chains collapse into nanoparticles in sufficiently dilute regimes. The deprotected polymers displayed a decrease in the number-average molecular weight (M_n) upon irradiation with 350 nm light as evident by the increased retention time in a size exclusion chromatography (SEC) experiment. Atomic force microscopy (AFM) results indicated the formation of single chain nanoparticles depending on polymer and sample preparation: drop casting with slow evaporation of the solvent allows concentration gradients on the surface leading to the formation of aggregates as the drop slowly concentrates. DLS measurements are in good agreement with the AFM results and support single-chain nanoparticles being 16 nm in diameter in extremely dilute regimes and 200 nm in

diameter for more concentrated solutions. As a result, well-defined metastable polymer particles via the supramolecular intramolecular crosslinking of single polymer chains were successfully prepared.

Meijer and co-workers¹⁴⁹ additionally described a novel method for fabricating nanoparticles from single polymer chains which have been expanded both in scope and utility. The well-defined linear polymers functionalized with an *o*-nitrobenzyl-protected 2-ureidopyrimidinone (UPy) pendant moiety were synthesized by a combination of living radical polymerization (LRP) and modular ligation chemistry. The alkyne functionalized linear PMMA chains were prepared via SET-LRP and subsequently the UPy-urethane moiety was ligated to the polymer to afford UPy functionalized precursor polymers; the remaining alkyne groups enable further functionalization of the nanoparticles. Subsequent UV irradiation induced the collapse of the single polymer chain into a nanoparticle via intramolecular cross-linking of the UPy urethane side groups in diluted solution (see Figure 2.8). The copolymers displayed a decreased hydrodynamic volume after deprotection in high diluted solution due to supramolecular cross-linking. The observed decrease in apparent molecular weight is a result of UPy dimerization after removal of the protecting group and the subsequent formation of single chain polymeric nanoparticles. AFM studies also indicated that after 90 min of irradiation the particle size decreases from ~100 nm to ~50 nm in diameter. The objects observed in the AFM images are single particles, indicating that the particles have a constant size in the diluted solution. SEC and AFM studies evidence that the intramolecular collapse is efficiently functioning.

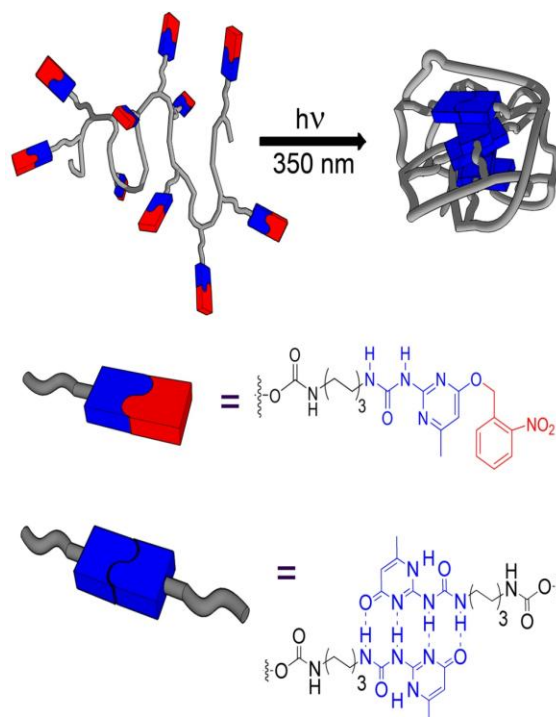


Figure 2.8 UV irradiation induced collapse of a single polymer chain into a nanoparticle via the supramolecular cross-linking of the UPy-urethane side groups as reported by Meijer and colleagues.¹⁴⁹ Reproduced with kind permission from the American Chemical Society.

Meijer and co-workers¹⁵⁰ also tuned the size of supramolecular single-chain polymer nanoparticles by synthesizing the polymers in various molecular weights, forming nanoparticles and subsequently by comparing their sizes via AFM. In this report,^[150] photodegradable UPy monomers were polymerized via ROMP using a second generation Grubbs' catalyst at ambient temperature in dichloromethane to afford a range of molecular weights of the linear polymers ($52\ 000\ \text{Da} \leq M_n \leq 1\ 200\ 000\ \text{Da}$). Polymeric nanoparticles were generated from functional linear polymers via the supramolecular cross-linking of the UPy urethane moieties in diluted solution as described previously.^[149] The data from the AFM measurements demonstrate the relationship between molecular weight and nanoparticle size. These results revealed that the size of single

chain polymeric nanoparticle can be adjusted by controlling the molecular weight of the parent polymer as followed by AFM. For instance, linear polymers with number-average molecular weight distributions of 52 000 Da and 550 000 Da self-fold in appropriate conditions, forming polymeric nanoparticles of 70 nm and 185 nm, respectively. It is clear that the diameter of polymeric nanoparticles depends on the molecular weight of the linear precursor. Furthermore, the UPy functional linear polymers were prepared without urea and urethane motifs. AFM studies indicated that these motifs are required to form well-defined nanostructures. As a result, the authors defined a relationship between the molecular weight of the non-folded polymer and the size of the nanoparticle using intramolecular supramolecular interactions.

Further, Palmans, Meijer and co-workers¹⁵¹ detailed the single chain folding of polymeric chains carrying catalytic units in water. The water-soluble random copolymer of chiral benzene-1,3,5-tricarboxamide methacrylate (BTAMA) and poly(ethylene glycol) methyl ether methacrylate (PEGMA) containing catalytic sites were synthesized by $\text{RuCl}_2(\text{PPh}_3)_3$ -catalyzed living radical polymerization. The well-defined random copolymers were characterized by SEC and ^1H NMR spectroscopy. Ruthenium (Ru) was efficiently incorporated into the copolymers via a ligand-exchange reaction during the polymerization as indicated by UV/Vis spectroscopy. All copolymers with various composition of benzene-1,3,5-tricarboxamide (BTA) units fold into well-defined functional nanostructures in water mimicking the folding basic folding elements of biomolecules. The intramolecular folded single-chain nanoparticles are characterized by DLS, diffusion ordered spectroscopy (DOSY) NMR, cryogenic transmission electron microscopy (cryo-TEM) and circular dichroism (CD) spectroscopy. The folded polymers carrying Ru were

fold from the work of Palmans and Meijer.¹⁵² Reproduced with kind permission from Wiley-VCH.

The above discussed studies represent apart from the studies in the present PhD thesis – to the best of our knowledge – the only examples of single chain folding driven by the formation of the non-covalent bonds. While the described studies are certainly remarkable, it is also clear that the field is only at an early stage. Avenues that need to be followed in the future – if true mimetic systems for e.g. proteins are to be achieved – include the placement more than two mutually orthogonal hydrogen bond donor/acceptor pairs and periodically repetitive (e.g. helical) elements into the polymer chains as well as the detailed study of the folding behavior of such systems and the associated folding dynamics as function of variable polymer types. It is believed that long term aim of constructing truly biomimetic functional macromolecules is – based on the progress made so far – most likely possible within the next 10 to 15 years.

2.8 References

- [1] J. Chiefari, Y. K. Chong, F. Ercole, J. Krstina, J. Jeffery, T. P. T. Le, R. T. A. Mayadunne, G. F. Meijs, C. L. Moad, G. Moad, E. Rizzardo, S. H. Thang, *Macromolecules* **1998**, *31*, 5559.
- [2] C. Barner-Kowollik, S. Perrier, *J. Polym. Sci. Part A: Polym. Chem.* **2008**, *46*, 5715.
- [3] M. K. Georges, R. P. N. Veregin, P. M. Kazmaier, G. K. Hamer, *Macromolecules* **1993**, *26*, 2987.
- [4] C. J. Hawker, A.W. Bosman, E. Harth, *Chem. Rev.* **2001**, *101*, 3661.
- [5] M. Kato, M. Kamigaito, M. Sawamoto, T. Higashimura, *Macromolecules* **1995**, *28*, 1721.
- [6] M. Ouchi, T. Terashima, M. Sawamoto, *Chem. Rev.* **2009**, *109*, 4963.
- [7] J. S. Wang, K. Matyjaszewski, *Macromolecules* **1995**, *28*, 7901.
- [8] F. Di Lena, K. Matyjaszewski, *Prog. Polym. Sci.* **2010**, *35*, 959.
- [9] V. Percec, B. Barboiu, *Macromolecules* **1995**, *28*, 7970.

- [10] B. M. Rosen, V. Percec, *Chem. Rev.* **2009**, *109*, 5069.
- [11] K. Matyjaszewski and J. Xia, *Chem. Rev.* **2001**, *101*, 2921.
- [12] L. Barner, T. P. Davis, M. H. Stenzel, C. Barner-Kowollik, *Macromol. Rapid Commun.* **2007**, *28*, 539.
- [13] Y. Yagci, M. A Tasdelen, *Prog. Polym. Sci.* **2006**, *31*, 1133.
- [14] J. S. Wang, K. Matyjaszewski, *Macromolecules* **1995**, *28*, 7901.
- [15] M. Kato, M. Kamigaito, M. Sawamoto, T. Higashimura, *Macromolecules* **1995**, *28*, 1721.
- [16] V. Percec, B. Barboiu, *Macromolecules* **1995**, *28*, 7970.
- [17] T. E. Patten, K. Matyjaszewski, *Acc. Chem. Res.* **1999**, *32*, 895.
- [18] H. Fischer, *J. Polym. Sci. Part A: Polym. Chem.* **1999**, *37*, 1885.
- [19] A. Goto and T. Fukuda, *Macro. Rapid Comm.* **1999**, *20*, 633.
- [20] K. Matyjaszewski, *J. Macro. Sci. Pure and App. Chem.* **1997**, *A34*, 1785.
- [21] T. Pintauer, K. Matyjaszewski, *Chem. Soc. Rev.*, **2008**, *37*, 1087.
- [22] W. A. Braunecker, K. Matyjaszewski, *Prog. Polym. Sci.* **2007**, *32*, 93.
- [23] W. Jakubowski, K. Matyjaszewski, *Macromolecules* **2005**, *8*, 4139.
- [24] K. Min, H. Gao, K. Matyjaszewski, *J. Am. Chem. Soc.* **2005**, *127*, 3825.
- [25] H. Tang, M. Radosz, Y. Shen, *Macromol. Rapid. Commun.* **2006**, *27*, 1127.
- [26] W. Jakubowski, K. Matyjaszewski, *Macromolecules* **2005**, *38*, 4139.
- [27] K. Min, H. Gao, K. Matyjaszewski, *J. Am. Chem. Soc.* **2005**, *127*, 3825.
- [28] J. K. Oh, C. Tang, H. Gao, N. V. Tsarevsky, K. Matyjaszewski, *J. Am. Chem. Soc.* **2006**, *128*, 5578.
- [29] J. K. Oh, H. Dong, R. Zhang, K. Matyjaszewski, *J. Polym. Sci. Part A: Polym. Chem.* **2007**, *45*, 4764.
- [30] W. Jakubowski, K. Matyjaszewski, *Angew. Chem. Int. Ed.* **2006**, *45*, 4482.
- [31] W. Jakubowski, K. Min and K. Matyjaszewski, *Macromolecules* **2006**, *39*, 39.
- [32] K. Min, H. Gao, K. Matyjaszewski, *Macromolecules* **2007**, *40*, 1789.
- [33] K. Matyjaszewski, W. A. Braunecker, K. Min, W. Tang, J. Huang, N. V. Tsarevsky, *PNAS* **2006**, *103*, 15309.

- [34] V. Percec, A. V. Popov, E. Ramierez-Castillo, M. Monteiro, B. Barboiu, O. Weichold, A. D. Asandei, C. M. J. Mitchell, *J. Am. Chem. Soc.* **2002**, *124*, 4940.
- [35] G. Lligadas, B. M. Rosen, C. A. Bell, M. J. Monteiro, V. Percec, *Macromolecules* **2008**, *41*, 8365.
- [36] V. Percec, T. Guliashvili, J. S. Ladislaw, A. Wistrand, A. Stjerndahl, M. J. Sienkowska, M. J. Monteiro, S. Sahoo, *J. Am. Chem. Soc.* **2006**, *128*, 14156.
- [37] V. Percec, A. V. Popov, E. Ramirez-Castillo, O. Weichold, *J. Polym. Sci. Part A: Polym. Chem.* **2003**, *41*, 3283.
- [38] G. Lligadas, V. Percec, *J. Polym. Sci. Part A: Polym. Chem.* **2007**, *45*, 4685.
- [39] G. Lligadas, J. S. Ladislaw, T. Guliashvili, V. Percec, *J. Polym. Sci. Part A: Polym. Chem.* **2008**, *46*, 278.
- [40] B. M. Rosen, V. Percec, *J. Polym. Sci. Part A: Polym. Chem.* **2007**, *45*, 4950.
- [41] W. Zhang, W. Zhang, Z. Zhang, Z. Cheng, Y. Tu, Y. Qiu, X. Zhu, *J. Polym. Sci. Part A: Polym. Chem.* **2010**, *48*, 4268.
- [42] U. Tunca, T. Erdogan, G. Hizal, *J. Polym. Sci. Part A: Polym. Chem.* **2002**, *40*, 2025.
- [43] D. A. Shipp, J.-L. Wang, K. Matyjaszewski, *Macromolecules* **1998**, *31*, 8005.
- [44] U. Tunca, B. Karlıga, S. Ertekin, A. L. Ugur, O. Sirkecioglu, G. Hizal, *Polymer* **2000**, *42*, 8489.
- [45] D. Mecerreyes, G. Moineau, P. Dubois, R. Jerome, J. L. Hedrick, C. J. Hawker, E. E. Malmstrom, M. Trollsas, *Angew. Chem. Int. Ed.* **1998**, *37*, 1274.
- [46] O. Altintas, G. Hizal, U. Tunca, *J. Polym. Sci. Part A: Polym. Chem.* **2006**, *44*, 5699.
- [47] J. A. Opsteen, J. C. M. Van Hest, *Chem. Comm.* **2005**, 57.
- [48] J. A. Opsteen, J. C. M. Van Hest, *J. Polym. Sci. Part A Polym. Chem. Ed.* **2007**, *45*, 2913.
- [49] J.-F. Lutz, *Angew. Chem. Int. Ed.* **2007**, *46*, 1018.
- [50] B. S. Sumerlin, N. V. Tsarevsky, G. Louche, R. Y. Lee, K. Matyjaszewski, *Macromolecules* **2005**, *38*, 7540.

- [51] H. Gao, G. Louche, B. S. Sumerlin, N. Jahed, P. Golas, K. Matyjaszewski, *Macromolecules* **2005**, *38*, 8979.
- [52] J.-F. Lutz, H. G. Boerner, K. Weichenhan, *Macromol. Rapid Commun.* **2005**, *26*, 514.
- [53] P. L. Golas, N. V. Tsarevsky, B. S. Sumerlin, L. M. Walker, K. Matyjaszewski, *Aust. J. Chem.* **2007**, *60*, 1.
- [54] H. Gao, K. Matyjaszewski, *Macromolecules* **2006**, *39*, 4960.
- [55] H. Gao, K. Matyjaszewski, *J. Am. Chem. Soc.* **2007**, *129*, 6633.
- [56] H. Durmaz, F. Karatas, U. Tunca, G. Hizal, *J. Polym. Sci. Part A: Polym. Chem.* **2006**, *44*, 3947
- [57] H. Gao, K. Min and K. Matyjaszewski, *Macromol. Chem. Phys.* **2007**, *208*, 1370.
- [58] M. K. Georges, R. P. N. Veregin, P. M. Kazmaier, G. K. Hamer, *Macromolecules* **1993**, *26*, 2987.
- [59] S. O. Hammouch, J. M. Catala, *Macromol. Rapid. Commun.* **1996**, *17*, 149.
- [60] T. Fukuda, T. Terauchi, A. Goto, K. Ohno, Y. Tsujii, T. Miyamoto, S. Kobatake, B. Yamada, *Macromolecules* **1996**, *29*, 6393.
- [61] D. Benoit, V. Chaplinski, R. Braslau, C. J. Hawker, *J. Am. Chem. Soc.* **1999**, *121*, 3904.
- [62] D. Benoit, S. Grimaldi, S. Robin, J. P. Finet, P. Tordo, Y. Gnanou, *J. Am. Chem. Soc.* **2000**, *122*, 5929.
- [63] C. J. Hawker, A.W. Bosman, E. Harth, *Chem. Rev.* **2001**, *101*, 3661.
- [64] S. Grimaldi, J. P. Finet, F. Le Moigne, A. Zeghdaoui, P. Tordo, D. Benoit, M. Fontanille, Y. Gnanou *Macromolecules* **2000**, *33*, 1141.
- [65] S. Robin, O. Guerret, J. L. Couturier, Y. Gnanou, *Macromolecules* **2002**, *35*, 2481.
- [66] K. J. Ivin, T. Saegusa, *Ring-opening Polymerization*, **1984**, Elsevier, London.
- [67] J. E. McGrath, *Ring-opening Polymerization: Kinetics, Mechanism, and Synthesis* **1985**, American Chemical Society, Washington D. C.

- [68] J. Chiefari, Y. K. Chong, F. Ercole, J. Krstina, J. Jeffery, T. P. T. Le, R. T. A. Mayadunne, G. F. Meijs, C. L. Moad, G. Moad, E. Rizzardo, S. H. Thang, *Macromolecules* **1998**, *31*, 5559.
- [69] C. Barner-Kowollik, *Handbook of Raft Polymerization* **2008**, Wiley-VCH, Weinheim.
- [70] G. Moad, E. Rizzardo, S. H. Thang, *Acc. Chem. Res.* **2008**, *41*, 1133.
- [71] G. Moad, J. Chiefari, Y. K. Chong, J. Krstina, R. T. A. Mayadunne, A. Postma, E. Rizzardo, S. H. Thang, *Poly. Inter.*, **2000**, *49*, 993.
- [72] A. J. Convertine, N. Ayres, C. W. Scales, A. B. Lowe, C. L. McCormick, *Biomacromolecules* **2004**, *5*, 1177.
- [73] J. F. Quinn, E. Rizzardo, T. P. Davis, *Chem. Comm.* **2001**, 1044.
- [74] H. C. Kolb, M. G. Finn, K. B. Sharpless, *Angew. Chem. Int. Ed.* **2001**, *40*, 2004.
- [75] B. S. Sumerlin and A. P. Vogt, *Macromolecules* **2010**, *43*, 1.
- [76] R. K. Iha, K. L. Wooley, A. M. Nystrom, D. J. Burke, M. J. Kade, C. J. Hawker, *Chem. Rev.* **2009**, *109*, 5620.
- [77] K. Khanna, S. Varshney, A. Kakkar, *Polym. Chem.* **2010**, *1*, 1171.
- [78] U. Mansfeld, C. Pietsch, R. Hoogenboom, C. R. Becer, U. S. Schubert, *Polym. Chem.* **2010**, *1*, 1560.
- [79] O. Altintas, U. Tunca *Chem. Asian J.* **2011**, *6*, 2584.
- [80] P. L. Golas, K. Matyjaszewski, *Chem. Soc. Rev.* **2010**, *39*, 1338.
- [81] P. Lecomte, R. Riva, C. Jerome, R. Jerome, *Macromol. Rapid Commun.* **2008**, *29*, 982.
- [82] C. R. Becer, R. Hoogenboom, U. S. Schubert, *Angew. Chem. Int. Ed.* **2009**, *48*, 4900.
- [83] O. Altintas, A. P. Vogt, C. Barner-Kowollik, U. Tunca, *Poly. Chem.* **2012**, *3*, 34.
- [84] C. Barner-Kowollik, A. J. Inglis, *Macromol. Chem. Phys.* **2009**, *210*, 987.
- [85] C. Barner-Kowollik, F. E. Du Prez, P. Espeel, C. J. Hawker, T. Junkers, H. Schlaad, W. Van Camp, *Angew. Chem. Int. Ed.* **2011**, *50*, 60.
- [86] V. V. Rostovtsev, L. G. Green, V. V. Fokin, K. B. Sharpless, *Angew. Chem. Int. Ed.* **2002**, *41*, 2596.

- [87] C. W. Tornøe, C. Christensen, M. Meldal, *J. Org. Chem.* **2002**, *67*, 3057.
- [88] J. A. Opsteen, J. C. M. van Hest, *Chem. Comm.* **2005**, 57.
- [89] H. Kwart, K. King, *Chem. Rev.* **1968**, *68*, 415.
- [90] G. Hizal, U. Tunca and A. Sanyal, *J. Polym. Sci. Part A: Polym. Chem.* **2011**, *49*, 4103.
- [91] A. J. Inglis, C. Barner-Kowollik, *Macromol. Rapid Commun.* **2010**, *31*, 1247.
- [92] A. J. Inglis, T. Paulohrl, C. Barner-Kowollik, *Macromolecules* **2010**, *43*, 33.
- [93] M. L. Szalai, D. V. McGrath, D. R. Wheeler, T. Zifer and J. R. McElhanon, *Macromolecules* **2007**, *40*, 818.
- [94] A. J. Inglis, L. Nebhani, O. Altintas, F. G. Schmidt, C. Barner-Kowollik, *Macromolecules* **2010**, *43*, 5515.
- [95] J. A. Syrett, G. Mantovani, W. R. S. Barton, D. Pricec and D. M. Haddleton, *Polym. Chem.* **2010**, *1*, 102
- [96] H. Durmaz, B. Colakoglu, U. Tunca and G. Hizal, *J. Polym. Sci., Part A: Polym. Chem.* **2006**, *44*, 1667.
- [97] A. J. Inglis, S. Sinnwell, M. H. Stenzel and C. Barner-Kowollik, *Angew. Chem. Int. Ed.* **2009**, *48*, 2411.
- [98] M. J. Kade, D. J. Burke and C. J. Hawker, *J. Polym. Sci. Part A: Polym. Chem.* **2010**, *48*, 743.
- [99] C. E. Hoyle, A. B. Lowe, C. N Bowman, *Chem. Soc. Rev.* **2010**, *39*, 1355.
- [100] A. B. Lowe, *Polym. Chem.* **2010**, *1*, 17.
- [101] X.-P. Qiu, F. M. Winnik, *Macromol. Rapid Commun.* **2006**, *27*, 1648.
- [102] A. H. Soeriyadi, G.-Z. Li, S. Slavin, M. W. Jones, C. M. Amos, C. R. Becer, M. R. Whittaker, D. M. Haddleton, C. Boyera and T. P. Davis, *Polym. Chem.* **2011**, *2*, 815.
- [103] S. P. S. Koo, M. M. Stamenovic, R. A. Prasath, A. J. Inglis, F. E. Du Prez, C. Barner-Kowollik, W. van Camp and T. Junkers, *J. Polym. Sci. Part A: Polym. Chem.* **2010**, *48*, 1699.
- [104] W. Lin, Q. Fu, Y. Zhang, J. Huang, *Macromolecules* **2008**, *41*, 4127.

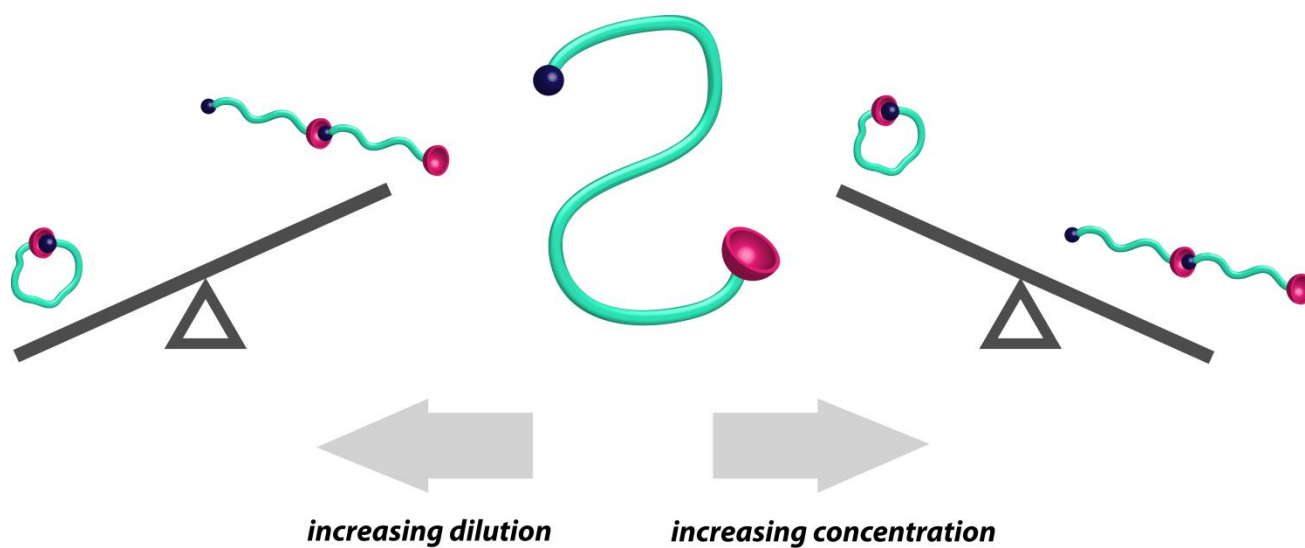
- [105] V. Percec, T. Guliashvili, J. S. Ladislaw, A. Wistrand, A. Stjern Dahl, M. J. Sienkowska, M. J. Monteiro, S. Sahoo, *J. Am. Chem. Soc.* **2006**, *128*, 14156.
- [106] H. Durmaz, G. Hizal, U. Tunca, *J. Polym. Sci. Part A: Polym. Chem.* **2011**, *49*, 1962.
- [107] N. Hadjichristidis, M. Pitsikalis, S. Pispas, H. Iatrou, *Chem. Rev.* **2001**, *101*, 3747
- [108] N. Hadjichristidis, H. Iatrou, M. Pitsikalis, J. Mays, *Prog. Poly. Sci.* **2006**, *31*, 1068.
- [109] A. Hirao, M. Hayashi, S. Loykulnant, K. Sugiyama, *Prog. Poly. Sci.* **2005**, *30*, 111.
- [110] N. Hadjichristidis, *J. Polym. Sci. Part A: Polym. Chem.* **1999**, *37*, 857.
- [111] H. Gao, K. Matyjaszewski, *Prog. Poly. Sci.* **2009**, *34*, 317.
- [112] S. Chen, A. Bertrand, X. Chang, P. Alcouffe, C. Ladaviere, J.-F. Geerard, F. Lortie, J. Bernard, *Macromolecules* **2010**, *43*, 5981.
- [113] J.M. Lehn, *Science* **1993**, *260*, 1762.
- [114] J. M. Lehn, *Supramolecular Chemistry* **1995**, Wiley-VCH, Weinheim.
- [115] W. H. Binder, R. Zirbs, *Adv. Polym. Sci.* **2007**, *207*, 1.
- [116] Felix H. Beijer, Huub Kooijman, Anthony L. Spek, Rint P. Sijbesma, E. W. Meijer, *Angew. Chem. Int. Ed.* **1998**, *37*, 75.
- [117] C. Fouquey, J. M. Lehn, A. M. Levelut, *Adv. Mater.* **1990**, *5*, 254.
- [118] M. Kotera, J.M. Lehn, J. P. Vigneron, *Tetrahedron* **1995**, *51*, 953
- [119] K. Hirschberg, J. Brunsveld, A. Ramiz, J.A.J. Vekemans, R.P. Sijbesma, E.W. Meijer, *Nature* **2000**, *407*, **167**.
- [120] R. F. M. Lange, E. W. Meijer, *Macromolecules* **1995**, *28*, 782.
- [121] S. K. Chang, A. D. Hamilton, *J. Am. Chem. Soc.* **1998**, *110*, 1318.
- [122] Pauling L, Corey RB, Branson HR (1951). *Proc Natl Acad Sci USA* **1951**, *37*, 205.
- [123] C. Branden, J. Tooze, *Introduction to Protein Structure* **1999**, New York and London, Garland Science
- [124] A. Bruce, A. Johnson, J. Lewis, M. Raff, K. Roberts, P. Walters, *The shape and structure of proteins* **2002**, New York and London, Garland Science.
- [125] C. Anfinsen, *Biochem. J.* **1972**, *128*, 737.

- [126] D. Mecerreyes, V. Lee, C. J. Hawker, J. L. Hedrick, A. Wursch, W. Volksen, T. Magbitang, E. Huang, R. D. Miller, *Adv. Mater.* **2001**, *13*, 204.
- [127] E. Harth, B. Van Horn, V. Y. Lee, D S. Germack, C. P. Gonzales, R. D. Miller, C. J. Hawker, *J. Am. Chem. Soc.* **2002**, *124*, 8653.
- [128] J. Pyun, C. Tang, T. Kowalewski, J. M. J. Fréchet, C. J. Hawker, *Macromolecules* **2005**, *38*, 2674.
- [129] Y. Kim, J. Pyun, J. M. J. Fréchet, C. J. Hawker, C. W. Frank, *Langmuir* **2005**, *21*, 10444.
- [130] J. Jiang, S. Thayumanavan, *Macromolecules* **2005**, *38*, 5886.
- [131] T. A. Croce, S. K. Hamilton, M. L. Chen, H. Muchalski, E. Harth, *Macromolecules* **2007**, *40*, 6028.
- [132] A. E. Cherian, F. C. Sun, S. S. Sheiko, G. W. Coates, *J. Am. Chem. Soc.* **2007**, *129*, 11350.
- [133] H. C. Kolb, M. G. Finn, K. B. Sharpless, *Angew. Chem. Int. Ed.* **2001**, *40*, 2004.
- [134] C. Barner-Kowollik, F. E. Du Prez, P. Espeel, C. J. Hawker, T. Junkers, H. Schlaad, W. van Camp, *Angew. Chem., Int. Ed.* **2011**, *50*, 60.
- [135] A. R. de Luzuriaga, N. Ormategui, H. J. Grande, I. Odriozola, J. A. Pomposo, I. Loinaz, *Macromol. Rapid Commun.* **2008**, *29*, 1156.
- [136] J. B. Beck, K. L. Killops, T. Kang, K. Sivanandan, A. Bayles, M. E. Mackay, K. L. Wooley, C. J. Hawker, *Macromolecules* **2009**, *42*, 5629.
- [137] C. T. Adkins, H. Muchalski, E. Harth, *Macromolecules* **2009**, *42*, 5786.
- [138] L. Oria, R. Aguado, J. A. Pomposo, J. Colmenero, *Adv. Mater.* **2010**, *22*, 3038.
- [139] B. S. Murray, D. A. Fulton, *Macromolecules* **2011**, *44*, 7242.
- [140] B. Zhu, J. Ma, Z. Li, J. Hou, X. Cheng, G. Qian, P. Liu, A. Hu, *J. Mater. Chem.* **2011**, *21*, 2679.
- [141] B. Zhu, G. Qian, Y. Xiao, S. Deng, M. Wang, A. Hu, *J. Polym. Sci. Part A: Polym. Chem.* **2011**, *49*, 5330.
- [142] X. Jiang, H. Pu, P. Wang, *Polymer* **2011**, *52*, 3597.
- [143] P. Wang, H. Pu, M. Jin, *J. Polym. Sci. Part A: Polym. Chem.* **2011**, *49*, 5133.

- [144] J. He, L. Tremblay, S. Lacelle, Y. Zhao, *Soft Matter* **2011**, 7, 2380.
- [145] B. V. K. J. Schmidt, N. Fechler, J. Falkenhagen, J.-F. Lutz, *Nat. Chem.* **2011**, 3, 234.
- [146] M. Zamfir, P. Theato, J.-F. Lutz, *Poly. Chem.*, **2012**, 3, DOI: 10.1039/c1py00514f.
- [147] M. Seo, B. J. Beck, J. M. J. Paulusse, C. J. Hawker, S. Y. Kim, *Macromolecules* **2008**, 41, 6413.
- [148] E. J. Foster, E. B. Berda, E. W. Meijer, *J. Am. Chem. Soc.* **2009**, 131, 6964.
- [149] Erik B. Berda, E. J. Foster, E. W. Meijer, *Macromolecules* **2010**, 43, 1430.
- [150] E. J. Foster, E. B. Berda, E. W. Meijer, *J. Polym. Sci. Part A: Polym. Chem.* **2011**, 49, 118.
- [151] T. Terashima, T. Mes, T. F. A. De Greef, M. A. J. Gillissen, P. Besenius, A. R. A. Palmans, E. W. Meijer, *J. Am. Chem. Soc.* **2011**, 133, 4742.
- [152] T. Mes, R. van der Weegen, A. R. A. Palmans, E. W. Meijer, *Angew. Chem. Int. Ed.* **2011**, 50, 5085.

Single-Chain Self-Folding of α,ω -Functional Linear Polymers

Chapter 3

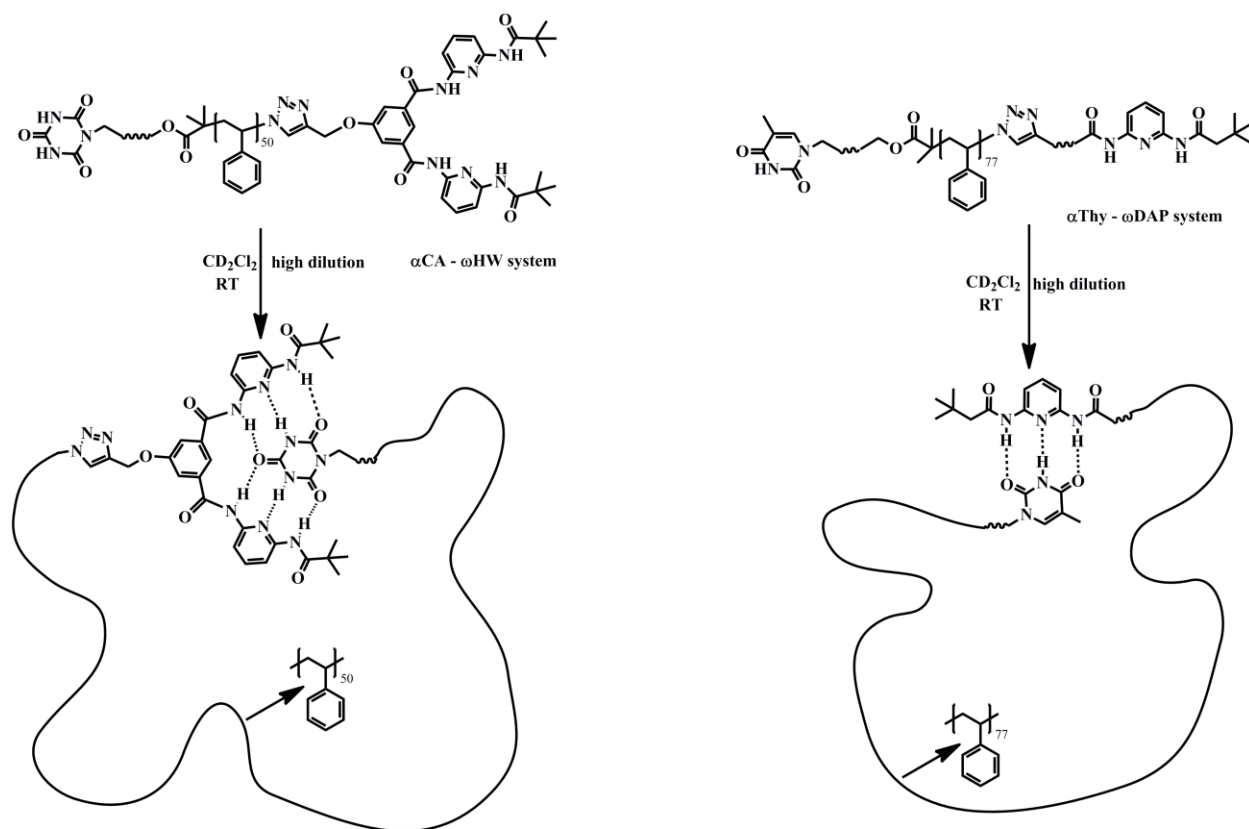


α,ω -Hydrogen donor/acceptor functional polymer strands are prepared via a combination of living radical polymerization and orthogonal conjugation and subsequently self-assembled as single chains to emulate – on a simple level – the self-folding behavior of natural biomacromolecules.

3.1 Introduction

Controlled-living radical polymerization techniques have been extensively employed for the synthesis of well-defined polymers.¹⁻³ Atom transfer radical polymerization (ATRP) is one of the most versatile and robust of the controlled-living radical polymerization techniques, allowing for fine control over the molecular architecture, molecular weight, and polydispersity of synthetic polymers.⁴⁻⁷ Combined with recent modular and orthogonal polymer ligation protocols, a powerful toolset exists with which well-defined polymer chains can be constructed.⁸⁻¹¹ Such advanced synthetic methodologies can be applied towards the construction of well-defined macromolecules that carry variable supramolecular recognition units at pre-selected positions along the polymer chain. The defining features of supramolecular chemistry are the characteristic reversible, non-covalent interactions, which play a key role in the behavior, such as self-assembly and conformational structure of these systems.¹² These reversible non-covalent interactions generally include H-bonding,^{13,14} metal ligand coordination,¹⁵⁻¹⁸ π - π stacking^{19,20} and ion-dipole interactions.^{21,22} Therefore, it follows that supramolecular polymers can be classified as polymeric systems that are generated from these reversible non-covalent interactions, which define the self-assembly, conformation and other properties of such polymers.²³⁻²⁵ Elaborate macromolecular designs can be achieved via the complexation of polymeric entities by hydrogen donor/acceptor pairs. An elegant example of the controlled folding of a single polymeric chain into a nanoparticle, through the interaction of donor/acceptor groups along the polymer backbone, has recently been reported.²⁶⁻²⁸ In addition, the self-assembly of block copolymers,^{29,30} poly(oxynorbornenes) and poly(thiophenes)^{31,32} has also been achieved by the modification of these polymers with donor/acceptor groups. Inspired by the synthetic systems that are now achievable through the combination of controlled living radical synthesis, orthogonal modular

conjugation and self-assembly driven by hydrogen bonding. Thus, it is the aim of the current chapter to explore the synthesis of α,ω -donor/acceptor functional single polymer chains and to study their single chain self-assembly as a first step towards mimicking the folding behavior of natural biomacromolecules. Self-assembly was achieved through the functionalization of α,ω -polymer chains with terminal α,ω -donor/acceptor groups, which were subsequently employed as reversible linkages of a single chain at its ends (see Scheme 3.1).³³



Scheme 3.1 Formation of single chain circular systems from cyanuric acid-poly(styrene)-Hamilton wedge (CA-PS-HW) (**8**) and thymine-poly(styrene)-diaminopyridine (Thy-PS-DAP) (**23**) at ambient temperature in CD_2Cl_2 .

The ultimate aim of the current efforts is to generate well-defined macromolecules that have variable orthogonal hydrogen donor/acceptor pairs at predetermined points within the backbone of the macromolecule, which would permit the defined folding/unfolding of the backbone into a specific geometry similar to a natural protein. Cyanuric acid / Hamilton wedge (CA/HW) and thymine / diaminopyridine (Thy / DAP) as complementary recognition motifs in conjugation with ATRP and copper catalyzed azide alkyne cycloaddition (CuAAC) as techniques for the preparation of well-defined telechelic polymers are chosen for the following considerations: (i) These recognition units are well-studied in supramolecular polymer science to generate advanced macromolecular architectures. Linear homopolymers, block copolymers and star polymers can be prepared using these motifs that are able to bring together precursor polymers. (ii) Before preparing more complex structures, it is advisable to understand the basic requirements for the self-folding of single-chain polymers by preparing α,ω -functional linear polymers that contain these motifs. (iii) Further, these recognition units are orthogonal to each other both on a small molecule level as well as when attached to a polymer backbone, suggesting that more complex dual or multi-orthogonal designs should be achievable. (iv) These motifs are stable under radical polymerization conditions and thus radical transformations. (v) ATRP is one of the premier radical polymerization techniques to synthesis α,ω -functional linear polymers with high end-group fidelity. (vi) CuAAC is a selective and very efficient type of reaction that can be performed under extremely mild conditions with high yields, good functional group tolerance and essentially no by-products. (vii) ATRP-made synthetic polymers can be easily and almost quantitatively functionalized using CuAAC.

Here, the synthesis of a novel well-defined α Thy or α CA functionalized poly(styrene) using an initiator with appropriate functional group in conjunction with ATRP is described. The

halogen end group of the polymers is subsequently transformed into an azide moiety, which can be ligated to an acetylene functionalized hydrogen acceptor DAP or HW to provide the ω -end (see Scheme 3.1). Investigations into the self-assembly of the resulting polymer systems α CA - ω HW and α Thy - ω DAP (under conditions of low polymer concentrations) is carried out via nuclear magnetic resonance (NMR) and dynamic light scattering (DLS) studies. In addition, the single chain self-folding of α,ω -functional poly(styrene) capped with CA and HW bonding motifs subjected to a solvent study. The reason for this study is due to the realization that analysis of the system with ^1H NMR is drastically improved when CD_2Cl_2 , rather than CDCl_3 , is employed as a solvent. Chronologically, this discovery was made after the initial study of the α CA - ω HW study was carried out in $\text{CHCl}_3/\text{CDCl}_3$ (please refer to chapter 5 for details). Consequently, the α CA and ω HW functional polymer was subjected to self-assembly in CD_2Cl_2 to reconfirm the previous results and to – additionally – investigate the effect of sterics on the self-assembly process, albeit with an improved NMR analytical procedure.

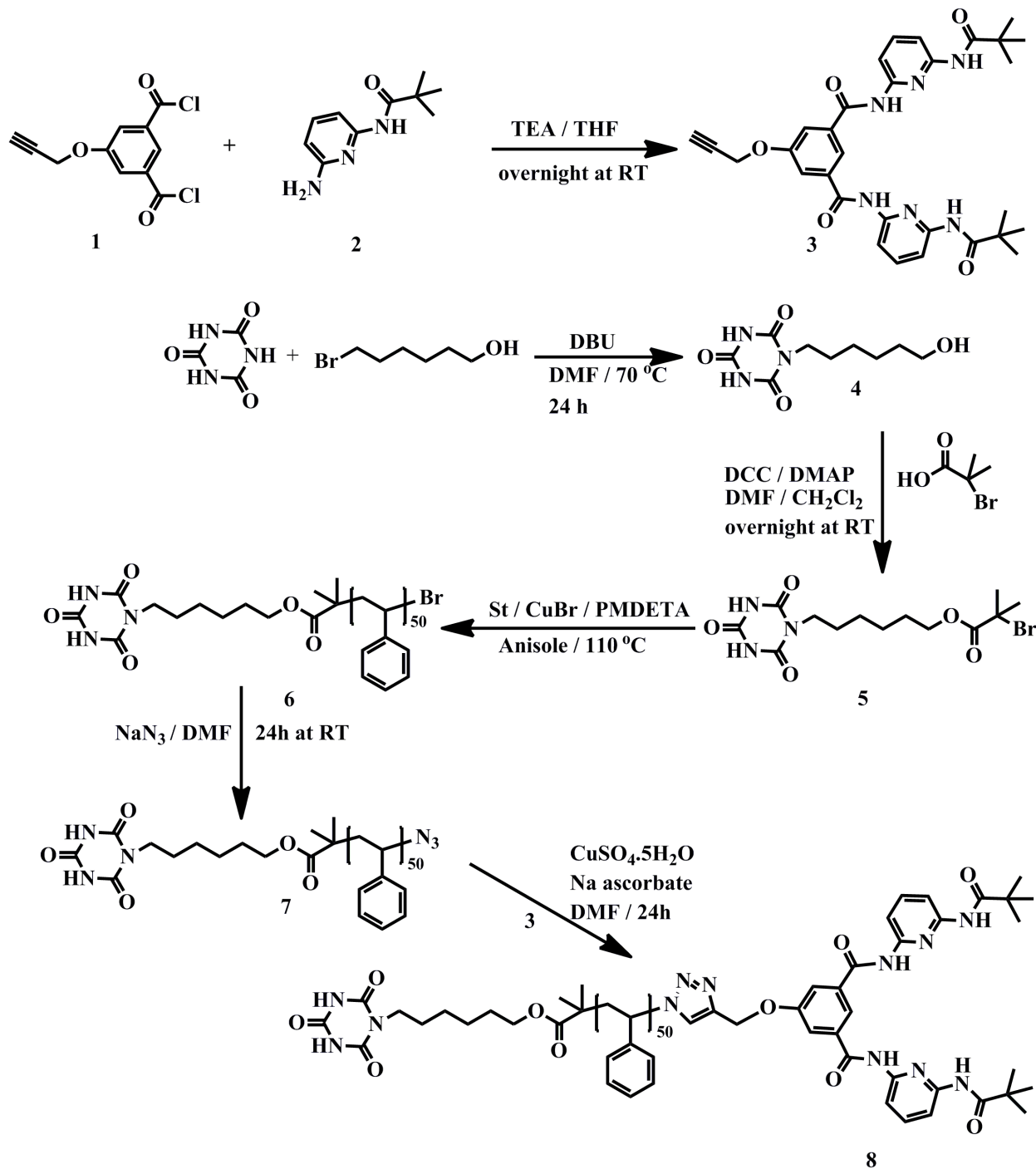
3.2 Preparation of α CA and ω HW Functionalized Polystyrene

3.2.1 Synthesis

5-(prop-2-ynyloxy)isophthaloyl dichloride (**1**)³⁴ and *N*-(6-aminopyridin-2-yl)-3,3-dimethylbutanamide (**2**)³⁵ were synthesized according to the literature.

3.2.1.1 Synthesis of *N*¹, *N*³-bis(6-pivalamidopyridin-2-yl)-5-(prop-2-ynyloxy)isophthalamide

(3): A solution of compound **1** (1 g, 3.89 mmol) in dry THF (20 mL) was added dropwise to a solution of compound **2** (1.8 g, 9.33 mmol) and triethylamine (1.62 mL, 11.67 mmol) in dry THF (20 mL) at ambient temperature. The solution was stirred at ambient temperature for 16 h, the residue filtered off and the solvent removed under reduced pressure. Purification by column



Scheme 3.2 General strategy for preparing α -cyanuric acid and ω -Hamilton wedge functional polymers.

chromatography on silica gel (CH_2Cl_2 /ethyl acetate (4:1) as eluent) gave a white solid. (1.62 g, 73%). ^1H NMR (400 Hz, DMSO-d_6) δ (ppm) 1.25 (s, 18H), 2.31 (s, 4H) 3.36 (s, 1H), 5.01 (s, 2H), 7.78-7.9 (m, 8H), 8.23 (s, 1H), 9.29 (s, 2H), 10.59 (s, 2H). ^{13}C NMR (100 Hz, DMSO-d_6) δ (ppm) 28.0, 39.4, 57.0, 76.4, 78.8, 105.2, 115.1, 117.4, 135.3, 141.0, 149.1, 156.3, 160.9, 164.8, 176.8 MS-ESI ($\text{M}+\text{Na}$) $^+$ calculated for $\text{C}_{31}\text{H}_{34}\text{N}_6\text{O}_5$: 621.25, found 621.37.

3.2.1.2 Synthesis of 1-(6-hydroxyhexyl)-1,3,5-triazinane-2,4,6-trione (4): 6-Bromohexan-1-ol (1.81 g, 10 mmol) and cyanuric acid (6.50 g, 50 mmol) were dissolved in dry DMF (50 mL). 1,8-Diazabicyclo[5.4.0]undec-7-ene (DBU, 1.5 mL, 10 mmol) was added dropwise to the solution. The mixture was heated to 70 °C and stirred for 24 h. The solvent was evaporated and the crude mixture was dissolved with methanol and filtered. The solvent was evaporated off and the residual purified via chromatography on silica gel, eluting with $\text{CH}_2\text{Cl}_2/\text{CH}_3\text{OH}$ (15:1) to obtain compound **4** as a white solid (1.35 g, 59%). ^1H NMR (400 Hz, DMSO-d_6) δ (ppm) 1.26 (m, 4H), 1.39 (m, 2H), 1.49 (m, 2H), 3.36-3.35 (t, 2H), 3.58-3.64 (t, 2H), 4.35 (bs, 1H), 11.37 (bs, 2H). ^{13}C NMR (100 Hz, DMSO-d_6) δ (ppm) 28.52, 30.40, 32.50, 33.45, 45.60, 62.64, 72.23, 153.85, 155.13, 175.99.

3.2.1.3 Synthesis of 6-(2,4,6-trioxo-1,3,5-triazinan-1-yl)hexyl 2-bromo-2-methylpropanoate (5): Precursor **4** (1 g, 4.36 mmol) was dissolved in 5 mL dry (DMF). 2-Bromo-2-methyl propionic acid (0.947 g, 5.67 mmol) and 4-dimethylaminopyridine (DMAP) (0.069 g, 0.56 mmol) were dissolved in 10 mL dry DCM and subsequently added to the mixture. DCC (1.75 g, 8.5 mmol) was dissolved in 5 mL dry DCM and then added to the solution at 0 °C. The reaction was carried out at ambient temperature overnight. Solids were filtered off, the filtrate was concentrated and the crude product was purified by column chromatography on silica gel, eluting

with $\text{CH}_2\text{Cl}_2/\text{MeOH}$ (25/1) to give the ATRP initiator as a white solid (0.615 g, 37%). ^1H NMR (400 Hz, DMSO-d_6) δ (ppm) 1.26 (m, 4H), 1.39 (m, 2H), 1.49 (m, 2H), 1.86 (s, 6H), 3.58-3.64 (t, 2H), 4.07-4.12 (t, 2H), 11.37 (brs, 2H). ^{13}C NMR (100 Hz, DMSO-d_6) δ (ppm) 28.52, 30.40, 32.50, 33.45, 45.60, 72.23, 153.85, 155.13 MS-ESI ($\text{M}+\text{Na}$) $^+$ calculated for $\text{C}_{13}\text{H}_{20}\text{BrN}_3\text{O}_5$: 400.05, found 400.08.

3.2.1.4 Synthesis of α -cyanuric acid functional polystyrene (6): Into a 50 mL of Schlenk tube, styrene (8.0 mL, 52.89 mmol), PMDETA (0.073 mL, 0.264 mmol), CuBr (0.050 g, 0.264 mmol), and **5** (0.13 g, 0.264 mmol) in 2 mL of anisole were added and the reaction mixture was degassed by three freeze-pump-thaw cycles and left under argon. The tube was subsequently placed in a thermostatted oil bath at 110 °C for min. The polymerization mixture was diluted with THF, passed through an alumina column to remove the catalyst, and precipitated in methanol. The polymer was dried for 24 h in a vacuum oven at 25 °C to give a white solid (0.6 g) Yield: 11%. ^1H NMR (400 Hz, CDCl_3) δ (ppm) 7.98 (s, 2H of cyanuric acid), 7.01-6.39 (5H, ArH of PS), 4.42-4.33 (1H, CHBr), 3.73 (2H, $\text{CH}_2\text{-N}$), 3.45(2H, $\text{CH}_2\text{-O}$), 1.78-1.18 (aliphatic protons of PS), 0.90-077 (6H, $\text{NCH}_2(\text{CH}_2)_3\text{CH}_2\text{O}$). $M_{n,\text{NMR}} = 5500$ Da, $M_{n,\text{SEC}} = 5000$ Da, $PDI = 1.04$.

3.2.1.5 Synthesis of α -cyanuric acid functional polystyrene with azide (7): **6** (0.5 g, 0.09 mmol) was dissolved in DMF (15 mL), and sodium azide (0.24 g, 3.6 mmol) was added. The reaction mixture was stirred for 24 h at room temperature. It was filtered and evaporated to remove DMF. Dichloromethane (100 mL) was added, and the reaction mixture was washed three times with distilled water. The organic layer was dried with anhydrous Na_2SO_4 , and the solvent was removed in rotary. The polymerization mixture was diluted with THF and precipitated in

methanol. The polymer was dried for 24 h in a vacuum oven at 25 °C. FTIR (cm^{-1}): 2095 (N_3 stretching). $M_{n,\text{NMR}} = 5400$ Da, $M_{n,\text{SEC}} = 5000$ Da, $PDI = 1.04$. After the reaction with sodium azide the CH-Br disappears completely, indicating ~100% transformation.

3.2.1.6 Synthesis of α,ω -donor-acceptor single chain polystyrene (8): Compound **7** (0.2 g, 0.036 mmol), compound **3** (43.65 mg, 0.073 mmol), copper (II) sulfate pentahydrate (17.63 mg, 0.11 mmol) and sodium ascorbate (21.89 mg, 0.11 mmol) were dissolved in DMF (5 mL). The resulting mixture was stirred at ambient temperature for 24 h before the copper catalyst was removed by passage through a short column of neutral alumina. The solvent was removed under reduced pressure and subsequently diluted with the addition of THF. The polymer was precipitated in 100 mL of methanol, filtered and dried under vacuum at 25 °C for 24 h to obtain a white solid (0.238 g) Yield: 98%. ^1H NMR (400 Hz, CDCl_3) δ (ppm) 7.96-7.76 (9H, ArH of host), 7.01-6.39 (5H, ArH of PS), 5.13-5.03 (2H, OCH_2 linked to triazole), 3.73 (2H, $\text{CH}_2\text{-N}$), 3.45(2H, $\text{CH}_2\text{-O}$), 1.78-1.18 (aliphatic protons of PS), 0.90-0.77 (6H, $\text{NCH}_2(\text{CH}_2)_3\text{CH}_2\text{O}$). $M_{n,\text{NMR}} = 6000$ Da, $M_{n,\text{SEC}} = 6100$ Da, $PDI = 1.04$.

3.2.1.7 Self-assembly studies between 3 and 6: Six different samples were prepared with dissolved polymer **6** (21.9 mg) in 1 mL CDCl_3 in an NMR tube. The concentration of **6** was kept constant at 4 mM. Compound **3** was added to the each solution in 1, 2, 3, 4, and 5 equiv., respectively. The mixtures were left to assemble overnight (12 h) at ambient temperature; subsequently ^1H NMR spectra were recorded (Figure 3.9).

3.2.1.8 Single chain self-assembly studies of polymer 8 with ^1H NMR: 6.0 mg, 12.0 mg, and 24.0 mg of the polymer **8** were dissolved in 1 mL CDCl_3 in an NMR tube and left to assemble overnight (12 h); ^1H NMR spectra were subsequently recorded (Figure 3.9).

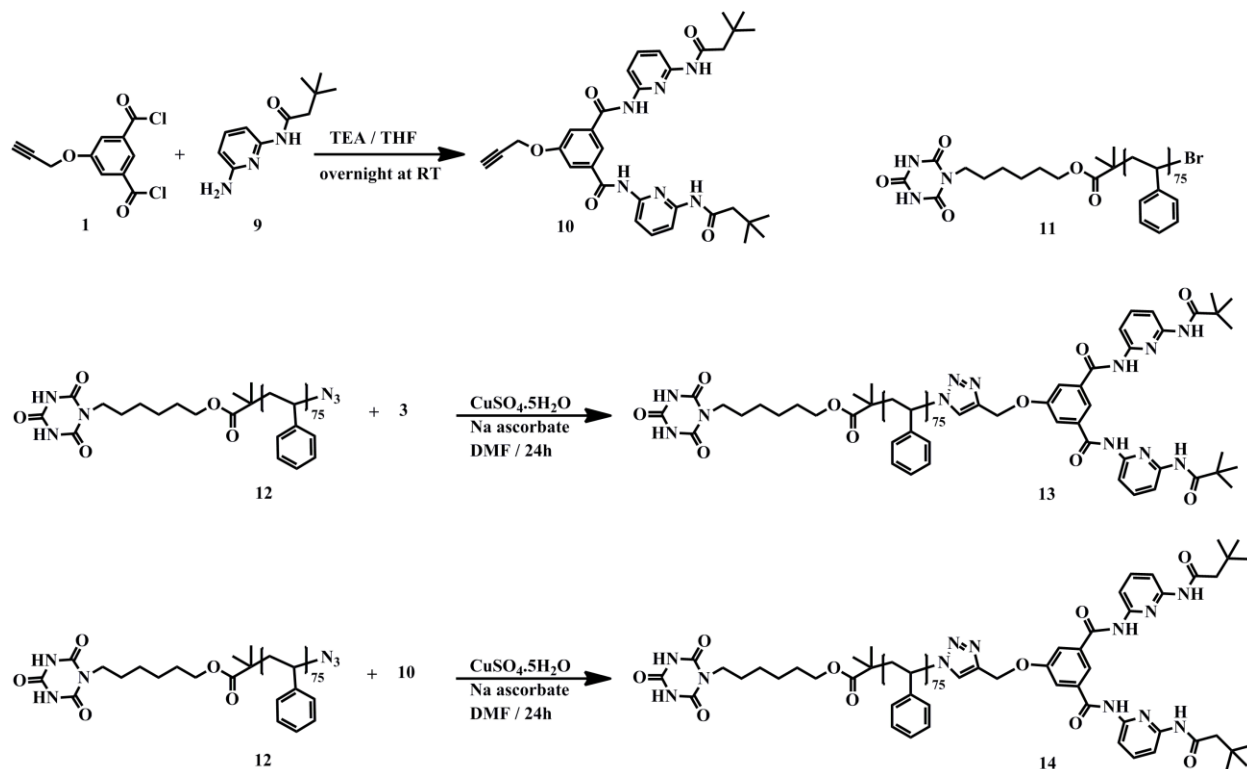
3.2.1.9 Single chain self-assembly studies of polymer 8 via DLS: Solutions of **8** were prepared by dissolving 3.0 mg, 4.5 mg, 6.0 mg, 9.0 mg, 12.0 mg, and 18.0 mg of the polymer **8** in 1 mL CHCl_3 to obtain six concentrations. A few solutions of polystyrene standards were also prepared in a similar fashion. Solvents and polymer solutions were filtered through 0.2 μm and 0.5 μm PTFE filters, respectively, and measured after 12 h assembly at ambient temperature in the scattering cell. One polystyrene (PS) standard (9100 Da) was measured in several concentrations showing no measurable difference in hydrodynamic diameter D_h . Such an observation confirms that one can neglect the influence of concentration and the scattering angle on the diffusion coefficient and consequently also on the hydrodynamic radii R_h for the molecule sizes and concentrations in our experiments. Thus, any change in D_h as a function of concentrations observed with polymer **8** is a result of the hydrogen-bonding associations. The constant values of D_h at lower concentrations of **8** clearly indicate that the smallest possible folding has occurred, i.e. the circular self-assembly of a single chain of **8**. The theoretical values provided in Table 3.2 are calculated as follows. Starting from the Einstein equation of viscosity, it follows that: $[\eta] \cdot M_n = ((10 \cdot \pi \cdot N_A) / 3) \cdot R_h^3$ or $R_h = ([\eta] \cdot M_n / (10 \cdot \pi \cdot N_A))^{1/3}$ with $D_h = 2 \cdot R_h$, where $[\eta]$ is the intrinsic viscosity, M_n the number average molecular weight and $N_A = \text{Avogadro's constant}$. For the calculation of $[\eta]$, Mark-Houwink parameters K_η and α_η from the Polymer Handbook were employed⁶ (two values for polystyrene in chloroform at 25 °C were employed [$K_\eta^1 = 7.2 \cdot 10^{-5} \text{ dL g}^{-1}$, $\alpha_\eta^1 = 0.76$ and $K_\eta^2 = 11.2 \cdot 10^{-5} \text{ dL g}^{-1}$, $\alpha_\eta^2 = 0.73$]); the resulting R_h values are averaged.

3.2.1.10 Preparation of compound and polymers that are described in Scheme 3.3

Compound **10** was prepared as described above for **3**. Polymer **11**, **12**, **13** or **14** were prepared as described above for **6**, **7** and **8**, respectively.

3.2.1.11 Self-assembly studies between polymer 12 and compound 3 or 10. A sample of polymer **12** (24.3 mg) was mixed with compound **3** or **10** dissolved in 1 mL CD_2Cl_2 or CDCl_3 in a NMR tube. The concentration of **12** was kept constant at 3 mM. Compound **3** or **10** was added in 1 equivalent relative to polymer **12**. The mixtures were left to interact overnight (12 h) at ambient temperature; ^1H NMR spectra were subsequently recorded (see Figure 3.11).

3.2.1.12 Single chain self-assembly studies of polymer 13 and 14. Polymer **13** (8.7 mg) in 1 mL CDCl_3 or CD_2Cl_2 and polymer **14** (8.7 mg) in 1 mL CD_2Cl_2 were dissolved and placed in an NMR tube, respectively and left to assemble overnight (12 h); ^1H NMR spectra were subsequently recorded (see Figure 3.12).



Scheme 3.3 Schematic presentation of the related structure that are utilized for the effect of the solvent and steric hindrance on the self-assembly.

3.2.2 Results and Discussion of Synthesis α CA and ω HW Functionalized Polystyrene

The target system was designed to feature a cyanuric acid functionality in the α -position and a Hamilton wedge functionality at the ω -position of polymer chain with the aim of generating well-defined heterotelechelic polymers via a combination of ATRP and copper catalyzed azide and alkyne cycloaddition (CuAAC). The synthetic pathway used to generate the target **CA-PS-HW (8)** heterotelechelic supramolecular polymer are outlined in Scheme 3.2.

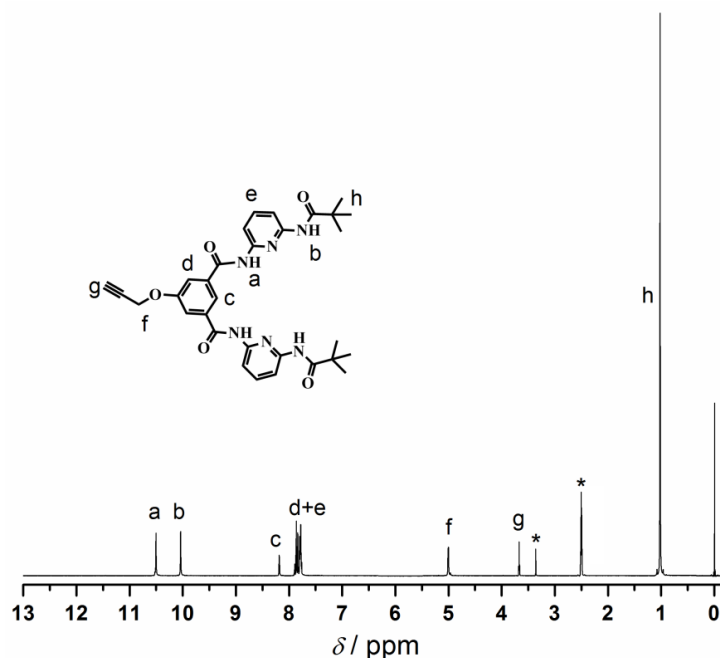


Figure 3.1 ^1H NMR of N^1,N^3 -bis(6-(3,3-dimethylbutanamido)pyridin-2-yl)-5-(prop-2-yn-1-yloxy)isophthalamide (**3**) in $\text{DMSO}-d_6$. The peaks marked with an asterisk are due to solvent/water.

To tether the Hamilton wedge (HW) motif to the end of polymer chain, an alkyne functional HW had to be synthesized first. To achieve these compounds, first, 5-(prop-2-ynyloxy)isophthaloyl dichloride (**1**) was reacted with N -(6-aminopyridin-2-yl)-3,3-dimethylbutanamide (**2**) in the presence of triethylamine as a catalyst and THF as solvent to obtain N^1,N^3 -bis(6-(3,3-dimethylbutanamido)pyridin-2-yl)-5-(prop-2-yn-1-yloxy)isophthalamide (**3**).

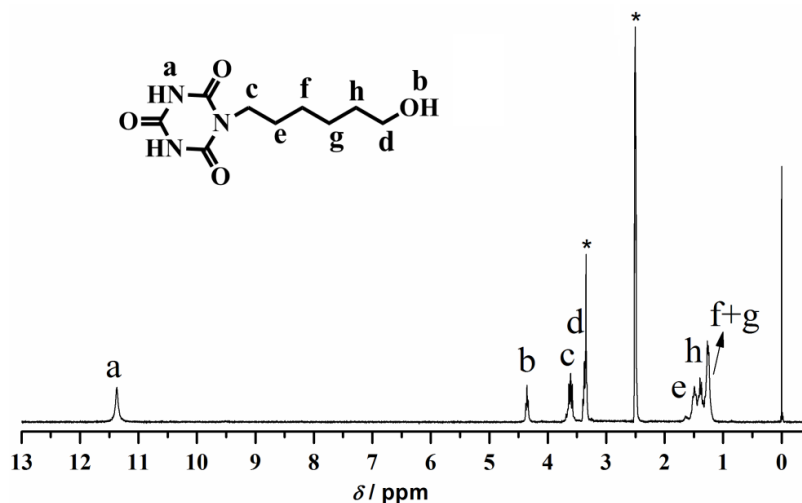


Figure 3.2 ^1H NMR of 1-(6-hydroxyhexyl)-1,3,5-triazinane-2,4,6-trione (**4**) in $\text{DMSO-}d_6$. The peaks marked with an asterisk are due to solvent/water.

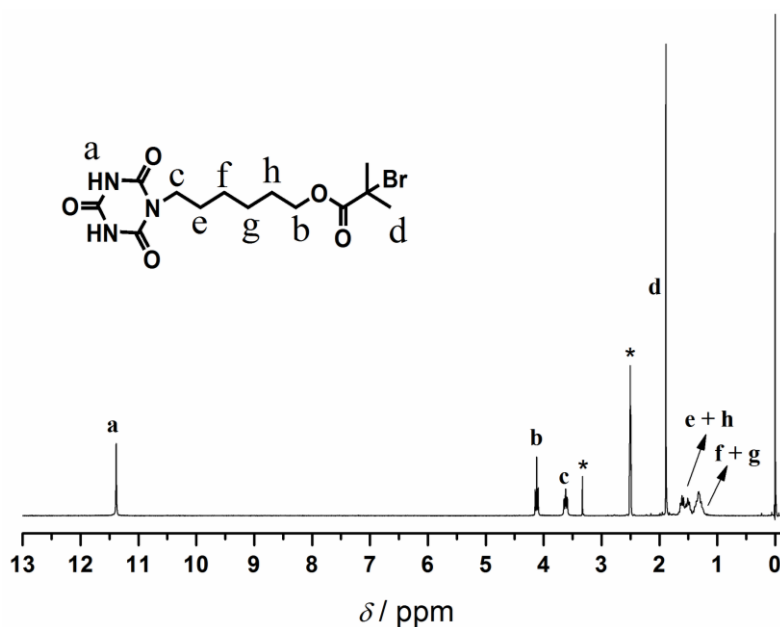


Figure 3.3 ^1H NMR of 6-(2,4,6-trioxo-1,3,5-triazinan-1-yl)hexyl 2-bromo-2-methylpropanoate (**5**) in $\text{DMSO-}d_6$. The peaks marked with an asterisk are due to solvent/water.

The ^1H NMR spectrum of **3** indicates the characteristic signals of *t*-butyl group at 1.01 ppm and also ether protons adjacent to alkyne group at 5.01 ppm. Moreover, the amide protons of **3** showed the related signals at 10.50 and 10.04 ppm (see Figure 3.1). A nucleophilic substitution reaction was carried between 6-bromohexanol and cyanuric acid catalyzed by DBU in DMF to afford hydroxyl functional cyanuric acid (**4**). The ^1H NMR spectrum of **4** indicates that the cyanuric acid protons and hydroxyl protons appeared at 11.37 ppm and 4.35 ppm, respectively (see Figure 3.2). Subsequently, an esterification reaction was carried out between **4** and 2-bromo-2-methylpropanoic acid in the presence of DCC/DMAP as catalysts to obtain the cyanuric acid functional ATRP initiator (**5**) which was characterized by ^1H NMR, ^{13}C NMR, and ESI-MS. The ^1H NMR spectrum of **5** indicates the characteristic signals of initiator at 1.91 ppm and also ester protons at 4.21 ppm (see Figure 3.3). The halogen terminus of the polymer is transformed into an azide moiety, which is subsequently ligated to an alkyne functional hydrogen acceptor (**3**) to provide the ω -end. Figure 3.4A depicts the size exclusion chromatogram of the bromide functional hydrogen donor chain **6**, of its azide variant **7** as well as of the α,ω -functional hydrogen donor/acceptor system **8**. The size exclusion chromatography (SEC) traces clearly indicate the low polydispersity of the polymer and that the transition from **7** to **8** leads to a shift in the molecular weight commensurate with the addition of **3**. The integral areas of the N-H bond of the cyanuric acid signal and that of the CH-Br of PS in the corresponding ^1H NMR spectrum have been compared and the bromo functionality of polymer **6** has been determined as being close to 100% relative to cyanuric acid termini (Figure 3.5). The successful transformation of **7** and **3** to **8** is further supported by inspection of the ATR-IR spectra of the polymers. Figure 3.4B depicts the ATR-IR spectra of **6** and **7**, where the absorption associated with the azide-terminal polymer **7** at 2095 cm^{-1} is clearly visible. After the conjugation reaction, the azide band has

disappeared (compound **8**). Table 3.1 summarises the molecular weights of the polymers depicted in Scheme 3.2 as determined via both SEC as well as ^1H NMR spectroscopy.

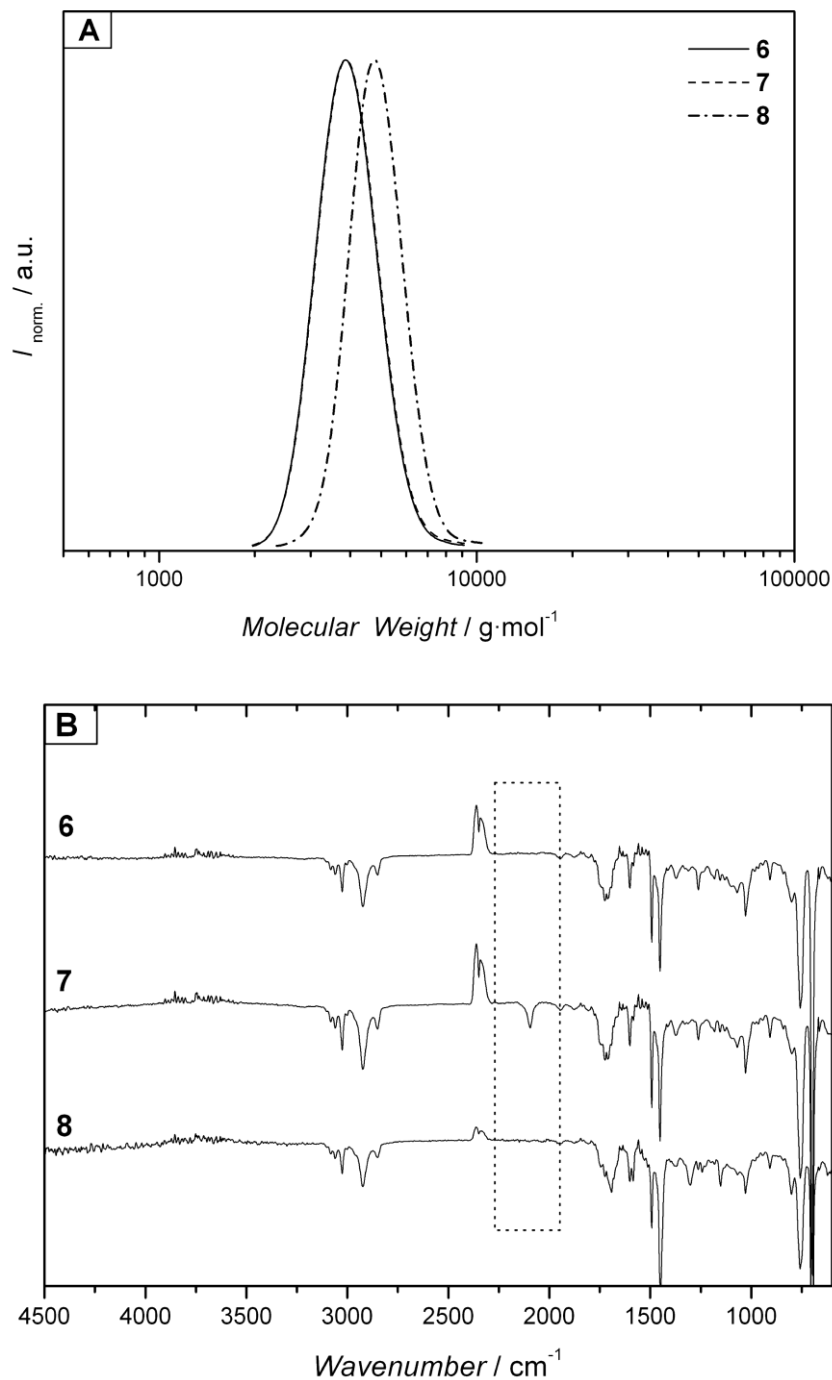


Figure 3.4 (a) Evolution of SEC chromatograms for **6**, **7**, and **8**. (b) ATR-IR spectra of **6**, **7**, and **8**.

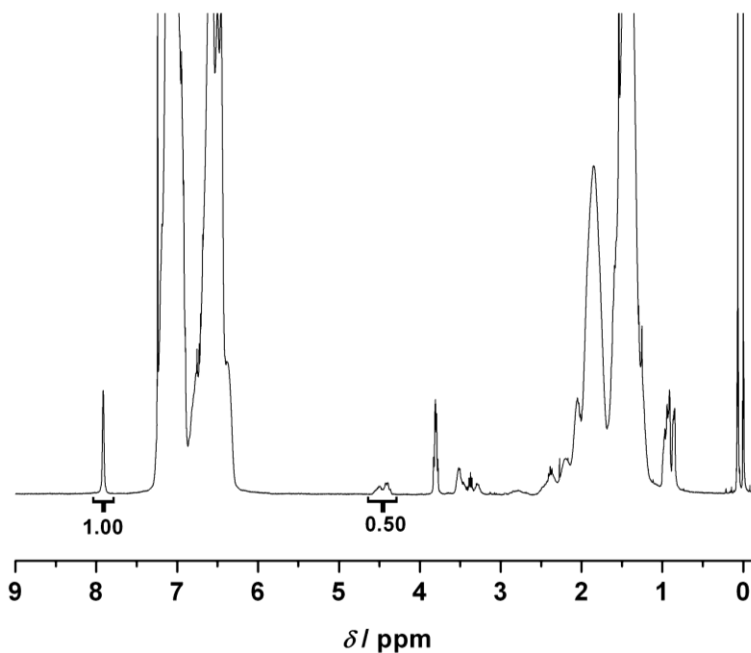


Figure 3.5 ^1H NMR spectrum of **6** in CDCl_3 at ambient temperature. From the ratio of the peak areas NH_2 of CA to CHBr (integral values shown), the end group functionalization can be deduced as being close to $\sim 100\%$.

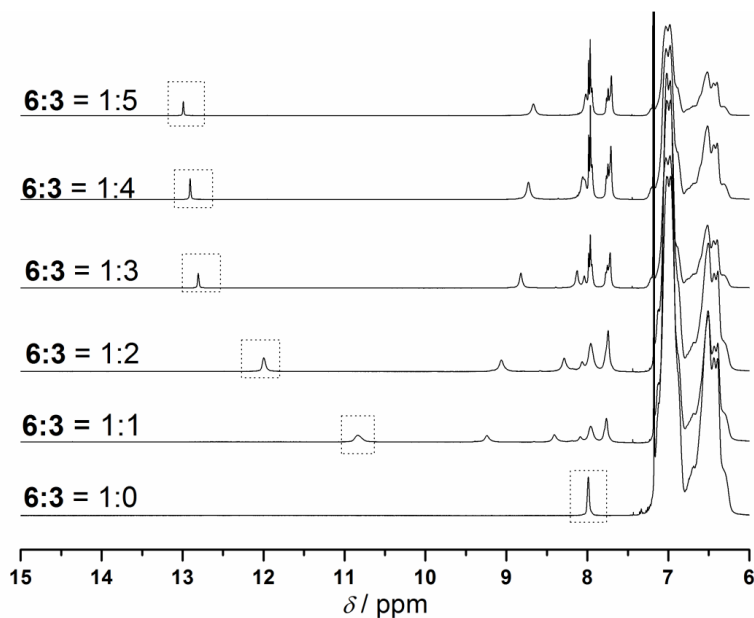


Figure 3.6 Expanded ^1H NMR spectra of the **6•3** self-assembly system in different concentration ratios in CDCl_3 at ambient temperature. The concentration of **6** was kept constant at 4 mM.

Table 3.1 Molecular weight of the precursor and the final polymers. The related structures can be found in Scheme 3.2 and Scheme 3.3.

Polymers	Monomer	$[\text{M}_0]/[\text{I}_0]$	Initiator	Time (min.)	M_n^b	M_w/M_n	M_n^c
6	Styrene	200	5	50	5000	1.04	5500
7	-	-	-	-	5000	1.04	5400
8	-	-	-	-	6100	1.04	6000
11	Styrene	200	5	70	7500	1.04	8100
12	-	-	-	-	7500	1.04	8100
13 or 14	-	-	-	-	8200	1.04	8700

^a $[\text{I}]_0/[\text{PMDETA}]_0/[\text{CuBr}]_0 = 1:1:1$; at 110 °C. ^bDetermined via RI detection SEC using linear PS standards. ^cDetermined from ^1H NMR spectroscopy.

Before undertaking the self-assembly reaction between the α,ω -donor/acceptor chain ends of **8**, it seemed mandatory to establish what a full associated system (in its non-circular form) would behave like in the NMR analysis. The interaction of **6** with compound **3** was investigated by ^1H NMR spectroscopic titration carried out in CDCl_3 . For the ^1H NMR studies, the concentration of **6** was kept constant at 4 mM and the change in the chemical shift was followed as a function of increasing concentrations of **3**. The NMR titration experiments revealed a significant downfield shift of the signal associated with the imide protons due to the complexation of **3**. As shown in Figure 3.6 and Figure 3.7, the peak at $\delta = 7.98$ ppm was assigned to the N-H protons of the cyanuric acid recognition unit at the α -end of the polymer **6**. When polymer **6** (4 mM) was mixed with 1 equiv. of compound **3** in CDCl_3 , the chemical shift of the proton resonance of the imide protons of polymer **6** changed from 7.98 to 10.83 ppm. When the polymer **6** (4 mM) was

mixed with 2, 3, 4, and 5 equiv. of the compound **3** in CDCl_3 , the chemical shift for the proton resonance of the imide protons of polymer **6** changed from 7.98. When polymer **6** was mixed with compound **3**, the N-H protons of the Hamilton wedge appeared at 9.24 and 8.40 ppm due to the self-assembly.

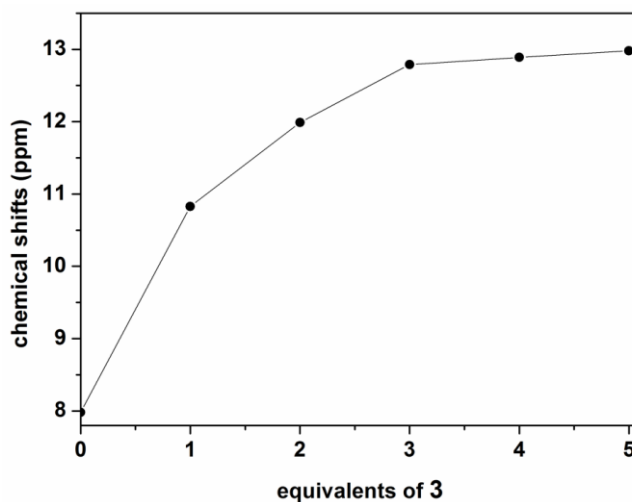


Figure 3.7 Chemical shifts of the imide protons of polymer **6** as a function of equivalents of **3**. The concentration of **6** was kept constant at 4 mM.

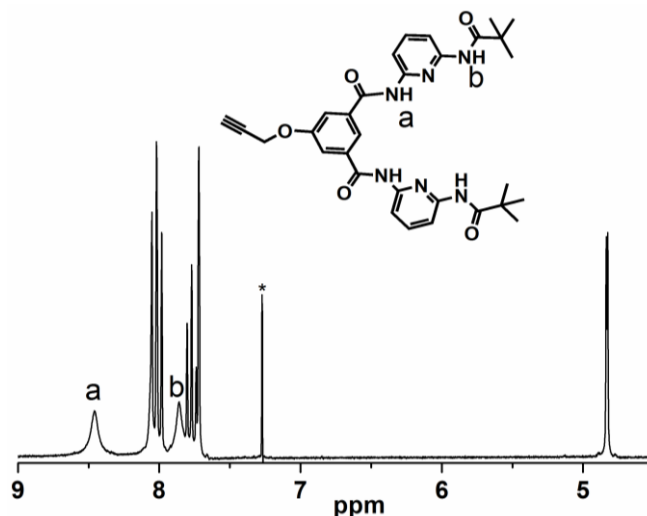


Figure 3.8 Expanded ^1H NMR spectrum of N^1,N^3 -bis(6-(3,3-dimethylbutanamido)pyridin-2-yl)-5-(prop-2-yn-1-yloxy)isophthalamide (**3**) in CDCl_3 . The peak marked with an asterisk is due to solvent. Only the amide protons are indicated.

With increasing concentration of the compound **3**, the N-H protons of the Hamilton wedge shifted slightly further up-field due to the formation of the strong assembly between **6** and **3**. These changes are characteristic for the formation of a multiple-hydrogen bonding complex.³⁶

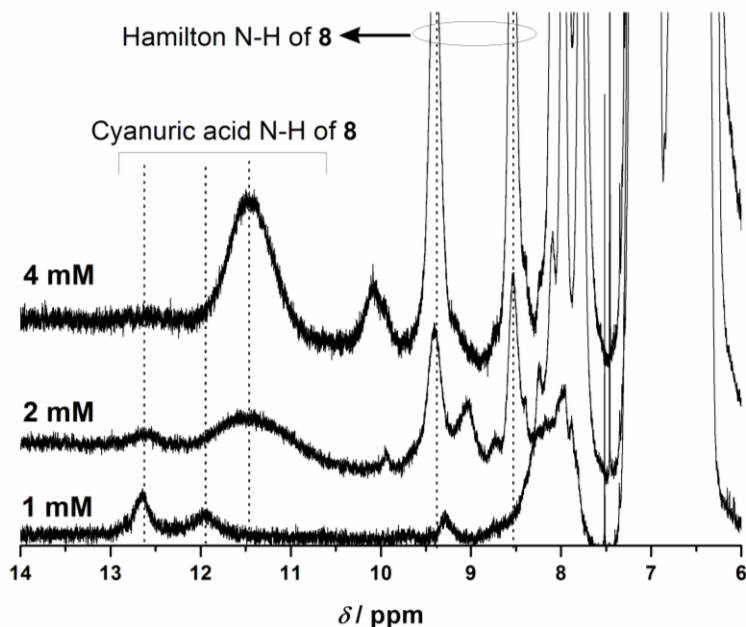


Figure 3.9 Expanded ¹H NMR of the polymer **8** in different concentrations in CDCl₃.

Evidence for the formation of the (single chain) hydrogen-bonded self-assembly of **8** in CDCl₃ came from ¹H NMR and dynamic light scattering (DLS) studies. For the ¹H NMR studies, a solution of the polymer **8** was prepared in CDCl₃ of 4 mM and left for 12 h at ambient temperature to allow self-assembly. The chemical shift for the proton resonance of the imide protons of the cyanuric acid unit of **8** changed from $\delta = 7.98$ to a strong resonance at $\delta = 11.49$ ppm and a weaker signal at $\delta = 12.63$ ppm, indicating the presence of species with different stabilities. A significant downfield shift of the imide protons of the cyanuric acid moieties is observed. When a 2 mM solution of **8** is prepared, the resonances at $\delta = 11.49$ ppm become weaker relative to the resonance at $\delta = 12.63$ ppm. When the polymer **8** was prepared as a 1 mM

solution, the signal at $\delta = 11.49$ ppm shifted to $\delta = 11.98$ and the peak at $\delta = 12.63$ ppm further increased. Thus, the ^1H NMR spectra show a downfield shift of the imide protons as the concentration of polymer **8** is decreased. This shift – in significant excess of the expected 10.83 ppm from the 1:1 association of **3** and **6** (see Figure 3.6) – indicates the formation of stabilized (circular) structures via an entropy driven preferential assembly. These results indicate that in more dilute solutions (<1 mM) stable self-assemblies are formed with significantly reduced exchange processes (Figure 3.9) congruent with ring formation.

While the NMR experiments indicate that stabilized structures due to (circular) entropy driven self-assembly occur, only a measurement of the hydrodynamic diameter, D_h , can provide evidence for the single chain circular self-assembly. Thus, D_h of self-assemblies of **8** and polystyrene (PS) standards were determined by DLS in CHCl_3 at 20 °C. The D_h of the polystyrene standards ($M_n = 9100$ Da and $M_n = 3400$ Da) were measured as 4.6 nm and 2.4 nm, respectively, which is in excellent agreement with the theoretical values (see Table 3.2). The polymer **8** ($M_{n,\text{NMR}} = 6000$ Da) was subjected to DLS in six concentrations. The D_h of the polymers in these solutions were measured to be 4.1 nm, 4.1 nm, 4.3 nm, 4.6 nm, 5.0 nm, and 5.0 nm, respectively. Concomitantly, a PS standard (9100 Da) was analysed via DLS at variable concentrations (Figure 3.10). The mean hydrodynamic diameter of polymer **8** increases with increasing concentrations in contrast to the PS standard ($D_h(c)=\text{const.}$), indicating the formation of inter-chain assemblies of **8**. As its concentration is reduced, the diameter of **8** is observed to progressively lower, thus supporting the formation of the more compact single-chain self-assembled cyclic structures.

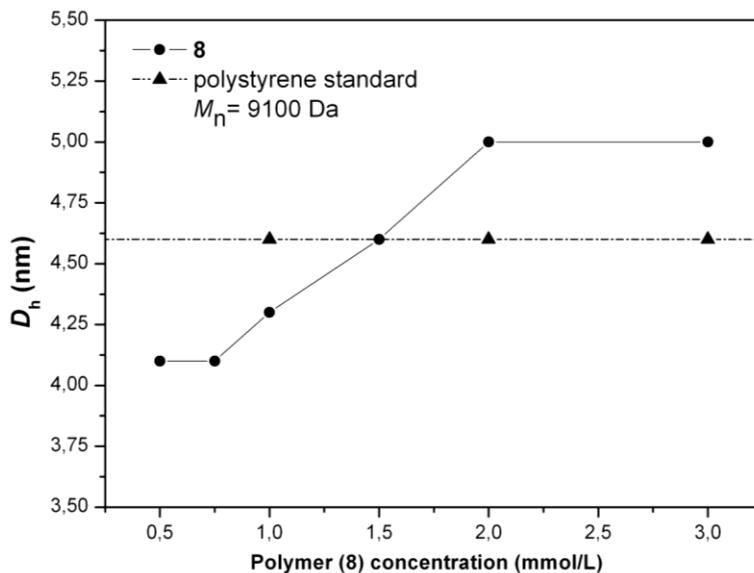


Figure 3.10 Hydrodynamic diameter of polymer **8** in different concentrations (mM) in CHCl_3 .

Table 3.2 Hydrodynamic diameter, D_h , of the polymer **8** in different concentrations as well as polystyrene standards in CHCl_3 at 25 °C.

Polymer	$D_h^{\text{exp}} / \text{nm}$	$D_h^{\text{theo}} / \text{nm}^{37}$
1 mM PS-standard ($M_n=9100$ Da)	4.6	4.6
2 mM PS-standard ($M_n=9100$ Da)	4.6	4.6
3 mM PS-standard ($M_n=9100$ Da)	4.6	4.6
10 mM PS-standard ($M_n=3400$ Da)	2.4	2.4
3 mM of 8	5.0	-
2 mM of 8	5.0	-
1.5 mM of 8	4.6	-
1 mM of 8	4.3	-
0.75 mM of 8	4.1	-
0.5 mM of 8	4.1	-

In summary, it is demonstrated that the single chain self-assembly of very narrow polydispersity synthetic macromolecules through α,ω -hydrogen-bonding between a cyanuric acid and a Hamilton wedge is possible. ^1H NMR and DLS analyses support the existence of strong entropically driven hydrogen-bonding interactions between the α -donor and ω -acceptor of the polymer **8** leading to single chain circular self-assembly. Predominant single

chain self-assembly of **8** occurs at (or below) concentrations of approximately 0.5 mM.

In chapter 5, supramolecular miktoarm star polymers achieved via hydrogen bonding between CA / HW are reported. Here, variable deuterated solvents, which are useful for studying self-assembly achieved via multiple hydrogen bonding are discussed. In the context of the solvent investigation it was found that deuterated CD_2Cl_2 is preferable over CDCl_3 as NMR solvent for studying. Thus, it seemed a matter of priority to revisit the single-chain self-folding of αCA and ωHW functionalized linear polymers. Thus, **11** and **12** ($M_{n,\text{NMR}} = 8100$ Da, $M_{n,\text{GPC}} = 7500$ Da, $PDI = 1.04$), **13** and **14** ($M_{n,\text{NMR}} = 8700$ Da, $M_{n,\text{GPC}} = 8200$ Da, $PDI = 1.04$) are synthesized using the above reported procedure for **6**, **7** and **8**. In addition, it was to be established whether there is any steric effect from the trimethylacetyl or *t*-butylacetyl groups of the HW (**3** or **10**) (see Scheme 3.2 and Scheme 3.3) on the *intermolecular* / *intramolecular* self-assembly.

As expected, the results obtained confirm the previous conclusions. For the *intermolecular* self-assembly, the interaction of **11** with compound **3** or **10** was investigated by ^1H NMR spectroscopic titration carried out in CD_2Cl_2 to compare NMR solvents. Figure 3.11a demonstrates that when **11** (4 mM) was mixed with 1 equivalent of compound **3** in CDCl_3 , the chemical shift of the imide proton signal of **11** changed from 7.98 ppm to 11.09 ppm. Similarly, Figure 3.11b shows that when **11** (4 mM) was mixed with 1 equivalent of compound **3** in CD_2Cl_2 , the chemical shift of the imide proton signal of **11** changed from 7.98 ppm to 10.83 ppm. Finally, as shown in Figure 3.11c when **11** (4 mM) was mixed with 1 equivalent of compound **10** in CD_2Cl_2 , the chemical shift of the imide proton signal of **11** changed from 7.98 ppm to 13.14 ppm.

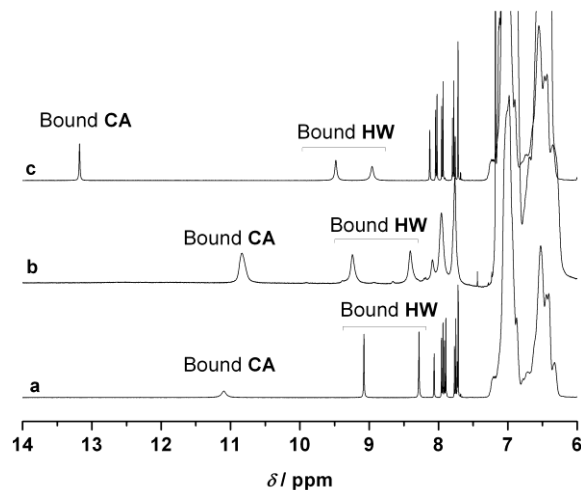


Figure 3.11 Chemical shifts of the imide proton signals of **11** as a function of equivalent of **3** or **10**. The concentration of **11** was kept constant at 4 mM. (a) Expanded ¹H NMR spectra of the **3•11** self-assembly system in 1 : 1 ratio in CDCl₃ at ambient temperature. (b) Expanded ¹H NMR spectra of the **3•11** self-assembly system in 1 : 1 ratio in CD₂Cl₂ at ambient temperature. (c) Expanded ¹H NMR spectra of the **10•11** self-assembly system in 1 : 1 ratio in CD₂Cl₂ at ambient temperature.

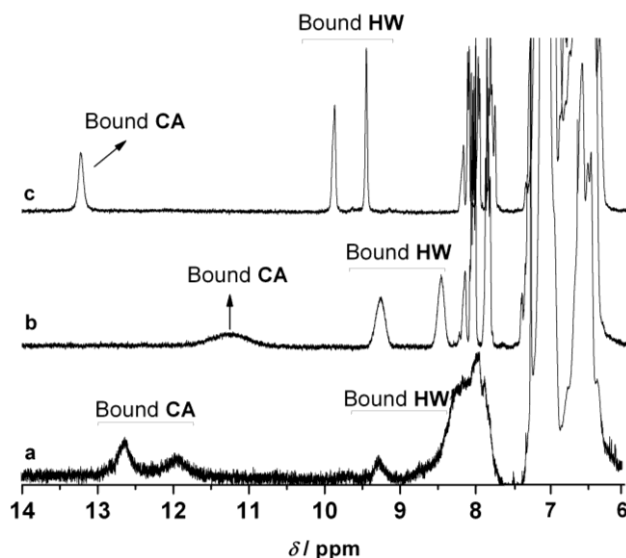


Figure 3.12 Expanded ¹H-NMR of entropy driven single chain self-assemblies of heterotelechelic polymers at ambient temperature. The concentration of polymers was kept constant at 1 mM. (a) **8** in CDCl₃ (b) **13** in CD₂Cl₂ (c) **14** in CD₂Cl₂.

For the investigation of the *intramolecular* self-assembly of **13**, a solution of **13** was prepared in CDCl_3 and the ^1H NMR was recorded (see Figure 3.12a). The resulting NMR spectrum revealed the presence of two peaks between 12 ppm and 13 ppm. Unfortunately, it is challenging to conclude which peak belongs to circularly bound cyanuric acid. When **13** was dissolved in CD_2Cl_2 and characterized by ^1H NMR (see Figure 3.12b), however, it became clear that CD_2Cl_2 is a much better solvent as compared to CDCl_3 for studying supramolecular structures achieved through the hydrogen-bonding of CA with HW. The self-assembly of CA protons with the HW appear as a single peak at 11.25 ppm in the ^1H NMR spectrum in CD_2Cl_2 at ambient temperature.

Next, it was investigated whether different functional groups on the HW affect the ability of HW to H-bond and therefore affect the self-assembly of αCA and ωHW functionalized macromolecules. More specifically, the effect of trimethylacetyl functionalized HW (linked to a polymer chain) **13** on single chain self-assembly, as compared to the effect of the corresponding *t*-butylacetyl macromolecule **14**, was analyzed. A solution of **13** was prepared in CD_2Cl_2 at a 1 mM concentration and left for 12 h at ambient temperature to allow for self-assembly. The ^1H NMR spectrum of **13** revealed that the imide proton signal of the cyanuric acid unit of **13** shifted downfield from δ 7.98 to δ 11.25 ppm (see Figure 3.12b). Similarly, a solution of **14** was prepared using the same protocol as that employed for **13**. The chemical shift observed for the imide proton of the cyanuric acid unit of **14** was similar to the shift seen for the imide proton of **13**; however, a greater downfield shift, from δ 7.98 ppm to δ 13.15 ppm, was observed. These results (see Figure 3.12c) suggest that the *t*-butylacetyl group allows for a stronger HW – CA interaction and therefore increased (circular) self-assembly (in CD_2Cl_2 at ambient temperature)

than the trimethylacetyl group. Thus, the best result for the self-assembly (**14**) was obtained with a *t*-butylacetyl group (see Scheme 3.2 and Scheme 3.3) in CD_2Cl_2 , which was confirmed by ^1H NMR spectroscopy (see Figure 3.12c). Such a result does not come entirely surprising as a *t*-butyl acetyl group may leave more space for the cyanuric acid unit to enter the HW than less flexible *t*-butyl group. The chemical shifts of the titration experiments between **3** and **10** (from 7.98 ppm to 13.14 ppm) are in good agreement with the chemical shifts (from 7.98 ppm to 13.15 ppm) of circular system of **14**. In addition, in agreement with literature,³⁸ the strong hydrogen binding of cyanuric acid protons results in imide proton signals that emerge close to 13 ppm in ^1H NMR.

To verify the afore mentioned ^1H NMR results, the D_h of **13** was investigated in dichloromethane at ambient temperature. The D_h of **13** in these solutions were measured to be 1.1, 1.3, 4.0, 4.9 and 5.1 nm, respectively. The D_h of **13** increases with increasing concentrations. These results indicate the formation of single chain self-assemblies of **13**. The D_h values of **13** were found to be smaller in dichloromethane than in CDCl_3 for low concentrations of **13** (see Figure 3.13). These results are in good agreement with the corresponding ^1H NMR results for **13** in CDCl_3 . Specifically, at low concentrations of **13** in CDCl_3 more than one peak is observed between 12 and 13 ppm in the ^1H NMR spectrum. Such an observation implies that there are some nonspecific interactions occurring in CDCl_3 at low concentration of **13** and these interactions increase the mean D_h of **13**.

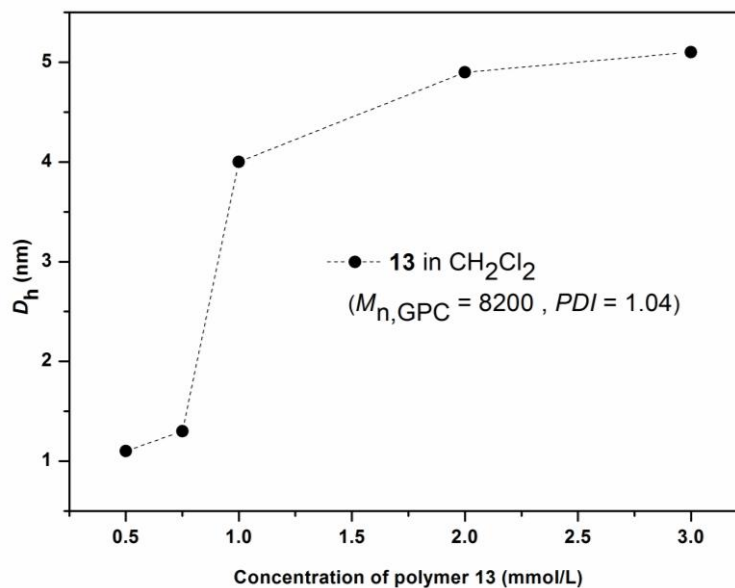


Figure 3.13 Hydrodynamic diameter (D_h) of polymer **13** in variable concentrations (mM) in CH_2Cl_2 (•).

3.3 Preparation of α -Thy and ω -DAP Functionalized Polystyrene

In the previous section of the current chapter, the single chain self-folding of α CA and ω HW functional linear polymers was established investigating concentration and appropriate solvents for the self-folding. Moreover, the cyanuric acid functional initiator was for the first time used under metal-mediated radical polymerization conditions, evidencing that the initiator containing hydrogen donor-acceptor moieties does not interfere with the mechanism of the ATRP. In next part of present chapter, Thy and DAP complementary recognition units are prepared as new pairs of suitable functional groups for single chain self-folding. The reason for additionally investigating these pairs is based on the desire to combine them with α CA and ω HW in a single polymer chain to generate more complex single chain folding structures, featuring two mutually orthogonal binding pairs. Fortunately, the self-folding of α Thy and ω DAP functional linear polymers (see Scheme 3.4) can also be properly examined, i.e. in the same depth for the

α CA and ω HW functional linear polymers. These below results provide strong encouragement for bringing together these recognition units in the same polymer chain at pre-defined positions for a detailed discussion of the dual chain folding systems. (please see chapter 4).

Below the synthesis of a novel well-defined α -thymine functionalized poly(styrene) using a thymine-based initiator in conjunction with ATRP is described first. The halogen end group of the polymer is subsequently transformed into an azide moiety, which can be ligated to an acetylene functionalized hydrogen acceptor (diaminopyridine) to provide the ω -end. Investigations into the self-assembly (i.e., cyclization) of the resulting polymer (under conditions of low polymer concentrations) is carried out via nuclear magnetic resonance (NMR) and dynamic light scattering (DLS) studies.

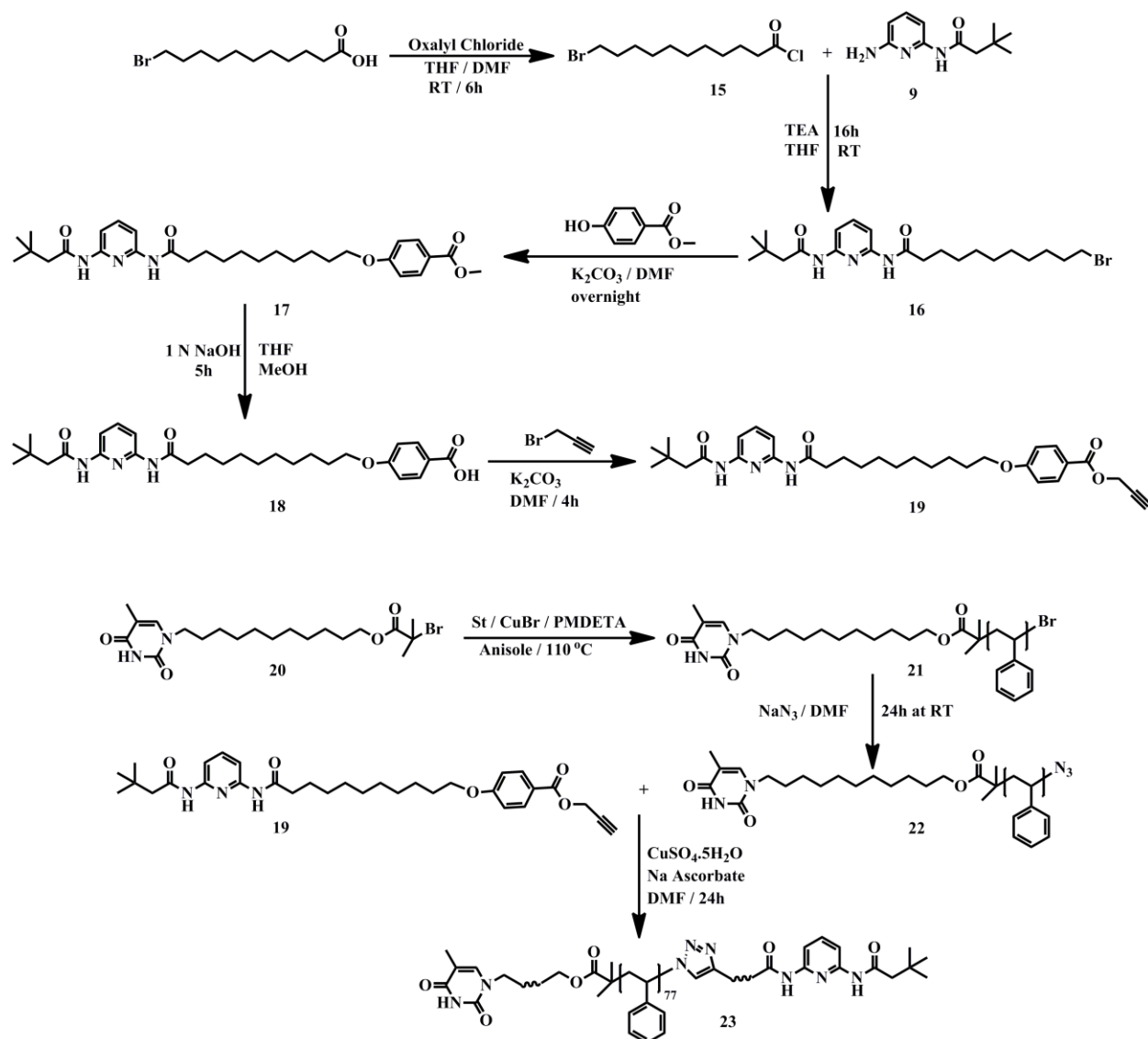
3.3.1 Synthesis

11-(5-methyl-2,4-dioxo-3,4-dihydro pyrimidin-1(2*H*)-yl)undecyl 2-bromo-2-methylpropanoate (**20**) was synthesized according to the literature.

3.3.1.1 Synthesis of 11-bromoundecanoyl chloride (15). 11-bromo-undecanoic acid (2.88 g, 10.86 mmol) was dissolved in 30 mL of dry THF in a three-neck round-bottom flask and 0.5 mL of dry DMF was added to this solution. Oxalyl chloride (1.65 mL, 18.62 mmol) was added dropwise over 10 min to the solution of 11-bromo-undecanoic acid. The mixture was stirred for 6 h at ambient temperature. The solvent was removed under reduced pressure and the crude product was subsequently dried under vacuum for 3 h to yield 11-bromoundecanoyl chloride (**15**) as a yellowish solid.

3.3.1.2 Synthesis of 11-bromo-*N*-(6-(3,3-dimethylbutanamido)pyridin-2-yl)undecanamide (16). **15** was dissolved in 40 mL of dry THF and added dropwise to a solution of compound **9**

(1.5 g, 7.24 mmol) and triethylamine (1.18 mL, 8.53 mmol) in 20 mL of dry THF at 0°C. The solution was stirred at ambient temperature for 16 h. The precipitate formed during the reaction was filtered off and the solvent was subsequently removed under reduced pressure. The crude product was purified by column chromatography (dry packed column; silica gel, CH₂Cl₂/ethyl acetate (4:1))



Scheme 3.4 Synthetic strategy for preparing α -Thy and ω -DAP functionalized polystyrene.

eluent), giving a white solid **16** after removal of solvent (3.14 g, yield 92%). ^1H NMR (400 MHz, DMSO- d_6) δ (ppm) 1.00 (s, 9H), 1.25 (brs, 14H), 1.55 (bs, 2H), 1.80-1.74 (q, 2H), 2.29 (s, 2H), 2.35-2.41 (t, 2H), 3.53 (t, 2H), 7.72-7.74 (bs, 3H), 9.89 (s, 1H), 10.00 (s, 1H). ^{13}C NMR (100 MHz, DMSO- d_6) δ (ppm) 24.89, 25.34, 28.42, 28.48, 28.62, 28.65, 28.71, 28.84, 29.44, 30.76, 35.97, 49.04, 60.67, 108.60, 141.79, 148.76, 171.73, 173.07. ESI-MS ($\text{M}+\text{Na}$) $^+$ $\text{C}_{22}\text{H}_{36}\text{BrN}_3\text{O}_2$ theoretical: 453.20, experimental: 453.17.

3.3.1.3 Synthesis of methyl 4-(11-(6-(3,3-dimethylbutanamido)pyridin-2-ylamino)-11-oxoundecyloxy) benzoate (17). Compound **16** (1.5 g, 3.40 mmol) was dissolved in 30 mL of DMF. Methyl 4-hydroxybenzoate (0.622 g, 4.09 mmol) and K_2CO_3 (0.847 g, 6.13 mmol) were subsequently added to the solution. The reaction mixture was stirred overnight at ambient temperature. After this time, the reaction mixture was poured into water and extracted with a mixture of DCM and diethyl ether (1:1). The organic phase was washed with water, dried over Na_2SO_4 , and concentrated. The product was purified by recrystallization from ethyl acetate affording a white

solid **17** (1.494 g, 86%). ^1H NMR (400 MHz, CD_2Cl_2) δ (ppm) 1.03 (s, 9H), 1.6 (bs, 14H), 1.63 (bm, 2H), 1.76 (brm, 2H), 2.17 (s, 2H), 2.30-2.33 (t, 2H), 3.80 (s, 3H), 3.96 (s, 2H), 6.84-6.88 (d, 2H), 7.63 (bm, 3H), 7.89-7.92 (bm, 4H). ^{13}C NMR (100 MHz, DMSO- d_6) δ 24.89, 25.34, 28.42, 28.48, 28.62, 28.65, 28.71, 28.84, 29.44, 37.82, 39.82, 51.83, 68.17, 109.28, 109.32, 114.07, 122.33, 131.56, 162.96, 166.94. ESI-MS ($\text{M}+\text{Na}$) $^+$ $\text{C}_{30}\text{H}_{43}\text{N}_3\text{O}_5$ theoretical: 525.32, experimental: 525.29.

3.3.1.4 Synthesis of 4-(11-(6-(3,3-dimethylbutanamido)pyridin-2-ylamino)-11-oxoundecyloxy)benzoic acid (18): NaOH (1 N, 10 mL) was added to a solution of compound **17**

(1 g, 1.95 mmol) in THF and MeOH (2:1, 30 mL). The solution was stirred at ambient temperature for 5 h and subsequently concentrated to a volume of 15 mL. The reaction mixture was poured into 150 mL of water and concentrated HCl was added dropwise to generate a white precipitate, which was filtered, washed with water, and dried under vacuum to give compound **18** as a white solid (0.914 g, 94%). ^1H NMR (400 MHz, DMSO- d_6) δ (ppm) 1.00 (s, 9H), 1.27 (bs, 14H), 1.55 (bm, 2H), 1.68-1.73 (t, 2H), 2.28 (s, 2H), 2.34-2.40 (t, 2H), 4.01 (s, 2H), 6.97-7.00 (d, 2H), 7.71 (s, 3H), 7.85-7.87 (d, 2H), 9.89 (s, 1H), 10.00 (s, 1H), 12.58 (s, 1H). ^{13}C NMR (100 MHz, DMSO- d_6) δ (ppm) 24.89, 25.34, 28.42, 28.48, 28.62, 28.65, 28.71, 28.84, 29.44, 30.76, 35.97, 48.94, 67.64, 108.92, 114.09, 122.65, 139.68, 150.14, 150.24, 162.19, 166.90, 170.73, 172.09. ESI-MS ($\text{M}+\text{Na}$) $^+$ $\text{C}_{29}\text{H}_{42}\text{N}_3\text{O}_5$ theoretical: 511.3, experimental: 511.28.

3.3.1.5 Synthesis of prop-2-ynyl 4-(11-(6-(3,3-dimethylbutanamido)pyridin-2-ylamino)-11-oxoundecyl- oxy) benzoate (19). Compound **18** (0.7 g, 1.36 mmol) was dissolved in 15 mL of dry DMF. Propargyl bromide (0.202 g, 1.71 mmol) and K_2CO_3 (0.375 g, 2.72 mmol) were subsequently added to this solution. The reaction was stirred at ambient temperature for 4 h. The precipitate formed during the reaction was removed by filtration. The filtrate was dried using a rotary evaporator and the crude product obtained was dissolved in DCM. The organic phase was washed with water, dried over Na_2SO_4 , filtered, dried using a rotary evaporator, and then dried under vacuum. Purification by recrystallization from *n*-hexane gave compound **19** as a white solid (0.71 g, 94%). ^1H NMR (400 MHz, DMSO- d_6) δ (ppm) 1.00 (s, 9H), 1.27 (bs, 14H), 1.55 (bm, 2H), 1.68-1.73 (t, 2H), 2.29 (s, 2H), 2.35-2.41 (t, 2H), 3.60 (s, 1H), 4.03 (s, 2H), 4.91 (s, 2H), 7.02-7.06 (d, 2H), 7.72 (s, 3H), 7.89-7.92 (d, 2H), 9.89 (s, 1H), 10.00 (s, 1H). ^{13}C NMR (100 MHz, DMSO- d_6) δ (ppm) 24.89, 25.34, 28.42, 28.48, 28.62, 28.65, 28.71, 28.84, 29.44,

30.76, 35.97, 48.94, 67.80, 77.65, 78.51, 108.92, 114.09, 120.84, 139.68, 150.14, 150.24, 162.80, 164.54, 170.73, 172.09. ESI-MS ($M+Na$)⁺ $C_{32}H_{43}N_3O_5$ theoretical: 549.32, experimental: 549.27

3.3.1.6 Synthesis of α -thymine functional poly(styrene) (Thy-PS-Br) (21). Styrene (8.0 mL, 6.98 mmol), PMDETA (0.073 mL, 0.349 mmol), and **20** (0.155 g, 0.349 mmol) in 2 mL of anisole were added to a 50 mL schlenk tube. The reaction mixture was degassed via three successive freeze-pump-thaw cycles and left under argon. CuBr (0.050 g, 0.349 mmol) was added to the solution under argon. The tube was subsequently sealed and placed in an oil bath at 110 °C for 45 min. The polymerization mixture was rapidly cooled in an ice bath, diluted with THF, and passed through an alumina column to remove the catalyst. The solvent was removed under reduced pressure and the remaining crude product was subsequently diluted with DCM (50 mL) and washed with 0.1 M EDTA (10 mL) solution to remove any remaining Cu, which might be complexed by to the recognition unit. The organic phase was dried over Na_2SO_4 , concentrated and precipitated in 80 mL methanol twice. The polymer was dried for 24 h under vacuum to give α -thymine functional poly(styrene) as a white solid (0.545 g). ($[M]_0/[I]_0 = 200$, $[I]_0:[CuBr]_0:[PMDETA]_0 = 1:1:1$). $M_{n,NMR} = 8500$ Da, $M_{n,SEC} = 8600$ Da, $PDI = 1.05$, end group fidelity (with respect to thymine and Br) close to 98%.

3.3.1.7 Synthesis of α -thymine functional poly(styrene) with azide endgroup (Thy-PS- N_3) (22). **21** (0.5 g, 0.06 mmol) was dissolved in DMF (15 mL), and sodium azide (0.16 g, 2.4 mmol) was added. The reaction mixture was stirred for 24 h at room temperature. It was filtered and evaporated to remove DMF. Dichloromethane (100 mL) was added, and the reaction mixture was washed three times with distilled water. The organic layer was dried with anhydrous Na_2SO_4 , and the solvent was removed in rotary. The polymerization mixture was diluted with

THF and precipitated in methanol. The polymer was dried for 24 h in a vacuum oven at 25 °C. FTIR (cm^{-1}): 2095 (N_3 stretching). $M_{n,\text{NMR}} = 8500$ Da, $M_{n,\text{SEC}} = 8600$ Da, $PDI = 1.05$.

3.3.1.8 Synthesis of α,ω -donor-acceptor single chain poly(styrene) (**23**) (Thy-PS-DAP).

Polymer **22** (0.2 g, 0.023 mmol), compound **19** (0.039 g, 0.07 mmol), copper (II) sulfate pentahydrate (0.017 g, 0.07 mmol) and sodium ascorbate (0.014 g, 0.07 mmol) were dissolved in DMF (5 mL). The resulting mixture was stirred at ambient temperature for 16 h and subsequently passed through a short column of neutral alumina to remove the copper catalyst. The solvent was removed under reduced pressure and the crude product was diluted with DCM (50 mL) and washed with 0.1 M EDTA solution (10 mL) to remove any Cu that might be complexed to the recognition units. The organic phase was dried over Na_2SO_4 , concentrated, and precipitated in 80 mL of cold methanol twice, filtered, and dried under vacuum at 25°C for 24 h to obtain a white solid (0.234 g, yield 98%). ^1H NMR (400 MHz, CDCl_3) δ (ppm) 7.96-7.76 (9H, ArH of host), 7.01-6.39 (5H, ArH of PS), 5.13-5.03 (2H, OCH_2 linked to triazole), 3.73 (2H, $\text{CH}_2\text{-N}$), 3.45(2H, $\text{CH}_2\text{-O}$), 1.78-1.18 (aliphatic protons of PS), 0.90-0.77 (6H, $\text{NCH}_2(\text{CH}_2)_3\text{CH}_2\text{O}$). $M_{n,\text{NMR}} = 9100$ Da, $M_{n,\text{SEC}} = 9300$ Da, $PDI = 1.04$

3.3.1.9 Self-assembly studies between compound 17 and polymer 21. Five different samples were prepared with polymer **21** (25.5 mg) dissolved in 1 mL CD_2Cl_2 in a NMR tube. The concentration of **21** was kept constant at 3 mM. Compound **17** was then added in 1, 2, 3, 4, or 5 equivalents relative to polymer **21**. The mixtures were left to interact overnight (12 h) at ambient temperature; ^1H NMR spectra were subsequently recorded (see Figure 3.21 and 3.22).

3.3.1.10 Single chain self-assembly studies of polymer 23. Polymer **23** (9.1 mg, 18.2 mg, or 27.3) was dissolved in 1 mL CD_2Cl_2 and placed in an NMR tube, and left to assemble overnight (12 h); ^1H NMR spectra were subsequently recorded (see Figure 3.24).

3.3.2 Results and Discussion of α -Thy and ω -DAP Functionalized Polystyrene

The target structure was designed to feature a thymine functionality in the α -position and a diaminopyridine functionality group at the ω -position of polymer chain with the aim of generating well-defined heterotelechelic supramolecular self-assembly systems via a combination of ATRP and modular conjugation chemistry. The synthetic pathway used to generate the target **Thy-PS-DAP (23)** heterotelechelic supramolecular polymer is outlined in Scheme 3.4.

The thymine functional ATRP initiator (**20**) was synthesized in two steps following published literature and subsequently was characterized by ^1H NMR (see Figure 3.14).

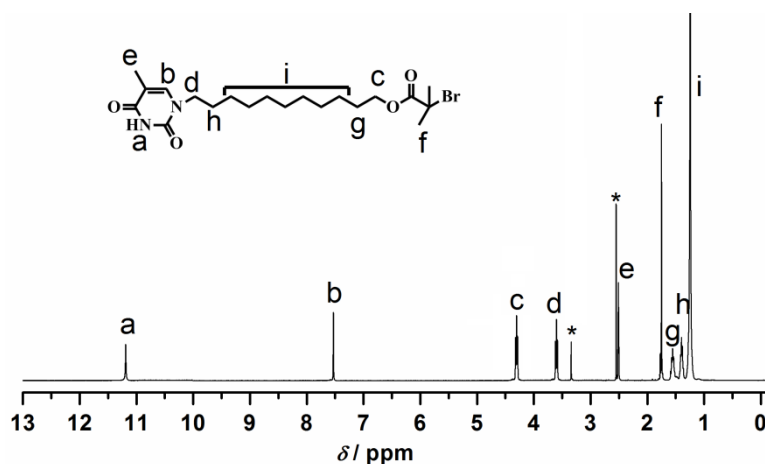


Figure 3.14 ^1H -NMR spectrum of 11-(5-methyl-2,4-dioxo-3,4-dihydropyrimidin-1(2H)-yl)undecyl 2-bromo-2-methylpropanoate (**20**) in $\text{DMSO}-d_6$. The peaks marked with an asterisk are due to solvent/water.

To incorporate a diaminopyridine (DAP) motif at the end of the polymer chain, an alkyne containing DAP compound had to be synthesized first. This was achieved by treating 11-bromoundecanoic acid with oxalyl chloride to generate the acid chloride **15**, which was subsequently reacted with *N*-(6-aminopyridin-2-yl)-3,3-dimethylbutanamide (**9**) in the presence of triethylamine to obtain compound **16**. The ^1H NMR spectrum of **16** shows the characteristic signals for pyridine protons and those of $-\text{CH}_2\text{Br}$, which appeared at 7.73 and 3.53 ppm, respectively (see Figure 3.15).

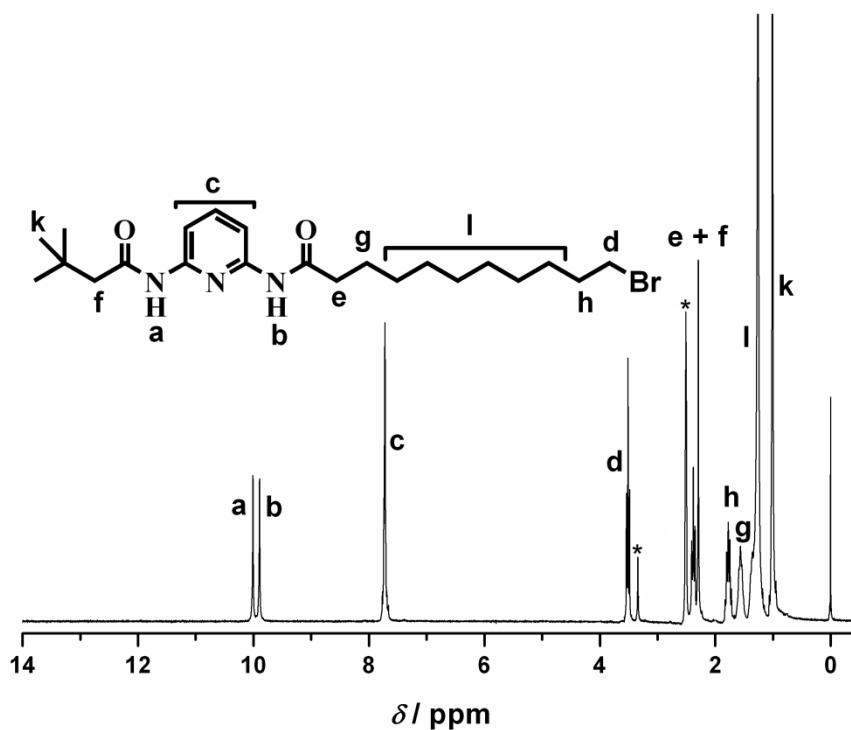


Figure 3.15 ^1H -NMR spectrum of 11-bromo-*N*-(6-(3,3-dimethylbutanamido)pyridin-2-yl)undecanamide (**16**) in $\text{DMSO}-d_6$. The peaks marked with an asterisk are due to solvent/water.

In the second step, compound **16** was subjected to an etherification reaction with methyl 4-hydroxybenzoate in the presence of K_2CO_3 and DMF to afford compound **17**. In the ^1H NMR spectrum of **17** the proton signals associated with $-\text{CH}_2\text{Br}$ and $-\text{CH}_2\text{CH}_2\text{Br}$ at 3.40 ppm and 1.8

ppm, respectively, disappear and new proton signals corresponding to the phenyl group, $-CH_2O-$, and $-COOCH_3$ can be observed at 7.92-6.88 ppm, 3.96 ppm, and 3.80 ppm, respectively (see Figure 3.23). Next, the deprotection of the carboxylic acid group of **17** was readily accomplished in the presence of 1 N NaOH in a THF/methanol mixture. This was confirmed by 1H NMR: the proton signal for the carboxylic acid of **18** was observed at 12.58 ppm and the proton signal for the methyl group was no longer observed at 3.80 ppm (see Figure 3.16). Finally, the alkyne functional DAP compound was synthesized by esterification of compound **18** with propargyl bromide in the presence of K_2CO_3 and DMF. The 1H NMR spectrum of **19** indicates that the proton signal corresponding to $-COOH$ has disappeared and the new proton signals for $-COOCH_2C-$ and $-CCH$ are observed at 4.91 ppm and 3.60 ppm, respectively (Figure 3.17). Compound **20** was employed as an initiator in the CuBr/PMDETA complex catalyzed ATRP of styrene in anisole to yield the α -thymine end capped polymer **21** ($M_n = 8500 \text{ g mol}^{-1}$, $PDI = 1.06$). The end group fidelity of **21** has been assessed via quantitative integration of its NMR spectrum (see Figure 3.18) and found to be close to 98%. The ω -end bromo functionality was quantitatively converted to an azide group employing NaN_3 in DMF (see Figure 3.20). Next, copper catalyzed azide-alkyne conjugation chemistry was used to couple **22** and compound **19** in the presence of $CuSO_4$ /sodium ascorbate in DMF at ambient temperature to give the corresponding α,ω -donor/acceptor substituted heterotelechelic macromolecule **23** (see Scheme 3.4). The number average molecular weight, M_n , of Thy-PS-DAP (**23**) was determined to be 9100 Da and 9300 Da ($PDI = 1.04$) using 1H -NMR and SEC (Figure 3.19) (molecular weight was reported relative to PS standards), respectively. The M_n , as well as the corresponding polydispersity values, of compounds **21**, **22**, and **23** can be found in Table 3.3.

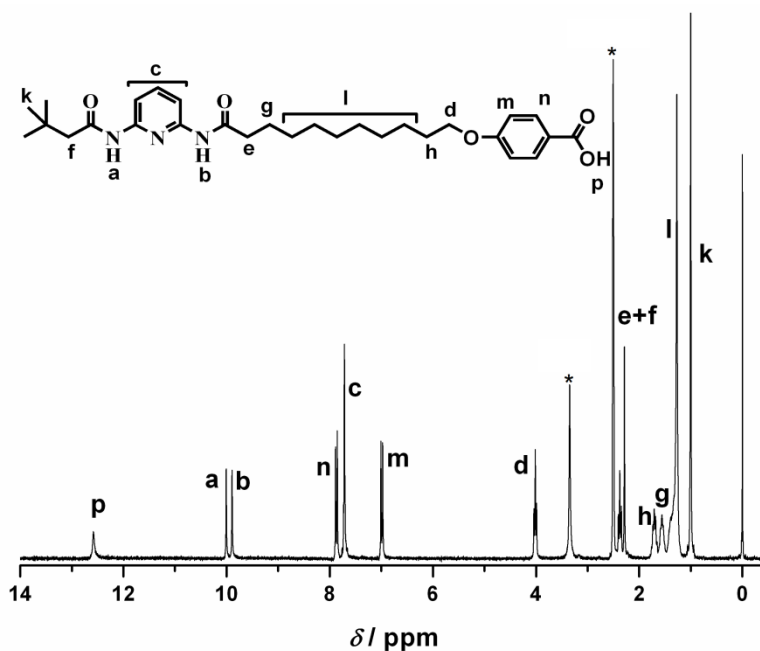


Figure 3.16 $^1\text{H-NMR}$ spectrum of 4-(11-(6-(3,3-dimethylbutanamido)pyridin-2-ylamino)-11-oxoundecyloxy)benzoic acid (**18**) in $\text{DMSO-}d_6$. The peaks marked with an asterisk are associated with solvent/water.

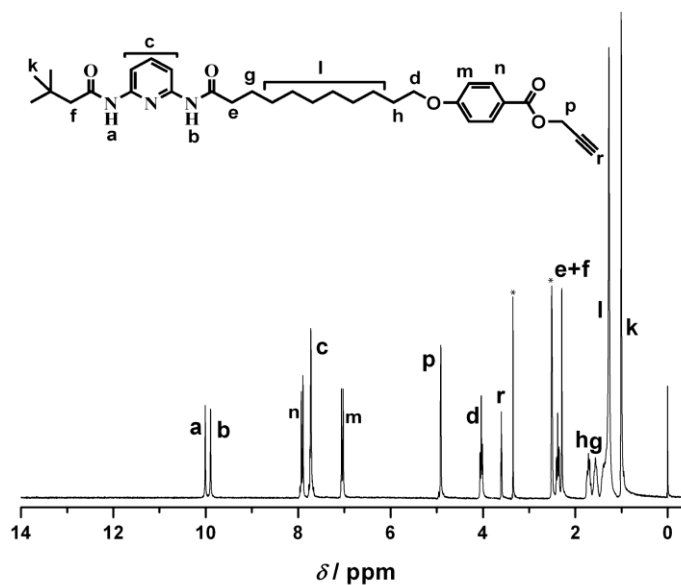


Figure 3.17 $^1\text{H-NMR}$ spectrum of prop-2-ynyl 4-(11-(6-(3,3-dimethylbutanamido)pyridin-2-ylamino)-11-oxoundecyloxy)benzoate (**19**) in $\text{DMSO-}d_6$. The peaks marked with an asterisk are associated with solvent/water.

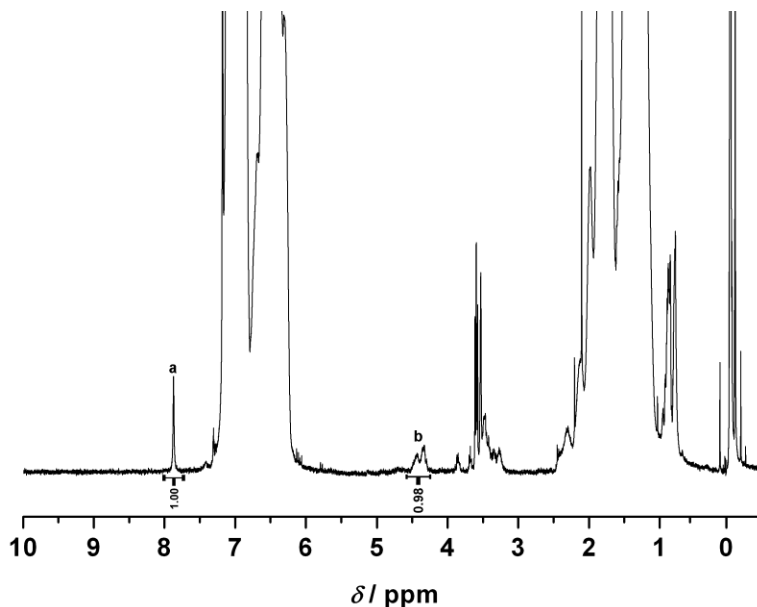


Figure 3.18 ^1H NMR spectrum of polymer **21** in CDCl_3 at ambient temperature with the integral values of the relevant resonances. The ratio of the peak areas **a** (NH of thymine at the α -end of polymer **21**) to **b** (CH-Br of ω -end of polymer **21**) indicate a chain fidelity close to $\sim 98\%$.

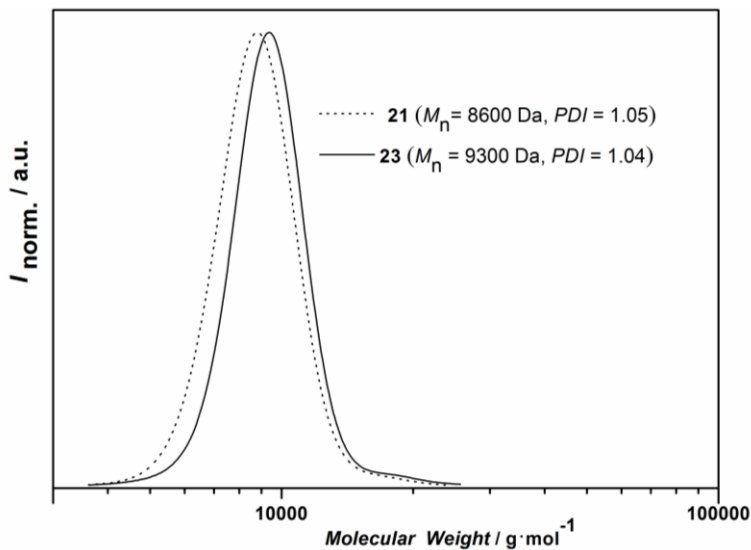
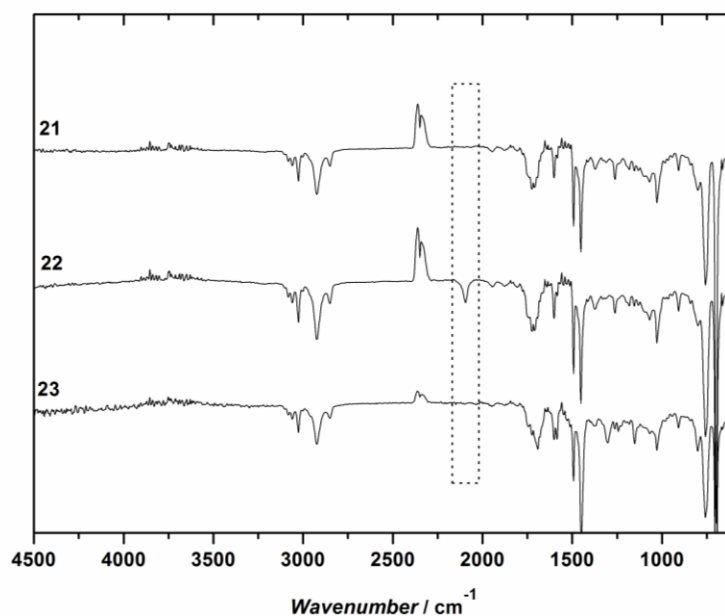


Figure 3.19 SEC traces of Thy-PS-Br (**21**) and Thy-PS-DAP (**23**).

Table 3.3 Molecular weight of the precursor and the final polymers. The related structures can be found in Scheme 3.4.

Polymers	Monomer	$[M_0]/[I_0]$	Initiator	Time (min.)	M_n^b	M_w/M_n	M_n^c
21^a	Styrene	200	20	45	8600	1.05	8500
22	-	-	-	-	8600	1.05	8500
23	-	-	-	-	9300	1.04	9100

^a $[I]_0/[PMDETA]_0/[CuBr]_0 = 1:1:1$; at 110 °C. ^b Determined via RI detection SEC using linear PS standards. ^c Determined from 1H NMR spectroscopy.

**Figure 3.20** ATR-IR spectra of Thy-PS-Br (**21**), Thy-PS-N₃ (**22**), Thy-PS-DAP (**23**).

Before discussing in detail the self-assembly of polymer **23** resulting from the recognition of its hydrogen donor/acceptor motifs, the *intermolecular* interaction of **21** with compound **17** was investigated by a 1H NMR spectroscopic titration carried out in CD_2Cl_2 . For the 1H NMR studies, the concentration of **21** was kept constant at 3 mM and the change in the chemical shift

was followed as a function of increasing concentrations of **17**. The NMR titration experiments revealed a significant downfield shift of the signal associated with the imide protons due to the complexation of **17**. As shown in Figure 3.18 or Figure 3.21, the peak at δ 7.87 ppm was assigned to the NH proton of the thymine recognition unit at the α -end of polymer **21**.

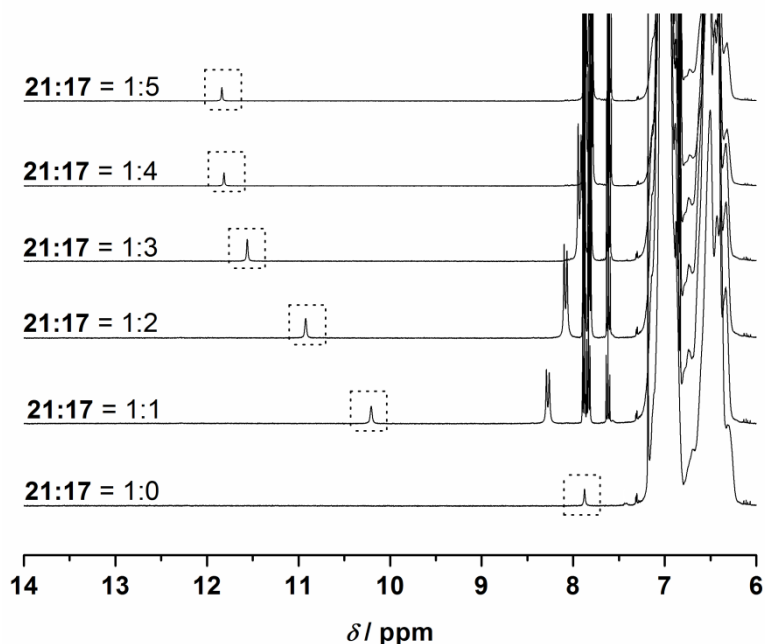


Figure 3.21 Expanded ¹H NMR spectra of the **21•17** self-assembly system with varied concentration ratios in CD₂Cl₂ at ambient temperature. The concentration of **21** was kept constant at 3 mM.

When polymer **21** was mixed with 1 equivalent of compound **17** in CD₂Cl₂, the ¹H NMR revealed a downfield shift, from δ 7.98 ppm to δ 10.14 ppm, of the imide proton signal for polymer **21**. When polymer **21** was mixed with 2, 3, 4, and 5 equiv. of the compound **17** in CD₂Cl₂, the chemical shift for the proton resonance of the imide proton of polymer **21** changed from 7.98 to 10.91, 11.54, 11.81, and 11.83 ppm, respectively, indicating an increase in the complexation (Figure 3.21 and Figure 3.22).

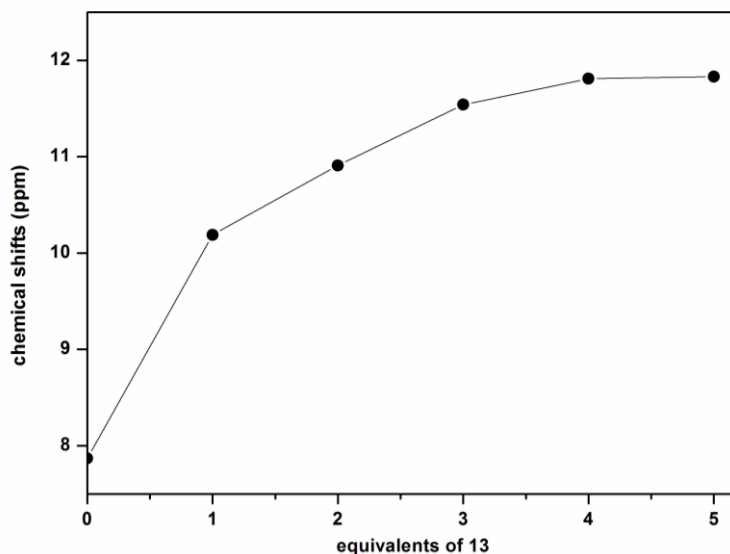


Figure 3.22 Chemical shifts of the imide protons of polymer **21** as a function of equivalents of **17**. The concentration of **21** was kept constant at 3 mM.

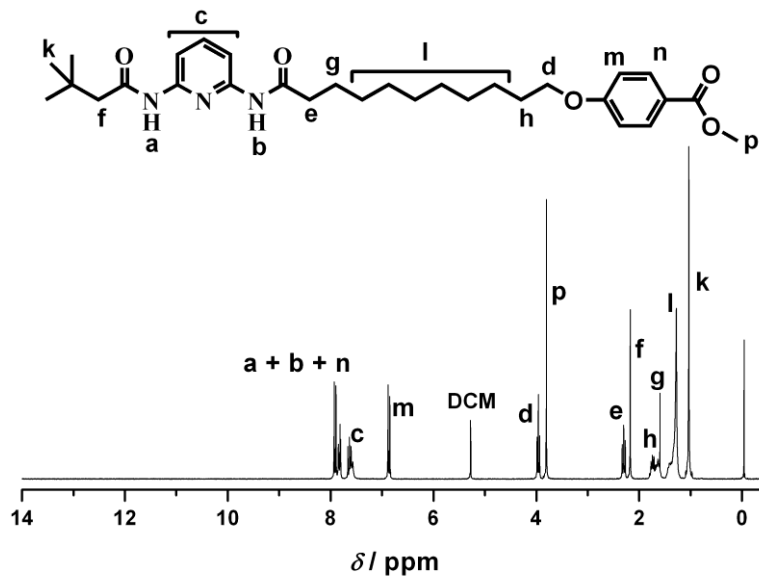


Figure 3.23 ¹H-NMR spectrum of methyl 4-(11-(6-(3,3-dimethylbutanamido)pyridin-2-ylamino)-11-oxoundecyloxy) benzoate (**17**) in CD₂Cl₂.

Moreover, the proton signals at δ 7.81 ppm and δ 7.84 ppm were assigned to the *NH* protons of the DAP of **17** in CD_2Cl_2 (see Figure 3.23). When polymer **21** was mixed with compound **17**, the *NH* protons of the DAP appeared at 8.24 and 8.27 ppm due to the self-assembly. With increasing concentration of compound **17**, the *NH* protons of the DAP shifted slightly further upfield due to the formation of the strong assembly between **21** and **17**. These changes in the NMR spectra are characteristic for the formation of a three-point hydrogen bonding complex.

Evidence for the formation of the (single chain) self-folding, through hydrogen-bonding, of **23** in CD_2Cl_2 was provided by ^1H NMR and dynamic light scattering (DLS) studies. For the ^1H NMR studies, a solution of the polymer **23** was prepared in CD_2Cl_2 of 1 mM and left for 12 h at ambient temperature to allow to self-assemble. The chemical shift of the imide proton signal of the thymine unit of **23** changed from δ 7.87 to δ 8.21 ppm. When a 2 mM solution of **23** is prepared, the chemical shift at δ 8.21 ppm shifts downfield to δ 8.41 ppm. When the concentration of the solution of polymer **23** was increased to 3 mM, the signal shifted further downfield to δ 8.53 ppm. This downfield shift of the imide proton signal as the concentration of polymer **23** is increased is shown in the ^1H NMR spectra in Figure 3.24. These shifts are less than expected, considering the chemical shift of the imide proton signal to 10.14 ppm that occurs with a 1:1 association of **17** and **21** (see Figure 3.21). However, these values are in good agreement with previous reports³⁹ in which Bernard and colleagues describe that the supramolecular association between thymine and DAP (small molecules) through a selective three-point H-bonding complexation in deuterated chloroform resulted in a significant downfield shift of the *NH* thymine proton signal (from 8.22 ppm to 10.45 ppm). They also observed that the chemical shifts are much less (from 8.08 to 8.72 ppm) than of the H-bonding of small molecules, indicating that the presence of the polymeric chains slightly affects the ability of thymine to

associate with DAP moieties, possibly due to the altered accessibility within the polymeric system. Given these observations, the chemical shift of the imide proton of **23** that is observed indicates the formation of stabilized (cyclic) structures via entropy driven preferential self-assembly. These results indicate that in more dilute solutions stable self-assemblies are formed with significantly reduced exchange processes congruent with ring formation.

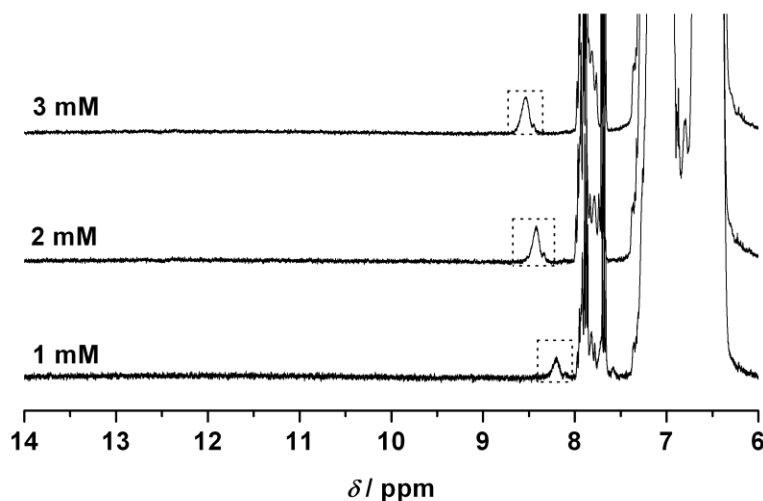


Figure 3.24 Expanded $^1\text{H-NMR}$ of the polymer **23** at different concentrations in CD_2Cl_2 .

While the NMR experiments suggest that stabilized structures occur, due to entropy driven (circular) self-assembly, only the measurement of the hydrodynamic diameter, D_h , can provide unequivocal evidence for the single chain circular self-assembly. Thus, the D_h of self-assembled **23** and poly(styrene) standards were determined by DLS in CH_2Cl_2 at 25°C . The polymer **23** ($M_{n,\text{NMR}} = 9100$ Da) was characterized by DLS at five concentrations (0.5, 0.75, 1, 2 and 3mM). The D_h of the polymers in these solutions were measured to be 1.2 nm, 1.4 nm, 4.1 nm, 5.4 nm, and 6.1 nm, respectively. Concomitantly, a PS standard (9100 Da) was analysed via DLS at variable concentrations. The mean hydrodynamic diameter of polymer **23** increases with

increasing concentrations in contrast to the PS standard ($D_h(c)=\text{const.}$), indicating that higher concentrations favor the formation of inter-chain assemblies of **23** (see Figure 3.25). As the concentration is reduced, the diameter of **23** is observed to progressively decrease, thus suggesting that more compact single-chain self-assembled cyclic structures are formed.

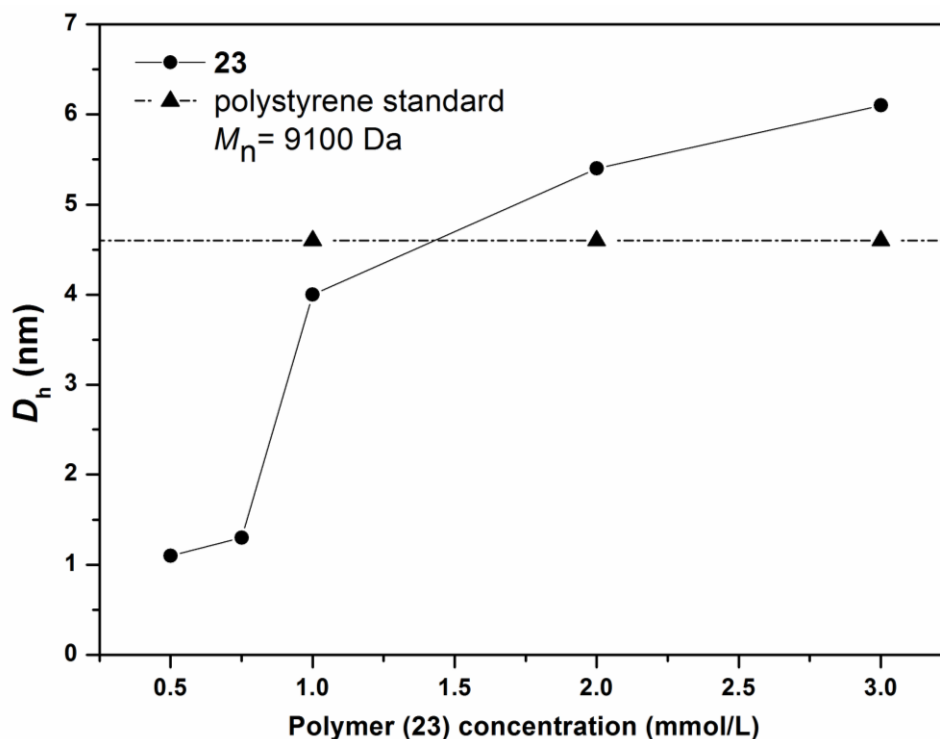


Figure 3.25 Hydrodynamic diameter of polymer **23** at various concentrations (0.5, 0.75, 1, 2 and 3 mM) in CH_2Cl_2 .

3.4 Conclusions

In the current chapter, novel cyanuric acid and thymine functional initiators were synthesized and characterized ^1H NMR, ^{13}C NMR and ESI-MS. Styrene polymerization was for the first time performed using these initiator under metal-catalyzed radical polymerization condition. CA or Thy functional linear polymers obtained with narrow molecular weight distribution and high end group fidelity. Alkyne functional complementary recognition motifs ()

(HW and DAP) were also synthesized and characterized by ^1H NMR, ^{13}C NMR and ESI-MS. Finally, α,ω -Hydrogen donor-acceptor functional polymer strands are generated by a combination of ATRP and CuAAC and characterized by ^1H NMR, GPC and FT-IR. It was demonstrated that entropy driven single chain self-assembly of very narrow polydispersity synthetic macromolecules could be achieved through the α,ω -hydrogen bonding complementary recognition units. The results from ^1H NMR and DLS analyses in dichloromethane provide support for the existence of strong entropically driven hydrogen-bonding interactions between complementary recognition units of the heterotelechelic polymers, leading to single chain circular self-assembly. Single chain self-assemblies predominantly occur at low concentrations. The effects of solvents and steric hindrance, (i.e. from trimethylacetyl vs *t*-butylacetyl alkyl groups within the Hamilton wedge), on the self-assembly of the complementary recognition (CA / HW) units of heterotelechelic polymer were investigated and it was established that the sterically less demanding *t*-butyl acetyl group leads to a better assembly process. Dichloromethane is the preferred solvent over chloroform, as the non-specific interactions between the cyanuric acid protons and the solvent are avoided. In summary, optimum solvents and concentrations for the self-folding of α,ω -hydrogen donor-acceptor functional single chain polymers were established. The employed CA, HW, Thy and DAP recognition motifs thus hold great promise for the preparation of dual self-folding single polymer chains via multiple and pairwise orthogonal hydrogen bonding.

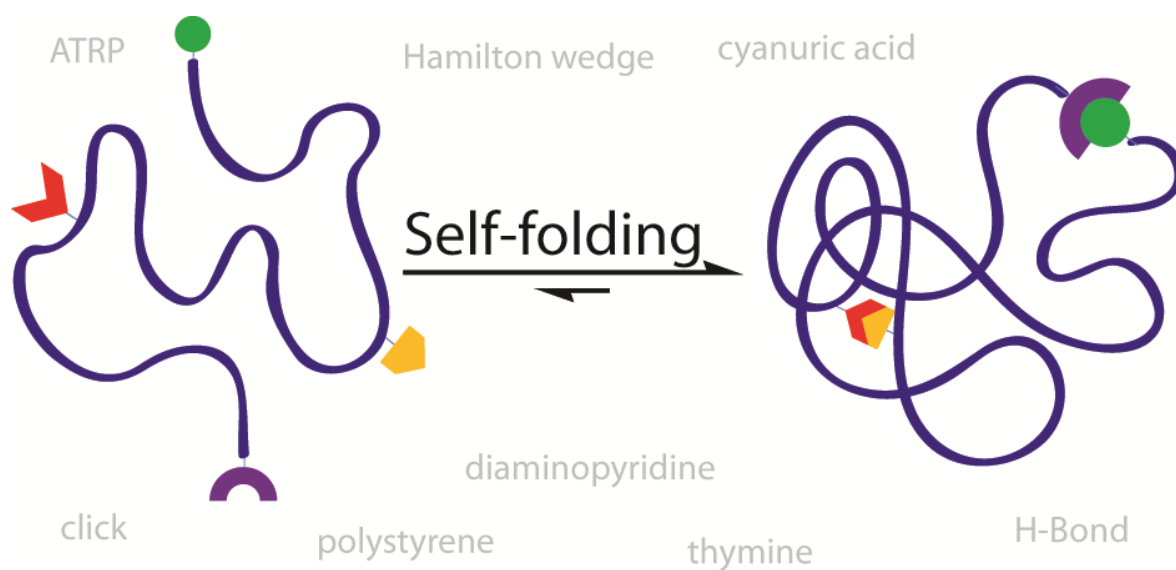
3.5 References

- [1] M. Kato, M. Kamigaito, M. Sawamoto, T. Higashimura, *Macromolecules* **1995**, 28, 1721.
- [2] V. Percec, B. Barboiu, *Macromolecules* **1995**, 28, 7970.
- [3] J. S. Wang, K. Matyjaszewski, *Macromolecules* **1995**, 28, 7901.
- [4] K. Matyjaszewski, J. Xia, *Chem. Rev.* **2001**, 101, 2921.
- [5] K. Matyjaszewski, J. Xia, *Chem. Rev.* **2001**, 101, 2921.
- [6] M. Ouchi, T. Terashima, M. Sawamoto, *Chem. Rev.* **2009**, 109, 4963.
- [7] K. Matyjaszewski, *Macromolecules* **2012**, DOI: 10.1021/ma3001719
- [8] H. C. Kolb, M. G. Finn, K. B. Sharpless, *Angew. Chem. Int. Ed.* **2001**, 40, 2004.
- [9] C. Barner-Kowollik, A. J. Inglis, *Macromol. Chem. Phys.* **2009**, 210, 987.
- [10] W. H. Binder, R. Sachsenhofer, *Macromol. Rapid Commun.* **2008**, 29, 952.
- [11] C. J. Hawker, K. L. Wooley, *Science* **2005**, 309, 1200.
- [12] J. M. Lehn, *Chem. Soc. Rev.* **2007**, 36, 151.
- [13] M. J. Krische, J. M. Lehn, *Struct Bonding* **2000**, 96, 3.
- [14] F. H. Beijer, H. Kooijman, A. L. Spek, R. P. Sijbesma, E. W. Meijer, *Angew. Chem. Int. Ed.* **1998**, 37, 75.
- [15] R. Knapp, A. Schott, M. Rehahn, *Macromolecules* **1996**, 29, 478.
- [16] J. P. Sauvage, J. P. Collin, J. C. Chambron, S. Guillerez, C. Coudret, *Chem. Rev.* **1994**, 94, 993.
- [17] M. Chiper, M. A. R. Meier, D. Wouters, S. Hoepfener, C. A. Fustin, J. F. Gohy, U. S. Schubert, *Macromolecules* **2008**, 41, 2771.
- [18] O. Altintas, I. Yilmaz, G. Hizal, U. Tunca, *J. Polym. Sci. Part A: Polym. Chem.* **2006**, 44, 3242.
- [19] C. Nuckolls, T. J. Katz, G. Katz, P. J. Collings, L. Castellanos, *J. Am. Chem. Soc.* **1999**, 121, 79.
- [20] L. Brunsveld, E. W. Meijer, R. B. Prince, J. S. Moore, *J. Am. Chem. Soc.* **2001**, 123, 7978.
- [21] Yamaguchi, N.; Gibson, H. W. *Angew Chem Int Ed* 1999, 38, 143.

- [22] P. R. Ashton, P. J. Campbell, E. J. T. Chrystal, P. T. Glink, S. Menzer, D. Philp, N. Spencer, J. F. Stoddart, P. A. Tasker, D. J. Williams, *Angew. Chem. Int. Ed.* **1995**, *34*, 1865.
- [23] J. D. Fox, S. J. Rowan, *Macromolecules* **2009**, *42*, 6823.
- [24] L. Brunsveld, B. J. B. Folmer, E. W. Meijer, R. P. Sijbesma, *Chem. Rev.* **2001**, *101*, 4071.
- [25] T. F. A De Greef, M. M. J. Smulders, M. Wolfs, A. P. H. J. Schenning, R. P. Sijbesma, E. W. Meijer, *Chem. Rev.* **2009**, *109*, 5687.
- [26] E. J. Foster, E. B. Berda, E. W. Meijer, *J. Am. Chem. Soc.* **2009**, *131*, 6964.
- [27] E. B. Berda, E. J. Foster, E. W. Meijer, *Macromolecules* **2010**, *43*, 1430.
- [28] E. B. Berda, E. J. Foster, E. W. Meijer, *J. Polym. Sci. Part A: Polym. Chem.* **2011**, *49*, 118.
- [29] J. M. Pollino, L. P. P. Stubbs, M. Weck, *J. Am. Chem. Soc.* **2004**, *126*, 563.
- [30] M. N. Higley, J. M. Pollino, E. Hollebeak, M. Weck, *Chem. Eur. J.* **2005**, *11*, 2946.
- [31] W. H. Binder, C. Kluger, *Macromolecules* **2004**, *37*, 9321.
- [32] C. Enders, S. Tanner, W. H. Binder, *Macromolecules* **2010**, *43*, 8436.
- [33] O. Altintas, P. Gerstel, N. Dingenouts, C. Barner-Kowollik, *Chem. Commun.* **2010**, *46*, 6291.
- [34] F.Y. Ji, L. L. Zhu, X. Ma, Q. C. Wang, H. Tian, *Tetrahedron Lett.*, **2009**, *50*, 597.
- [35] A. B. Eldrup, C. Christensen, G. Haaima, P. E. Nielsen, *J. Am. Chem. Soc.* **2002**, *124*, 3254.
- [36] C. Burd, M. Weck *Macromolecules* **2005**, *38*, 7225.
- [37] The Mark-Houwink parameter for the calculation of $[\eta]$ has been taken from: I. Brandrup, E. Immergut, *Polymer Handbook*, Wiley & Sons 4th edition, New York, **2003**.
- [38] S. K. Yang, A. V. Ambade, M. Weck, *J. Am. Chem. Soc.* **2010**, *132*, 1637.
- [39] S. Chen, A. Bertrand, X. Chang, P. Alcouffe, C. Ladaviere, J. F. Gerard, F. Lortie, J. Bernard, *Macromolecules* **2010**, *43*, 5981.

Dual Self-Folding of Single Polymer Chains via Reversible Hydrogen Bonding

Chapter 4

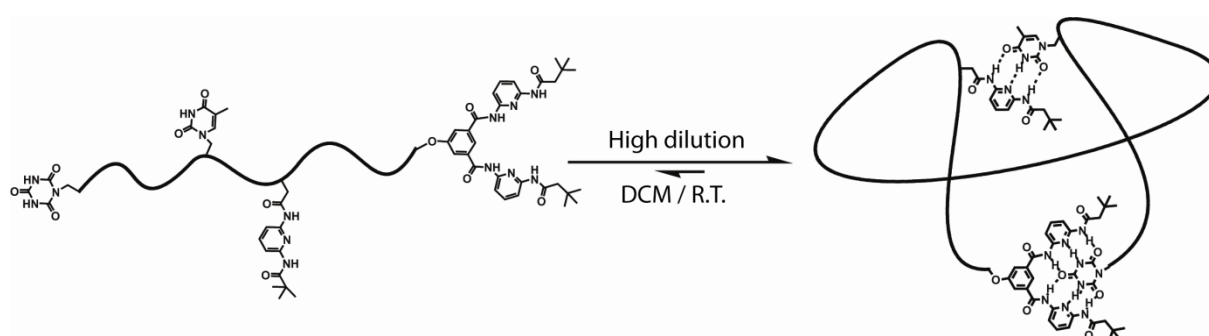


Well-defined functional polymers containing two distinct and mutually orthogonal hydrogen bonding recognition motifs are prepared via a combination of atom transfer radical polymerization (ATRP) and copper catalyzed azide–alkyne cycloaddition (CuAAC). The complementary recognition units are subsequently self-folded as single cyclic chains to emulate – on a simple level – the self-folding behavior of natural biomacromolecules.

4.1 Introduction

The emulation of natural processes and the design of chemical reaction sequences inspired by nature is – or at least should be – one of the most important driving forces for synthetic macromolecular design. Reversible self-folding processes are nature's way to control the conformation of biological polymers. Many proteins undergo folding in solution to yield delicate molecular assemblies stabilized by non-covalent or – in some case – covalent interactions.¹⁻³ Recently, a wide array of synthetic approaches has been designed to conjugate synthetic macromolecules with biological entities, e.g. peptides and proteins,⁴⁻⁶ with a view to employing them as drug or gene delivery vectors.^{7,8} Many of these approaches make use of radical polymerization processes that feature living characteristics⁹⁻¹¹ combined with modular conjugation protocols,¹² some of which fulfill the criteria of a *click* reaction.^{13,14} While such approaches are highly notable, they do not emulate naturally occurring molecules in the strict sense yet rather aim at imparting additional specific characteristics to biomolecules that aid in fulfilling their function within a defined biological context. Only very recently have attempts been made to emulate the folding behavior of natural biomacromolecules – such as proteins – on a simple level, yet based entirely on synthetic polymeric systems.¹⁵⁻¹⁸ The key binding principle in nature revolves around the formation of reversible hydrogen bonds between suitable hydrogen donor and acceptor systems. Thus, it seems appropriate to transfer this concept when attempting to fold synthetic macromolecules to mimic naturally occurring systems. In addition, hydrogen bond-mediated self-assembly is a powerful strategy within supramolecular polymer chemistry.^{19,20} Hydrogen donor/acceptor systems have featured strongly in polymer chemistry – especially over the last decade – and have been employed to construct reversibly forming block copolymers²¹⁻²⁷ star polymers²⁸⁻³² and nanoparticles.³⁴⁻³⁹ Biomolecules typically entail several hydrogen donor/acceptor systems, which lead to the

formation of specific tertiary structures that enable the biomolecules to fulfill a certain function. Importantly, biomolecules undergo single chain folding without the participation of other (identical) biomolecule entities. In the present chapter, the first time generation – based on earlier results of a single chain entropy driven circular α,ω -self-folding presented in chapter 3 of this thesis – of a well-defined synthetic macromolecule which features two pairs of mutually orthogonal hydrogen bonding motifs (cyanuric acid-Hamilton wedge and thymine-diaminopyridine) at well-defined points within the polymer chains is discussed. To achieve the above synthetic aim, atom transfer radical polymerization protocols alongside copper catalyzed [2+3] dipolar cycloaddition chemistry were employed. The orthogonal nature of the employed hydrogen binding motifs is established and evidence – via dynamic and static light scattering and ^1H NMR experiments – that the system undergoes strong, entropy-driven single chain self folding with a high equilibrium constant. The present system thus represents the to-date closest fully synthetic analogue to prepare via statistical polymerization process a biological self-folding macromolecule forming a tertiary structure. Scheme 4.1 represents the generic nature of the target molecule as well as its entropy driven self-folding action.



Scheme 4.1 Mimicking natural protein structures based on two pairs of mutually orthogonal recognition motifs (thymine-diaminopyridine and cyanuric acid-Hamilton wedge) alongside its reversible self-folding process.

4.2 Synthesis

4-(11-Oxo-11-(6-pivalamidopyridin-2-ylamino)undecyloxy)benzoic acid (**1**),¹⁶ propargyl 2-hydroxymethyl-2-(α -bromoisobutyl oxy methyl)-propionate (**2**),⁴⁰ methyl 11-(5-methyl-2,4-dioxo-3,4-dihydropyrimidin-1(2*H*)-yl)undecanoate (**4**),⁴¹ 6-(2,4,6-trioxo-1,3,5-triazinan-1-yl)hexyl 2-bromo-2-methylpropanoate (**7**)¹⁵ and *N*¹,*N*³-bis(6-(3,3-dimethylbutanamido)pyridin-2-yl)-5-(prop-2-ynyloxy)isophthalamide (**13**)¹⁵ were synthesized according to literature procedures.

4.2.1 Synthesis of 2-((2-bromo-2-methylpropanoyloxy)methyl)-2-methyl-3-oxo-3-(prop-2-ynyloxy) propyl 4-(11-oxo-11-(6-pivalamidopyridin-2-ylamino)undecyloxy)benzoate (3**):** Precursor **1** (1 g, 2.01 mmol) was dissolved in 5 mL dry (DMF). Compound **2** (0.516 g, 1.6 mmol) and 4-dimethylaminopyridine (DMAP) (0.025 g, 0.2 mmol) were dissolved in 10 mL of dry DCM and subsequently added to the solution. DCC (0.622 g, 3.01 mmol) was dissolved in 5 mL dry DCM and subsequently added to the mixture. The reaction was carried out at ambient temperature overnight. Solids were filtered off, the filtrate was concentrated and the crude product was purified by column chromatography on silica gel, eluting with *n*-hexane/ethylacetate (2/1) to give the diaminopyridine bearing linker **3** as a viscous liquid (0.874 g, 68%). ¹H NMR (400 MHz, DMSO-*d*₆) δ (ppm) 10.17 (s, 1H), 9.16 (s, 1H), 7.89-7.87 (d, 2H), 7.79-7.71 (m, 2H), 7.61-7.59 (d, 1H), 7.05-7.02 (d, 2H), 4.79 (s, 2H), 4.40 (m, 4H), 4.04 (t, 2H), 3.58 (s, 1H), 2.35 (t, 2H), 1.88 (s, 6H), 1.72 (m, 2H), 1.55 (m, 2H) 1.39-1.18(bm, 26H). ¹³C NMR (100 MHz, DMSO-*d*₆) δ (ppm) 176.63, 172.16, 171.53, 170.25, 164.80, 162.82, 150.42, 150.13, 139.79, 131.34, 121.07, 114.46, 109.93, 109.10, 77.96, 77.92, 67.84, 66.46, 65.28, 59.71, 56.80, 52.60, 46.42, 40.13, 35.96, 30.07, 28.91, 28.79, 28.70, 28.53, 28.46, 26.88, 25.40, 24.95, 20.72, 17.16, 14.05. ESI-MS (M+Na)⁺ C₄₀H₅₄BrN₃O₉ theoretical: 822.29, experimental: 822.30.

4.2.2 Synthesis of 11-(5-methyl-2,4-dioxo-3,4-dihydropyrimidin-1(2*H*)-yl)undecanoic acid (5): A solution of NaOH (1 N, 10 mL) was added to a solution of compound **4** (2 g, 6.17 mmol) in THF/MeOH (2:1, 30 mL). The solution was stirred at ambient temperature for 5 h and subsequently concentrated to a volume of 15 mL. The reaction mixture was poured into 150 mL of water and concentrated HCl was added in a dropwise fashion to generate a white precipitate, which was filtered, washed with water, and dried under vacuum to give compound **5** as a white solid (1.85 g, 97%). ¹H NMR (400 MHz, DMSO-*d*₆) δ (ppm) 11.97 (s, 1H), 11.19 (s, 1H), 7.54 (s, 1H), 3.62 (t, 2H), 2.21 (t, 2H), 1.75 (s, 3H), 1.57-1.48 (bm, 4H), 1.25 (s, 14H). ¹³C NMR (100 MHz, DMSO-*d*₆) δ (ppm) 174.45, 164.17, 150.67, 141.49, 108.08, 46.95, 33.47, 28.79, 28.77, 28.66, 28.55, 28.50, 28.38, 28.27, 25.75, 24.45, 11.78. ESI-MS (M+Na)⁺ C₁₇H₂₈N₂O₄ theoretical: 333.2, experimental: 333.3.

4.2.3 Synthesis of 2-((2-bromo-2-methylpropanoyloxy)methyl)-2-methyl-3-oxo-3-(prop-2-ynyloxy) propyl 11-(5-methyl-2,4-dioxo-3,4-dihydropyrimidin-1(2*H*)-yl)undecanoate (6): Precursor **5** (0.5 g, 1.61 mmol) was dissolved in 5 mL dry (DMF). Compound **2** (0.414 g, 1.29 mmol) and 4-dimethylaminopyridine (DMAP) (0.02 g, 0.16 mmol) were dissolved in 10 mL dry DCM and subsequently added to the solution. DCC (0.498 g, 2.41 mmol) was dissolved in 5 mL dry DCM and subsequently added to the mixture. The reaction was carried out at ambient temperature overnight. Solids were filtered off, the filtrate was concentrated and the crude product was purified by column chromatography on silica gel, eluting with *n*-hexane/ethylacetate (1/1) to give the thymine bearing linker **6** as a viscous liquid (0.656 g, 83%). ¹H NMR (400 MHz, DMSO-*d*₆) δ 11.19 (s, 1H), 7.53 (s, 1H), 4.75 (s, 2H), 4.26-4.19 (d, 4H), 3.58 (t, 3H), 2.28 (t, 2H), 1.88 (s, 6H), 1.75 (s, 3H), 1.55-1.52 (bm, 4H), 1.49-1.24 (bs, 17H). ¹³C NMR (100 MHz, DMSO-*d*₆) δ (ppm) 172.37, 171.43, 170.19, 164.24, 150.82, 141.39, 108.31, 77.91, 77.87, 66.35, 64.69, 59.57, 56.78, 52.55, 47.08, 46.14, 40.13, 39.92,

39.71, 39.50, 39.29, 39.08, 38.87, 33.46, 33.28, 30.08, 28.79, 28.74, 28.58, 28.39, 28.33, 25.76, 24.41, 24.32, 17.08, 14.05, 11.87. ESI-MS ($M+Na$)⁺ C₂₈H₄₁BrN₂O₈ theoretical: 635.2, experimental: 635.3.

4.2.4 Synthesis of α CA and ω Br Functional Polystyrene (8): To a 50 mL Schlenk tube, styrene (8.0 mL, 6.98 mmol), PMDETA (73 μ L, 0.35 mmol) and **7** (132 mg, 0.35 mmol) in 2 mL of anisole were added and the reaction mixture was degassed by three freeze-pump-thaw cycles and left under argon. CuBr (50 mg, 0.35 mmol) was added to the solution under argon flow. The tube was subsequently placed in a thermostatted oil bath at 110 °C for 30 min. The polymerization mixture was cooled in an ice-bath, diluted via the addition of THF and the copper catalyst was removed by passing through a short column of neutral alumina. The solvent was removed under reduced pressure, subsequently diluted with the addition of DCM and extracted with EDTA solution to remove Cu (a catalyst also complexed by the recognition unit).²⁹ The organic phase was dried over Na₂SO₄, concentrated and subsequently precipitated two times into 80 mL methanol. The polymer was dried for 24 h under high vacuum and afforded a white solid (0.87 g). $M_{n,NMR} = 3100$ Da, $M_{n,SEC} = 3000$ Da, $M_w/M_n = 1.06$. The bromide of polymer **8** was subsequently converted to an azide functionality as described in the chapter 3 (end group fidelity 100%).

4.2.5 Synthesis of α CA and ω Thy Functional Polystyrene (9): α -CA- ω -azide polystyrene (820 mg, 0.26 mmol), compound **6** (244 mg, 0.39 mmol), copper (II) sulfate pentahydrate (132 mg, 0.52 mmol) and sodium ascorbate (105 mg, 0.52 mmol) were dissolved in DMF (10 mL). The resulting mixture was stirred at ambient temperature for 24 h. 40 mL of DCM was added to the solution and extracted two times with 10 mL of EDTA solution to remove Cu (a catalyst also complexed by the recognition unit). The organic phase was dried over Na₂SO₄, concentrated and subsequently precipitated twice in 80 mL methanol. The polymer was dried

for 24 h in a high vacuum to give a yellowish solid (0.92 g). $M_{n,NMR} = 3700$ Da, $M_{n,SEC} = 3900$ Da, $PDI = 1.04$.

4.2.6 Synthesis of CA-PS-Thy-PS-Br (10): Into a 50 mL of Schlenk tube, styrene (6.9 mL, 0.06 mol), PMDETA (12.6 μ L, 0.06 mmol) and **9** (223 mg, 0.06 mmol) in 3.45 mL of anisole were added and the reaction mixture was degassed by three freeze-pump-thaw cycles and left under argon. CuBr (8.6 mg, 0.06 mmol) was added to the solution under argon flow. The tube was subsequently placed in a thermostatted oil bath at 110 °C for 60 min. The crude polymer was purified and dried as described above for **8** to give **10** as white solid (473 mg). $M_{n,NMR} = 7500$ Da, $M_{n,SEC} = 7100$ Da, $PDI = 1.11$. Subsequently, the terminal bromide of polymer **10** was converted to the azide functionality as described above for **8**. ATR-IR (cm^{-1}): 2095 (N_3 stretching). $M_{n,NMR} = 7900$ Da, $M_{n,SEC} = 7700$ Da, $PDI = 1.11$ (end group fidelity 100%).

4.2.7 Synthesis of CA-PS-Thy-PS-DAP (11): CA-PS-Thy-PS-azide (430 mg, 0.054 mmol), compound **3** (65 mg, 0.081 mmol), copper (II) sulfate pentahydrate (27 mg, 0.108 mmol) and sodium ascorbate (21 mg, 0.108 mmol) were dissolved in DMF (10 mL). The resulting mixture was stirred at ambient temperature for 24 h. The crude polymer was purified and dried as described above for **9** to give **11** as white solid (454 mg). $M_{n,NMR} = 8700$ Da, $M_{n,SEC} = 8800$ Da, $PDI = 1.11$.

4.2.8 Synthesis of CA-PS-Thy-PS-DAP-PS-Br (12): Into a 50 mL Schlenk tube, styrene (5.9 mL, 51.5 mmol), PMDETA (9 μ L, 0.043 mmol) and **11** (0.373 g, 0.043 mmol) in 2.95 mL of anisole were added and the reaction mixture was degassed by three freeze-pump-thaw cycles and left under argon. CuBr (6.1 mg, 0.043 mmol) was added to the solution under argon flow. The tube was subsequently placed in a thermostatted oil bath at 110 °C for 40 min. The crude polymer was purified and dried as described above for **8** to give **12** as a white solid (570 mg). $M_{n,SEC} = 14300$ Da, $PDI = 1.16$. Subsequently, the terminal bromide of polymer **12** was

converted to the azide functionality as described above for **8**. ATR-IR (cm^{-1}): 2095 (N_3 stretching). $M_{n,\text{SEC}} = 14200$ Da, $PDI = 1.17$ (end group fidelity 100%).

4.2.9 Synthesis of CA-PS-Thy-PS-DAP-PS-HW (14): The polymer CA-PS-Thy-PS-DAP-PS-Azide (450 mg, 0.031 mmol), compound **13** (65 mg, 0.093 mmol), copper (II) sulfate pentahydrate (23 mg, 0.093 mmol) and sodium ascorbate (19 mg, 0.093 mmol) were dissolved in DMF (10 mL). The resulting mixture was stirred at ambient temperature for 24 h. The crude polymer was purified and dried as described above for **9** to give **14** as white solid. $M_{n,\text{SEC}} = 15400$ Da, $PDI = 1.12$. For an end group fidelity assessment refer to Table 4.1.

4.3 Result and Discussion

In the following the synthesis of the dual self-folding system will be discussed in detail, inclusive of an assessment of the pairwise orthogonal nature of the recognition units. The synthetic section is followed by the investigation of the single chain self-assembly process itself. The self-assembly section can be read independently of the synthetic part.

4.3.1 Synthesis of the Dual Self-Folding System and Orthogonality Assessment

A well-defined dual foldable polymer was sequentially prepared by atom transfer radical polymerization (ATRP) and modular ligation chemistry, which permitted the inclusion of defined folding/unfolding points along the backbone mimicking – on a simple level – a natural protein. The resulting polymer contains two competitive yet pairwise orthogonal hydrogen-bonding pairs. The hydrogen bonding recognition units were based on the three-point thymine-diaminopyridine and the six-point cyanuric acid-Hamilton wedge interactions. The selection of these two pairs is driven by the fact that the selected recognition units must be orthogonal to each other, i.e. no cross-association should take place. The four pair-wise

selected hydrogen-bonding motifs are – to the best of our knowledge – the only combination that fulfills this criterion.⁴¹ It is important to note that the thymine-diaminopyridine features weaker binding than the cyanuric acid-Hamilton wedge system (see below for quantitative binding constant data determined on these system). However, It will be demonstrated that these interactions – which are frequently employed in H-bonding driven polymer assembly – are sufficient to induce single chain-self assembly. The target system was designed to feature a cyanuric acid functional group at the α -position, bearing a thymine and a diaminopyridine functionality at a pre-selected position on the polymer backbone as well as the Hamilton wedge functionality at the ω -position of the single polymer chain (see Scheme 4.1). To tether these functionalities to a single polymer backbone, a cyanuric acid ATRP initiator, linkers bearing a thymine or diaminopyridine, and the alkyne-Hamilton wedge had to first be synthesized. The detailed characterization of the cyanuric acid functional ATRP initiator, the diaminopyridine with carboxylic acid group and the Hamilton wedge with alkyne group can be found in our previously published procedures.¹⁵⁻¹⁶ ¹H NMR spectra of the trifunctional linker compound (**2**), the thymine bearing ester group (**4**) or carboxyl acid (**5**) can be found in the Figure 4.1, Figure 4.2 and Figure 4.3, respectively.

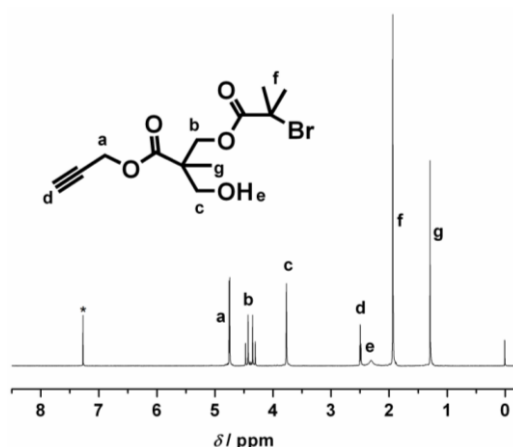


Figure 4.1 ¹H NMR spectrum of 2-hydroxymethyl-2-(α -bromoisobutyloxymethyl)-propionate (**2**) in CDCl₃. The resonance marked with an asterisk is associated with solvent.

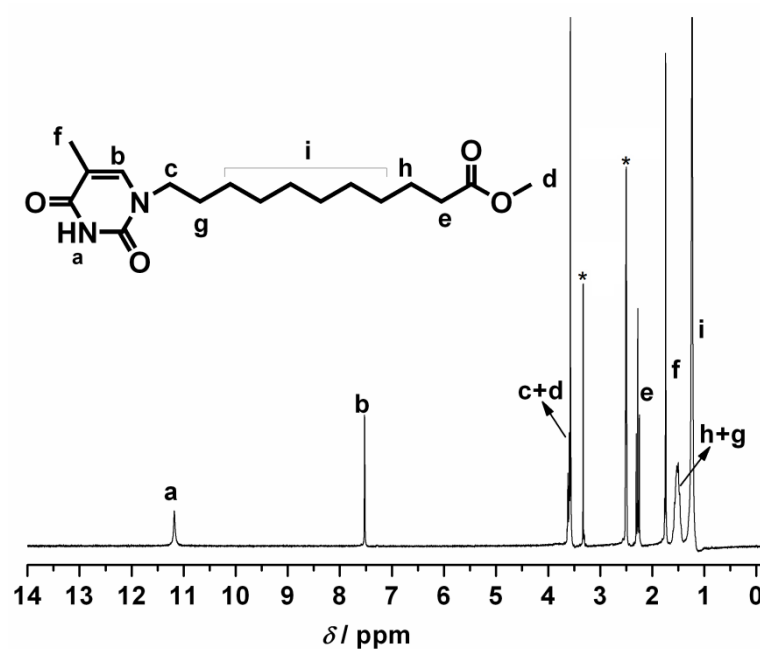


Figure 4.2 ¹H NMR spectrum of methyl 11-(5-methyl-2,4-dioxo-3,4-dihydropyrimidin-1(2H)-yl)undecanoate (4) in DMSO-*d*₆. The resonances marked with an asterisk are associated with solvent/water.

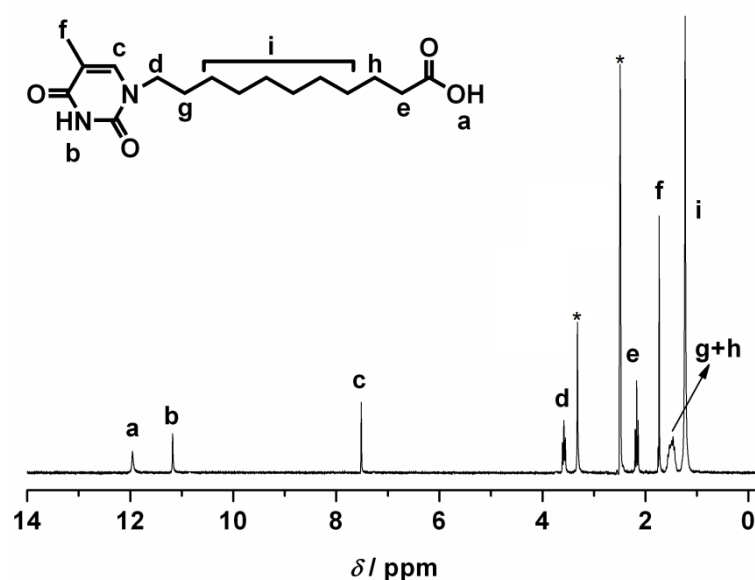
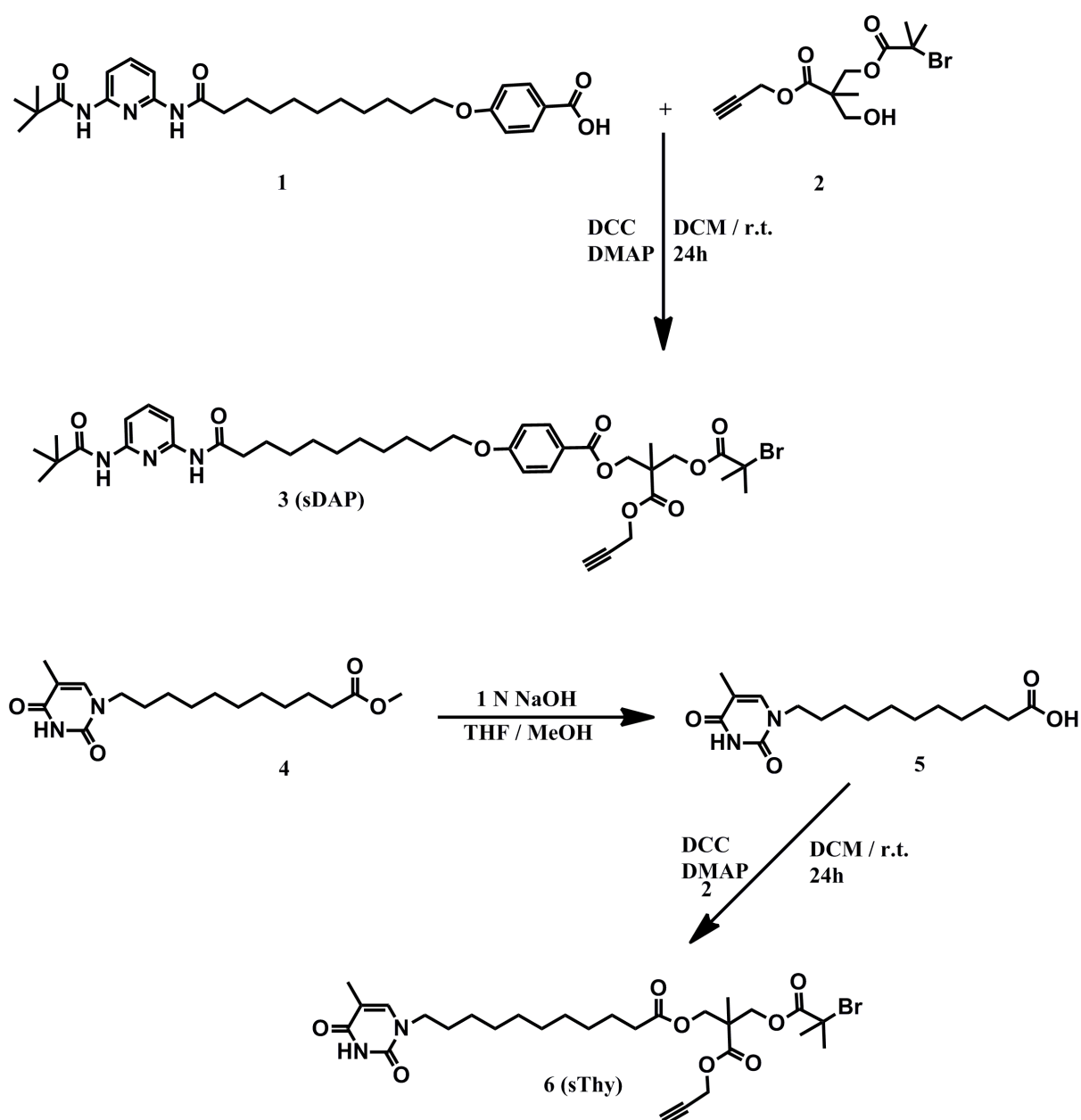


Figure 4.3 ¹H NMR spectrum of 11-(5-methyl-2,4-dioxo-3,4-dihydropyrimidin-1(2H)-yl)undecanoic acid (5) in DMSO-*d*₆. The resonances marked with an asterisk are associated with solvent/water.



Scheme 4.2 Synthetic strategy for the preparation of diaminopyridine (sDAP) (**3**) and thymine (sThy) (**6**) bearing linker compounds.

Initially, a compound bearing diaminopyridine was synthesized via esterification of **1** with **2** in the presence of DCC/DMAP as catalysts and DCM/DMF as solvents. The ^1H NMR spectrum of **3** indicates that the proton signal corresponding to COOH has disappeared and

new characteristic proton signals for the $CCCH_2O$ and $C(CH_3)Br$ are observed at 4.75 ppm and 1.88 ppm, respectively (see Figure 4.4).

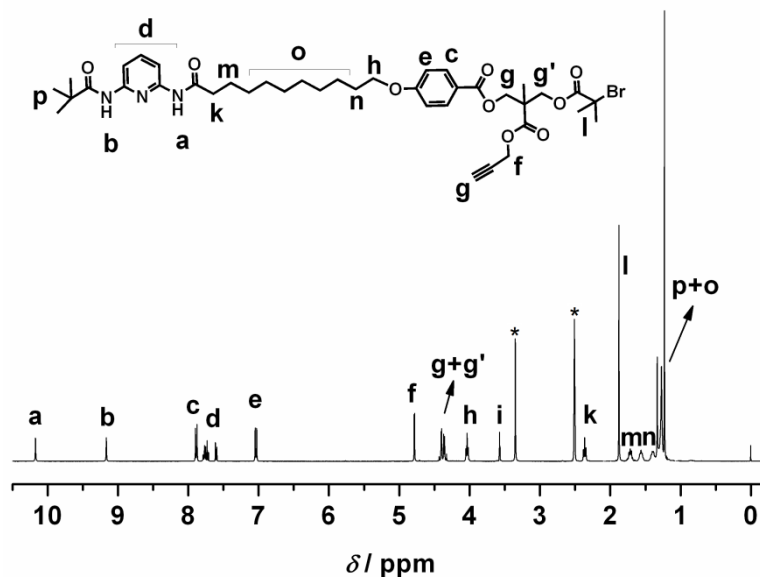


Figure 4.4 1H NMR spectrum of 2-((2-bromo-2-methylpropanoyloxy)methyl)-2-methyl-3-oxo-3-(prop-2-ynyloxy)propyl 11-(5-methyl-2,4-dioxo-3,4-dihydropyrimidin-1(2H)-yl) undecanoate (**3**) in $DMSO-d_6$. The resonances marked with an asterisk are associated with solvent/water.

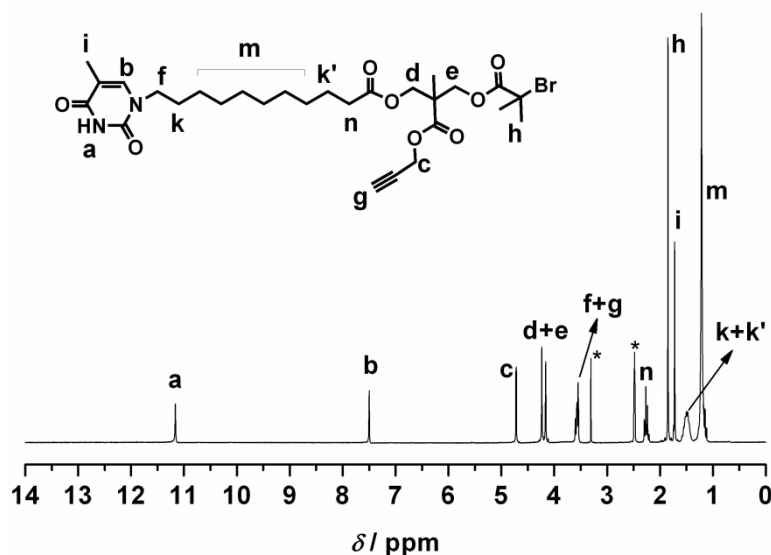


Figure 4.5 1H NMR spectrum of 2-((2-bromo-2-methylpropanoyloxy)methyl)-2-methyl-3-oxo-3-(prop-2-ynyloxy)propyl 11-(5-methyl-2,4-dioxo-3,4-dihydropyrimidin-1(2H)-yl) undecanoate (**6**) in $DMSO-d_6$. The resonances marked with an asterisk are associated with solvent/water.

Subsequently, the hydrolysis of the methyl ester group of **4** was readily accomplished in the presence of 1 N NaOH in a THF/methanol (2/1) mixture. The hydrolytic success was confirmed by ^1H NMR which indicates that the proton signal from the carboxylic acid of **5** can be observed at 12.02 ppm and the proton signal for the methyl group can no longer be seen at 3.80 (see Figure 4.3). The compound bearing a thymine group was synthesized by esterification of compound **2** with compound **5** in the presence of DCC/DMAP as catalysts and DCM/DMF as solvents. The ^1H NMR spectrum of **6** indicates that the proton signal corresponding to COOH has disappeared and new characteristic proton signals for CCCH_2O and $\text{C}(\text{CH}_3)\text{Br}$ are observed at 4.75 ppm and 1.88 ppm, respectively (see Figure 4.5). The structures of the compounds bearing either thymine or diaminopyridine were also confirmed by ^{13}C NMR and ESI-MS.

Before discussing the synthesis of the single polymer chains with two complementary yet orthogonal recognitions pairs at specific positions on the polymer chain (**14**), it is mandatory to investigate the orthogonality of these recognition units to one another via their small (denoted with the prefix 's') molecule analogues (sThy, sCA, sDAP, sHW). The orthogonality of cyanuric acid, the Hamilton wedge, thymine and diaminopyridine has been demonstrated previously by ^1H NMR spectroscopy between a pendant functional polymer and small molecules, yet not in their small molecule state.⁴¹ The orthogonality of the functional recognition units was evidenced in the current study by ^1H NMR spectroscopy in deuterated dichloromethane (CD_2Cl_2)³² solution at the ambient temperature. The self-assembly studies were carried out with the following compounds: sDAP (**3**), sThy (**6**) (see Scheme 4.2 for a structural imagine), sCA (**7**) (see Scheme 4.3 for a structural imagine) and sHW (**13**) (see Scheme 4.4 for structural imagine). The ^1H NMR spectra of sThy (**6**) and sCA (**7**) were independently measured in CD_2Cl_2 at ambient temperature and the NH protons of sThy and

sCA were assigned to peaks at 9.07 ppm and 8.81 ppm, respectively (Figure 4.6a for sCA and Figure 4.6b for sThy). Upon the addition of 1 equiv. of sThy to the solution containing 1 equiv. of sCA, the ^1H NMR spectrum of the mixture of sThy and sCA revealed that there is no interaction between these molecules, however, there is a small shift of the NH signals of sThy and sCA and the signals appear at 9.00 and 8.88 ppm, respectively (see Figure 4.6c). Next, upon the addition of 1 equiv. of sDAP (**3**) to 1 equiv. of sHW (**13**), the ^1H NMR spectrum of the mixture of sDAP and sHW reveals that there is no interaction between sDAP and sHW (see Figure 4.6d). When adding 1 equiv. of sDAP to a mixture of 1 equiv. each of sThy and sCA, the ^1H NMR spectrum of the sDAP-sThy complexes reveal a shift of the imide protons of sThy from 9.00 ppm to 9.52 ppm as well as new proton signals of the complexed sDAP at 8.11 and 8.21 ppm (see Figure 4.7e). The NH protons of sCA are visible at 9.14 ppm (see Figure 4.7e). Subsequently, the addition of 1 equiv. of sHW to a mixture of sCA and the sDAP-sThy complex results in a strong shift of the imide protons of sCA from 9.14 to 12.38 ppm and a new proton signal of the bound sHW at 9.86 and 9.43 ppm was observed in the ^1H NMR spectrum. Furthermore, the NH proton signal of sThy shifts from 9.52 to 9.31 ppm and the NH proton signals of sDAP shifts from 8.11 and 8.21 ppm to the aromatic region (see Figure 4.7f). These results demonstrate the orthogonality of both the three-point sDAP (**3**) – sThy (**6**) and six-point sCA (**7**) – sHW (**13**) interactions on small molecules and evidence no interfering hydrogen-bonding interactions between the two individual recognition pairs. Moreover, the results of these interactions with the small molecules provide useful insights into the NH protons signal shifts, which will aid in the analysis of the precursor and final polymer for the single chain self-assembly.

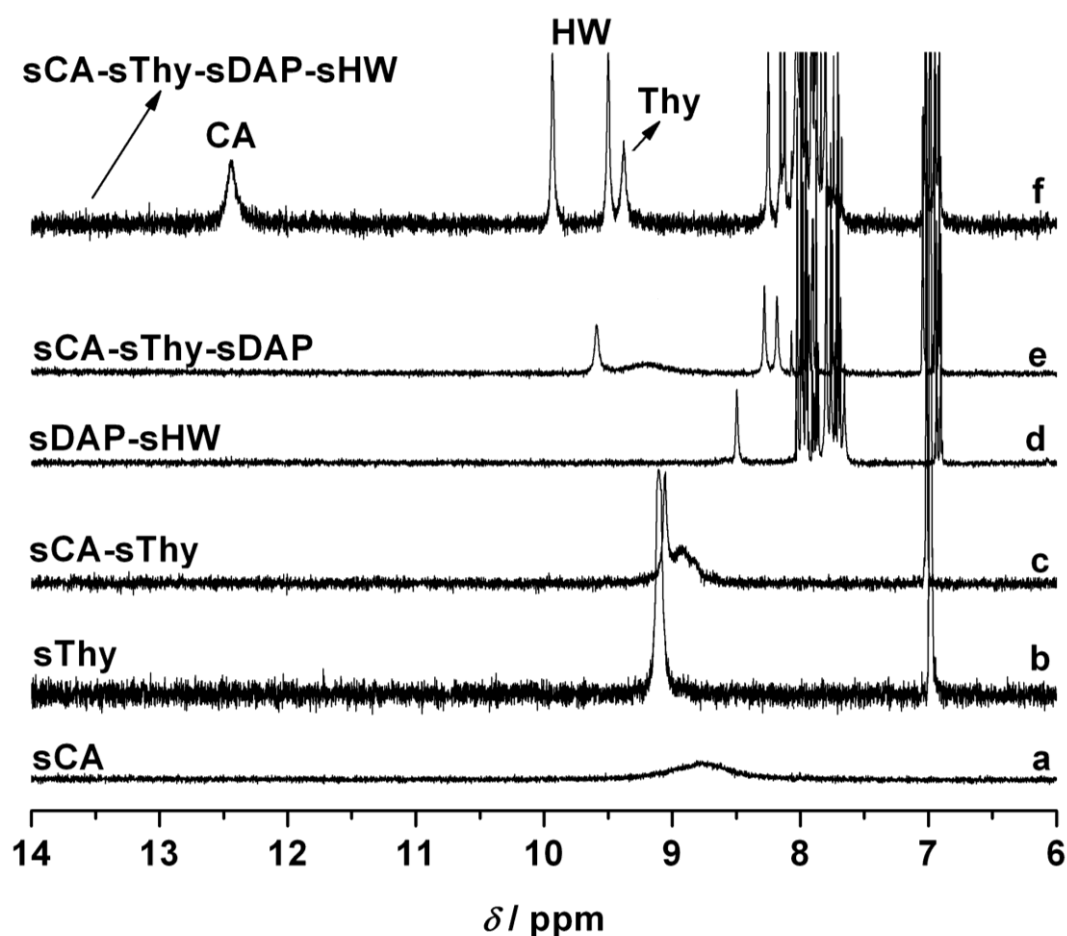


Figure 4.6 ^1H NMR spectra demonstrating the mutually orthogonal hydrogen bonding of Thy-DAP and CA-HW in CD_2Cl_2 at ambient temperature. (a) sCA (**7**), (b) sThy (**6**), (c) sCA-sThy (**6+7**), (d) sDAP-sHW (**3+13**), (e) sCA-sThy-sDAP (**7+6+13**), (f) sCA-sThy-sDAP-sHW (**7+6+3+13**). The concentration of all recognition units was kept constant at 1 mM.

After the synthesis of the functional small molecules and establishing the orthogonal characteristics of the two recognition pairs, a single polymer chain that contained all these complementary recognition pairs at specific positions in its backbone was designed. ATRP and modular ligation chemistry are the preferred synthetic methodologies for the preparation of the complex polymer chain. Subsequently, the halogen end group of the polymers can readily be converted into an azide group enabling the installation of any desired functionality on the polymer chain-end via copper catalyzed azide / alkyne [2+3] dipolar cycloaddition.

To incorporate a cyanuric acid motif at the α -end of a polymer, a **CA-PS-Br (8)** polystyrene was prepared by using **7** as an initiator in the ATRP of styrene with anisole as the solvent in the presence of a CuBr/PMDETA catalytic system at 110 °C for 30 min. The end group fidelity of **8** (i.e. the percentage of chains featuring both a cyanuric acid and bromide terminus) is almost quantitative (calculated from the integral areas of the α -cyanuric acid imide and ω -CHBr protons) in the CA-PS-Br (see Figure 4.7). The NMR derived number average molecular weight ($M_{n,NMR} = \text{Degree of polymerization } (DP_{n,NMR}) \times \text{Molecular weight (MW) of monomer} + \text{MW of initiator (7)} = 26 \times 104.15 + 377 = 3100 \text{ g}\cdot\text{mol}^{-1}$) of CA-PS-Br was calculated by comparing the integrated areas of the aromatic protons of PS at 6.5-7.5 ppm and the two protons of the cyanuric acid end-group at 7.91 ppm. It was found that $M_{n,NMR}$ ($3100 \text{ g}\cdot\text{mol}^{-1}$) was consistent with the number average molecular weight from SEC ($M_{n,SEC} = 3000 \text{ Da}$ with $M_w/M_n = 1.06$) relative to PS standards. The ω -bromide end group of the polymer was quantitatively converted into an azide with NaN_3 in DMF at ambient temperature. From the ^1H NMR spectrum of CA-PS-azide (**8**) (see Figure 4.8), it was observed that a signal at 4.5-4.4 corresponding to CH-Br at the ω -end of the polymer had completely disappeared and a new signal of the CH- N_3 was detected at 3.94 ppm ($M_{n,SEC} = 3000 \text{ Da}$ with $M_w/M_n = 1.06$). Subsequently, copper catalyzed azide-alkyne conjugation chemistry was employed to couple the **8** and **6** in the presence of $\text{CuSO}_4 \times \text{H}_2\text{O}$ /sodium ascorbate in DMF at ambient temperature to give the corresponding **CA-PS-Thy (9)** hetero-functional macroinitiator. The number average molecular weights ($M_{n,NMR} = DP_{n,NMR} \times 104.15 \text{ g}\cdot\text{mol}^{-1} + 990 \text{ g}\cdot\text{mol}^{-1} = 26 \times 104.15 + 990 = 3700 \text{ g}\cdot\text{mol}^{-1}$) and ($M_{n,SEC} = 3900$ with $M_w/M_n = 1.04$) of **CA-PS-Thy (9)** were determined via ^1H NMR and SEC (relative to linear PS standards), respectively.

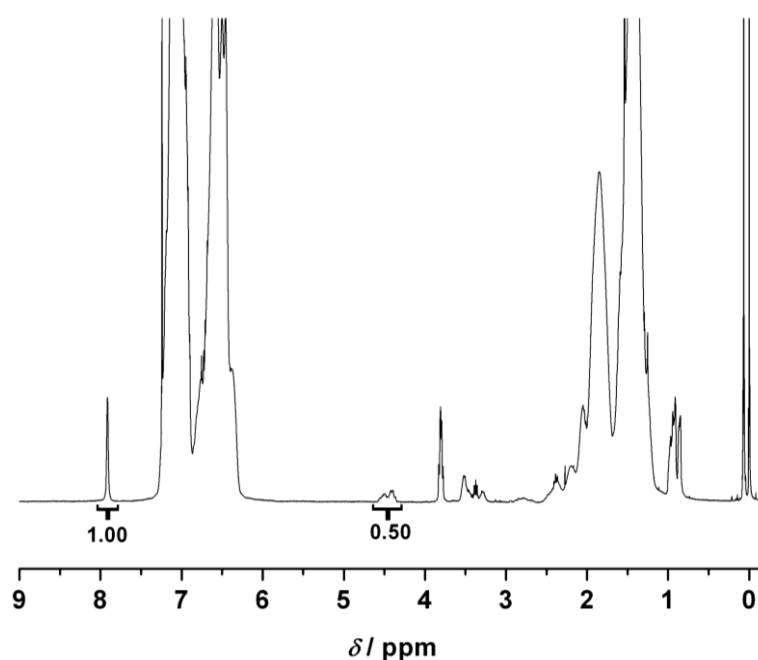


Figure 4.7 ^1H NMR spectrum of **8** in CDCl_3 at ambient temperature. From the ratio of the peak areas NH_2 of CA to CHBr (integral values shown), the end group functionalization can be deduced as being close to $\sim 100\%$.

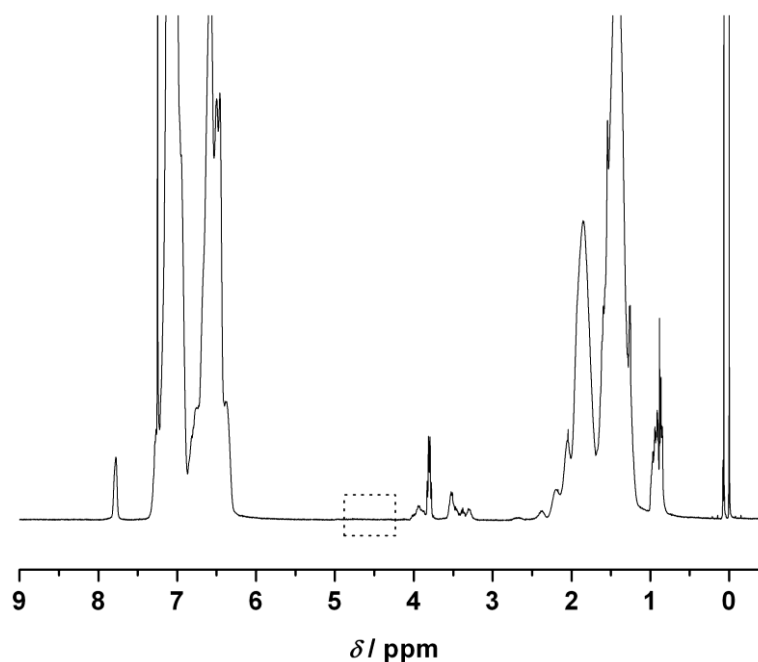
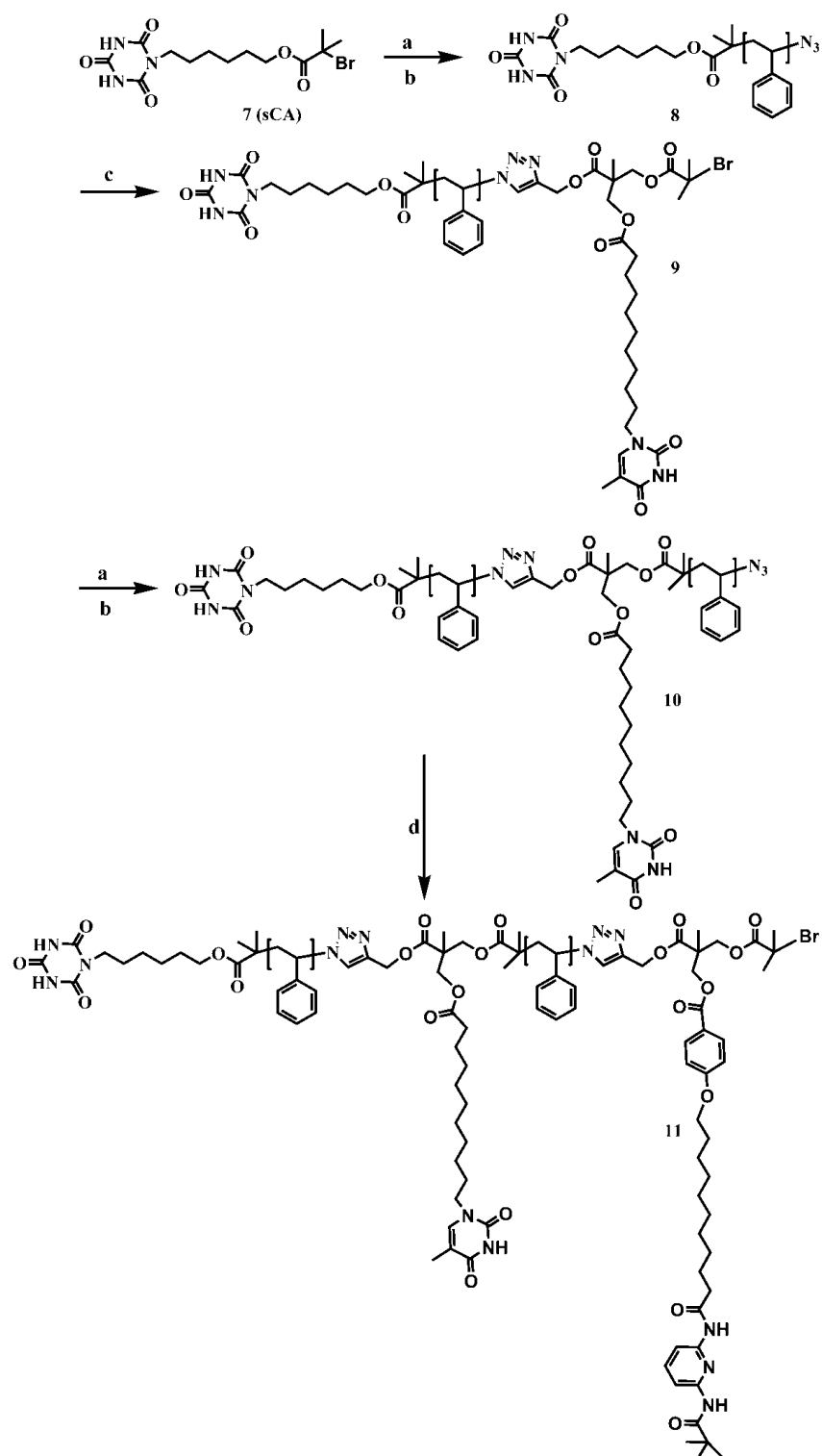


Figure 4.8 ^1H NMR spectrum of **8** with azide functionality in CDCl_3 at ambient temperature. The dashed box within the figure shows that CH-Br of polymer **8** was quantitatively converted to its azide functionality.



Scheme 4.3 Synthetic strategy for preparing α -cyanuric acid, thymine bearing and ω -diaminopyridine functional linear polystyrene. Reagent and conditions: (a) styrene, CuBr, PMDETA, anisole, 110 °C; (b) NaN_3 , DMF, room temperature (r.t.); (c) $CuSO_4 \cdot 5H_2O$, Na ascorbate, **6**, DMF, r.t.; (d) $CuSO_4 \cdot 5H_2O$, Na ascorbate, **3**, DMF, r.t.

From the ^1H NMR spectrum of **9**, it can be observed that a signal at 3.9 corresponding to CH-N_3 of ω -end of the polymer had completely disappeared and new signals of the CH_2 and CH next to triazole ring were detected at 5.22 ppm. The corresponding ester protons of **6** were assigned at 4.22 ppm (see Figure 4.9). Moreover, the SEC trace of **9** indicated a clear shift to the higher molecular weight region (from 3000 Da to 3900 Da), confirming the introduction of **6**.

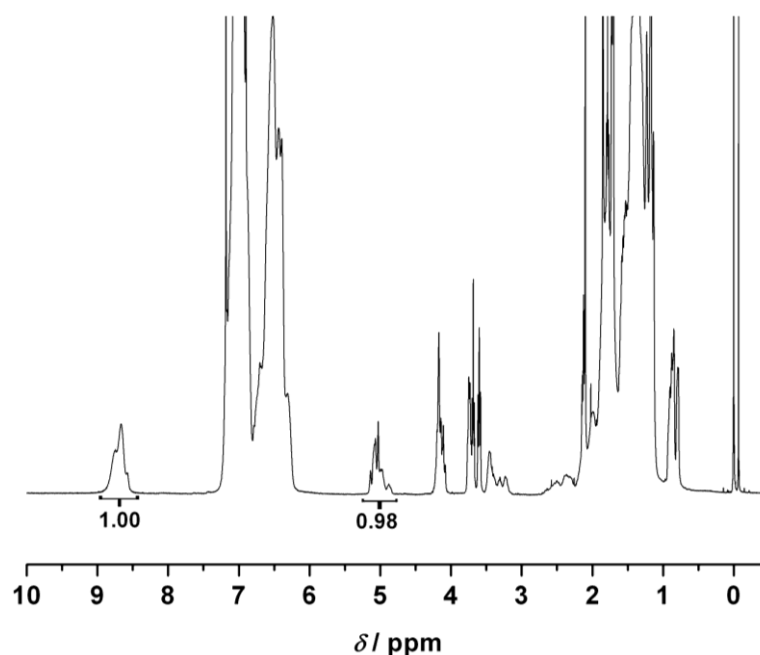


Figure 4.9 ^1H NMR spectrum of **9** in CDCl_3 at ambient temperature. From the ratio of the peak areas NH_2 of CA to CH_2 and CH (next to triazole ring) (integral values shown), the end group functionalization can be deduced as being close to ~98 %.

These results indicate that the **CA-PS-Thy (9)** macroinitiator was quantitatively synthesized via the reaction between the **CA-PS-azide (8)** and compound **6** at ambient temperature. **CA-PS-Thy-PS (10)** was prepared by using **9** as a macroinitiator for the ATRP of St with anisole as a the solvent and a CuBr/PMDETA catalytic system at $110\text{ }^\circ\text{C}$ for 60 min. The SEC elugram for **CA-PS-Thy-PS-Br (10)** shows a clear shift to the higher molecular weight region compared with its corresponding polymeric precursor. The end

group fidelity is ca. 93% (calculated from the integral areas of the imide protons of CA-Thy and ω -CHBr protons) in the **CA-PS-Thy-PS-Br (10)** (see Figure 4.10).

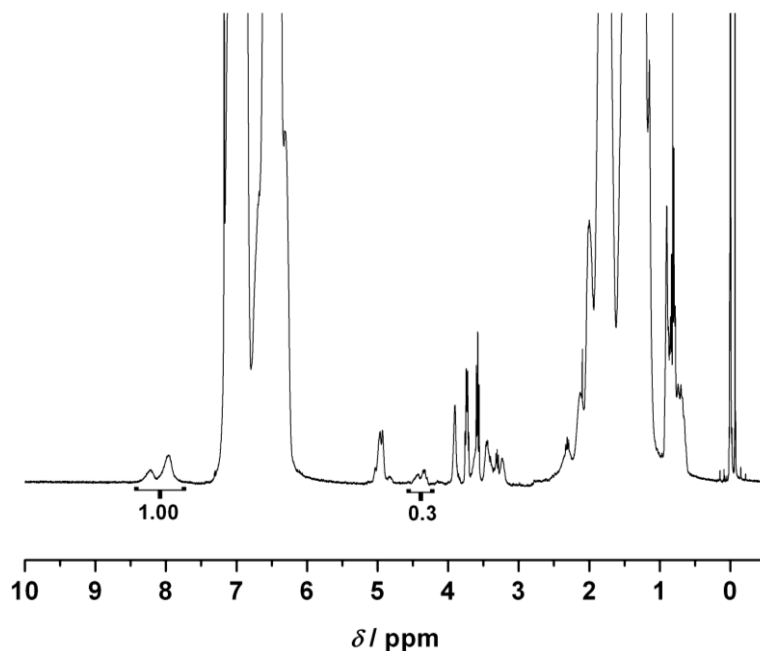
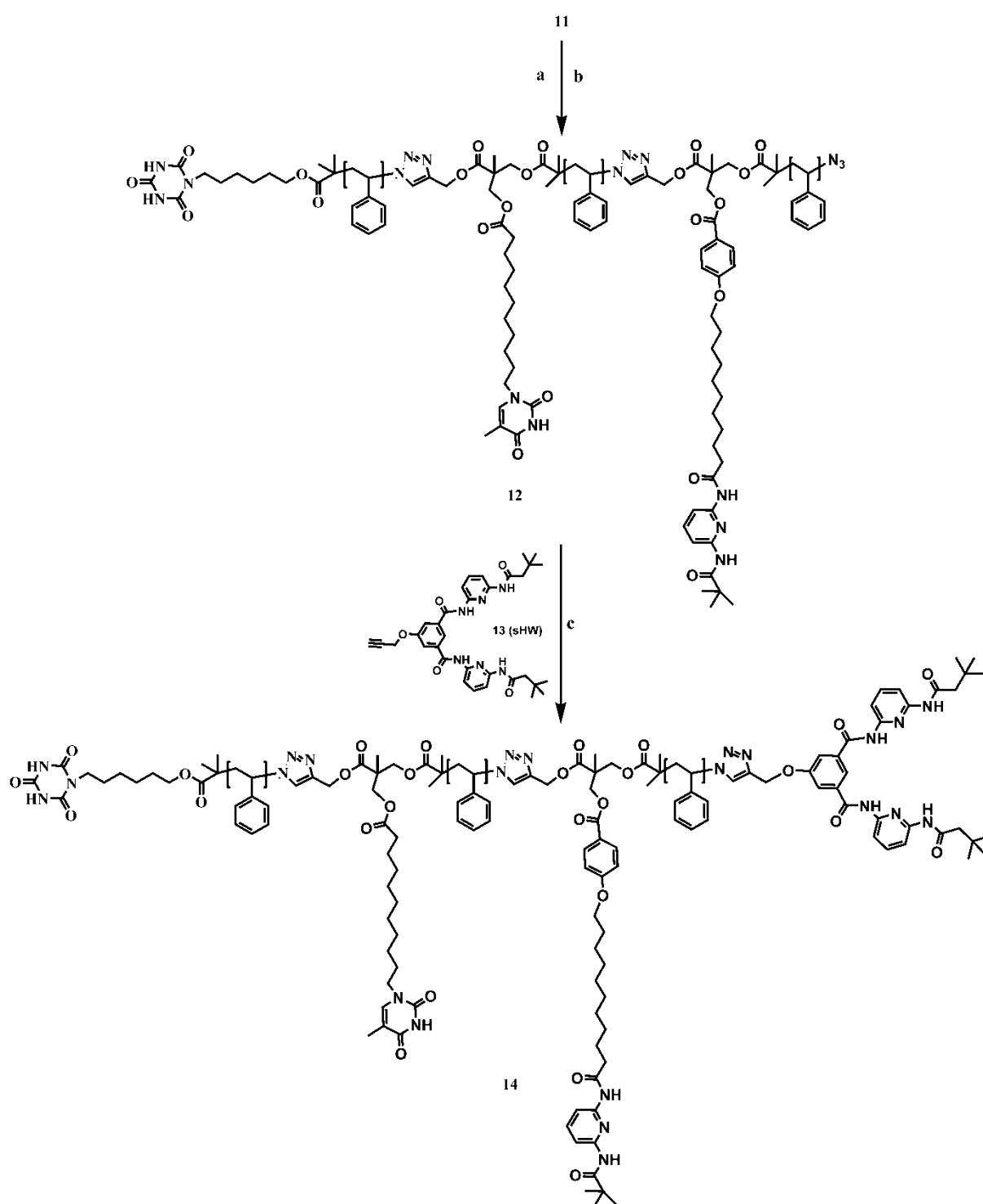


Figure 4.10 ^1H NMR spectrum of **10** in CDCl_3 at ambient temperature. From the ratio of the peak areas **NH** (three protons) of CA and Thy to **CHBr** (one proton) (integral values shown), the end group functionalization can be deduced as being close to ~87 %.

The NMR number average molecular weight ($M_{n,\text{NMR}} = DP_{n,\text{NMR}} \times 104.15 \text{ g}\cdot\text{mol}^{-1} + 990 \text{ g}\cdot\text{mol}^{-1} = 67 \times 104.15 + 990 = 7900 \text{ g}\cdot\text{mol}^{-1}$) of **CA-PS-Thy-PS-Br (10)** was calculated by comparing the integrated areas of the aromatic protons of PS at 6.5 – 7.5 ppm and the three protons of cyanuric acid and thymine imide protons at 7.96 – 8.22 ppm. It is found that $M_{n,\text{NMR}}$ was consistent with the number-average molecular weight from SEC ($M_{n,\text{SEC}} = 7700 \text{ Da}$ with $M_w/M_n = 1.11$). The ω -bromide end group of the polymer was quantitatively converted into an azide in a similar fashion as **8**.



Scheme 4.4 Synthetic strategy for the preparation of α -cyanuric acid, thymine and diaminopyridine bearing and ω -Hamilton wedge functional linear polystyrene. Reagent and reaction conditions: (a) styrene, CuBr, PMDETA, anisole, 110 °C; (b) NaN₃, DMF, ambient temperature (r.t.); (c) CuSO₄×5H₂O, Na ascorbate, **13**, DMF, r.t.

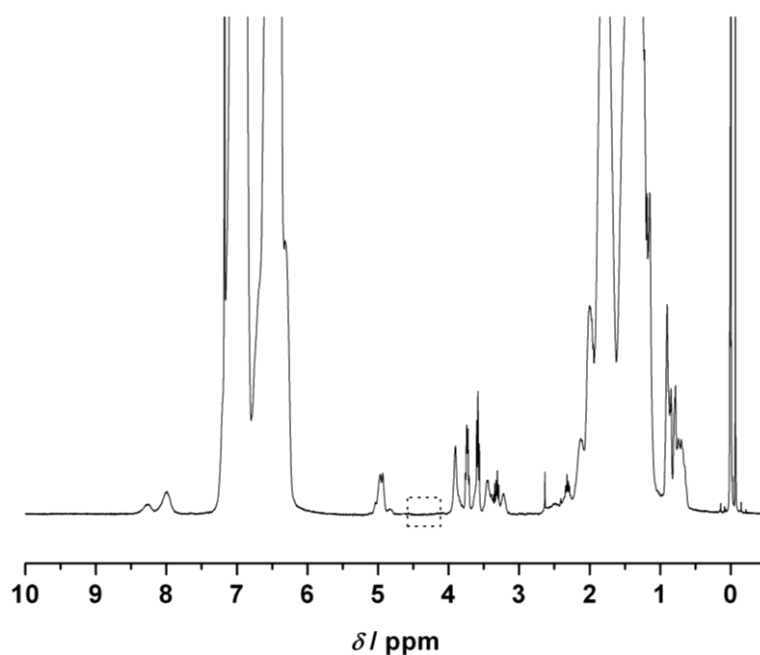


Figure 4.11 ^1H NMR spectrum of **10** with azide functionality in CDCl_3 at ambient temperature. The dashed box within the figure shows that **CH-Br** of polymer **10** was quantitatively converted to its azide functionality.

The ^1H NMR spectrum of **CA-PS-Thy-PS-azide** indicates that a signal at 4.4 corresponding to **CH-Br** of ω -end of the polymer have disappeared (see Figure 4.11). Next, the copper catalyzed azide-alkyne conjugation was undertaken to couple the **CA-PS-Thy-PS-azide** and compound **3** in the same fashion as **9** to give the corresponding **CA-PS-Thy-PS-DAP** heterofunctional macroinitiator. The ^1H NMR spectrum of **CA-PS-Thy-PS-DAP** (**11**) shows that new signals of aromatic protons of **3** at 7.65-7.87 ppm and the corresponding ester protons at 4.28-4.33 ppm of **3** (see Figure 4.12). The SEC trace for **CA-PS-Thy-PS-DAP** (**11**) was clearly shifted to the higher molecular weight region (from 7700 Da to 8800 Da), confirming the introduction of the small molecule **3**. Subsequently, **CA-PS-Thy-PS-DAP-PS-Br** (**12**) was prepared by using **11** as a macroinitiator in the ATRP of St with anisole as a solvent and CuBr/PMDETA as the catalyst system $110\text{ }^\circ\text{C}$ for 40 min. The degree of end group functionalization of **12** cannot be calculated using ^1H NMR, due to the absence of a

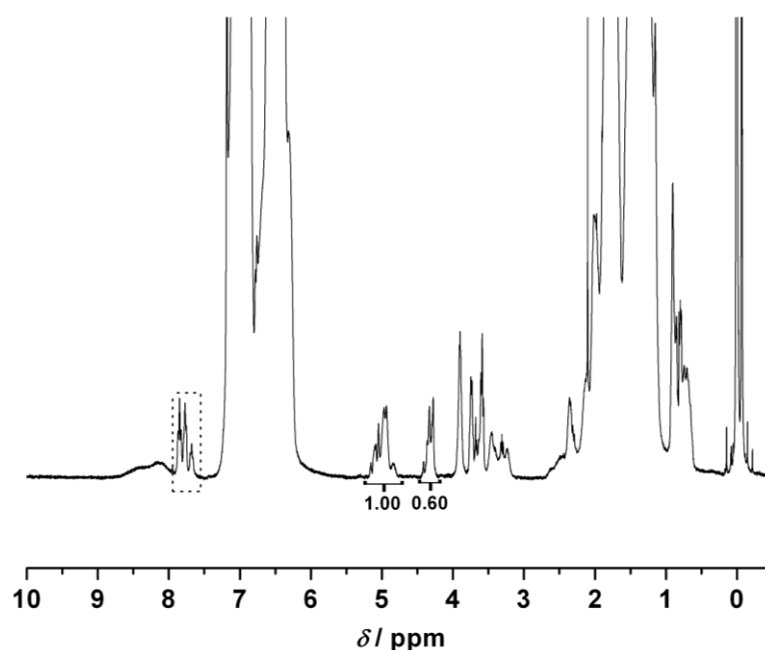


Figure 4.12 ^1H NMR spectrum of **11** in CDCl_3 at ambient temperature. From the ratio of the peak areas $(\text{CH}_2)_2$ and $(\text{CH})_2$ (next to triazole ring) and $\text{C}(\text{OCH}_2)_2$ (integral values shown), the end group fidelity can be deduced as being close to $\sim 91\%$. The dashed box within the figure shows that the aromatic protons of the compound **3**.

separate, non-overlapping peak to compare with the $\omega\text{-CHBr}$ protons of **12**. However, it is reasonable to assume that the end group fidelity of **12** was formed in high yield similar to **8** or **10**. The SEC trace for **CA-PS-Thy-PS-DAP-PS-Br (12)** is clearly shifted to the higher molecular weight region compared with its corresponding polymeric precursor. The ω -bromide end group of the polymer was quantitatively converted into an azide in a similar fashion to **8** and **10**. Copper catalyzed azide-alkyne conjugation chemistry was subsequently employed to couple the **CA-PS-Thy-PS-DAP-PS-azide** and compound **13** in the same fashion as **9** and **11** to give the corresponding **CA-PS-Thy-PS-DAP-PS-HW (14)** heterofunctional polymer chain. The SEC traces (refer to Figure 4.13) indicate a clear shift to higher molecular weight region (from 14300 Da to 15400 Da), confirming the introduction of small molecules **13**. Notably, it was observed that all the SEC curves are monomodal with

low polydispersity index, thus confirming the introduction of functional small molecules and chain extension of the precursor polymers through ATRP and modular ligation chemistry.

Table 4.1 Reaction condition of the ATRP process and the properties of generated polymers, alongside the characteristics of the polymers modified via modular conjugation

Polymer	Monomer	[M ₀]/[I ₀]	Init.	Time (min.)	M _n ^b	M _w /M _n	M _n ^c	Funct. ^d
8^a	Styrene	200	7	30	3000	1.07	3100	100%
9	<i>Modular ligation of polymer-azide and 6</i>				3900	1.04	3700	98%
10^a	Styrene	1000	9	60	7700	1.11	7900	90%
11	<i>Modular ligation of polymer-azide and 3</i>				8800	1.11	8700	91%
12^a	Styrene	1200	11	40	14300	1.16	- ^f	-
14	<i>Modular ligation of polymer-azide and 13</i>				15400	1.12	- ^f	- ^g

^a[I]₀/[PMDETA]₀/[CuBr]₀ = 1:1:1; at 110 °C.

^bDetermined via RI detection SEC using linear PS standards.

^cDetermined from ¹H NMR spectroscopy.

^dDegree of end group functionalization. More details can be found both in the text and the Supporting Information section in Figures S4, S6, S7 and S8.

^eCA-PS-azide; ^fCA-PS-Thy-PS-azide; ^gCA-PS-Thy-PS-DAP-PS-azide.

^fThe end group fidelity of **12** cannot be calculated using ¹H NMR due to the absence of a separate, non-overlapping peak to compare with the ω-CHBr protons of **12**.

^gDue to the absence of a separate peak, it is not possible to calculate the functionalization fidelity. However, based on the efficiency of the previous transformations (which incur an average functionalization loss of 2 to 3% per step), it is expected to be close to 85% for **14**, given the fact that two additional transformations have been carried out going from **11** to **14**.

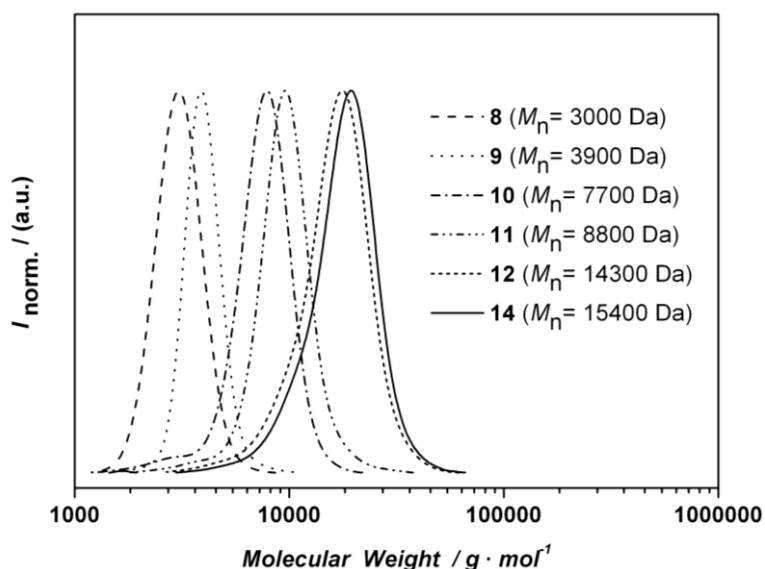


Figure 4.13 SEC traces of the precursor polymers and final polymers. The detailed reaction conditions can be found in Table 1. The structure images of the related polymers can be found in the Scheme 4.3 and Scheme 4.4.

4.3.2 Single Chain Self-Folding of Dual Hydrogen Bonding Macromolecules

The characterization of supramolecular polymers is not feasible with most common polymer characterization techniques due to the fact that H-bonding depends on variables such as solvent, concentration, temperature and pressure. However, ¹H NMR is an efficient, non-invasive and well-known technique to characterize the H-bonding directed self-assembly of polymers, allowing the study of self-assembly in a wide range of concentrations and temperatures. In addition – and critically important – static and dynamic light scattering are key techniques to study self-assembly processes, especially in the present case where it needs to be established whether *true* single chain self-folding occurs or if higher order agglomerates are formed.

Consequently, evidence for the formation of the efficient assembly of **14** through hydrogen bonding was provided by variable temperature ¹H NMR and – most importantly – light scattering methods (SLS and DLS) in CH₂Cl₂ studies at ambient temperature confirm the

single chain self-folding (see below). The hydrogen bond driven self-assembly of a self-folded single polymer chain should lead to a significant down-field shift of the NH protons of the cyanuric acid, Hamilton wedge and thymine moieties. For the ^1H NMR studies, a solution of polymer **14** was prepared in CD_2Cl_2 of 1 mM and left for 12 h at ambient temperature to allow for self-assembly. It was observed that the ^1H NMR spectrum (see Figure 4.14) reveals strong shifts of the amide protons³² of the Hamilton receptor from 7.80 and 8.52 ppm to 9.35 and 9.78 ppm, respectively. New signals appear at 11.93 and 8.46 ppm that correspond to the bound imide protons of cyanuric acid and thymine, respectively, in the self-assembly motif. However, the bound amide protons of diaminopyridine overlap with the resonances of aromatic protons present in **14**.²⁷ It should also be noted that the observed chemical shifts are much smaller for the polymeric systems (i.e. bound imide protons of cyanuric acid at 11.93 ppm) (see Figure 4.14) compared with signals for small molecules (i.e. bound imide protons of cyanuric acid at 12.38 ppm) (see Figure 4.6), indicating that the presence of the bulky polymeric chains affect the association ability of complementary hydrogen-bonding moieties, possibly due to the altered accessibility within the polymeric system.^{16,31} The temperature and time stability of these hydrogen bonds were additionally investigated via ^1H NMR. The ^1H NMR spectra (see Figure 4.14 of the polymer **14** did not show any significant change after prolonged standing (ca. 7 days), an observation which revealed that the single chain self-folding of **14** was stable in CD_2Cl_2 solution for long periods. The supramolecular hydrogen-bonded assemblies undergo continuous self-assembly and disassembly processes; the dynamic character of these systems can be revealed by temperature dependent ^1H NMR spectroscopy.⁴² For temperature based ^1H NMR studies, a solution of **14** was prepared in $[\text{D}_2]$ tetrachloroethane at a concentration of 1 mM and left for 12 h at ambient temperature to allow for self-assembly.

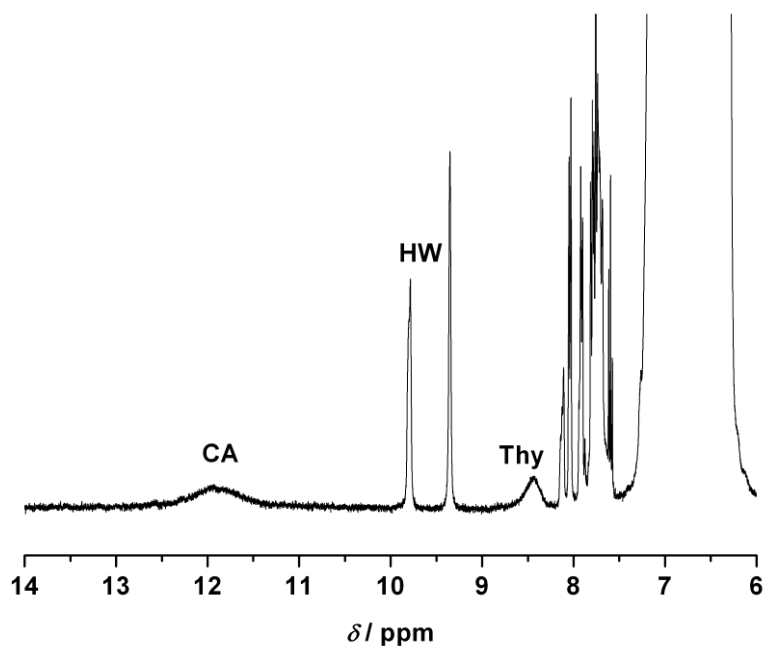


Figure 4.14 Expanded ^1H NMR of (single chain) self-folded of the polymer **14** (proven by DLS and SLS, see below) in CD_2Cl_2 at ambient temperature showing bound imide protons of cyanuric acid (CA) and thymine (Thy) as well as amide protons of the Hamilton wedge (HW). The bound amide protons of diaminopyridine (DAP) are overlapping with aromatic protons.

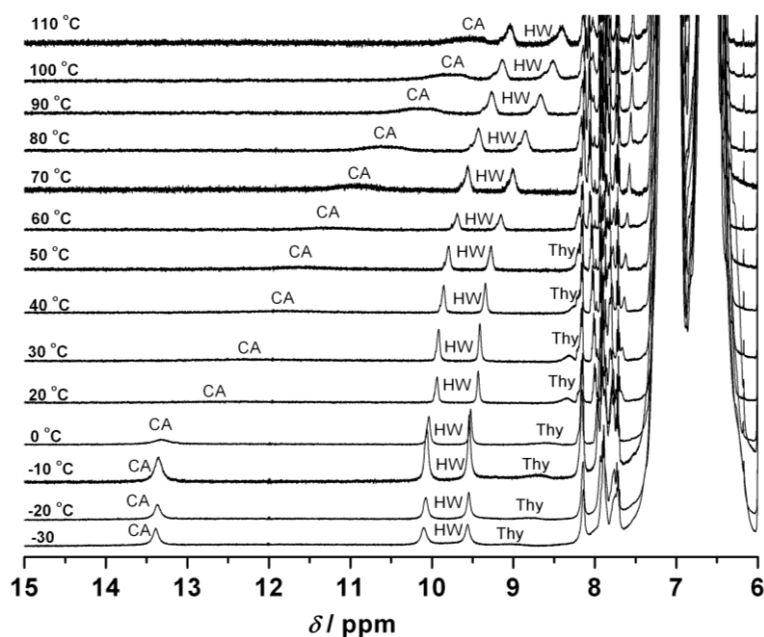


Figure 4.15 Expanded ^1H NMR of single chain self-folding of the polymer **14** (proven by DLS and SLS, see text) in $[\text{D}_2]\text{tetrachloroethane}$ at variable temperatures showing bound

imide protons of cyanuric acid (CA) and thymine (Thy) as well as amide protons of the Hamilton wedge (HW).

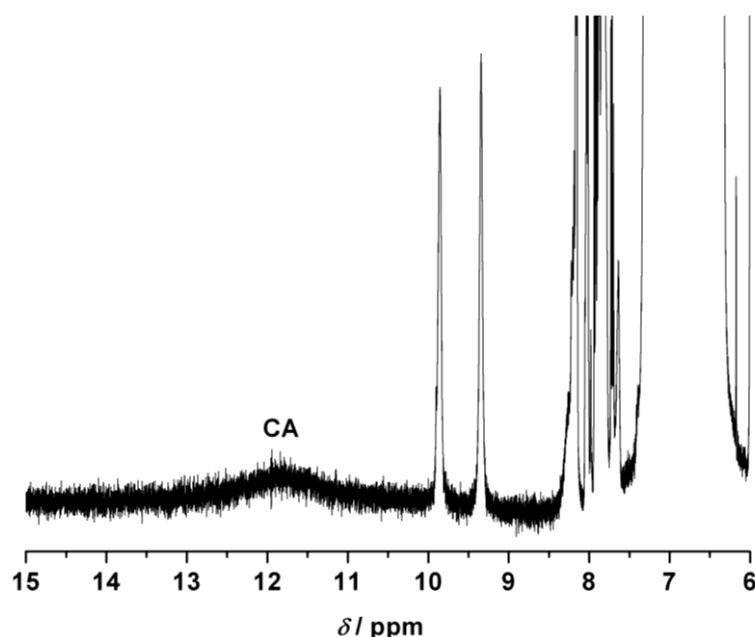


Figure 4.16. Magnified ^1H NMR of single chain self-folded of the polymer **14** in $[\text{D}_2]$ tetrachloroethane at $+40\text{ }^\circ\text{C}$ showing bound imide protons of cyanuric acid (CA).

When the solution is heated from -30 to $110\text{ }^\circ\text{C}$, the ^1H NMR spectra (see Figure 4.15) show a significant down-field shift of the resonances associated with the protons that undergo self-assembly (starting at 13.4 ppm for **CA**, at 10.11 and 9.56 for **HW**, and at 9.10 ppm for **Thy** of polymer **14** at $-30\text{ }^\circ\text{C}$ due to the stronger associations between the recognition units).⁴² These results suggest that at low temperatures the association-dissociation equilibrium is slow on the NMR time scale. Moreover, it can be concluded that by lowering the temperature the thermodynamic equilibrium is shifted towards the self-folded species and indicates the formation of stabilized structures.⁴³ It is also evident from Figure 4.15 that in the temperature range between $+20$ and $+50\text{ }^\circ\text{C}$ the imide protons of **CA** and between 0 and $-30\text{ }^\circ\text{C}$ the imide protons of **Thy** are in a coalescence regime, where the signals of the bounded NH protons are very broad or cannot be detected anymore.^{43,44} The up-field shift of these signals upon

increasing the temperature indicates the decreasing stability of the self-folded single polymer chain.^{42,43} When the solution of polymer **14** is cooled (inside the NMR probe head) from -110 to -30 °C, the same NMR spectra as depicted in Figure 4.15 are obtained. Thus, the changing chemical shifts for the imide protons of **14** evidence the gradual reversibility of the single chain folding/unfolding process as a function of temperature. Moreover, upon magnification the CA imide protons between +30 and +60 are clearly visible as a broad signal (see Figure 4.16). Furthermore, an earlier reported and established mathematical model^{31,45} was employed to deduce the binding constants (K_{ass}) between Thy and DAP, which were found to be close to 653 M^{-1} for the Thy-DAP and $2.4 \times 10^6 \text{ M}^{-1}$ for the CA-HW system.

Mathematical model chosen to determine K_{ass} : The data were fitted to the following equation to provide K_{ass} :

$$\delta_{\text{obs}} = \delta_{\text{H}} + \frac{(\delta_{\text{HG}} - \delta_{\text{H}}) \left\{ \left([\text{H}_t] + [\text{G}_t] + \frac{1}{K_a} \right) - \left(\left([\text{H}_t] + [\text{G}_t] + \frac{1}{K_a} \right)^2 - 4[\text{H}_t][\text{G}_t] \right)^{1/2} \right\}}{2[\text{H}_t]} \quad (\text{eq. 4.1})$$

where the experimentally determined parameters are as follows: $[\text{G}_t]$ and $[\text{H}_t]$, the total guest and host concentrations, respectively, δ_{obs} the observed shift, and δ_{H} , the shift of the host in the absence of guest and δ_{HG} the shift in the fully associated system. K_a is obtained by implicitly solving the above equation via a fitting exercise to match the resulting δ_{obs} with its experimentally found value.

The values provided in the table 4.2 are taken from chapter 3 where the small molecule association between Thy (polymer terminus, **21**, in the Scheme 3.4 of the chapter 3), DAP (small molecule, **17**, in the Scheme 3.4 of the chapter 3) and CA (polymer terminus, **11**, in the Scheme 3.3 of the chapter 3) as well as HW (small molecule, **10**, Scheme 3.3 of the chapter)

was followed by ^1H NMR in a concentration dependent series going to full association (to obtain δ_{HG}), whose values are listed in the below table.

Table 4.2 Chemical shifts and concentrations of the recognition units, which are used in the mathematical model above.

Recognition Units	Concentrations	δ_{obs} / ppm	δ_{H} / ppm ⁴⁶	δ_{HG} / ppm ⁴⁶
Thymine	1×10^{-3} mol L ⁻¹	9.10	7.87	11.83
Cyanuric acid	1×10^{-3} mol L ⁻¹	13.39	7.98	13.50

The six-point hydrogen bonding (CA-HW) exhibits – not surprisingly – significantly larger binding interactions between host and guest than the three-point hydrogen bonding system (Thy-DAP). These binding constants are in the range of those observed and successfully employed in typical H-bonding polymeric systems. For example, the K_{ass} of the H-bonding polymeric chains in halogenated solvents are between 10^2 and 10^3 M⁻¹ for the Thy-DAP and 10^6 to 10^7 M⁻¹ for the CA-HW system, respectively.^{31,47} In addition, it is important to establish if **14** can be folded and unfolded at will and the switch can be observed via ^1H NMR. The disassembly of **14** can be achieved by adding a co-solvent that perturbs the hydrogen bond formation such as methanol.⁴⁸ After recording an ^1H NMR spectrum of polymer **14** in CD_2Cl_2 in 1 mM concentration (see Figure 4.14), 7 μL d-methanol (approximately one drop, leading to a methanol concentration of 0.17 mol L⁻¹) were added to the solution and the ^1H NMR spectrum (see Figure 4.17) was recorded again. Inspection of Figure 4.17 clearly indicates that no resonances are visible anymore between 8.5 ppm and 13.5 ppm corresponding to the protons of Thy, HW and CA in their bound state (compare to the spectrum depicted in Figure 4.14).

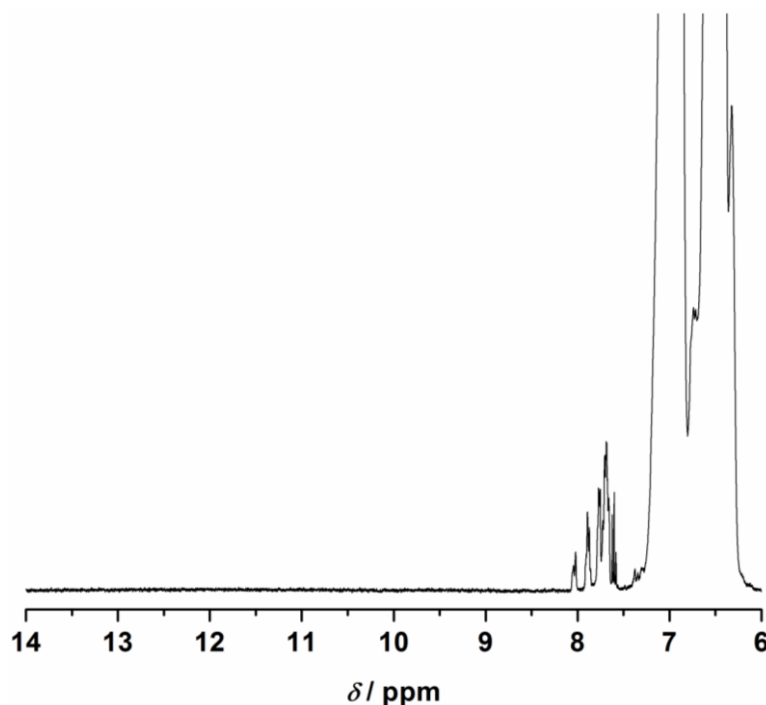


Figure 4.17 Magnified ^1H NMR of polymer **14** in CD_2Cl_2 and CD_3OD ($c_{\text{d-methanol}} = 0.17 \text{ mol}\cdot\text{L}^{-1}$) in 2 mM concentration at the ambient temperature.

While ^1H NMR is very useful to assess the magnitude of the association process, only light scattering techniques can provide information about the single chain folded nature of the bioinspired material **14**. Via SLS it is possible to demonstrate that the molecular weight of polymer **14** at high dilutions corresponds to the molecular weight determined *via* SEC analysis of the same polymer. Such an observation implies that polymer **14** is a truly single chain folded system, as otherwise a higher molecular weight – caused by chain-chain association – would be observed.

SLS provides information on the time-averaged properties of the system. The apparent weight average molecular weight (M_w) can be obtained by the Debye relationship:

$$\frac{KC}{I_r} = \frac{1}{M_w} \left(1 + \frac{R_g^2 q^2}{3} \right) + 2A_2 C \quad (\text{eq. 1})$$

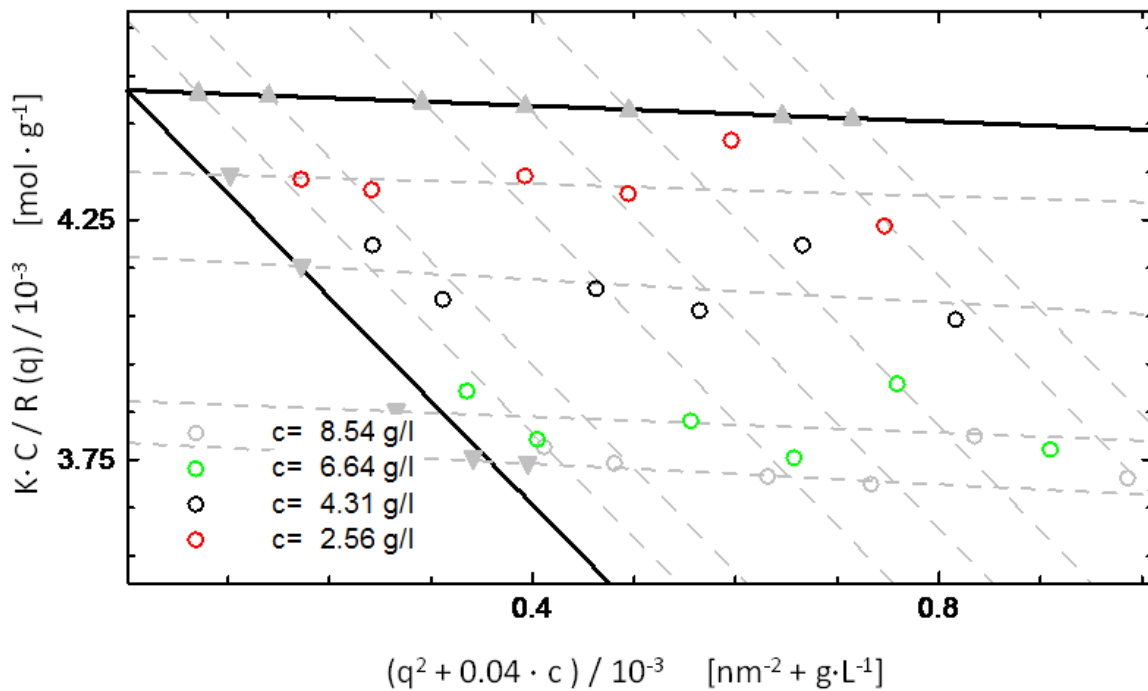


Figure 4.18 Zimm-plot obtained by SLS measurement for polymer **14** dissolved in dichloromethane.

where C is the concentration (in $\text{g}\cdot\text{L}^{-1}$), I_r is the relative excess scattering intensity, K gathered optical parameters, R_g is the radius of gyration, q is scattering wave vector, and A_2 is the second virial coefficient. Plotting all Kc/R points for polymer **14** in dichloromethane at different values of concentration and angle result on a Zimm plot which is showed Figure 4.18. The M_w was obtained by extrapolating $\frac{KC}{I_r}$ values to $q = 0$ (higher black line) and $C = 0$ (left most black line) according to eq. 1. SLS obtained molecular weights are collected in Table 4.3, alongside the SEC determined numbers. Inspection of Table 4.3 immediately demonstrates that the SEC in THF and SLS in dichloromethane determined molecular weight averages are identical for polymer **14**. In addition, we have also determined

the average molecular weight of **14** in dichloromethane with small amount of methanol (7 μL), in which the same value is obtained as in dichloromethane alone. The reason for adding methanol will be detailed in the below DLS section. The SLS measurements are benchmarked against polystyrene (PS) standards ($M_w=17500 \text{ g}\cdot\text{mol}^{-1}$), which are also included in Table 4.3. Furthermore (see Table 4.3), one can notice a difference in the value of the second virial coefficient A_2 – which characterize the interactions polymer/solvent – between the polystyrene standard and polymer **14**. The value of A_2 turns from positive for PS to negative for polymer **14** caused by the presence of the complementary recognition units.

Table 4.3 Characteristics of polystyrene standard and polymer **14** determined by SEC in THF and by SLS in dicholormethane (DCM).

Polymer	M_n^{SEC} (Da)	M_w^{SEC} (Da)	M_w^{SLS} (Da)	A_2^{SLS} ($\text{cm}^3\cdot\text{mol}\cdot\text{g}^2$)
PS standard	17000	17500	17600	$1.01\cdot 10^{-3}$
14	15400	17250	20600	$-6.36\cdot 10^{-4}$
			20400 ^a	$-6.06\cdot 10^{-4}$ ^a

^aDetermined after adding methanol ($C_{\text{methanol}} = 0.17 \text{ mol}\cdot\text{L}^{-1}$) to the DCM solution.

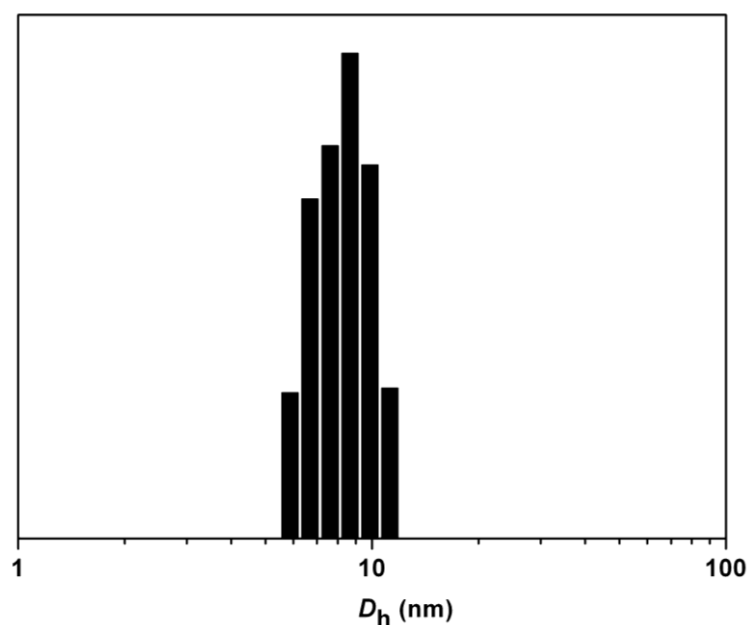


Figure 4.19 Mean hydrodynamic diameter of self-folded single polymer chains (**14**) determined at 90° , in 1 mM concentration in dichloromethane at ambient temperature.

DLS has developed into powerful and versatile tool for estimating the size distribution profile of small particles in suspension or polymers in solution, effective for particles in the size range of a few nanometers up to several micrometers. As a crucial assessment of the efficient formation of self-folded of single polymer chains through H-bonding, comparative DLS analyses were performed in dichloromethane solution. Although the above NMR and SLS experiments suggest that stabilized double cyclic structures occur – due to entropy driven self-assembly – only the measurement of the mean hydrodynamic diameter (D_h , which is the volume weight diameter of the distribution) at variable concentrations can provide unequivocal evidence for single chain circular self-folding.¹⁵⁻¹⁶

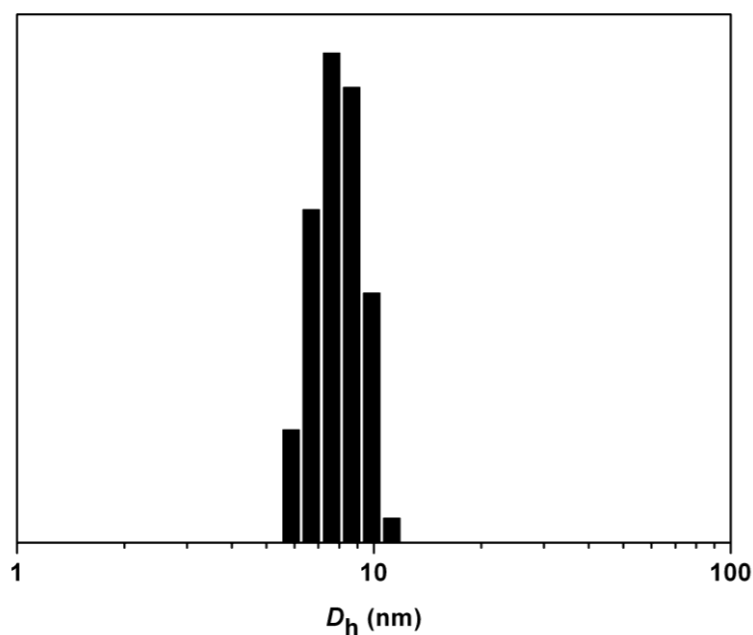


Figure 4.20. The mean diameter of self-folded single polymer chain **14** in 2 mM concentration in dichloromethane at ambient temperature.

Mono-modal particle size distributions could be detected for 1 mM (see Figure 4.19) and 2 mM (see Figure 4.20) solutions of **14**, indicating that – at low concentrations – the predominant species were the single chain self-folded polymers. The D_h of the polymers in these solutions were measured to be 8.0 nm and 8.1 nm at 1 mM and 2 mM, respectively. When the concentration was increased to 3 mM, two signal clusters were observed, a major peak at 8.0 nm and a secondary peak at 17.4 nm (see Figure 4.21). The percentage fractions of this mixture were calculated to be ca. 87% and ca. 13%, respectively. Thus, intermolecular interactions were observed at 3 mM solution of polymer **14**, which evidences that the formation of single chain self-folding of the polymer is dependent on concentration; at higher concentrations dual chain aggregates appear.

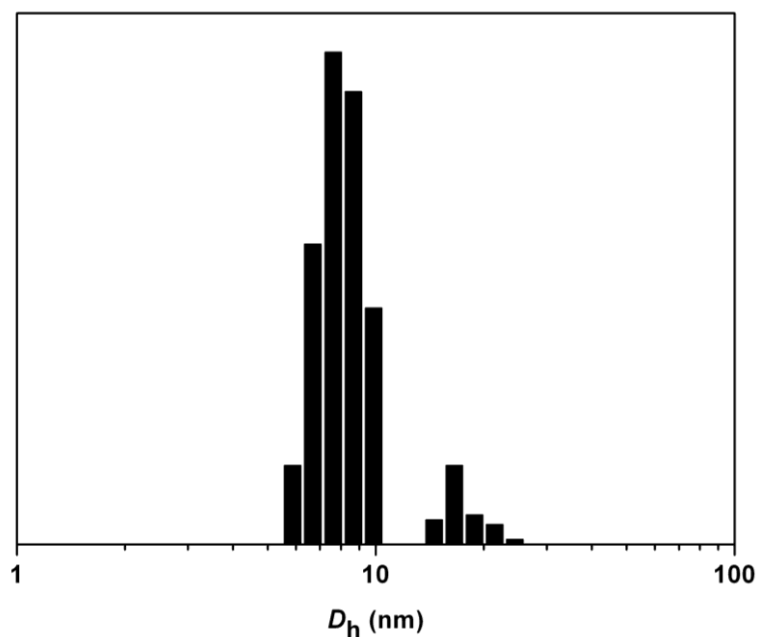


Figure 4.21 The mean hydrodynamic diameters of self-folded single polymer chain (**14**) determined at 90° , in 3 mM concentration in dichloromethane at ambient temperature.

The size distribution obtained at concentrations of 1 and 2 mM of the polymer **14** show that the mean hydrodynamic diameter of polymer **14** does not change with increasing concentrations which indicates the formation of intra-chain assemblies of **14** at these concentrations. Furthermore, the D_h of a system not capable of folding (i.e. PS standards, $M_w = 17500 \text{ g}\cdot\text{mol}^{-1}$) was also determined by DLS in dichloromethane. The D_h of the PS standards was measured as close 8 nm at variable concentrations. The direct comparison of D_h between pure PS and polymer **14** is not advisable as their structure are very different due to the presence of the large hydrogen bonding recognition units in polymer **14** and consequently their behavior in solution should be different. However – at high concentrations (3 mM) – pure PS does *not* present a bimodal size distribution, which indicates that hydrogen bonding is responsible for the formation of inter-chain assemblies of polymer **14** at high concentrations and thus supports the formation of the more compact single-chain self-folded structures of

polymer **14** at low concentrations. The combined ^1H NMR and – critically important – the LS results indicate that in dilute solutions stable self-assemblies with a single chain self-folded structure are formed with significantly reduced exchange processes.

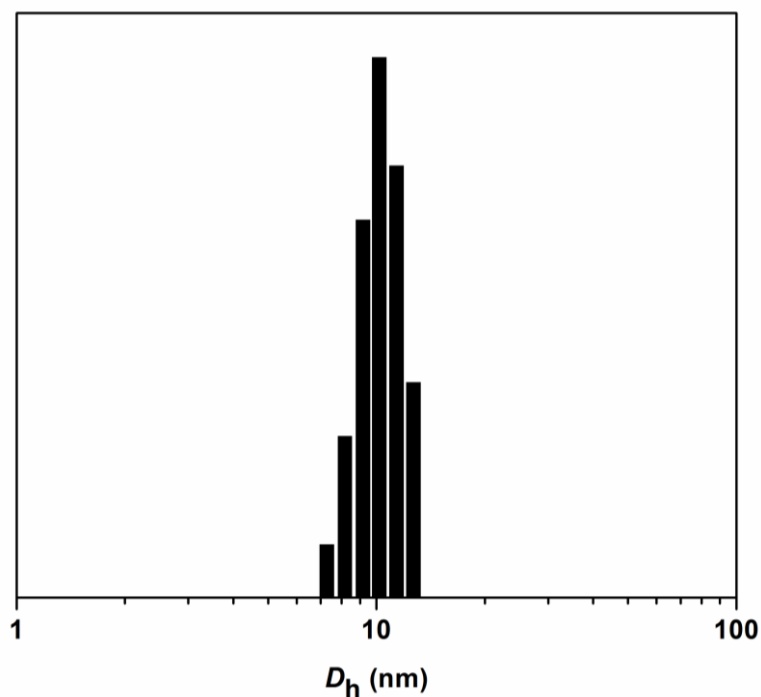


Figure 4.22 The mean diameter of the single polymer chain **14** determined at 90° , in 2 mM concentration in dichloromethane and methanol ($c_{\text{methanol}} = 0.17 \text{ mol}\cdot\text{L}^{-1}$) at ambient temperature.

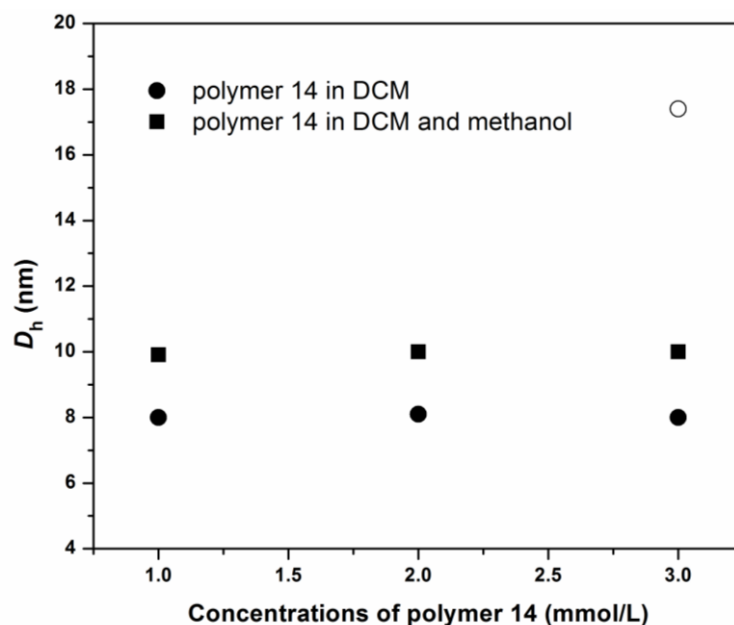


Figure 4.23 The mean diameter of folded structure of polymer **14** in DCM (●) and non-folded structure of polymer **14** in a mixture of dichloromethane and methanol ($c_{\text{methanol}} = 0.17 \text{ mol L}^{-1}$) (■) at different concentrations. Note that at a concentration of 3 mM^{-1} two distributions (open and closed circles) are observed in the system with non-perturbed self-assembly, as higher order structures (not only single chain self-assemblies, i.e. chain-chain assemblies) are formed (please also refer to the full distribution data in Figure 4.22).

Above we have demonstrated that the polymer folding behavior of polymer **14** can be switched at will as evidenced by ^1H NMR spectroscopy (see Figure 4.17). It is now mandatory to carry out DLS measurements to evidence that the D_h also changes upon the addition of the $7 \mu\text{L}$ of methanol.⁴⁸ The DLS measurements are carried out at variable concentrations in CH_2Cl_2 in the presence and absence of methanol (see Figure 4.23). The D_h of **14** in these solutions was determined to be 9.9 nm, 10.0 nm, and 10.0 nm (see Figure 4.23), respectively. Upon addition of methanol, the D_h values significantly increase (to 10 nm) as depicted in Figure 4.22, whereas no change of the M_w is observed by SLS (see Table 4.3). This increase is a substantial change in D_h , which is fully congruent with the disappearance of the resonances associated with the H-bonded system (compare Figure 4.16 vs Figure 4.17).

Notably, in the perturbed system higher aggregates are no longer formed as in the non-perturbed system at higher concentrations (see Figure 4.23, 3 mM⁻¹). These data thus confirm that polymer **14** features a folded structure in 1 mM and 2 mM solution in CH₂Cl₂ at ambient temperature.

4.4 Conclusions

The formation of self-folding of a single polymer chain based on two orthogonal non-covalent interactions, i.e. a cyanuric acid-Hamilton wedge multiple hydrogen bonding and thymine and diaminopyridine triple hydrogen bonding interaction has been demonstrated for the first time. Two linker compounds were prepared: 2-((2-bromo-2-methylpropanoyloxy)methyl)-2-methyl-3-oxo-3-(prop-2-ynyloxy)propyl 4-(11-oxo-11-(6-pivalamidopyridin-2-ylamino)undecyloxy)benzoate (**3**), which bears a diaminopyridine moiety, an alkyne unit, and an initiator for ATRP, as well as 2-((2-bromo-2-methylpropanoyloxy)methyl)-2-methyl-3-oxo-3-(prop-2-ynyloxy)propyl 11-(5-methyl-2,4-dioxo-3,4-dihydropyrimidin-1(2H)-yl)undecanoate (**6**), a thymine moiety, an alkyne unit and an initiator for ATRP. The mutual orthogonality of the two recognition units was confirmed by ¹H NMR in CD₂Cl₂ at ambient temperature. Subsequently – starting from a cyanuric acid functional ATRP initiator **7** – a heterofunctional single polymer chain was prepared by ATRP followed by the insertion of a linker compound through modular ligation chemistry. The well-defined precursor macromolecules were characterized via both ¹H NMR (end group functionalization) and SEC techniques. The self-folding was confirmed by the combination of SLS and DLS data, while temperature dependent ¹H NMR provided information about the magnitude and dynamics of the exchange processes. It was found that the single chain self-folding was dependent on concentration and temperature, with single chain self-folded

structures dominating – or even exclusively occurring – at low temperatures and high dilution regimes. The construction of even more complex single chain supramolecular polymers and their self-folding studies involving non-covalent interactions based on hydrogen bonds and guided by naturally occurring systems are underway in our laboratories, with the ultimate long term aim of developing synthetic methodologies for the preparation of synthetic protein-like structures that can eventually fulfill biological functions.

4.5 References

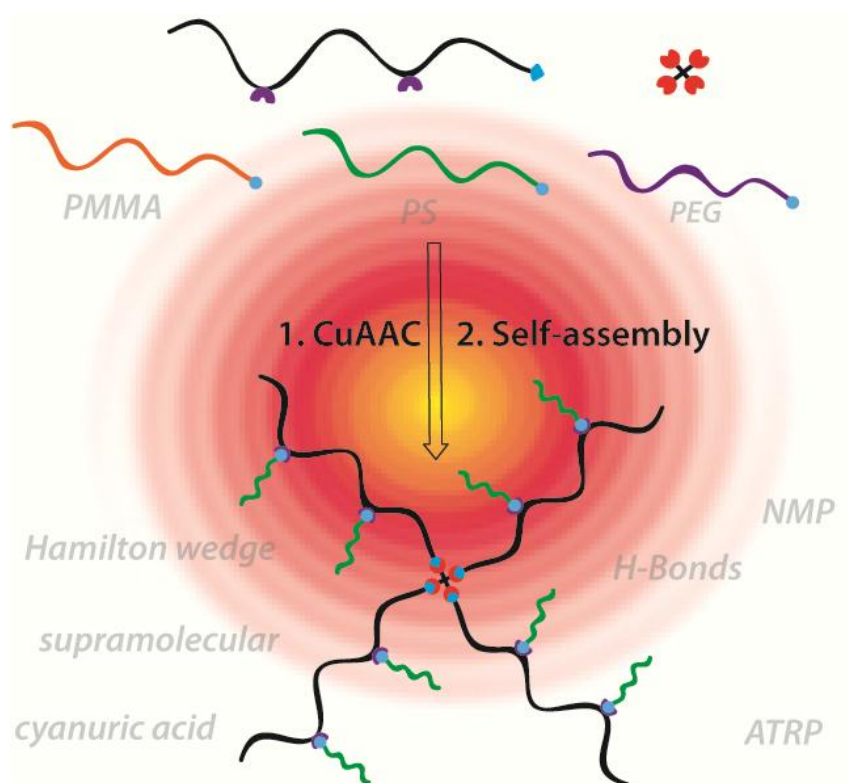
- [1] C. B. Anfinsen, *Science* **1973**, *181*, 223.
- [2] C. M. Dobson, *Nature* **2003**, *426*, 884.
- [3] G. Guichard, I. Huc, *Chem. Commun.* **2011**, *47*, 5933.
- [4] J. Geng, G. Mantovani, L. Tao, J. Nicolas, G. J. Chen, R. Wallis, D. A. Mitchell, B. R. G. Johnson, S. D. Evans and D. M. Haddleton, *J. Am. Chem. Soc.* **2007**, *129*, 15156.
- [5] K. L. Heredia, T. H. Nguyen, C. W. Chang, V. Bulmus, T. P. Davis, H. D. Maynard, *Chem. Commun.* **2008**, 3245.
- [6] V. Bulmus, *Polym. Chem.* **2011**, *2*, 1463.
- [7] P. A. Bertin, J. M. Gibbs, C. K. F. Shen, C. S. Thaxton, W. A. Russin, C. A. Mirkin, S. T. Nguyen, *J. Am. Chem. Soc.* **2006**, *128*, 4168.
- [8] F. J. Xu, W. T. Yang, *Prog. Polym. Sci.* **2011**, *36*, 1099.
- [9] K. Matyjaszewski and J. Xia, *Chem. Rev.* **2001**, *101*, 2921.
- [10] C. J. Hawker, A. W. Bosman, E. Harth, *Chem. Rev.* **2001**, *101*, 3661.
- [11] G. Moad, C. Barner-Kowollik, in *Handbook of RAFT Polymerization*, ed. C. Barner-Kowollik, Wiley-VCH, Weinheim, **2008**.
- [12] O. Altintas, A. P. Vogt, C. Barner-Kowollik, U. Tunca, *Poly. Chem.* **2012**, *3*, 45.
- [13] H. C. Kolb, M. G. Finn and K. B. Sharpless, *Angew. Chem. Int. Ed.* **2001**, *40*, 2004.
- [14] C. Barner-Kowollik, F. E. Du Prez, P. Espeel, C. J. Hawker, T. Junkers, H. Schlaad, W. V. Camp, *Angew. Chem. Int. Ed.* **2011**, *50*, 60.
- [15] O. Altintas, P. Gerstel, N. Dingenouts, C. Barner-Kowollik, *Chem. Commun.* **2010**, *46*, 6291.

- [16] O. Altintas, T. Rudolph, C. Barner-Kowollik, *J. Polym. Sci. Part A: Polym. Chem.* **2011**, *49*, 2566.
- [17] T. Mes, R. van der Weegen, A. R. A. Palmans, E. W. Meijer, *Angew. Chem. Int. Ed.* **2011**, *50*, 5085.
- [18] B. V. K. J. Schmidt, N. Fechler, J. Falkenhagen, J.-F. Lutz, *Nature Chem.* **2011**, *3*, 234.
- [19] L. Brunsveld, B. J. B. Folmer, E. W. Meijer, R. P. Sijbesma, *Chem. Rev.* **2001**, *101*, 4071.
- [20] J.-M. Lehn, *Chem. Soc. Rev.* **2007**, *36*, 151.
- [21] M. N. Highley, J. M. Pollino, E. Hollebeak, M. Weck, *Chem.-Eur. J.* **2005**, *11*, 2946.
- [22] O. A. Scherman, G. B. W. L. Ligthart, R. P. Sijbesma, E. W. Meijer, *Angew. Chem. Int. Ed.* **2006**, *45*, 2072.
- [23] K. E. Feldman, M. J. Kade, T. F. A. de Greef, E. W. Meijer, E. J. Kramer, C. J. Hawker, *Macromolecules* **2008**, *41*, 4694.
- [24] A. V. Ambade, S. K. Yang, M. Weck, *Angew. Chem. Int. Ed.* **2009**, *48*, 2894.
- [25] S. K. Yang, A. V. Ambade, M. Weck, *J. Am. Chem. Soc.* **2010**, *132*, 1637.
- [26] K. E. Feldman, M. J. Kade, E. W. Meijer, E. J. Kramer, C. J. Hawker, *Macromolecules* **2010**, *43*, 5121.
- [27] A. Bertrand, S. Chen, G. Souharce, C. Ladavieere, E. Fleury, J. Bernard, *Macromolecules* **2011**, *44*, 3694.
- [28] E. M. Todd, S. C. Zimmerman, *J. Am. Chem. Soc.* **2007**, *129*, 14534.
- [29] A. Likhitsup, S. Yu, Y.-H. Ng, C. L. L. Chai, E. K. W. Tam, *Chem. Commun.* **2009**, 4070.
- [30] J. Bernard, F. Lortie, B. Fenet, *Macromol. Rapid Commun.* **2009**, *30*, 83.
- [31] S. Chen, A. Bertrand, X. Chang, P. Alcouffe, C. Ladaviere, J.-F. Gerard, F. Lortie, J. Bernard, *Macromolecules* **2010**, *43*, 5981.
- [32] O. Altintas, U. Tunca, C. Barner-Kowollik, *Poly. Chem.* **2011**, *2*, 1146.
- [33] A. T. ten Cate, H. Kooijman, A. L. Spek, R. P. Sijbesma, E. W. Meijer, *J. Am. Chem. Soc.* **2004**, *126*, 3801.
- [34] E. Harth, B. Van Horn, V. Y. Lee, D. S. Germack, C. P. Gonzales, R. D. Miller, C. J. Hawker, *J. Am. Chem. Soc.* **2002**, *124*, 8653.

- [35] A. W. Bosman, A. Heumann, G. Klaerner, D. Benoit, J. M. J. Frechet, C. J. Hawker, *J. Am. Chem. Soc.* **2001**, *123*, 6461.
- [36] T. Terashima, M. Kamigaito, K. Y. Baek, T. Ando and M. Sawamoto, *J. Am. Chem. Soc.* **2003**, *125*, 5288.
- [37] E. J. Foster, E. B. Berda, E. W. Meijer, *J. Am. Chem. Soc.* **2009**, *131*, 6964.
- [38] E. B. Berda, E. J. Foster, E. W. Meijer, *Macromolecules* **2010**, *43*, 1430.
- [39] E. J. Foster, E. B. Berda, E. W. Meijer, *J. Polym. Sci. Part A: Polym. Chem.* **2011**, *49*, 118.
- [40] O. Altintas, G. Hizal, U. Tunca, *J. Polym. Sci. Part A: Polym. Chem.* **2008**, *46*, 1218.
- [41] C. Burd, M. Weck, *Macromolecules* **2005**, *38*, 7225.
- [42] V. Berl, M. Schmutz, M. J. Krische, R. G. Khoury, J.-M. Lehn, *Chem. Eur. J.* **2002**, *8*, 1227.
- [43] K. Hager, A. Franz, A. Hirsch, *Chem. Eur. J.* **2006**, *12*, 2663.
- [44] K. Hager, U. Hartnagel, A. Hirsch, *Eur. J. Org. Chem.* **2007**, *2007*, 1942.
- [45] F. Ilhan, M. Gray, V. M. Rotello, *Macromolecules* **2001**, *34*, 2597.
- [46] O. Altintas, T. Rudolph, C. Barner-Kowollik, *J. Polym. Sci. Part A: Polym. Chem.* **2011**, *49*, 2566.
- [47] W. H. Binder, M. J. Kunz, C. Kluger, G. Hayn, R. Saf, *Macromolecules* **2004**, *37*, 1749.
- [48] F. Wessendorf, Hirsch, *Tetrahedron* **2008**, *64*, 11480.

Complex Macromolecules Architectures via Multiple Hydrogen Bonding

Chapter 5



The self-assembly of well-defined ATRP and NMP prepared polymers with Hamilton Wedge as well as cyanuric acid binding motifs is demonstrated to be an efficient avenue to star, miktoarm star and star block copolymers. The self-assembly process was unambiguously evidenced via H NMR, DLS and SLS analysis.

5.1 Introduction

A branched polymer structure is described as a non-linear polymer with multiple backbone chains growing from junction points.^{1,2} It has been demonstrated that branching results in a more compact structure in comparison to linear counterparts of similar molecular weight, due to the higher segment density of the branched structure, which changes the melt, solution and solid-state properties of the polymer.¹ The properties of polymers depend on their composition and topology.^{3,4} Therefore, precision synthesis of complex macromolecular architectures to control the polymer properties is a key field of study in polymer chemistry.

Star polymers have been generally prepared by living ionic polymerization techniques until recently.^{5,6} In the last decade, with an advance in the living radical polymerization (LRP) routes,⁷⁻¹⁶ the facile synthesis of both linear and star polymers became possible and received widespread attention due to the variety of applicable monomers and greater tolerance to experimental conditions in comparison with living ionic polymerization routes.^{17,18} For instance, atom transfer radical polymerization (ATRP) and nitroxide mediated radical polymerization (NMP) are versatile and robust controlled-living radical polymerization techniques, allowing for fine control over the molecular architecture, molecular weight, and polydispersity of synthetic polymers.^{19,20} In recent years, orthogonal conjugation reactions and their combination with LRP techniques have been increasingly applied towards the preparation of both linear and star polymers due to their efficiency, orthogonality to various functional groups, simple workup as well as compatibility with LRP.²¹⁻²⁴ The connectivity between the individual structural elements of the complex architecture structure is thus covalent.

Supramolecular chemistry – in contrast – is characterized by non-covalent interactions, which play a key role in the assembly, conformation, and/or behavior of supramolecular systems.²⁵ These reversible non-covalent interactions mainly include H-bonding,^{26,27} metal ligand coordination,²⁸⁻³⁰ π - π stacking^{31,32} and ion-dipole interactions.^{33,34} In a similar way, supramolecular polymers can be classified as polymeric systems that utilize these reversible non-covalent interactions to define their assembly, conformation, and/or behavior.³⁵⁻³⁷ Thus, supramolecular polymers can be generated by a single or a combinations of these non-covalent interactions described above. H-bonding has proved to be one of the most prominent supramolecular motifs, due to its ease of accessibility and high binding constants.³⁷ Hydrogen bonds display sensitivity to temperature changes and can form stable associations in a range of solvents.³⁷ H-bonding or its combination with metal-ligand motif has been utilized for the generation of a wide variety of supramolecular polymers, such as homo, block copolymers (di- and multiblock), star, cyclic and dendrimeric polymers.³⁸⁻⁵⁶

However, relatively few studies focusing on the synthesis of supramolecular star polymers via H-bonding interaction have been reported until now. Recently, Zimmerman *et al.* produced linear poly(styrene) (PS) and polylactide terminated with a ditopic H-bonding module and converted these low molecular weight linear polymers into high molecular weight supramolecular star structures through a self-assembly process.⁵⁷ More recently, Tam *et al.* reported the synthesis of linear poly(methyl methacrylate) (PMMA) with a guanosine terminal group generated via atom transfer radical polymerization (ATRP), followed by its self-assembly into the final supramolecular star polymer with eight arms via an addition of potassium picrate as a self-assembling partner.^{58,59} Tam *et al.* demonstrated that the star polymers obtained via

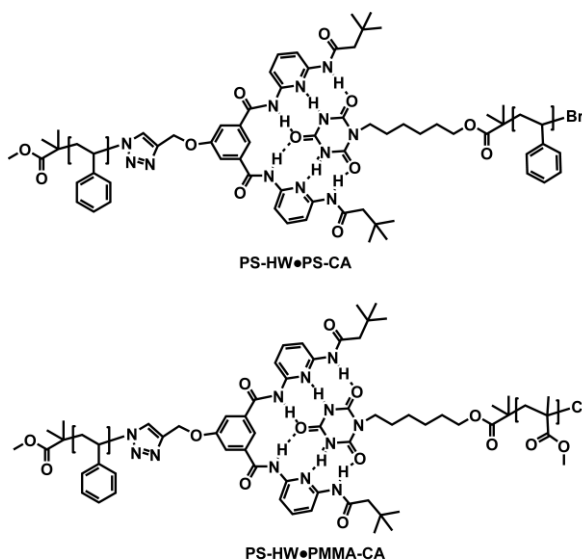
divergent and convergent approaches were identical. Meanwhile, Bernard and colleagues reported the synthesis of supramolecular poly(vinyl acetate) (PVA), which was achieved via reversible addition fragmentation chain transfer (RAFT) polymerized chains with H-bonding motifs – specifically thymine and diaminopyridine derivatives – located at the polymer chain's terminus as well as in a mid-chain position, respectively.⁶⁰ The self-assembly of the PVA chains into an A₃ star polymer in CDCl₃ was successfully demonstrated by ¹H NMR spectroscopy. The same group published the synthesis of AB₂ type miktoarm star polymers using similar supramolecular motifs.⁵⁰ In addition – in the context of the current thesis – the first time preparation of α,ω -hydrogen donor/acceptor (HW/CA) functional polymer strands prepared via a combination of living radical polymerization (ATRP) and orthogonal conjugation is reported. The species are shown to undergo self-assembly as single chains to emulate – on a simple level – the self-folding behavior of natural biomacromolecules.⁶¹

The characterization of supramolecular polymers is not feasible with most common polymer characterization techniques due to the fact that H-bonding depends on the solvent, concentration, temperature and pressure.³⁷ However, ¹H NMR is an efficient, non-invasive and well-known technique to characterize the H-bonding directed self-assembly of polymers, allowing the study of a wide range of concentrations and temperatures.³⁶ Moreover, the self-assembly properties can be characterized by dynamic as well as static light scattering (DLS and SLS) which provide unambiguous evidence for the effect the hydrogen-bonding interactions between the complementary recognition units such as Hamilton wedge (HW) and cyanuric acid (CA) have on the solution properties and sizes of the self-assembled polymers. The

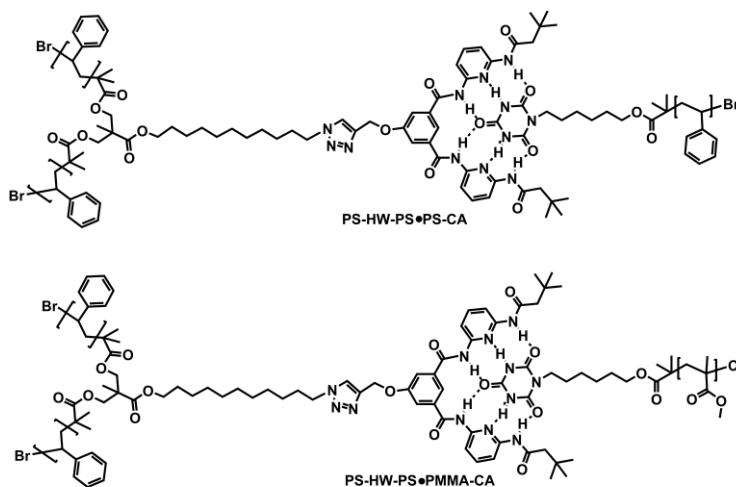
hydrodynamic diameter (D_h) and weight-average molecular weight (M_w) of supramolecular constructed star polymers can be obtained by DLS and SLS measurements, respectively.

In the first part of the current chapter, examples of supramolecular block, star and miktoarm star polymers were prepared using highly binding recognition (HW/CA) units through the combination of ATRP and copper catalyzed azide-alkyne chemistry (CuAAC)⁶². These six-hydrogen bonding motifs were deliberately chosen, as they have extremely high association constants ($K_{\text{ass}} = 10^6 \text{ M}^{-1}$ in CHCl_3).⁴² When HW/CA systems are compared with other motifs employed to produce supramolecular stars (such as the three-hydrogen bonding thymine and diaminopyridine motifs ($K_{\text{ass}} = 120\text{-}140 \text{ M}^{-1}$ in CDCl_3) employed by Bernard *et al.*)⁵⁰ there is an over four order of magnitude increase in the observed association constants. Moreover, the results reported herein provide – for the first time – a calculation of the degree of binding of these supramolecular assemblies via ^1H NMR spectroscopy. The synthesis of well-defined Hamilton Wedge (HW)⁶³ mid- and end-functionalized poly(styrene)s (PS-HW-PS and PS-HW), as well as cyanuric acid end-functionalized poly(methyl methacrylate) (PMMA-CA) and poly(styrene) (PS-CA) is reported. These base polymers are carefully characterized via NMR and size exclusion chromatography. Subsequently, the base macromolecular structures are self-assembled into supramolecular architectures, i.e. PS-HW-PS•PMMA-CA miktoarm star polymer, PS-HW-PS•PS-CA star polymer, PS-HW•PMMA-CA diblock copolymer and PS-HW•PS-CA extended homopolymer in CD_2Cl_2 at ambient temperature, respectively. The self-assembly into the respective PS-HW-PS•PMMA-CA, PS-HW-PS•PS-CA, PS-HW•PMMA-CA and PS-HW•PS-CA structures was established via an extensive ^1H -NMR study. The targeted

structures are depicted in Scheme 5.1 (block copolymers) and Scheme 5.2 (star and miktoarm star polymers). The molecular weight selection for the poly(styrene) and poly(methyl methacrylate) polymers in the range between $3700 \leq M_n / \text{g mol}^{-1} \leq 9000$ is guided by the following considerations: (i) The lower molecular weight material ($< 3000 \text{ g mol}^{-1}$) PS contains a HW, which is not soluble in common organic solvents. Thus, 3000 g mol^{-1} defines the lower molecular weight barrier. (ii) For the self-assembly systems, it is desirable to employ as pure as possible macromolecular building blocks. Unfortunately, when higher molecular weights are targeted ($> 9 \text{ k Da}$), radical-radical coupling reactions occur during the synthesis of high molecular weight poly(styrene) by ATRP (see Figure 5.11). Therefore, the molecular weights employed in the current study present an optimum between solubility and purity.



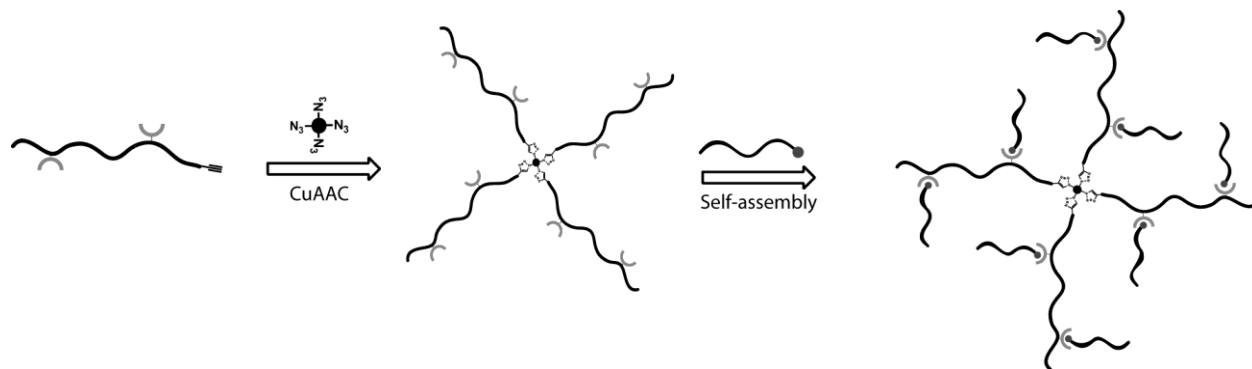
Scheme 5.1 Formation of poly(styrene)-Hamilton Wedge and poly(styrene)-cyanuric acid (PS-HW•PS-CA) as well as poly(styrene)-Hamilton Wedge and poly(methyl methacrylate)-cyanuric acid (PS-HW•PMMA-CA) block copolymers through H-bonding of Hamilton Wedge and cyanuric acid motifs.



Scheme 5.2 Formation of poly(styrene)-Hamilton Wedge and poly(styrene)-cyanuric acid (PS-HW-PS•PS-CA) three arm star and poly(styrene)-Hamilton Wedge and poly(methyl methacrylate)-cyanuric acid (PS-HW-PS•PMMA-CA) miktoarm star polymers through H-bonding via Hamilton Wedge and cyanuric acid motifs.

In the second part of current chapter, the supramolecular construction of well-defined star-shaped macromolecules using highly binding recognition (HW/CA) units. The precursor polymers bearing the recognition units are generated via NMP, ATRP and modular ligation chemistry. The synthesis of a novel alkyne functional NMP initiator, a simple approach to prepare the hydroxyl functional Hamilton wedge (HW) and cyanuric acid end-functionalized poly(ethylene glycol) (PEG-CA) as well as – ultimately – HW-functionalized well-defined star-shaped macromolecules are reported. The polymers are in-depth characterized by ^1H NMR and size exclusion chromatography (SEC). Subsequently, these base macromolecular structures are grafted by self-assembly to obtain supramolecular architectures, i.e. (PS-*g*-PS) $_4$, (PS-*g*-PMMA) $_4$, and (PS-*g*-PEG) $_4$ self-assembled star polymers in CH_2Cl_2 or CD_2Cl_2 at ambient

temperature, respectively. The overall synthetic design concept is depicted in Scheme 5.3. The self-assembled nature of the generated star polymers is verified by ^1H NMR, DLS and SLS studies.



Scheme 5.3 Supramolecular grafting of star-shaped macromolecules generated by NMP and CuAAC via HW/CA complementary recognitions motifs.

5.2 Preparation of Supramolecular Block, Star and Miktoarm Star polymers through Multiple Hydrogen Bonding

5.2.1 Syntheses

2,2,5-Trimethyl-1,3-dioxane-5-carboxylic acid (**1**)⁶⁴, 6-(2,4,6-trioxo-1,3,5-triazinan-1-yl)hexyl 2-bromo-2-methylpropanoate (**8**)⁶¹ mono azide end-functionalized PS (PS-N₃) (**11**)⁶⁵ and the N¹,N³-bis(6-(3,3-dimethylbutanamido)pyridin-2-yl)-5-(prop-2-ynyloxy)isophthalamide (**12**)⁶¹ were synthesized according to literature procedures.

5.2.1.1 Synthesis of 11-bromoundecyl 2,2,5-trimethyl-1,3-dioxane-5-carboxylate (2): 11-bromoundecan-1-ol (1.00 g, 3.98 mmol), **1** (1.04 g, 5.97 mmol) and DMAP (0.073 g, 0.60 mmol) were dissolved in dry DCM (20 mL). DCC (1.85 g, 8.95 mmol) was dissolved in 10 mL dry

DCM and subsequently added to the solution. The reaction was carried out at ambient temperature overnight. Solids were filtered off, the filtrate was concentrated and the crude product was purified via column chromatography on silica gel, eluting with ethyl acetate / *n*-hexane (1/10) to obtain compound **2** as a viscous liquid (1.18 g, yield: 73%). ¹H NMR (400 MHz, CDCl₃) δ (ppm) 4.21-4.10 (q, 2H, CH₂CH₂OCO), 3.66-3.61 (d, 4H, CCH₂O), 3.43-3.38 (t, 2H, BrCH₂), 1.9-1.79 (m, 2H, BrCH₂CH₂), 1.67-1.58 (m, 2H, OCH₂CH₂), 1.43 (s, 3H, CCH₃), 1.39 (s, 3H, CCH₃), 1.28 (bm, 14H, (CH₂)₇), 1.2 (s, 3H, CCH₃). ¹³C NMR (100 MHz, CDCl₃) δ (ppm) 176.05, 98.04, 68.69, 66.04 65.23, 49.06, 33.07, 32.17, 29.14, 29.13, 29.17, 29.75, 28.73, 28.51, 26.43, 26.43, 15.32. ESI-MS (M+Na)⁺ C₁₉H₃₅BrO₄ theoretical: 429.16, experimental: 429.12.

5.2.1.2 Synthesis of 11-bromoundecyl 3-hydroxy-2-(hydroxymethyl)-2-methylpropanoate

(3): Compound **2** (1.00 g, 2.45 mmol) was dissolved in 15 mL of THF and 15 mL of 1 M HCl (aq.) was slowly added to the solution. The reaction mixture was stirred for 4 h. The solution was diluted with DCM and then extract two times with water. The combined organic phases were dried over Na₂SO₄, filtered and evaporated. The crude product was purified via column chromatography on silica gel, eluting with ethyl acetate / *n*-hexane (1/10) to remove residual unreacted compound **2**, eluting with ethyl acetate / *n*-hexane (1/1) to obtain compound **3** as a white solid (0.83 g, yield: 93%). ¹H NMR (400 MHz, CDCl₃) δ (ppm) 4.19-4.14 (t, 2H, CH₂CH₂OCO), 3.94-3.89 (d, 2H, CCH₂O), 3.74-3.69 (d, 2H, CCH₂O), 3.43-3.38 (t, 2H, BrCH₂), 2.45 (bs, 2H, OH), 1.9-1.79 (m, 2H, BrCH₂CH₂), 1.67-1.58 (m, 2H, OCH₂CH₂), 1.28 (bm, 14H, (CH₂)₇), 1.2 (s, 3H, CCH₃). ¹³C NMR (100 Hz, CDCl₃) δ (ppm) 176.05, 68.55, 65.23, 49.08,

34.05, 29.42, 29.41, 29.17, 29.13, 28.83, 28.53, 28.71, 25.84, 17.15. ESI-MS ($M+Na$)⁺ $C_{16}H_{31}BrO_4$ theoretical: 389.13, experimental: 389.08.

5.2.1.3 Synthesis of 11-azidoundecyl 3-hydroxy-2-(hydroxymethyl)-2-methylpropanoate (4):

Compound **3** (0.80 g, 2.17 mmol) was dissolved in 15 mL of DMF and NaN_3 (0.7 g, 10.85 mmol) was added to the solution. The reaction mixture was stirred at 80°C for 24 h and subsequently cooled to ambient temperature. Distilled water was added to the solution and the product was extracted three times with diethyl ether. The combined organic phases were dried over Na_2SO_4 , filtered and evaporated. Product **4** was isolated as white solid (0.71 g, yield: 99%). ¹H NMR (400 MHz, $CDCl_3$) δ (ppm) 4.19-4.14 (t, 2H, CH_2CH_2OCO), 3.94-3.89 (d, 2H, CCH_2O), 3.74-3.69 (d, 2H, CCH_2O), 3.28-3.23 (t, 2H, N_3CH_2), 2.76 (bs, 2H, OH), 1.69-1.57 (m, 4H, OCH_2CH_2 and $N_3CH_2CH_2$), 1.28 (bm, 14H, $(CH_2)_7$), 1.2 (s, 3H, CCH_3). ¹³C NMR (100 MHz, $CDCl_3$) δ (ppm) 176.05, 68.55, 65.23, 51.49, 49.08, 29.42, 29.41, 29.17, 29.13, 28.83, 28.53, 28.71, 25.84, 17.15. ESI-MS ($M+Na$)⁺ $C_{16}H_{31}N_3O_4$, theoretical: 352.22, experimental: 352.12.

5.2.1.4 Synthesis of azide-functionalized ATRP initiator (5): Compound **4** (0.7 g, 2.12 mmol) was dissolved in 20 mL of dry THF. Et_3N (1.2 mL, 8.51 mmol) and DMAP (0.052 g, 0.42 mmol) were added to the solution and cooled to 0°C. 2-Bromoisobutyrylbromide (1.05 mL, 8.51 mmol) was dissolved in 10 mL of dry THF and subsequently added dropwise to the reaction mixture within 30 min. After the addition, the reaction mixture was warmed to ambient temperature and stirred further for 5 h. Solids were filtered off, the filtrate was concentrated and diluted with 100 mL of CH_2Cl_2 , and the mixture was extracted two times with 50 mL of a saturated aqueous solution of $NaHCO_3$. The organic phase was dried over Na_2SO_4 . The solution was purified by

column chromatography on silica gel with ethyl acetate / hexane (1:9) to give the product **5** as pale yellow (1.2 g, yield: 91%). ^1H NMR (400 MHz, CDCl_3) δ (ppm) 4.42-4.30 (q, 4H, CH_2OCO), 4.19-4.14 (t, 2H, $\text{CH}_2\text{CH}_2\text{OCO}$), 3.28-3.23 (t, 2H, N_3CH_2), 1.91 (s, 12H, $\text{C}(\text{CH}_3)_2\text{Br}$), 1.64-1.57 (m, 4H, OCH_2CH_2 and $\text{N}_3\text{CH}_2\text{CH}_2$), 1.28 (bm, 17H, $(\text{CH}_2)_7$ and CH_3). ^{13}C NMR (100 MHz, CDCl_3) δ (ppm) 172.41, 170.99, 66.37, 65.62, 55.32, 51.48, 46.65, 30.66, 29.42, 29.41, 29.19, 28.83, 28.71, 28.52, 26.70, 25.86, 17.94. ESI-MS ($\text{M}+\text{Na}$) $^+$ $\text{C}_{24}\text{H}_{41}\text{Br}_2\text{N}_3\text{O}_6$, theoretical: 648.13, experimental: 648.04.

5.2.1.5 Synthesis of azide mid-functionalized poly(styrene) (PS- N_3 -PS) (6): Into a 50 mL Schlenk tube, St (10 mL, 87 mmol), PMDETA (0.073 mL, 0.349 mmol), and **5** (0.109 g, 0.174 mmol) in 5 mL of anisole were added and the reaction mixture was degassed by three freeze-pump-thaw cycles and left under argon. CuBr (0.05 g, 0.349 mmol) was added to the solution under argon. The tube was subsequently placed in a thermostated oil bath at 80 °C for 60 min. After the specified time, the polymerization mixture was cooled in an ice bath and subsequently diluted with THF, passed through an alumina column to remove the catalyst, and two times precipitated in 100 mL cold methanol. The polymer was dried for 24 h under vacuum to afford PS- N_3 -PS as a white solid (0.54 g) ($[\text{M}]_0/[\text{I}]_0 = 250$, $[\text{I}]_0:[\text{CuBr}]_0:[\text{PMDETA}]_0 = 1:2:2$). $M_{n,\text{NMR}} = 3600$ Da, $M_{n,\text{SEC}} = 3800$ Da, $PDI = 1.08$.

5.2.1.6 Synthesis of Hamilton Wedge (HW) mid-functionalized poly(styrene) (PS-HW-PS) (7): PS- N_3 -PS (0.4 g, 0.11 mmol), **12** (0.2 g, 0.33 mmol), copper (II) sulfate pentahydrate (0.08 g, 0.33 mmol) and sodium ascorbate (0.07 g, 0.33 mmol) were dissolved in DMF (10 mL). The resulting mixture was stirred at ambient temperature for 24 h before the copper catalyst was removed by passing through a short column of neutral alumina. The solvent was removed under

reduced pressure, subsequently diluted with the addition of DCM and extracted with EDTA solution to remove Cu, which is complexed by the recognition unit.⁵⁸ The organic phase was dried over Na₂SO₄ and concentrated and then two times precipitated in 100 mL methanol, filtered and dried under vacuum for 24 h to obtain a white solid (0.45 g, yield: 98%). $M_{n,NMR} = 4200$ Da, $M_{n,SEC} = 4600$ Da, $PDI = 1.04$. ¹H NMR (400 MHz, CD₂Cl₂) δ (ppm) 7.96-7.76 (9H, ArH of HW), 7.01-6.39 (5H, ArH of PS), 5.23-5.03 (2H, OCH₂ linked to triazole), 3.45 (3H, CH₃-O), 1.78-1.18 (aliphatic protons of PS).

5.2.1.7 Synthesis of CA end-functionalized poly(styrene) (PS-CA) (9): Into a 50 mL of Schlenk tube, St (8.0 mL, 53 mmol), PMDETA (0.073 mL, 0.26 mmol), and **8** (0.13 g, 0.26 mmol) in 2 mL of anisole were added and the reaction mixture was degassed by three freeze-pump-thaw cycles and left under argon. CuBr (0.05 g, 0.26 mmol) was added to the solution under argon. The tube was subsequently placed in a thermostated oil bath at 110 °C for 45 min. The polymerization mixture was diluted with THF and passed through an alumina column to remove the catalyst. The solvent was removed under reduced pressure and subsequently diluted with the addition of DCM and extracted with EDTA solution to remove Cu, which is complexed by the recognition unit. The organic phase was dried over Na₂SO₄, concentrated and then two times precipitated in 100 mL methanol. The polymer was dried for 24 h in a Schlenk line to give a white solid (0.43 g) ($[M]_0/[I]_0 = 200$, $[I]_0:[CuBr]_0:[PMDETA]_0 = 1:1:1$). $M_{n,NMR} = 3600$ Da, $M_{n,SEC} = 3700$ Da, $PDI = 1.04$. ¹H NMR (400 MHz, CDCl₃) δ (ppm) 7.98 (s, 2H of cyanuric acid), 7.01-6.39 (5H, ArH of PS), 4.42-4.33 (1H, CHBr), 3.73 (2H, CH₂-N), 3.45 (2H, CH₂-O), 1.78-1.18 (aliphatic protons of PS), 0.90-0.77 (6H, NCH₂(CH₂)₃CH₂O).

5.2.1.8 Synthesis of CA end-functionalized poly(methyl methacrylate) (PMMA-CA) (10):

Into a 50 mL of Schlenk tube, MMA (5.0 mL, 46 mmol), PMDETA (0.048 mL, 0.23 mmol), and **8** (0.087 g, 0.23 mmol) in 5 mL of toluene were added and the reaction mixture was degassed by three freeze-pump-thaw cycles and left under argon. CuCl (0.023 g, 0.23 mmol) was added to the solution under argon. The tube was subsequently placed in a thermostated oil bath at 50 °C for 30 min. The polymerization mixture was diluted with THF and passed through an alumina column to remove the catalyst. The solvent was removed under reduced pressure, subsequently diluted with the addition of DCM and extracted with EDTA solution to remove Cu, which is complexed by the recognition unit. The organic phase was dried over Na₂SO₄ and two times precipitated in 100 mL *n*-hexane. The polymer was dried for 24 h in a Schlenk line to give a white solid (0.78 g) ($[M]_0/[I]_0 = 200$, $[I]_0:[CuCl]_0:[PMDETA]_0 = 1:1:1$). $M_{n,NMR} = 9000$ Da, $M_{n,SEC} = 8500$ Da, $PDI = 1.13$. ¹H NMR (400 MHz, CDCl₃) δ (ppm) 8.62 (s, 2H of cyanuric acid), 4.02 (brs, 2H, -CH₂OC=), 3.88 (brs, 2H, -NCH₂-), 3.60 (brs, -OCH₃ of PMMA), 1.78-1.18 (aliphatic protons of PMMA).

5.2.1.9 Synthesis of HW end-functionalized poly(styrene) (PS-HW) (13):

PS-N₃ (1.00 g, 0.2 mmol), **12** (0.36 g, 0.61 mmol), copper (II) sulfate pentahydrate (0.15 mg, 0.61 mmol) and sodium ascorbate (0.12 mg, 0.61 mmol) were dissolved in DMF (5 mL). The resulting mixture was stirred at ambient temperature for 24 h before the copper catalyst was removed by passing through a short column of neutral alumina. The solvent was removed under reduced pressure, subsequently diluted with the addition of DCM and extracted with EDTA solution to remove Cu which is complex by the recognition unit. The organic phase was dried over Na₂SO₄, concentrated and then two times precipitated in 100 mL methanol, filtered and dried under

vacuum at 25 °C for 24 h to obtain a white solid (1.07 g; yield: 96%). $M_{n,NMR} = 5500$ Da, $M_{n,SEC} = 5600$ Da, $PDI = 1.04$. 1H NMR (400 MHz, CD_2Cl_2) δ (ppm) 7.96-7.76 (9H, ArH of host), 7.01-6.39 (5H, ArH of PS), 5.23-5.03 (2H, OCH_2 linked to triazole), 3.45 (3H, CH_3-O), 1.78-1.18 (aliphatic protons of PS).

5.2.1.10 Self-Assembly Study between PS-HW and PS-CA: A sample was prepared with dissolved **PS-HW** (11 mg, $2 \cdot 10^{-3}$ mmol) and **PS-CA** (7.2 mg, $2 \cdot 10^{-3}$ mmol) in 1 mL CD_2Cl_2 in an NMR tube. The mixture was kept at 40 °C for 5 min and then left to assemble overnight (12 h) at ambient temperature; subsequently 1H NMR spectra were recorded.

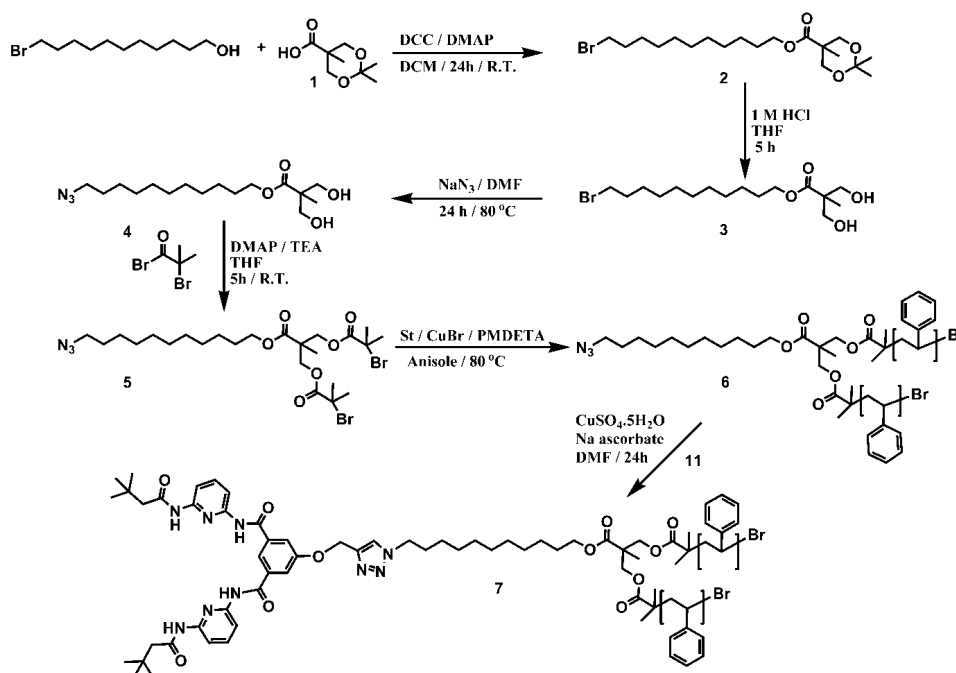
5.2.1.11 Self-Assembly Study between PS-HW-PS and PS-CA: A sample was prepared with dissolved **PS-HW-PS** (8.4 mg, $2 \cdot 10^{-3}$ mmol) and **PS-CA** (7.2 mg, $2 \cdot 10^{-3}$ mmol) in 1 mL CD_2Cl_2 in an NMR tube. The mixtures were kept at 40 °C for 5 min and then left to assemble overnight (12 h) at ambient temperature; subsequently 1H NMR spectra were recorded.

5.2.1.12 Self-Assembly Study between PS-HW and PMMA-CA: A sample was prepared with dissolved **PS-HW** (11 mg, $2 \cdot 10^{-3}$ mmol) and **PMMA-CA** (18 mg, $2 \cdot 10^{-3}$ mmol) in 1 mL CD_2Cl_2 in an NMR tube. The mixtures were kept at 40 °C for 5 min and then left to assemble overnight (12 h) at ambient temperature; subsequently 1H NMR spectra were recorded.

5.2.1.13 Self-Assembly Study between PS-HW-PS and PMMA-CA: A sample was prepared with dissolved **PS-HW-PS** (8.4 mg, $2 \cdot 10^{-3}$ mmol) and **PMMA-CA** (18 mg, $2 \cdot 10^{-3}$ mmol) in 1 mL CD_2Cl_2 in an NMR tube. The mixtures were kept at 40 °C for 5 min and then left to assemble overnight (12 h) at ambient temperature; subsequently 1H NMR spectra were recorded.

5.2.2 Results and Discussion of Supramolecular Block, Star and Miktoarm Star polymers through Multiple Hydrogen Bonding

In the first part of the present chapter, supramolecular complex macromolecular structures were prepared through multiple hydrogen bonding. The self-assembled structures were characterized and subsequently the degree of binding of these supramolecular assemblies were calculated via ^1H NMR in details. The Hamilton Wedge (HW) and cyanuric acid (CA) motifs, which were chosen as binding units due to their high self-assembly constant ($K_a = 10^6 \text{ M}^{-1}$) in CH_2Cl_2 at ambient temperature, were introduced into well-defined PS and PMMA as mid-chain (refer to Scheme 5. 2) and terminal (refer to Scheme 5.1) functionalities. The PS-HW-PS (**7**) building block was designed following the synthetic pathway outlined in Scheme 5.4.



Scheme 5.4 Synthetic strategy for preparing Hamilton Wedge mid-chain functionalized poly(styrene) (PS-HW-PS (**7**)).

To incorporate a HW motif into a mid-chain position, PS-N₃-PS (**6**) was synthesized in several steps. The first involves the reaction of 11-bromoundecan-1-ol with 2,2,5-trimethyl-1,3-dioxane-5-carboxylic acid to yield the corresponding compound **3**. The ¹H NMR spectrum of **3** shows the characteristic signals of $-CH_2OC=O$ and $-C-CH_2O-C-$ appearing at 4.18 and 3.62 ppm, respectively (see Figure 5.1). In a second step, the deprotection of the acetonide group of **2** was readily accomplished in the presence of 1 M HCl. The two hydroxyl groups of **3** can readily be observed at 2.45 ppm and the signal for the methyl group of the acetonide functionality is no longer identified at 1.39-1.43 ppm (see Figure 5.2).

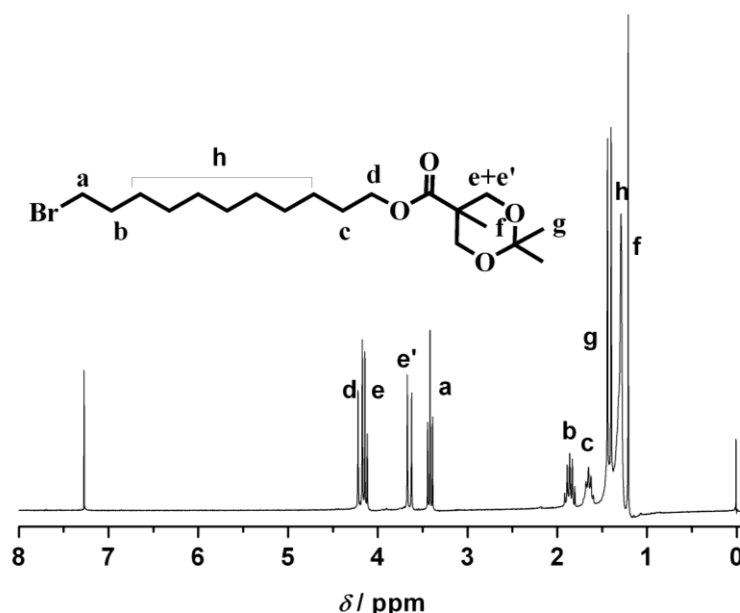


Figure 5.1 ¹H NMR spectrum of 11-bromoundecyl 2,2,5-trimethyl-1,3-dioxane-5-carboxylate (**2**) in CDCl₃.

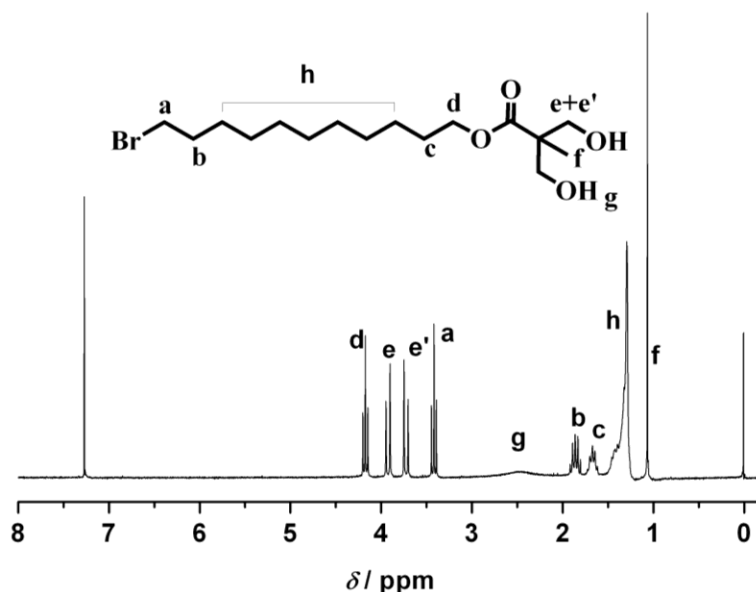


Figure 5.2 ¹H-NMR spectrum of 11-bromoundecyl 3-hydroxy-2-(hydroxymethyl)-2-methylpropanoate (3) in CDCl₃.

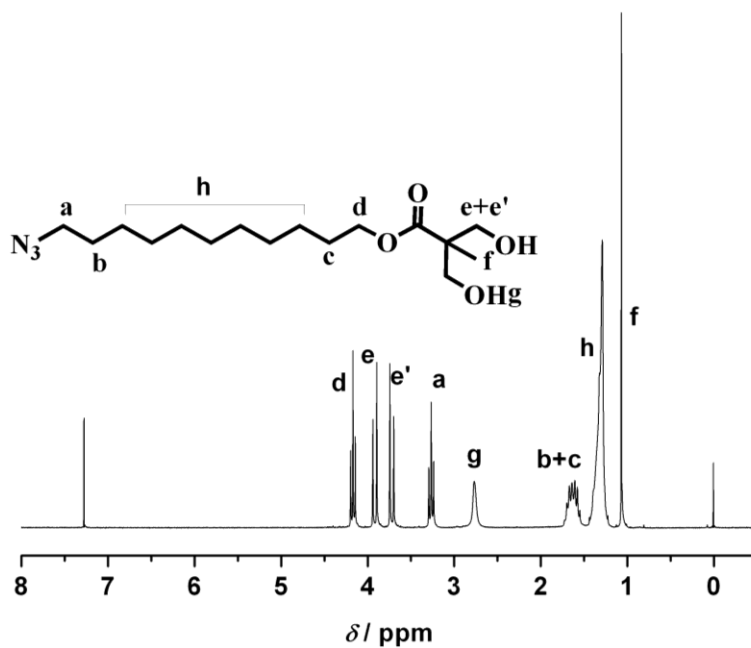


Figure 5.3 ¹H-NMR spectrum of 11-azidoundecyl 3-hydroxy-2-(hydroxymethyl)-2-methylpropanoate (4) in CDCl₃.

In a third step, the bromide functionality of **3** was almost quantitatively converted to an azide group in the presence of NaN_3 . The desired azide compound was isolated in quantitative yields and used without further purification in the subsequent step. The ^1H NMR spectrum of **4** (see Figure 5.3) indicates that the signals of $-\text{CH}_2\text{Br}$ and $-\text{CH}_2\text{CH}_2\text{Br}$ at 3.41 ppm and 1.8 ppm disappeared and a new signal associated with $-\text{CH}_2\text{N}_3$ emerged at 3.28 ppm. The ATRP initiator **5** was obtained via esterification of **4** with 2-bromoisobutyrylbromide in the presence of triethylamine. The initiator was purified via column chromatography and its purity was determined by ^1H NMR and ^{13}C NMR spectroscopy (see Figure 5.4 and Figure 5.5). The ^1H NMR spectrum of **5** indicates that the signals of $-\text{CH}_2-\text{OH}$ disappeared at 3.9-3.7 ppm and new signals associated with $-\text{CH}_2\text{OC}=\text{O}$ and $-\text{CCH}_3\text{Br}$ are observed at 4.40 ppm and 1.91 ppm, respectively.

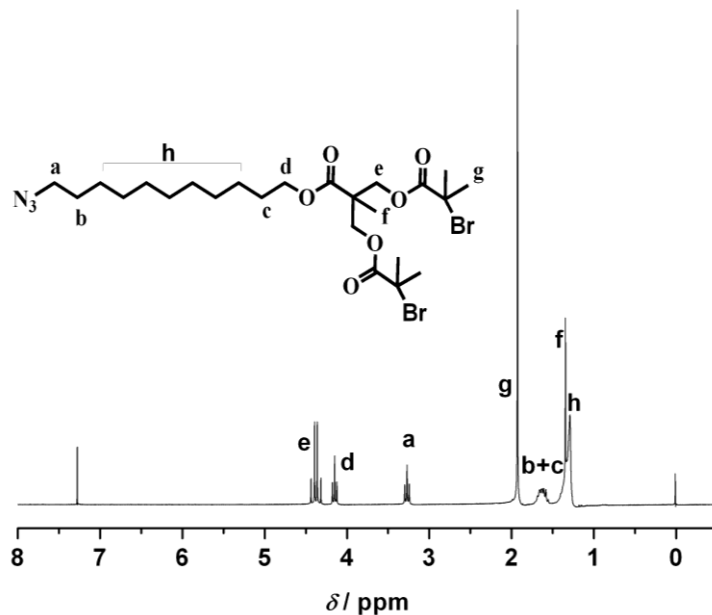


Figure 5.4 ^1H NMR spectrum of azido-functionalized ATRP initiator (**5**) in CDCl_3 .

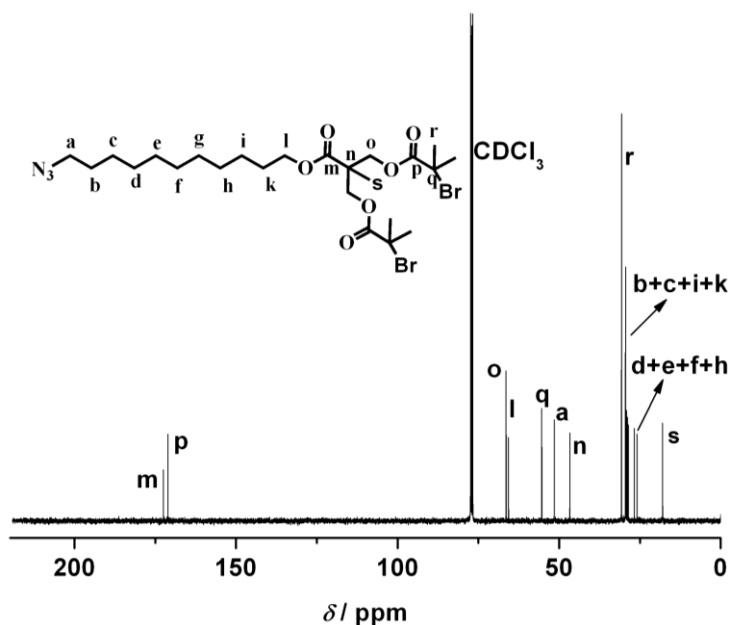


Figure 5.5 ^{13}C NMR spectrum of azido-functionalized ATRP initiator (**5**) in CDCl_3 .

In a final step, compound **5** was employed as an initiator for the ATRP of St in the presence of a $\text{CuBr}/\text{PMDETA}$ complex system as catalyst in anisole to yield polymer **6** ($M_n = 3700 \text{ g mol}^{-1}$, $PDI = 1.06$). Finally, utilizing copper catalyzed azide-alkyne conjugation chemistry, **6** and **12** were reacted to give the corresponding PS-HW-PS in the presence of CuSO_4 and sodium ascorbate in DMF at ambient temperature (see Figure 5.6). The number average molecular weight, M_n , of PS-HW-PS (**7**) was determined via SEC (molecular weight reported relatively to PS standards). The M_n of **7** deduced via SEC and ^1H NMR reads 4600 Da ($PDI = 1.04$) and 4200 Da, respectively. The number average molecular weights as well as the corresponding polydispersity values of all of the above compounds are collated in Table 5.1.

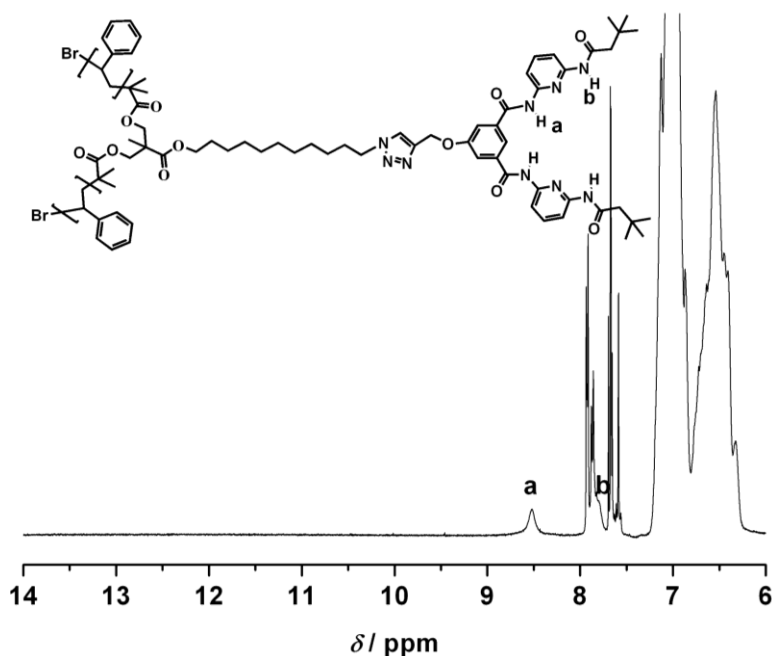


Figure 5.6 Expanded ^1H NMR spectrum of HW mid-functionalized polystyrene (PS-HW-PS) (**7**) in CD_2Cl_2 .

After the successful synthesis of **PS-HW-PS**, CA end-functionalized PS (**PS-CA**), CA end-functionalized PMMA (**PMMA-CA**), and HW end-functionalized PS (**PS-HW**) were prepared (see Scheme 5.5) to serve as blocks for the homopolymer, diblock copolymer, star and miktoarm star polymers. **PS-CA** was synthesized using **8** as an initiator for the ATRP of St in the presence of $\text{CuBr}/\text{PMDETA}$. Moreover, **PMMA-CA** was synthesized using **8** as an initiator during the ATRP of MMA in the presence of $\text{CuCl}/\text{PMDETA}$. Furthermore, **PS-N₃** was reacted with **12** to yield **PS-HW** through azide-alkyne conjugation employing the $\text{CuSO}_4/\text{ascorbate}$ catalyst system in DMF at ambient temperature. The ^1H NMR spectra (see Figure 5.7, 5.8 and 5.9) of **PS-CA**, **PMMA-CA** and **PS-HW** display all characteristic signals for the HW and CA moieties which were desired as end-group functionalities. The molecular weights of **PS-CA** (**9**),

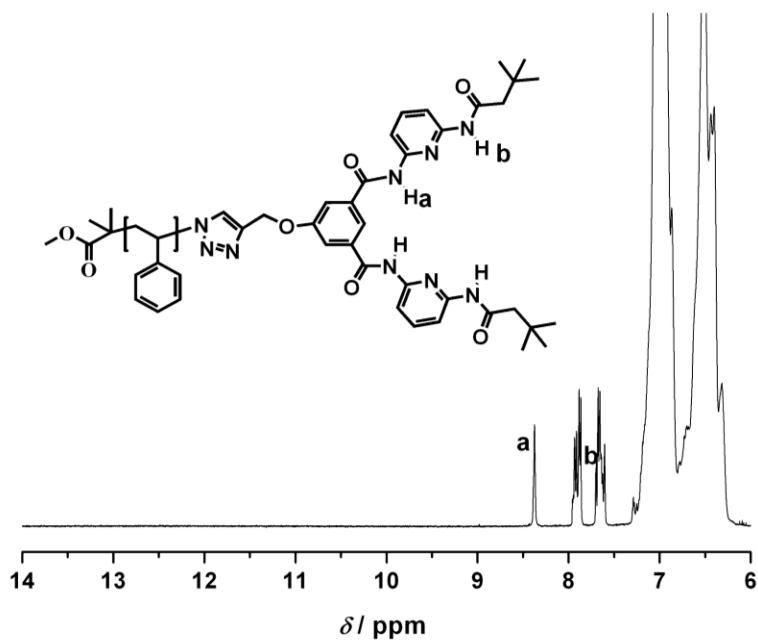


Figure 5.7 Expanded $^1\text{H-NMR}$ spectrum of HW end-functionalized polystyrene (**PS-HW**) in CD_2Cl_2 at ambient temperature.

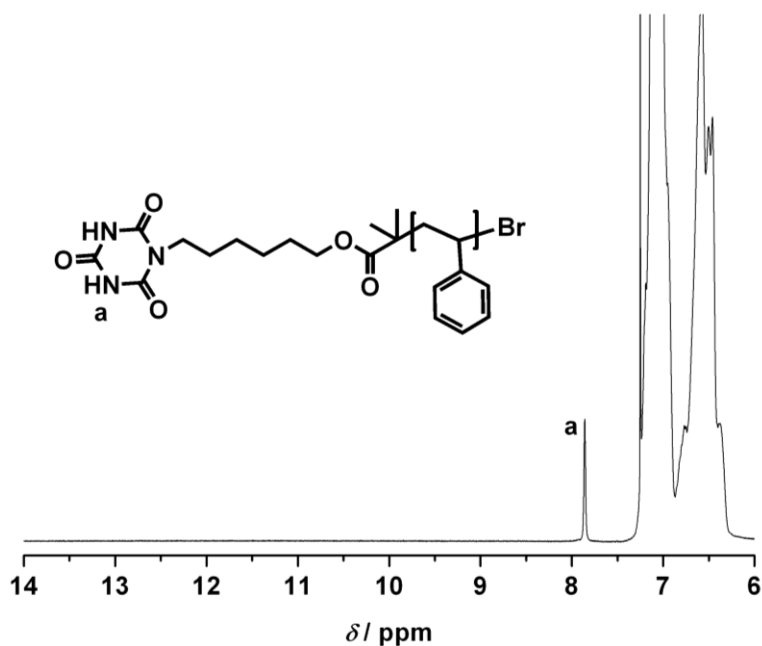


Figure 5.8 Expanded $^1\text{H-NMR}$ spectrum of CA end-functionalized polystyrene (**PS-CA**) in CDCl_3 .

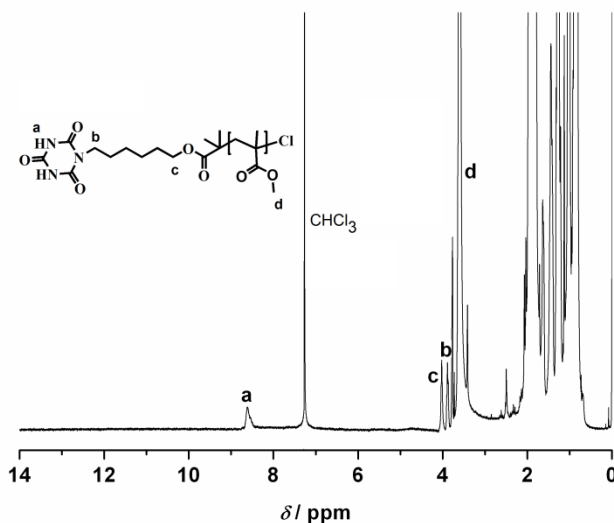


Figure 5.9 ¹H-NMR spectrum of CA end-functionalized poly(methyl methacrylate) (PMMA-CA) in CDCl₃.

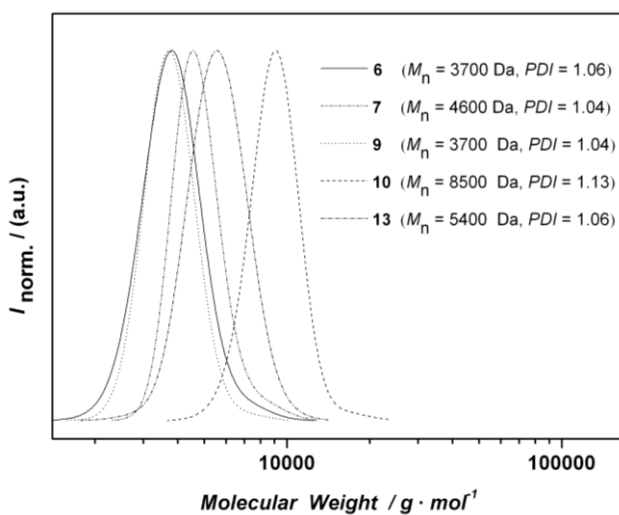


Figure 5.10 SEC traces of the precursor polymers depicted in Scheme 5.4 and 5.5. The detailed reaction conditions can be found in Table 5.1.

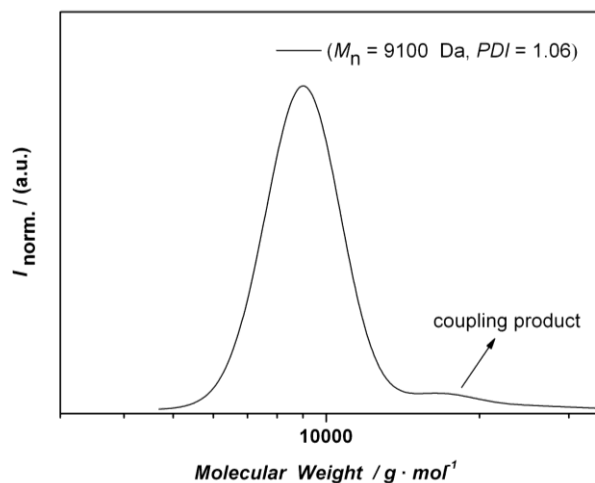


Figure 5.11 SEC trace of polymer prepared via ATRP using initiator **8**. The conditions were the same as those used to prepare polymer **9** (PS-CA) (see experimental section) with the exception that the reaction time was 2h.

Table 5.1 Characteristics of functional precursor polymers employed in the current study.

Polymers	Monomer	$[M_0]/[I_0]$	Initiator	time / min	M_n	M_w/M_n	M_n^g
6 ^a	St	250	5	60	3700 ^e	1.06	3600
7	-	-	-	-	4600 ^e	1.04	4200
9 ^b	St	200	8	45	3700 ^e	1.04	3600
10 ^c	MMA	200	8	30	8500 ^f	1.13	9000
11 ^d	St	200	MiBBr	45	4700 ^e	1.09	4900
13	-	-	-	-	5400 ^e	1.06	5500

^a $[I]_0/[PMDETA]_0/[CuBr]_0 = 1:2:2$; at 80 °C. ^b $[I]_0/[PMDETA]_0/[CuBr]_0 = 1:1:1$ at 110 °C.

^c $[I]_0/[PMDETA]_0/[CuCl]_0 = 1:1:1$; at 50 °C. ^d $[I]_0/[PMDETA]_0/[CuBr]_0 = 1:1:1$ at 110 °C.

^e Determined from RI detection SEC using linear PS standards. ^f Determined from RI detection SEC using linear PMMA standards. ^g Determined from ¹H NMR spectroscopy.

Before discussing in detail the self-assembly between the individual recognition motifs, CA and HW, it is appropriate to discuss the NMR solvents, which are to be used to achieve self-assembly. Initially, the ^1H NMR spectrum of **PS-HW (13)** was recorded in CDCl_3 and non-specific interactions between 13 ppm and 9 ppm (peaks labeled x, y, and z) were observed that can be attributed to the intermolecular H-bonding between the Hamilton receptors (see Figure 5.12). The same measurement was repeated for **PS-HW-PS (7)** and similar results were obtained. However, ^1H NMR spectra of **7** and **13** measured in CD_2Cl_2 evidence that the signals of the NH protons of the Hamilton receptor appear at 7.80 ppm and 8.52 ppm, which is in good agreement with theoretical expectations^{38u} (see Figure 5.6 and 5.7).

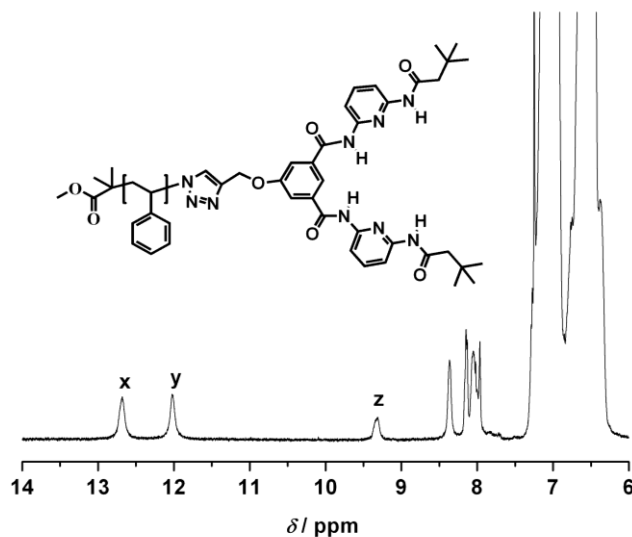


Figure 5.12 Expanded ^1H NMR spectrum of HW end-functionalized polystyrene (**PS-HW**) in CDCl_3 at ambient temperature.

Moreover, it should be pointed out that the more polar solvent CD_2Cl_2 solvates the Hamilton receptor better than CDCl_3 and prevents the formation of inter/intra-molecular H-bonding. Thus,

the polarity of CD_2Cl_2 is sufficient to prevent inter- and intramolecular H-bonding of the Hamilton receptors, yet appropriate to enable intermolecular H-bonding between HW and CA. On the basis of the above experimental data, CD_2Cl_2 is to be preferred over CDCl_3 as NMR solvent for investigating the self-assembly behavior between these recognition motifs.

Subsequently, the formation of diblock, star, and miktoarm star polymers via H-bonding between the HW receptor and the CA located at various places of the polymer backbone (as described in Scheme 5.1 and 5.2) was investigated. All self-assembly processes of the building blocks can be followed by monitoring characteristic changes in the chemical shifts of the *NH* protons of the two recognition pairs using ^1H NMR spectroscopy.

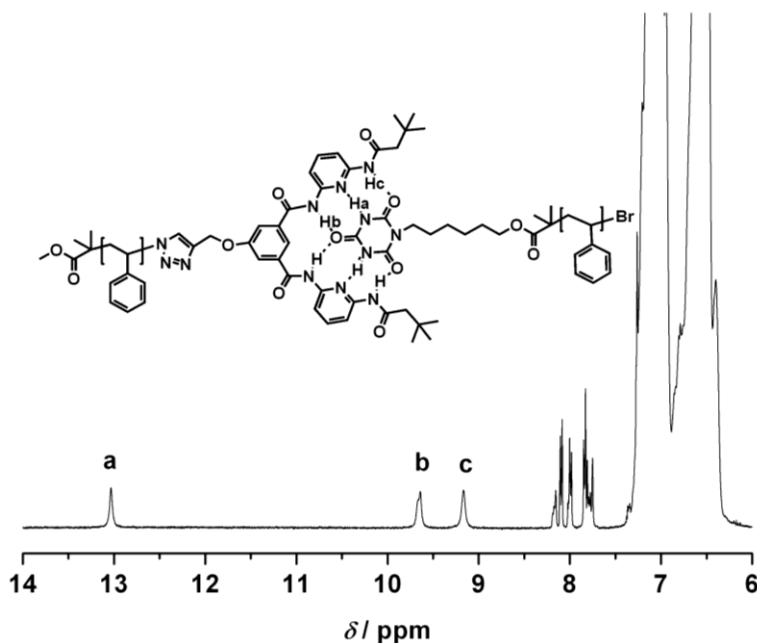


Figure 5.13 Expanded ^1H -NMR spectrum of the **PS-HW•PS-CA** self-assembly system in CD_2Cl_2 at ambient temperature. Equimolar amounts with respect to the HW and CA binding motifs were employed. The individual end group concentration for both motifs was close to 2 mM.

First, the formation of a PS-HW•PS-CA (PS-PS) self-assembled structure between **PS-HW** and **PS-CA** in CD₂Cl₂ at ambient temperature was studied. Upon the addition of 1 equiv. of **PS-CA** into 1 equiv. of **PS-HW** in CD₂Cl₂, it is observed that the ¹H NMR spectrum (see Figure 5.13) reveals strong shifts of the amide protons (H_b and H_c) of the Hamilton receptor from 7.80 and 8.52 ppm (see Figure 5.7) to 9.64 and 9.16 ppm, respectively, thus evidencing that the self-assembled homopolymer PS-HW•PS-CA (PS-PS) is formed. Furthermore, a new signal appears at 13.03 ppm (H_a) that corresponds to the (dynamically) bound cyanuric acid unit in the self-assembly motif.^{38u} The yield of supramolecular homopolymer can subsequently be deduced from the ratio between the peak area of –CHBr as an ω-end of **PS-CA** at 4.55–4.42 ppm and the peak area of bound NH as an α-end of **PS-CA** at 13.03 ppm: The amount of total chains carrying a cyanuric acid end group is directly proportional to the signal intensity of –CHBr, whereas the amount of these chains bound to the Hamilton receptor is directly proportional to the new NH signal at 13.03 ppm. Therefore – considering that the NH proton occurs with double intensity – the relative number of cyanuric acid terminal chains bound in the (dynamic) self-assembly at any point in time can be derived. The percentage of self-assembled polymer was thus deduced close to ~89% (see Figure 5.14 for the individual signals with their respective integral values). Moreover, during the addition of 1 equiv. of **PMMA-CA** to 1 equiv. of **PS-HW** in CD₂Cl₂, it is observed that the ¹H NMR spectrum (see Figure 5.15) also reveals strong respective shifts of the amide protons (H_b and H_c) of the Hamilton receptor from 7.80 and 8.52 ppm to 9.36 and 9.80 ppm, respectively, thus evidencing that a supramolecular block copolymer PS-HW•PMMA-CA (PS-PMMA) is formed.

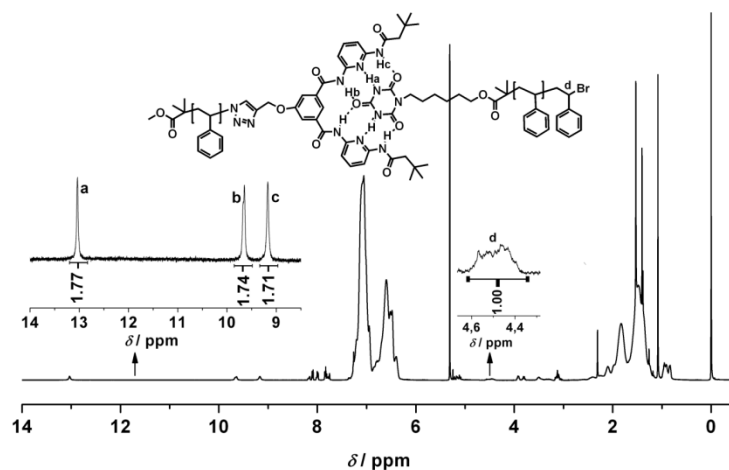


Figure 5.14 ^1H NMR spectrum of PS-HW•PS-CA supramolecular polymer system in CD_2Cl_2 at ambient temperature with the integral values of the relevant resonances. From the ratio of the peak areas **a** to **d**, the degree of self-assembly can be deduced as being close to ~89 %. Equimolar amounts with respect to the HW and CA binding motifs were employed. The individual end group concentration for both motifs was close to 2 mM.

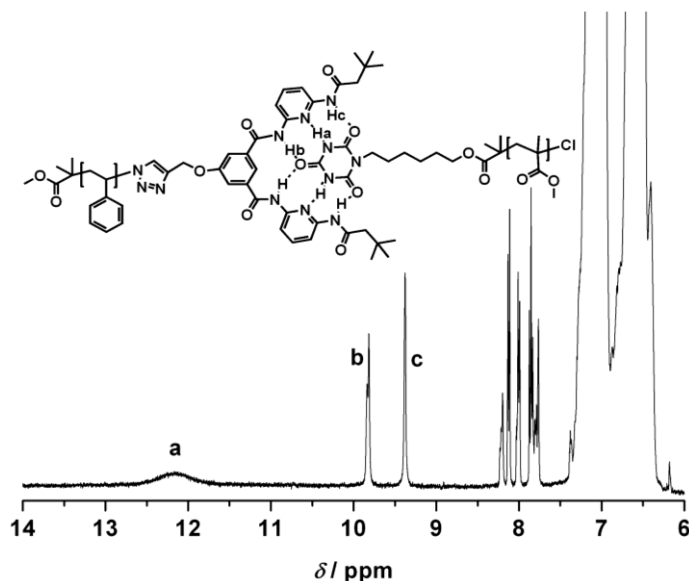


Figure 5.15 Expanded ^1H NMR spectrum of the PS-HW•PMMA-CA self-assembly system in CD_2Cl_2 at ambient temperature. Equimolar amounts with respect to the HW and CA binding motifs were employed. The individual end group concentration for both motifs was close to 2 mM.

Furthermore, a new (broad) signal^{38u} appears at 12.16 ppm (H_a) that corresponds to the bound cyanuric acid unit in the self assembled structure. In contrast to the PS-HW•PS-CA system, the percentage of self-assembled polymer cannot be calculated from the 1H NMR spectrum in this case due to the absence of a separate, non-overlapping peak to compare to the bound protons. The absence of a suitable comparative resonance is due to the methyl group present in methyl methacrylate, in contrast to the poly(styrene) system. In addition, no other resonances associated with the chain terminus are available for integration without overlap. However, it is reasonable to assume that supramolecular block copolymer, PS-HW•PMMA-CA (PS-PMMA) was formed in high yield similar to supramolecular miktoarm star polymer, $(PS)_2PMMA$ (see below), because 1H NMR spectra of the two self-assembly systems display almost the same chemical shifts of the imide protons in the Hamilton Wedge (in PS-PMMA: 9.36 and 9.80 ppm and in $(PS)_2PMMA$: 9.32 and 9.79 ppm).

As noted above, the formation of supramolecular star polymers via self-assembly between **PS-HW-PS** and **PS-CA** was also examined. When 1 equiv. of **PS-HW-PS** was mixed with 1 equiv. of **PS-CA** in CD_2Cl_2 at ambient temperature, the chemical shift of the imide protons of **PS-CA** changed from 7.85 (see Figure 5.8) to 13.05 ppm and the *NH* proton of the **PS-HW-PS** appeared at 9.64 and 9.14 ppm due to the self-assembly (see Figure 5.16). The yield of supramolecular three arm star polymer was calculated from the ratio between the peak area of $-CH_2CH_2-$ triazole of **PS-HW-PS** at 4.24 ppm and the peak area of bound *NH* as an α -end of **PS-CA** at 13.05 ppm, employing an identical rationale for arriving at the degree of self-assembly as described and employed above. The percentage of self-assembled star polymer $(PS)_3$ was thus calculated to be close to 90% by 1H NMR spectroscopy (see Figure 5.17 for the integrals of the

individual peak assignments). In principle, it should also be possible to use the $-CHBr$ proton (as in the PS-HW•PS-CA case discussed above) to assess the degree of binding within the miktoarm star system. However, using the methylene protons next to the triazole system is in principle the preferred option (if feasible), as due to the ATRP process not all chains may carry a bromide terminus. In the case of the PS-HW•PS-CA system, this option is not available, as no non-overlapping protons in the vicinity of the triazole system are present. It should be noted, however, that the chain end fidelity (i.e. the percentage of chains featuring both a cyanuric acid imide and bromide terminus) is close to 98% (calculated from the integral areas of the cyanuric acid imide and $-CHBr$ protons) in the PS-CA precursor macromolecule.

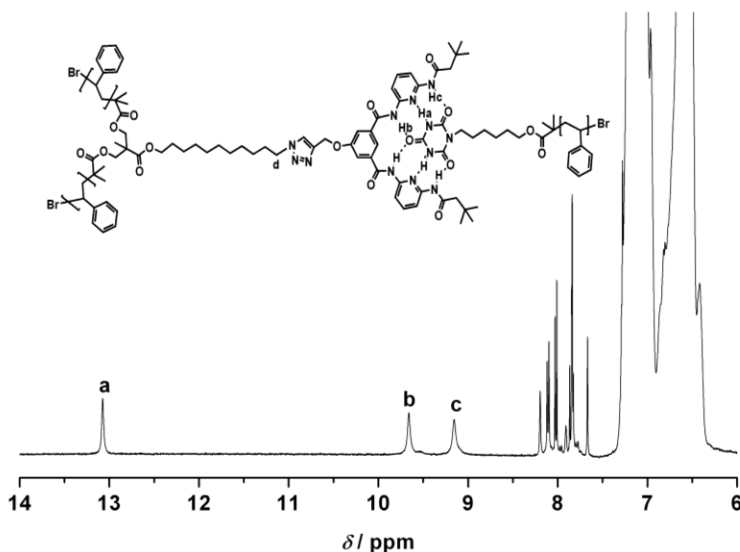


Figure 5.16 Expanded $^1\text{H-NMR}$ spectrum of the PS-HW-PS•PS-CA self-assembly system in CD_2Cl_2 at ambient temperature. Equimolar amounts with respect to the HW and CA binding motifs were employed. The individual end group concentration for both motifs was close to 2 mM.

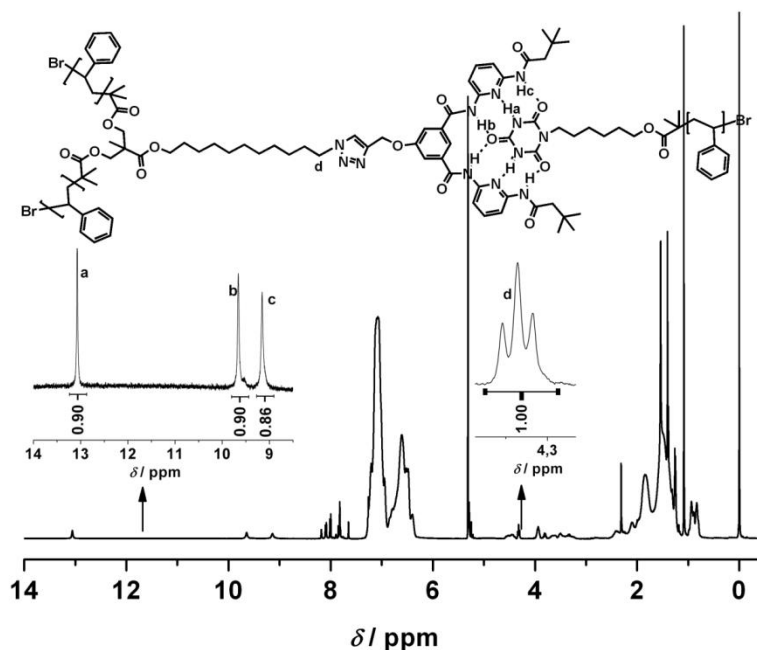


Figure 5.17 ^1H NMR spectrum of **PS-HW-PS•PS-CA** supramolecular star polymer system in CD_2Cl_2 at ambient temperature. From the ratio of the peak areas **a** to **d** (integral values shown), the degree of self-assembly can be deduced as being close to ~90 %. Equimolar amounts with respect to the HW and CA binding motifs were employed. The individual end group concentration for both motifs was close to 2 mM.

Finally, the preparation of a miktoarm star polymer **PS-HW-PS•PMMA-CA** (PS_2PMMA) was investigated through the self-assembly between **PS-HW-PS** and **PMMA-CA**. After the addition of 1 equiv. of **PMMA-CA** to 1 equiv. of **PS-HW-PS** in CD_2Cl_2 , it is observed that the ^1H NMR spectrum (see Figure 5.18) reveals similar strong shifts of the amide protons (H_b and H_c) of the Hamilton receptor from 7.80 and 8.52 ppm to 9.32 and 9.79 ppm, respectively, thus once more evidencing that a self-assembly – in this case a miktoarm star polymer **PS-HW-PS•PMMA-CA** (PS_2PMMA) – is formed. Furthermore, a new broad signal appears at 12.42 ppm (H_a) that

corresponds to the bound cyanuric acid unit in the self assembly. Following the above established calculation routine, the yield of supramolecular miktoarm star polymer was calculated from the ratio between the peak area of the $-\text{CH}_2\text{CH}_2-$ triazole of **PS-HW-PS** at 4.24 ppm and the peak area of bound *NH* as an α -end of **PMMA-CA** at 12.42 ppm. The percentage of self-assembled star polymer **PS₂PMMA** was calculated to be close to 98 % by ^1H NMR spectroscopy (see Figure 5.19 for the integrals of the individual peak assignments). Similar to the above discussed homo-three armed star system, the deduction of the degree of binding via the $-\text{CHBr}$ proton is the less preferred option (although it provides results within approximately similar range).

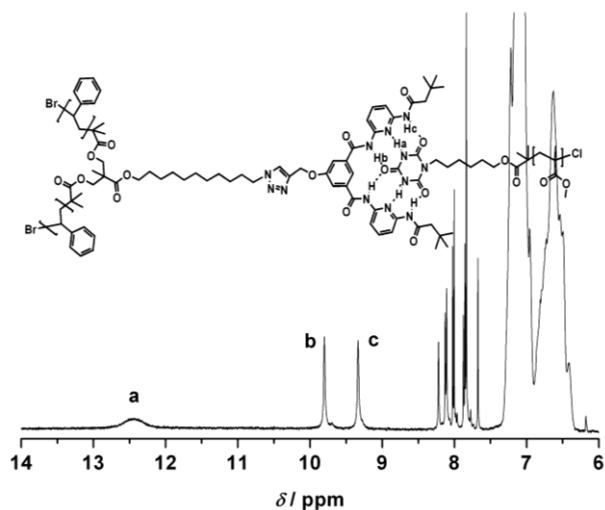


Figure 5.18 Expanded ^1H NMR spectrum of the **PS-HW-PS•PMMA-CA** self-assembly system in CD_2Cl_2 at ambient temperature. Equimolar amounts with respect to the HW and CA binding motifs were employed. The individual end group concentration for both motifs was close to 2 mM.

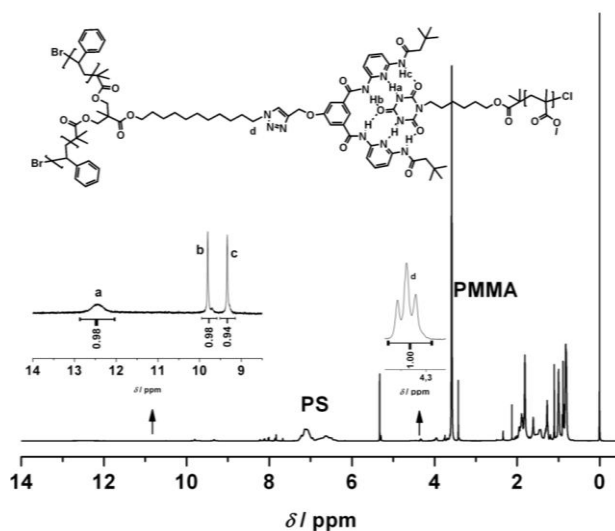


Figure 5.19 ¹H NMR spectrum of the **PS-HW-PS•PMMA-CA** supramolecular miktoarm star polymer system in CD₂Cl₂ at ambient temperature with integrated values from the ratio of the peak areas **a** to **d**. The degree of self-assembly can be deduced as being close to ~98 %. Equimolar amounts with respect to the HW and CA binding motifs were employed. The individual end group concentration for both motifs was close to 2 mM.

5.3 Construction of Star-shaped Macromolecules through Multiple Hydrogen Bonding

In the earliest part of the chapter, preparation and characterization of supramolecular complex structures are presented using multiple hydrogen bonding motifs. As a further step of the present chapter, the supramolecular constructions of star-shaped macromolecules through a strong complementary multiple hydrogen bond between Hamilton wedge (HW) functionalized well-defined star-shaped macromolecules and well-defined cyanuric acid (CA) functionalized linear polymers are detailedly discussed. The results of ¹H NMR, DLS and SLS studies indicate that ultimate complex structures are achieved.

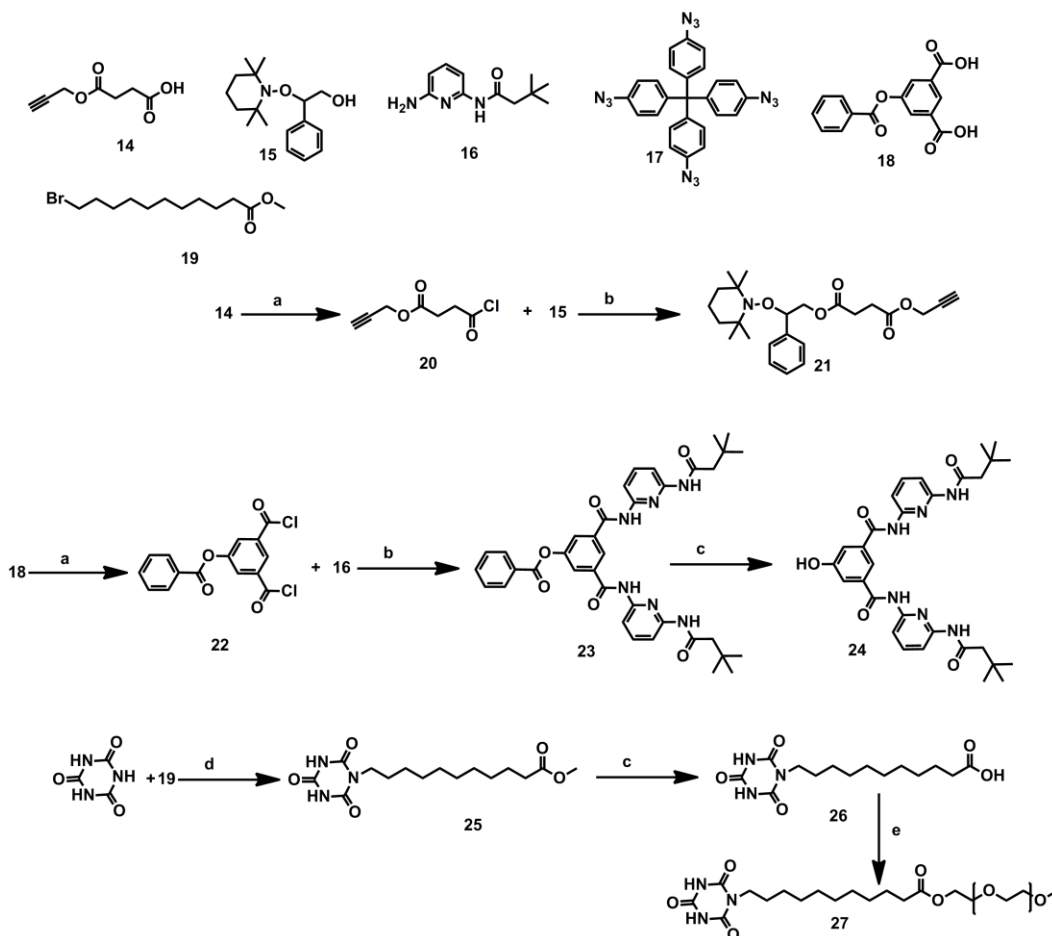
5.3.1 Synthesis

4-oxo-4-(prop-2-yn-1-yloxy)butanoic acid (**14**),^[66] 2-phenyl-2-((2,2,6,6-tetramethylpiperidin-1-yl)oxy)ethanol (**15**),^[67] *N*-(6-aminopyridin-2-yl)-3,3-dimethylbutanamide (**16**),^[68] tetrakis(4-azidophenyl)methane (**17**),^[69] dimethyl (benzoyloxy)isophthalate (**18**),^[70] methyl 11-bromoundecanoate (**19**)^[71] were synthesized according to literature procedures.

5.3.1.1 Synthesis of prop-2-yn-1-yl 4-chloro-4-oxobutanoate (20): **14** (1 g, 6.4 mmol) was dissolved in 30 mL of dry THF in a flame dried three-neck round-bottom flask and 0.1 mL of dry DMF was added to the solution. Subsequently, oxalyl chloride (0.83 mL, 9.6 mmol) was added dropwise over 10 min. The mixture was stirred for 6 h at ambient temperature. The solvent was removed under reduced pressure and the crude product was subsequently dried under vacuum for 3 h to yield **20** as a yellowish solid. The compound was directly used for the next step because of the sensitivity to moisture.

5.3.1.2 Synthesis of 2-phenyl-2-((2,2,6,6-tetramethylpiperidin-1-yl)oxy)ethyl prop-2-yn-1-yl succinate (21): All of **20** obtained in previous step was dissolved in 40 mL of dry THF and added dropwise to a solution of compound **15** (1.47 g, 5.3 mmol) and triethylamine (TEA, 1.06 mL, 7.7 mmol) in 20 mL of dry THF at 0°C. The solution was stirred at ambient temperature for 16 h. The precipitate formed during the reaction was filtered off and the solvent was subsequently removed under reduced pressure. The crude product was purified by column chromatography with *n*-hexane/ethyl acetate (9:1), giving a yellowish viscous liquid **21** after removal of solvent (1.91 g, yield 87%). ¹H NMR (400 MHz, CDCl₃) δ (ppm) 7.35 – 7.27 (m, 5H), 4.95 – 4.87 (m, 1H), 4.66 (d, *J* = 2.4 Hz, 2H), 4.64 – 4.56 (m, 1H), 4.28 (dd, *J* = 11.1, 6.6

Hz, 1H), 2.55 (t, $J = 3.0$ Hz, 4H), 2.47 (t, $J = 2.4$ Hz, 1H), 1.63 – 0.57 (m, 18H). ^{13}C NMR (101 MHz, CDCl_3) δ (ppm) 171.62, 171.37, 140.44, 128.01, 127.64, 83.72, 74.97, 66.50, 60.06, 52.17, 40.42, 34.00, 28.90, 28.76, 20.30, 17.13. ESI-MS ($\text{M}+\text{Na}$) $^+$ $\text{C}_{24}\text{H}_{33}\text{NO}_5$ theoretical: 438.23, experimental: 438.20



Scheme 5.6 Chemical structures used in current section and general strategy for the preparation of the alkyne functional NMP initiator, the hydroxyl functional Hamilton wedge, and cyanuric acid functional poly(ethylene glycol) (**CA-PEG**). *Experimental conditions:* (a) Oxalyl chloride, DMF, THF, 6h, r.t; (b) TEA, THF, overnight, r.t; (c) $\text{NaOH}_{(\text{aq})}$, MeOH/THF, 5h, r.t; (d) DBU, DMF, 24 h, 70 °C; (e) DCC, DMAP, DCM, MeO-PEG-OH.

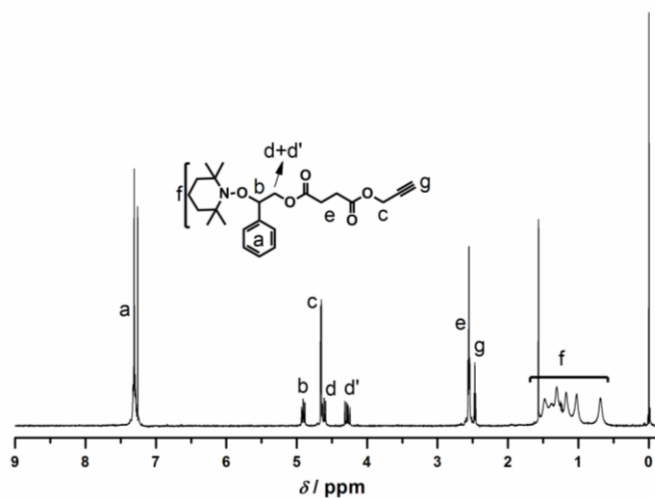


Figure 5.20 ^1H NMR spectrum of 2-phenyl-2-((2,2,6,6-tetramethylpiperidin-1-yl)oxy)ethyl prop-2-yn-1-yl succinate (**21**) in CDCl_3 at ambient temperature. The non-assigned resonance refers to solvent/water.

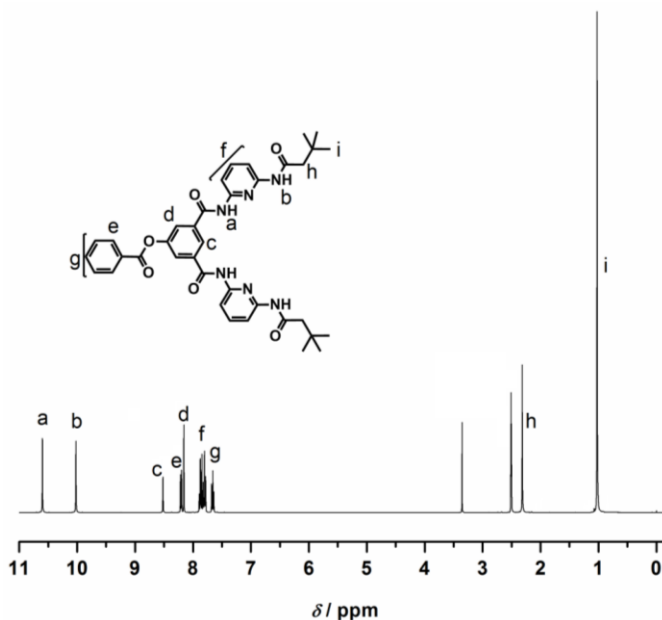


Figure 5.21 ^1H NMR spectrum of 3,5-bis((6-(3,3-dimethylbutanamido)pyridin-2-yl)carbamoyl)phenyl benzoate (**23**) in $\text{DMSO}-d_6$ at ambient temperature. The non-assigned resonances refer to solvent/water.

5.3.1.3 Synthesis of 3,5-bis(chlorocarbonyl)phenyl benzoate (22): **18** (1.33 g, 4.65 mmol) was dissolved in 30 mL of dry THF in a flame dried three-neck round-bottom flask and 1 mL of dry DMF was added to the solution. Subsequently, oxalyl chloride (1.22 mL, 14 mmol) was added dropwise over 10 min. The mixture was stirred for 6 h at ambient temperature. The solvent was removed under reduced pressure and the crude product was subsequently dried under vacuum for 3 h to yield **22** as a yellowish solid.

5.3.1.4 Synthesis of 3,5-bis((6-(3,3-dimethylbutanamido)pyridin-2-yl)carbamoyl)phenyl benzoate (23): **22** was dissolved in 40 mL of dry THF and added dropwise to a solution of **16** (2.12 g, 10.2 mmol) and triethylamine (2.1 mL, 15.3 mmol) in 30 mL of dry THF at 0°C. The solution was stirred at ambient temperature for 16 h. The precipitate formed during the reaction was filtered off and the solvent was subsequently removed under reduced pressure. The crude product was purified by column chromatography with dichloromethane/ethyl acetate (4:1) giving a white solid **23** after removal of solvent (2.51 g, yield 83%). ¹H NMR (400 MHz, DMSO-*d*₆) δ (ppm) 10.60 (s, 2H), 10.02 (s, 2H), 8.52 (t, *J* = 1.4 Hz, 1H), 8.2– 8.18 (m, 2H), 8.16 (d, *J* = 1.4 Hz, 2H), 7.91 – 7.75 (m, 7H), 7.66 (dd, *J* = 10.7, 4.8 Hz, 2H), 2.32 (s, 4H), 1.02 (s, 18H). ¹³C NMR (101 MHz, DMSO-*d*₆) δ (ppm) 170.89, 164.45, 164.25, 150.61, 150.54, 149.94, 140.01, 135.62, 134.29, 129.90, 129.04, 128.55, 125.06, 124.90, 110.60, 110.12, 49.04, 30.89, 29.54. ESI-MS (M+Na)⁺ C₃₇H₄₀N₆O₆ theoretical: 687.29, experimental: 687.42

5.3.1.5 Synthesis of N¹,N³-bis(6-(3,3-dimethylbutanamido)pyridin-2-yl)-5-hydroxyisophthalamide (24): 1.5 N NaOH solution (20 mL) was added to a solution of **23** (2.3 g, 3.46 mmol) in THF and MeOH (2:1, 45 mL). The reaction mixture was stirred at ambient

temperature for 5 h and subsequently concentrated to a volume of 20 mL. The solution was poured into 150 mL of distilled water and concentrated HCl was added dropwise to generate a white precipitate, which was filtered, washed with water, and dried under vacuum to give compound **24** as a white solid (1.91 g, 99%). ^1H NMR (400 MHz, $\text{DMSO-}d_6$) δ (ppm) 10.36 (s, 2H), 10.19 (s, 1H), 10.01 (s, 2H), 8.01 (s, 1H), 7.95 – 7.63 (m, 6H), 7.53 (d, $J = 0.8$ Hz, 2H), 2.32 (s, 4H), 1.03 (s, 18H). ^{13}C NMR (101 MHz, $\text{DMSO-}d_6$) δ (ppm) 170.81, 165.06, 157.57, 150.42, 149.99, 139.90, 135.43, 118.08, 117.66, 110.42, 109.88, 48.97, 30.79, 29.48 ESI-MS $(\text{M}+\text{Na})^+$ $\text{C}_{30}\text{H}_{36}\text{N}_6\text{O}_5$ theoretical: 583.26, experimental: 583.36

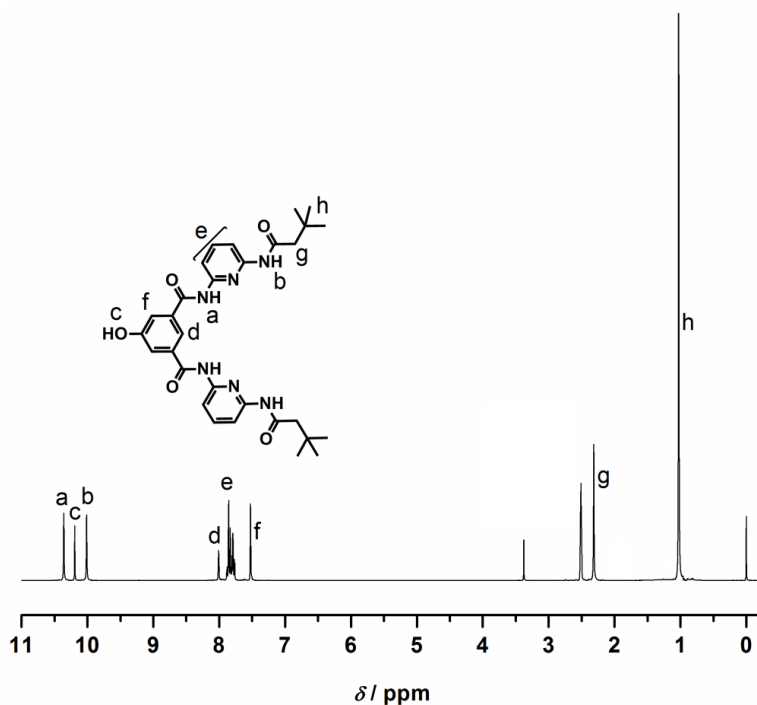


Figure 5.22 ^1H NMR spectrum of N^1,N^3 -bis(6-(3,3-dimethylbutanamido)pyridin-2-yl)-5-hydroxyisophthalamide (**24**) in $\text{DMSO-}d_6$ at the ambient temperature. The non-assigned resonances refer to solvent/water.

5.3.1.6 Synthesis of methyl 11-(2,4,6-trioxo-1,3,5-triazinan-1-yl)undecanoate (25): **19** (2.79 g, 10 mmol) and cyanuric acid (6.50 g, 50 mmol) were dissolved in dry DMF (50 mL). 1,8-Diazabicyclo[5.4.0]undec-7-ene (DBU, 1.47 g, 1.5 mL, 10 mmol) was added dropwise to the solution. The mixture was heated to 70 °C and stirred for 24 h. The solvent was evaporated and the crude mixture was dissolved in methanol and filtered. The solvent was evaporated off and the residual purified via chromatography on silica gel, eluting with *n*-hexane/ethyl acetate (1:1) to obtain compound **25** as a white solid (1.37 g, 42%). ¹H NMR (400 MHz, DMSO-*d*₆) δ (ppm) 11.39 (s, 2H), 3.66 – 3.54 (m, 5H), 2.28 (t, *J* = 11.8 Hz, 2H), 1.50 (bs, 4H), 1.24 (bs, 14H). ¹³C NMR (101 MHz, DMSO) δ (ppm) 173.26, 149.16, 148.55, 51.05, 33.17, 28.73, 28.69, 28.55, 28.53, 28.34, 27.18, 27.09, 26.01, 25.97, 24.33. ESI-MS (M+Na)⁺ C₁₅H₂₅N₃O₅ theoretical: 350.17, experimental: 350.28

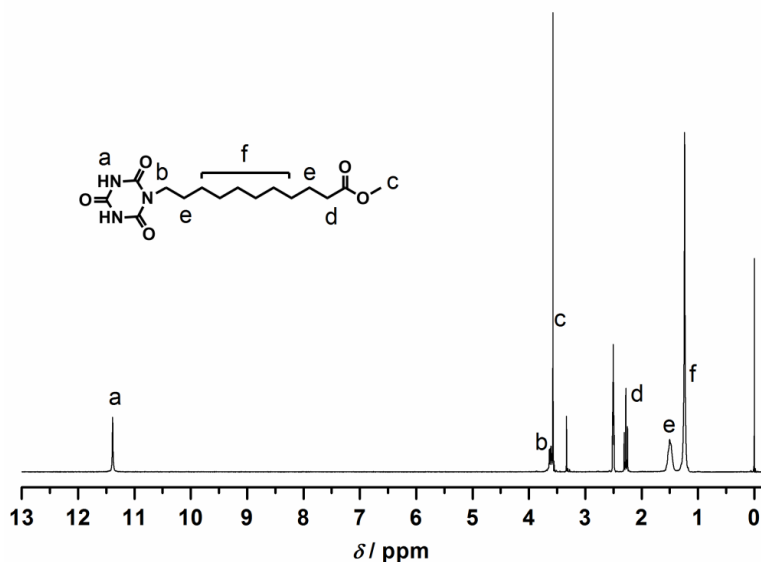


Figure 5.23 ¹H NMR spectrum of methyl 11-(2,4,6-trioxo-1,3,5-triazinan-1-yl)undecanoate (**25**) in DMSO-*d*₆ at ambient temperature. The non-assigned resonances refer to solvent/water.

5.3.1.7 Synthesis of 11-(2,4,6-Trioxo-1,3,5-triazinan-1-yl)undecanoic acid (26): 1 N NaOH solution (10 mL) was added to a solution of compound **25** (1.2 g, 3.66 mmol) in THF and MeOH (2:1, 15 mL). The reaction mixture was stirred at ambient temperature for 5 h and subsequently concentrated to a volume of 10 mL. The solution was poured into 150 mL of water and concentrated HCl was added dropwise to generate a white precipitate, which was filtered, washed with water and dried under vacuum to give compound **26** as a white solid (1.1 g, 96%). Melting point ^1H NMR (400 MHz, $\text{DMSO-}d_6$) δ (ppm) 11.96 (s, 1H), 11.39 (s, 2H), 3.61 (t, $J = 7.3$ Hz, 2H), 2.18 (t, $J = 7.3$ Hz, 2H), 1.48 (bs, 4H), 1.24 (bs, 14H). ^{13}C NMR (101 MHz, DMSO) δ (ppm) 174.24, 149.79, 148.62, 33.63, 28.82, 28.70, 28.53, 28.50, 28.34, 27.18, 27.09, 26.01, 25.47, 24.33. ESI-MS ($\text{M}+\text{Na}$) $^+$ $\text{C}_{14}\text{H}_{23}\text{N}_3\text{O}_5$ theoretical: 336.15, experimental: 336.26

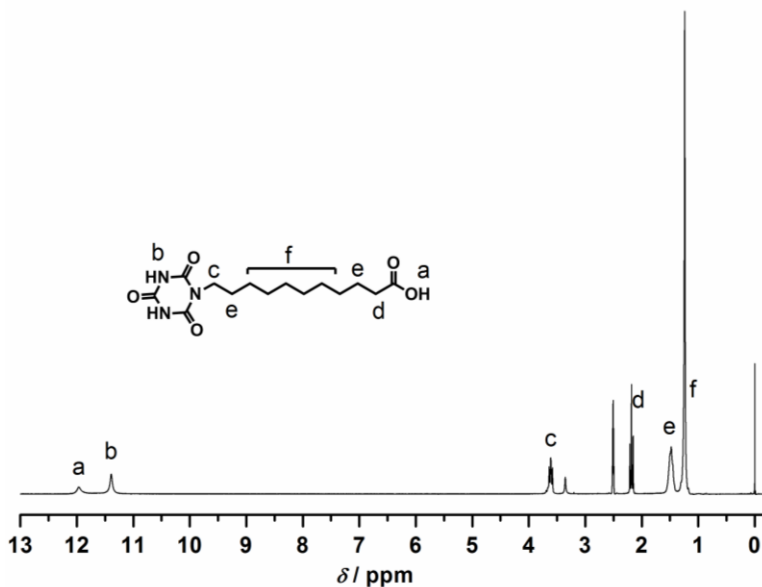


Figure 5.24 ^1H NMR spectrum of 11-(2,4,6-trioxo-1,3,5-triazinan-1-yl)undecanoic acid (**26**) in $\text{DMSO-}d_6$ at the ambient temperature. The peaks are not assigned that refer to solvent/water.

5.3.1.8 Synthesis of cyanuric acid functional poly(ethylene glycol) (CA-PEG) (27): **26** (0.5 g, 1.6 mmol) was dissolved in 5 mL of dry DMF. MeO-PEG-OH (0.585 g, 1.06 mmol) and 4-dimethylaminopyridine (DMAP) (0.130 g, 1.06 mmol) were dissolved in 5 mL dry DCM and subsequently added to the mixture. *N,N'*-Dicyclohexylcarbodiimide (DCC, 0.5 g, 2.4 mmol) was dissolved in 5 mL dry DCM and then added to the solution at 0 °C. The reaction was carried out at ambient temperature overnight. Solids were filtered off, the filtrate was concentrated and the crude product was purified by column chromatography on silica gel, eluting with CH₂Cl₂/MeOH (10/1) to give the CA-PEG (**27**) as a white solid (0.9 g, 97%). ¹H NMR (400 MHz, CDCl₃) δ (ppm) 8.81 (s, 2H), 4.20 (t, *J* = 7.5 Hz, 2H), 3.76 (d, *J* = 8.5 Hz, 2H), 3.60 (s, 44H), 3.55 – 3.44 (m, 2H), 3.33 (s, 3H), 2.27 (t, *J* = 7.5 Hz), 1.56 (s, 4H), 1.22 (s, 14H). (*M*_{n,SEC} = 1700 Da, *M*_w/*M*_n = 1.05).

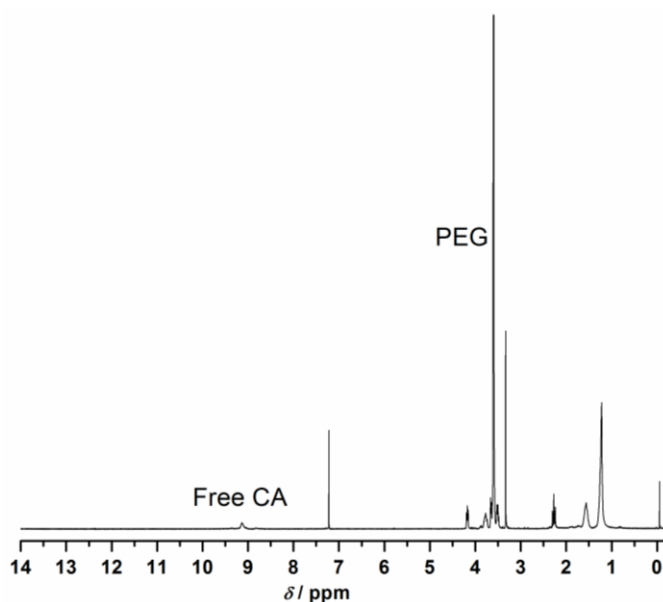
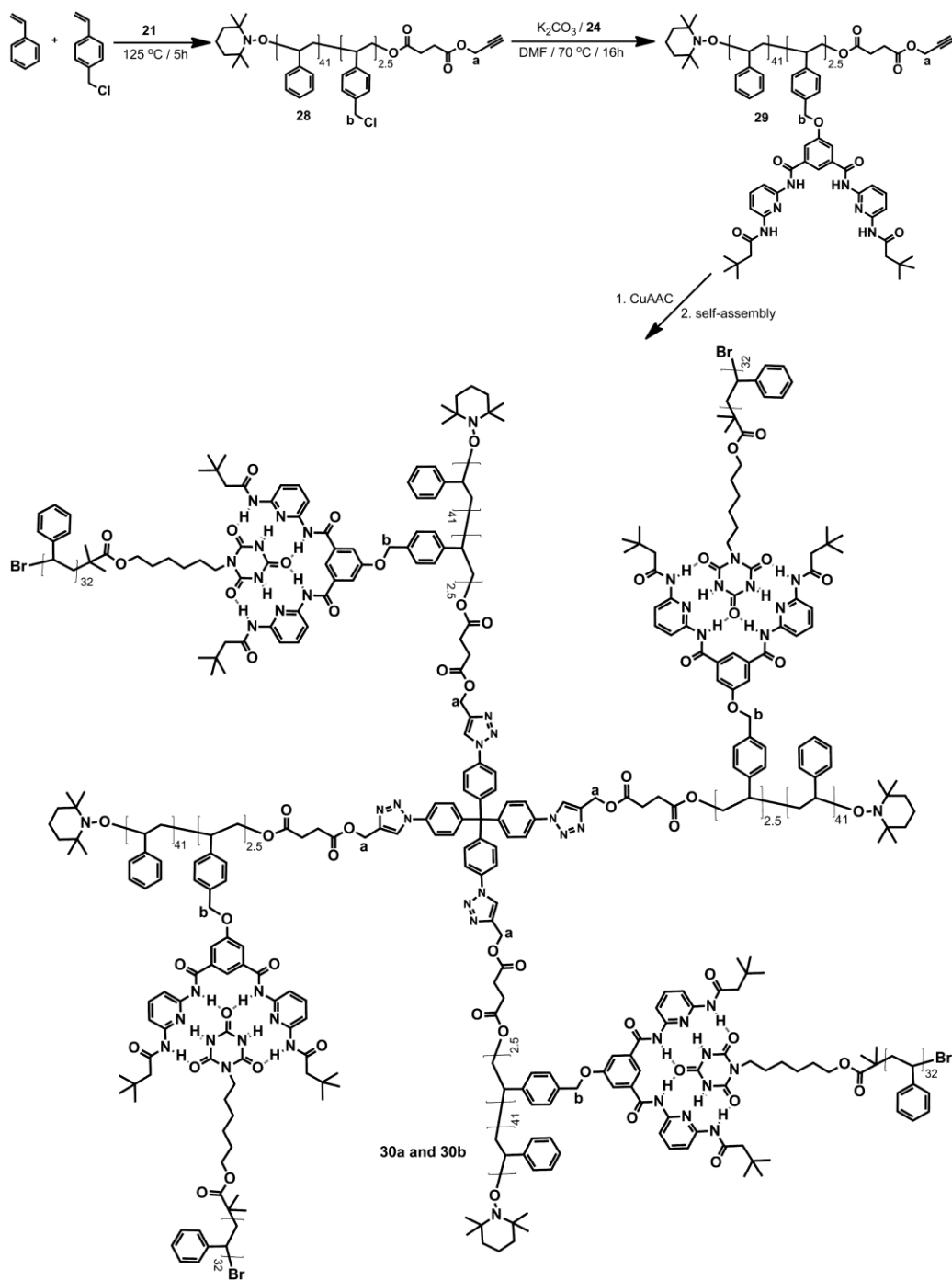


Figure 5.25 ¹H NMR spectrum of cyanuric acid functional poly(ethylene glycol) (CA-PEG) (**16**) in CH₂Cl₂ at ambient temperature.



Scheme 5.7. General chemical strategy for the preparation of supramolecular constructed (grafted) star-shaped macromolecules through hydrogen bonds via Hamilton wedge and cyanuric acid binding motifs. **30a** refers to non-self-assembled star-shaped macromolecules and **30b** refers to supramolecular grafted star-shaped macromolecules.

5.3.1.9 Preparation of alkyne end-functionalized P(S-co-CMS) copolymer (28): P(S-co-CMS) copolymers containing alkyne functionality was prepared via NMP of styrene (S) (5.5 mL) and chloromethylstyrene (CMS) (0.36 mL) in the presence of **21** (0.21 g, 0.087 mmol). The reaction mixture was degassed by three freeze-pump-thaw cycles and left under argon. The tube was then placed in an oil bath thermostated at 125 °C for 5 h. The polymerization mixture was diluted with THF, and precipitated in methanol. The obtained polymer was dried for 24 h in a vacuum oven at 25 °C to give a white solid (2.43 g). ¹H NMR (400 MHz, CDCl₃) δ (ppm) 7.17-6.15 (ArH of PS), 4.55 (2H, OCH₂CCH), 4.44 (2H, CH₂Cl), 3.95 (2H, CHCH₂-OCO), 2.52-2.30 (4H, OCCH₂CH₂CO), 1.78-1.18 (aliphatic protons of PS). ([M]₀/[I]₀ = 100, M_{n,NMR} = 5000 Da; M_{n,theo} = 5200 Da; M_{n,GPC} = 5500 Da; M_w/M_n = 1.13, conversion = 45%).

5.3.1.10 Preparation of alkyne end-functionalized P(S-co-HWS) copolymer (29): A solution of polymer **28** (1 g, 0.2 mmol), the hydroxyl functional Hamilton wedge (**24**) (0.56 g, 1.0 mmol), potassium carbonate (0.276 g, 2 mmol), and 3.5 mL of DMF was stirred at 70 °C for 24 h under an argon atmosphere. The resulting polymer was purified by column chromatography (silica gel), eluting with CH₂Cl₂/ethyl acetate (5/1) to give the P(S-co-HWS) copolymer (**29**) as a yellowish solid (1.25 g, 100%). ¹H NMR (400 MHz, CD₂Cl₂) δ (ppm) 8.46 (4H, NH of HW), 7.98-7.72 (ArH of HW), 7.17-6.15 (ArH of PS), 5.02 (2H, CH₂O), 4.62 (2H, OCH₂CCH), 3.95 (2H, CHCH₂-OCO), 2.52-2.30 (4H, OCCH₂CH₂CO), 1.78-1.18 (aliphatic protons of PS). M_{n,NMR} = 6300; M_{n,GPC} = 6200; M_w/M_n = 1.13).

5.3.1.11 Synthesis of Hamilton wedge functionalized star-shaped macromolecules (30a): An alkyne functional P(S-co-HWS) copolymer (**29**) (0.504 g, 0.08 mmol), compound **17** (0.01 g, 0.02 mmol), copper (II) sulfate pentahydrate (0.32 g, 1.65 mmol) and sodium ascorbate (0.4 g,

1.65 mmol) were dissolved in DMF (3 mL). The resulting mixture was stirred at 80 °C for 24 h. The polymerization mixture was cooled in an ice-bath, diluted by the addition of THF and the copper catalyst was removed by passing through a short column of neutral alumina. The solvent was removed under reduced pressure, subsequently diluted with the addition of CH₂Cl₂ and extracted with EDTA solution to remove the copper (a catalyst also complexed by the recognition unit). The organic phase was dried over Na₂SO₄, concentrated and subsequently precipitated two times into 80 mL methanol. The polymer was dried for 24 h under high vacuum and afforded a yellowish solid (0.41 g). ¹H NMR (400 MHz, CD₂Cl₂) δ (ppm) 8.54 (4H, NH of HW), 7.96-7.71 (ArH of HW), 7.05-6.56 (ArH of PS), 5.22 (2H, adjacent to the triazole ring), 5.02 (2H, CH₂O), 3.95 (2H, CHCH₂-OCO), 2.52-2.30 (4H, OCCH₂CH₂CO), 1.78-1.18 (aliphatic protons of PS). (*M*_{n,SEC} = 25100 Da, *M*_w/*M*_n = 1.08).

5.3.2 Results and Discussion of Construction of Star-shaped Macromolecules through Multiple Hydrogen Bonding

5.3.2.1 Preparation of Hamilton wedge functionalized star-shaped macromolecules

Hamilton wedge functionalized and well-defined star-shaped macromolecules were prepared through a combination of NMP and copper catalyzed azide and alkyne cycloaddition (CuAAC) (refer to Scheme 5.7). Initially, an alkyne functional NMP initiator was synthesized via esterification of compound **15** with **20** in the presence of TEA/DMAP as catalysts and THF as a solvent (refer to Scheme 5.6). The ¹H NMR spectrum of **21** indicated that new characteristic proton signals for the HCCCH₂O and COCH₂CH₂CO were observed at 4.66 ppm and 2.54 ppm, respectively (see Figure 5.20). The hydroxyl functional Hamilton wedge was prepared in a two

step process: First, a hydroxyl protected Hamilton wedge (**23**) was synthesized via an amidation reaction between compound **16** and **22** in the presence of TEA as catalyst and THF as a solvent. The ^1H NMR spectrum confirmed that new proton signals for the *NH* and $\text{COCH}_2(\text{CH}_3)_3$ hydrogens were observed at 10.60 ppm and 2.32 ppm (see Figure 5.21). Subsequently, hydrolysis of the benzoic ester group of **23** was readily accomplished in the presence of 1.5 N NaOH solution in a THF/methanol (2/1) mixture. The hydrolytic success was confirmed by ^1H NMR which indicates the appearance of the proton signal at 10.19 ppm of the hydroxyl of **24** and the disappearance of the proton signals at 8.20 ppm of the phenyl group (see Figure 5.22). Reaction of **19** with cyanuric acid afforded the substitution of product **25**, which was finally deprotected to yield compound **26**. The structures of these compounds were characterized by ^1H NMR (refer to Figure 5.23 and 5.24, respectively). The esterification of compound **26** and MeO-PEG-OH was carried out in the presence of DCC/DMAP as catalysts and DCM/DMF as solvents to give cyanuric acid functional PEG (PEG-CA) (**27**). The ^1H NMR spectrum of **27** indicates that new characteristic proton signals of ester group and cyanuric acid imide protons were observed at 4.17 ppm and at 9.10 ppm (see Figure 5.25). The structures of the compounds described above were also confirmed by ^{13}C NMR and ESI-MS. Alkyne functional well-defined linear poly(styrene-*co*-chloromethylstyrene) (**28**) was synthesized via NMP employing an alkyne functional initiator at 125 °C for 5 h and characterized by ^1H NMR and SEC (see Figure 5.26). The NMR derived number average molecular weight of **17** ($M_{n,\text{NMR}} = DP_{n,\text{NMR}}$ of St \times 104 $\text{g}\cdot\text{mol}^{-1}$ + $DP_{n,\text{NMR}}$ of CMS \times 152 $\text{g}\cdot\text{mol}^{-1}$ + MW of initiator $\text{g}\cdot\text{mol}^{-1}$ (**21**) = 41 \times 104 $\text{g}\cdot\text{mol}^{-1}$ +

$2.5 \times 152 \text{ g}\cdot\text{mol}^{-1} + 415 \text{ g}\cdot\text{mol}^{-1} = 5000 \text{ g}\cdot\text{mol}^{-1}$) of **28** was calculated by comparing the integrated areas of the aromatic protons of PS at 6.5-7.5 ppm and the two protons of the CH_2

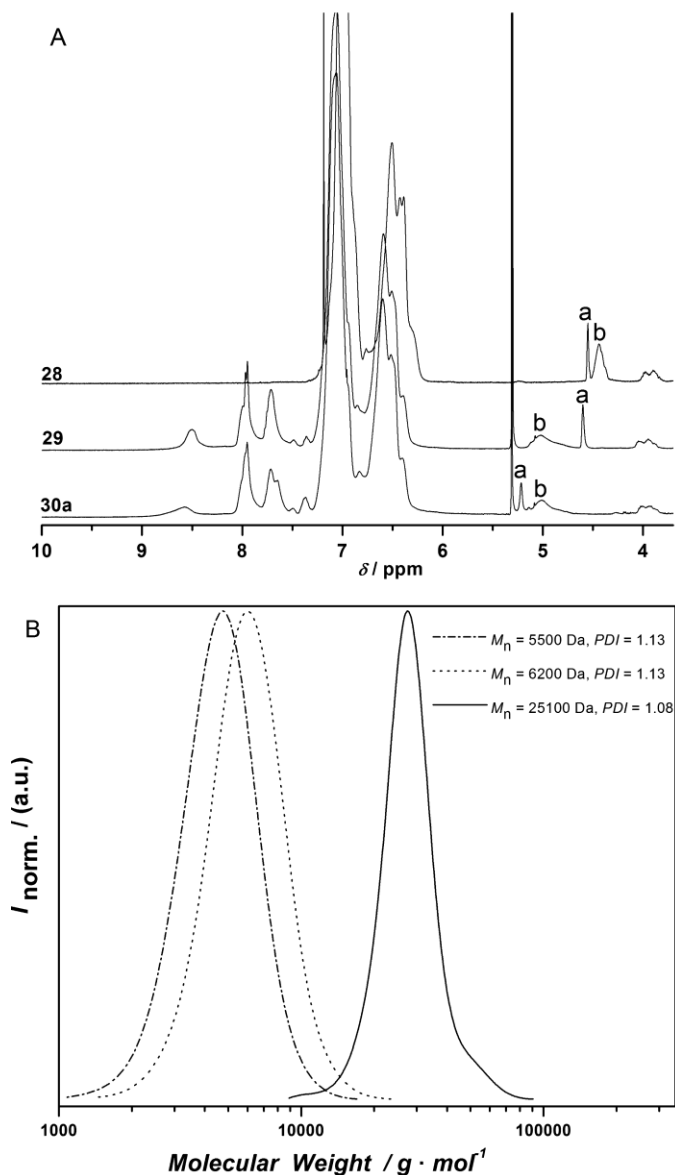


Figure 5.26 (a) Expanded ^1H NMR spectra of **28**, **29** and **30a** (b) SEC traces of the precursor polymers **17** (dash-dot line) and **18** (dot line) and final polymer **19a** (solid line). The chemical structures of the related polymers and ^1H NMR spectra labels can be found in Scheme 5.7.

adjacent to the alkyne group at 4.62 ppm. The number of the units of the chloromethylstyrene (CMS) can be calculated by the integral area of the CH_2 next to chlorine at 4.51 ppm and the CH_2 adjacent to the alkyne at 4.62 ppm. It was found that $M_{n,NMR}$ was consistent with error limits with the number average molecular weight from SEC ($M_{n,SEC} = 5500$ Da with $M_w/M_n = 1.13$ relative to PS standards). The hydroxyl functional Hamilton wedge was successfully introduced into the preformed P(S-*co*-CMS) copolymer backbone via an etherification reaction through nucleophilic substitution of the CMS units. The 1H NMR of the product **29** indicates 100% conversion of the chloromethylstyrene into its Hamilton wedge derivative as the signal at 4.51 ppm – corresponding to CH_2Cl – having completely disappeared and the new signals of the CH_2O group next to the Hamilton wedge being detected at 5.01 ppm (see Figure 5.26A). The SEC trace of P(S-*co*-HWS) (**29**) was clearly shifted to the higher molecular weight region (from 5500 Da to 6200 Da, with a theoretically expected shift of 6400 Da), confirming the introduction of the compound **24**. Finally, well-defined P(S-*co*-HWS) (**18**) with alkyne-end-functional group was reacted with tetrakis(4-azidophenyl)methane (**17**) to give the corresponding Hamilton wedge functional 4-arm star-shaped macromolecules. Copper-catalyzed azide and alkyne conjugation chemistry were successfully carried out with equimolar amounts of the reactants^[72] ([azide]/[alkyne] = 1/1) in DMF in the presence of $CuSO_4 \times H_2O$ /sodium ascorbate for 24 h at 80 °C. The SEC trace for the (P(S-*co*-HWS))₄ copolymer (**30a**) was clearly shifted to the higher molecular weight region (from 6200 Da to 25100 Da) featuring a monomodal distribution (refer

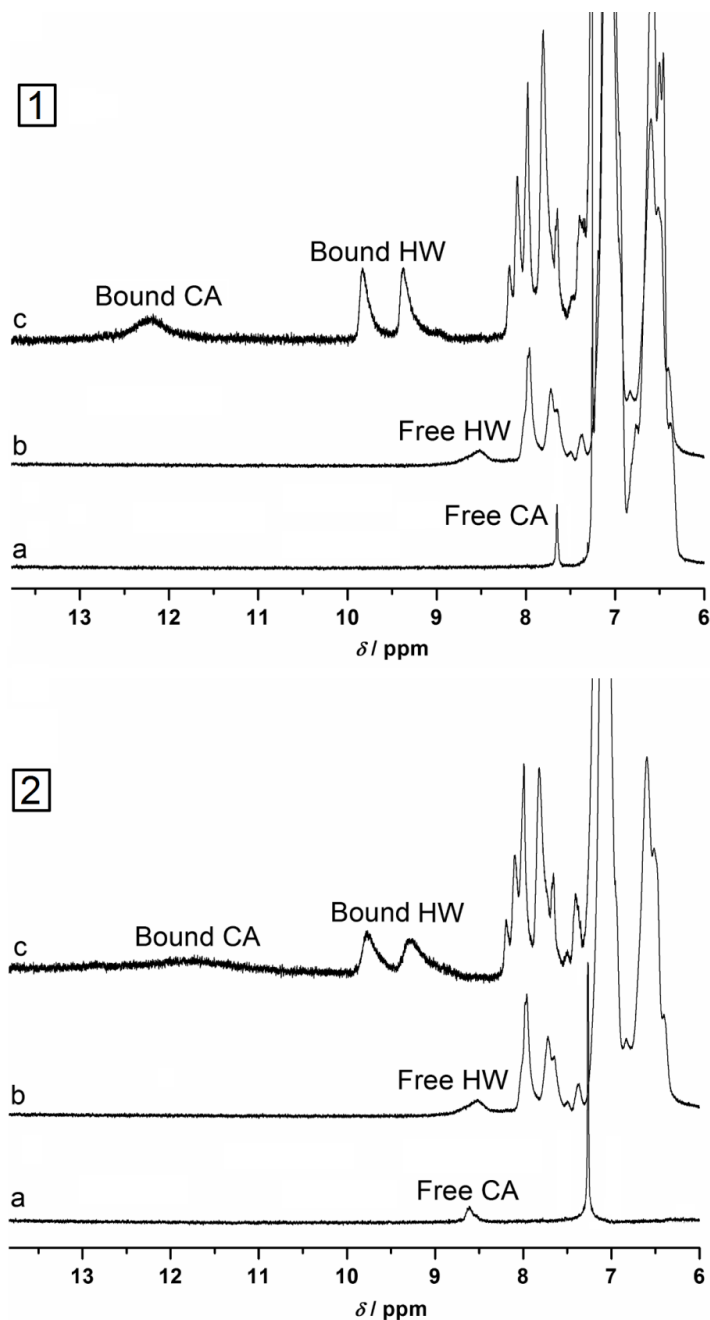


Figure 5.27 Expanded ^1H NMR spectrum of (1a) PS-CA (1b) $(\text{PS-co-HWS})_4$ (1c) $(\text{PS-g-PS})_4$ (2a) PMMA-CA (2b) $(\text{PS-co-HWS})_4$ (2c) $(\text{PS-g-PMMA})_4$ in CD_2Cl_2 at ambient temperature. Equimolar amounts with respect to the HW and CA binding motifs were employed. The NMR data for the poly(ethylene glycol) system can be found in the Figure 5.27.

to Figure 5.26B). The ^1H NMR spectrum of **30a** indicates that a signal at 4.62 ppm, corresponding to CH_2CCH , has completely disappeared and new signals of the CH_2 group next to the triazole ring was detected at 5.22 ppm (see Figure 5.26A).

5.3.2.2 Supramolecular construction of star-shaped macromolecules

The first evidence for the formation of the self-assembly between HW-functionalized star-shaped macromolecules and CA-functional linear polymer in CD_2Cl_2 was provided by ^1H NMR studies through hydrogen bonding. The chemical shifts of the amide protons of HW and the imide protons of CA in the ^1H NMR spectrum (see Figure 5.27) clearly evidences the complexation of these specific units in solution. The ^1H NMR spectrum of $(\text{P}(\text{S-co-HWS}))_4$ (**30a**) recorded in CD_2Cl_2 evidences that the signals of the NH protons of the Hamilton receptor appeared at 8.46 ppm (see 1b and 2b in the Figure 5.27). Subsequently, the formation of supramolecular grafted star-shaped polymers via H-bonding between the HW receptor and the CA end-functionalized well-defined linear polymers was investigated. All self-assembly processes of the building blocks can be followed by monitoring characteristic changes in the chemical shifts of the NH protons of the two recognition pairs using ^1H NMR spectroscopy (see Figure 5.27). Initially, the formation of a $(\text{PS-g-PS})_4$ (**30b**) self-assembled structure between $(\text{P}(\text{S-co-HWS}))_4$ (**30a**) and **PS-CA** (**9**) in CD_2Cl_2 at ambient temperature was studied. Upon the addition of **9** into **30a** (1:1 ratio in terms of recognition units) in CD_2Cl_2 , the ^1H NMR spectrum reveals strong shifts of the amide protons of the Hamilton receptor from 8.46 ppm to 9.83 and 9.38 ppm (see 1c in the Figure 5.27). Moreover, the chemical shift of the proton resonance of the imide protons of **PS-CA** (**9**) changed from 7.71 to ppm (see 1a in Figure 5.27) to 12.21 ppm (see 1c in Figure 5.27) thus evidencing that the self-assembled supramolecular grafted star-shaped polymer $(\text{PS-g-PS})_4$

was formed. Secondly, the formation of a **(PS-*g*-PMMA)₄** self-assembled structure between **30a** and **PMMA-CA (10)** in CD₂Cl₂ at ambient temperature was investigated. The ¹H NMR spectrum indicated that the amide protons of the Hamilton receptor shift from 8.46 ppm to 9.74 and 9.24 ppm (see 2c in Figure 5.27). Furthermore, a new signal appeared at 11.71 ppm that corresponds to the (dynamically) bound cyanuric acid unit in the self-assembled motif (see 2c in Figure 5.27). However, the imide protons of CA are in a coalescence regime, where the signals of the bounded NH protons appear very broad.^[73] When **PEG-CA (27)** was mixed with **30a** in CD₂Cl₂, the chemical shift of the imide protons of **PEG-CA (27)** changed from 9.10 to 12.02 ppm. Moreover, the peaks at 9.90 and 9.46 ppm were assigned to the NH protons of the Hamilton wedge in CD₂Cl₂ (see Figure 5.27).

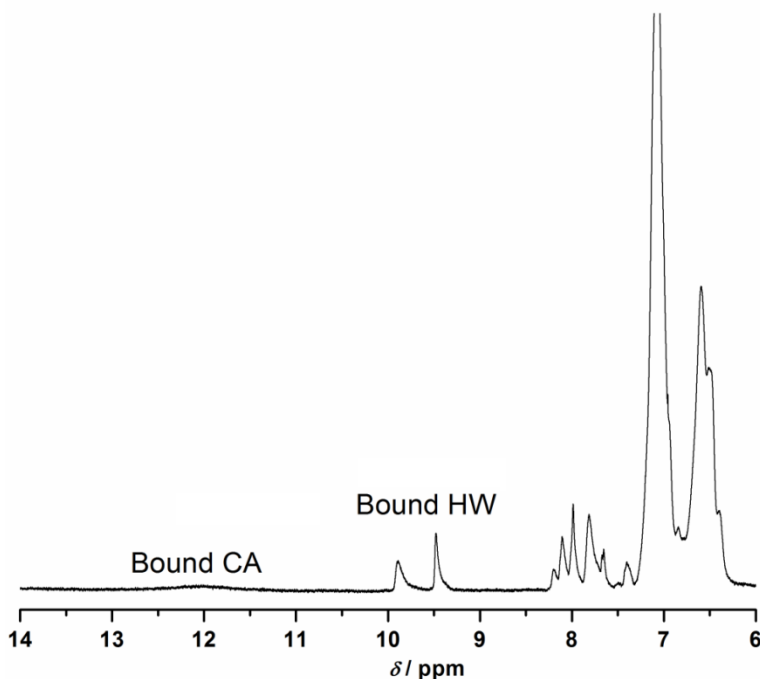


Figure 5.28 Expanded ¹H NMR spectrum of **(PS-*g*-PEG)₄** in CD₂Cl₂ at ambient temperature. Equimolar amounts with respect to the HW and CA binding motifs were employed.

Dynamic light scattering (DLS) has developed into a powerful and versatile tool for estimating the size distribution profile of small particles in suspension or polymers in solution, effective for particles in the size range of a few nanometers up to several micrometers. As a crucial assessment of the efficient formation of self-assembly of complex macromolecular architectures

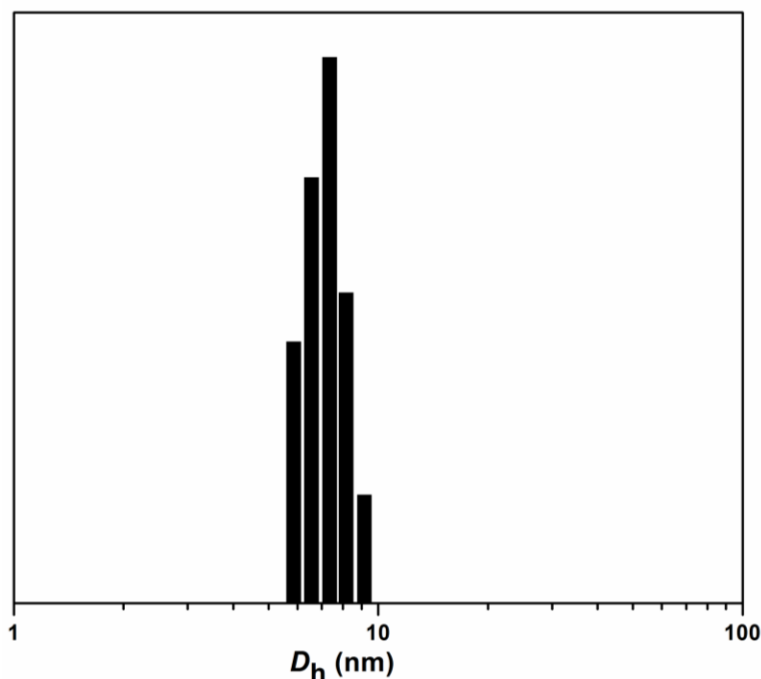


Figure 5.29 The mean hydrodynamic diameter of supramolecular grafted star-shaped macromolecules (PS-g-PS)₄ (**30b**) determined at 90° in dichloromethane at ambient temperature.

through H-bonding between host-guest (HW-CA) systems, comparative DLS analysis were performed in dichloromethane solutions. While the ^1H NMR experiments indicated that self-assembly occurred between HW-functional star polymer and CA-functional linear polymers, measurement of the hydrodynamic diameter (D_h) and weight-average molecular weight (M_w) can

provide evidence for supramolecular constructions of star-shaped macromolecules. Thus one of the systems, i.e. the linear polymer (**CA-PS**) (**9**) and star polymer **30a**, was exemplary subjected to DLS revealing a D_h of 2.6 nm and 1.4 nm, respectively by DLS measurements in CH_2Cl_2 . It might seem somewhat surprising that **30a** features a smaller D_h than **9**; however, the solubility of **30a** in CH_2Cl_2 is relatively poor thus leading to very compact nano-particles. In contrast, the supramolecular grafted star-shaped polymer (**PS-g-PS**)₄ (**30b**) in CH_2Cl_2 with an equimolar ratio of **CA-PS** (**9**) and **30a**) recognition motifs displayed a new population with a D_h equal to 7.5 nm, consistent with the formation of supramolecular grafted star-shaped polymer from the association via the binding motifs HW/CA. Moreover, no distribution in DLS corresponding to linear and star polymers could be observed, thus supporting the formation of the supramolecular graft star-shaped macromolecules (see Figure 5.29). Furthermore, the weight-average molecular weight (M_w) of the supramolecular grafted star-shaped polymers (**PS-g-PS**)₄ (**30b**) and (**PS-g-PEG**)₄ were determined by Static Light Scattering (SLS) in CH_2Cl_2 .

Table 5.2. Molecular weight of the precursor and the final polymers obtained by SEC and SLS

No	Precursor polymer		Grafted star polymer		
	M_w^a ,SEC of linear polymer	M_w^a ,SEC of 30a	M_w^b ,SLS	M_w^c ,theo	dn/dc^d
1	3800 Da (9)	27100 Da	59000 Da	65000 Da	0.16
2	1800 Da (27)	27100 Da	50000 Da	45000 Da	0.13

^a Determined via RI detection SEC using linear PS standards in THF.

^b Determined by SLS in dichloromethane via extrapolation of the Debye plots (refer to the Figure 5.31 and 5.32).

^c $M_{w,theo} = (M_{w,SEC} \text{ of the linear polymer} \times (10 \text{ is ratio between HW and CA})) \times M_{w,SEC} \text{ of the star polymer}$

^d Determined in dichloromethane.

Inspection of Table 5.2 shows a considerable increase of the molecular weight after converting the linear polymer to star-shaped polymer through hydrogen bonding. Again, sample systems were explored via SLS: When the well-defined linear polymers (**CA-PS** and **CA-PEG**) were

grafted to the HW-functionalized star-shaped macromolecules **30a** via complementary recognition motifs, the weight-average molecular weight of the **30a** increased from 27100 Da (M_w) to 59000 Da (with a theoretically expected increase to 65000 Da, matching error <10%) for **30b** and 50000 Da (with a theoretically expected increase to 45000 Da, matching error 10%) for **(PS-g-PEG)₄**. Thus, the DLS and SLS results carried out on the example of the supramolecular grafting of **(PS-g-PS (30b))** and **(PS-g-PEG)₄** unambiguously support the formation of supramolecular grafted star-shaped polymers between complementary recognition units.

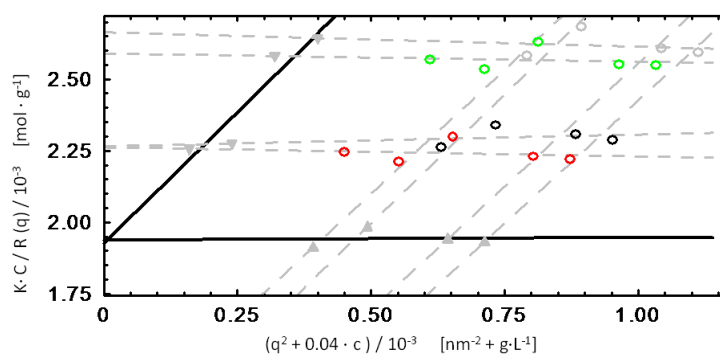


Figure 5.30 Zimm-plot obtained by SLS measurement of the mixture of CA-PS (**9**) and **30a** dissolved in dichloromethane at 8 g L⁻¹ (○), 6 g L⁻¹ (○) and 4 g L⁻¹ (○).

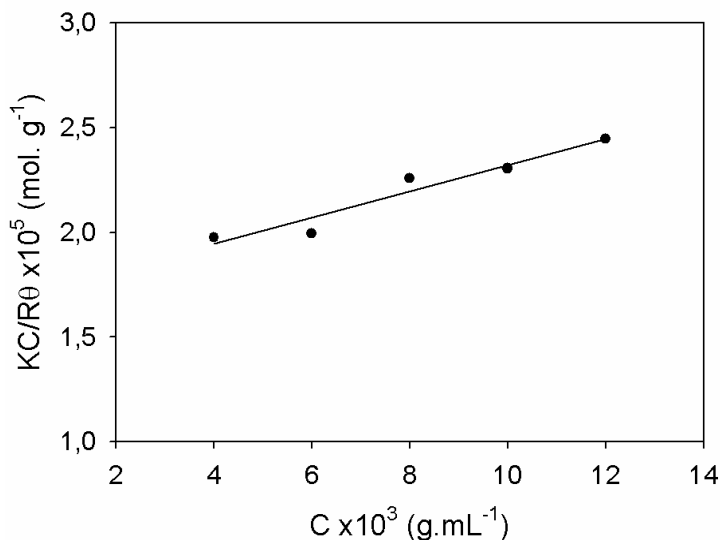


Figure 5.31 Debye-plot obtained by SLS measurement at 90° of the mixture of CA-PS (9) and 30a dissolved in dichloromethane (good solvent for polystyrene, thus $A_2 > 0$).

Static light scattering (SLS) is commonly used to measure the weight-average molecular weight (M_w) and the radius of gyration by extrapolating the concentration versus light scattering angle plot to zero. The M_w values that are presented in the text were, indeed, obtained by the extrapolation of the plot of concentration versus angle to zero and by plotting a Zimm diagram (see Figure 5.30). However, the size of the grafted polymers is too small to obtain fully reliable values from the SLS analysis via a Zimm plot. Figure 5.30 reveals that the Zimm plot obtained from the characterization of the mixture of CA-PS (9) and $(P(S-co-HWS))_4$ (30a) in dichloromethane features a certain degree of scattering. Therefore, the values obtained by extrapolation to zero of the concentration at 90° (i.e., Debye plots) were utilized. Both Debye plots (see Figure 5.31 and 5.32) for the molecular weights collated in Table 1 were thus shown.

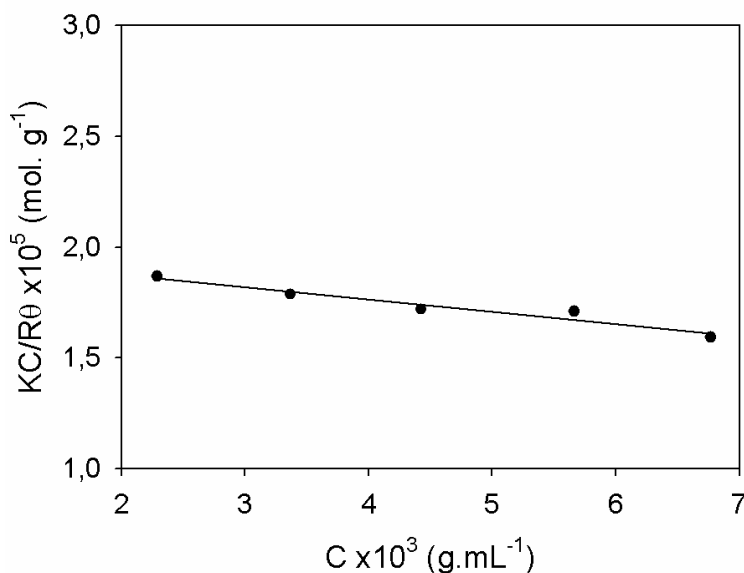


Figure 5.32 Debye-plot obtained by SLS measurement at 90° of the mixture of **PEG-CA (27)** and **30a** dissolved in dichloromethane (relatively poor solvent for PEG, thus $A_2 < 0$).

Furthermore, over the range of concentrations characterized by LS one can see that there is no concentration dependence of the H-bonding interactions, indicating that the bonds are relatively strong. However, the system was not characterized at lower concentrations to assess if the H-bonding achieved is still strong at a higher dilution. The analysis via Zimm plot reveals that the values of R_g were as low as around 3 nm, which is expected for such a system. However – as stated above – the expected values of R_g for small particles are below the detection limit, typically ranging from 20 to 500 nm, of the employed instrument. As previously suggested, this size range is not considered relevant to our system and supports the choice to rely on the Debye plot instead of the Zimm plot for the data analysis.

5.4 Conclusions

On the one hand, well-defined narrow polydispersity polymers containing a terminal and mid-chain functional Hamilton Wedge as well as cyanuric acid terminal motifs function efficiently during the self-assembly into block and star (co)polymer structures. The Hamilton Wedge and cyanuric acid functional macromolecular building blocks were prepared via a combination of atom transfer radical polymerization and copper catalyzed azide-alkyne ligation. Provided the binding motif decorated prepolymer systems carry a suitable unit allowing for the identification of individual chain terminal protons, the self-assembly process can be studied at ambient temperature via proton NMR spectroscopy, evidencing very high degrees of binding in two cases in excess of 90%, attesting the almost quantitative formation of block copolymer structures in CH_2Cl_2 . In addition, it has been evidenced that the six hydrogen bonds between the Hamilton Wedge and cyanuric acid offer stronger binding compared to other systems such as the three-hydrogen bond forming diaminopyridine-thymine assembly. This in turn offers a better option for the preparation of self-assembled polymers with variable topologies. The present data thus indicate that self-assembly driven macromolecular design is readily achievable employing Hamilton Wedge and cyanuric acid motifs based on ATRP polymers, even at ambient temperatures.

On the other hand, an alkyne functional nitroxide-mediated radical polymerization (NMP) initiator, hydroxyl functional Hamilton wedge and tetrakis(4-azidophenyl)methane were successfully synthesized to generate HW-functionalized star-shaped macromolecule *via* a combination of NMP and copper-catalyzed azide alkyne cycloaddition (CuAAC). Supramolecularly-constructed star shaped macromolecules were – for the first time – prepared

through H-bonds between a Hamilton wedge (HW) and cyanuric acid (CA) recognition motifs to generate (PS-*g*-PS)₄ (30b), (PS-*g*-PMMA)₄, and (PS-*g*-PEG)₄ star entities in CH₂Cl₂ or CD₂Cl₂ at ambient temperature. The self-assembly process was evidenced by proton nuclear magnetic resonance (¹H NMR) spectroscopy, dynamic as well as static light scattering (DLS and SLS) analysis. The present results evidence that the construction of complex macromolecular star entities on a very well-defined level is indeed possible employing high precision macromolecular design strategies.

5.5 References

- [1] J. Roovers, in *Star and Hyperbranched Polymers*; M. Mishra, S. Kobayashi, Ed.s, Marcel Dekker, New York, 1998, p. 285
- [2] W. Burchard, *Adv. Polym. Sci.* **1999**, *143*, 113.
- [3] K. Matyjaszewski, *Science* **2011**, *333*, 1104.
- [4] T. Yamamoto, Y. Tezuka, *Polym. Chem.* **2011**, *2*, 1930.
- [5] N. Hadjichristidis, M. Pitsikalis, S. Pispas, H. Iatrou, *Chem. Rev.* **2001**, *101*, 3747.
- [6] A. Hirao, M. Hayashi, S. Loykulnant, K. Sugiyama, S. W. Ryu, N. Haraguchi, A. Matsuo, T. Higashihara, *Prog. Polym. Sci.* **2005**, *30*, 111.
- [7] J. Chiefari, Y. K. Chong, F. Ercole, J. Krstina, J. Jeffery, T. P. T. Le, R. T. A. Mayadunne, G. F. Meijs, C. L. Moad, G. Moad, E. Rizzardo, S. H. Thang, *Macromolecules* **1998**, *31*, 5559.
- [8] C. Barner-Kowollik, S. Perrier, *J. Polym. Sci. Part A: Polym. Chem.* **2008**, *46*, 5715.
- [9] M. K. Georges, R. P. N. Veregin, P. M. Kazmaier, G. K. Hamer, *Macromolecules* **1993**, *26*, 2987.
- [10] C. J. Hawker, A. W. Bosman, E. Harth, *Chem. Rev.* **2001**, *101*, 3661.
- [11] M. Kato, M. Kamigaito, M. Sawamoto, T. Higashimura, *Macromolecules* **1995**, *28*, 1721.

- [12] M. Ouchi, T. Terashima, M. Sawamoto, *Chem. Rev.* **2009**, *109*, 4963.
- [13] J. S. Wang, K. Matyjaszewski, *Macromolecules* **1995**, *28*, 7901.
- [14] F. Di Lena, K. Matyjaszewski, *Prog. Polym. Sci.* **2010**, *35*, 959.
- [15] V. Percec, B. Barboiu, *Macromolecules* **1995**, *28*, 7970.
- [16] B. M. Rosen, V. Percec, *Chem. Rev.* **2009**, *109*, 5069.
- [17] K. Matyjaszewski, J. Xia, *Chem. Rev.* **2001**, *101*, 2921.
- [18] L. Barner, T. P. Davis, M. H. Stenzel, C. Barner-Kowollik, *Macromol. Rapid Commun.* **2007**, *28*, 539.
- [19] C. J. Hawker, A. W. Bosman, E. Harth, *Chem. Rev.* **2001**, *101*, 3661.
- [20] R. B. Grubbs, *Polym. Rev.* **2011**, *51*, 104.
- [21] B. S. Sumerlin, A. P. Vogt, *Macromolecules* **2010**, *43*, 1.
- [22] R. K. Iha, K. L. Wooley, A. M. Nystrom, D. J. Burke, M. J. Kade, C. J. Hawker, *Chem. Rev.* **2009**, *109*, 5620.
- [23] K. Khanna, S. Varshney, A. Kakkar, *Polym. Chem.* **2010**, *1*, 1171.
- [24] C. Barner-Kowollik, F. E. Du Prez, P. Espeel, C. J. Hawker, T. Junkers, H. Schlaad, W. Van Camp, *Angew. Chem. Int. Ed.* **2011**, *50*, 60.
- [25] J.-M. Lehn, *Chem. Soc. Rev.* **2007**, *36*, 151.
- [26] M. J. Krische, J.-M. Lehn, *Struct. Bonding (Berlin)* **2000**, *96*, 3.
- [27] F. H. Beijer, H. Kooijman, A. L. Spek, R. P. Sijbesma, E. W. Meijer, *Angew. Chem. Int. Ed.* **1998**, *37*, 75.
- [28] R. Knapp, A. Schott, M. Rehahn, *Macromolecules* **1996**, *29*, 478.
- [29] J. P. Sauvage, J.-P. Collin, J.-C. Chambron, S. Guillerez, C. Coudret, *Chem. Rev.* **1994**, *94*, 993.
- [30] M. Chiper, M. A. R. Meier, D. Wouters, S. Hoepfener, C.-A. Fustin, J.-F. Gohy, U. S. Schubert, *Macromolecules* **2008**, *41*, 2771.
- [31] C. Nuckolls, T. J. Katz, G. Katz, P. J. Collings, L. Castellanos, L. *J. Am. Chem. Soc.* **1999**, *121*, 79.

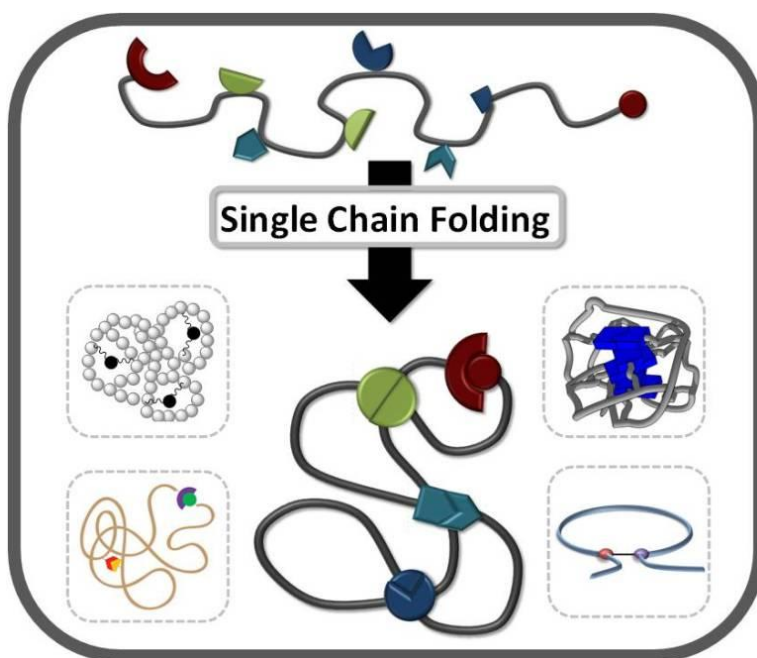
- [32] L. Brunsveld, E. W. Meijer, R. B. Prince, J. S. Moore, *J. Am. Chem. Soc.* **2001**, *123*, 7978.
- [33] N. Yamaguchi, H. W. Gibson, *Angew. Chem. Int. Ed.* **1999**, *38*, 143.
- [34] P. R. Ashton, P. J. Campbell, E. J. T. Chrystal, P. T. Glink, S. Menzer, D. Philp, N. Spencer, J. F. Stoddart, P. A. Tasker, D. J. Williams, *Angew. Chem. Int. Ed.* **1995**, *34*, 1865.
- [35] J. D. Fox, S. J. Rowan, *Macromolecules* **2009**, *42*, 6823.
- [36] L. Brunsveld, B. J. B. Folmer, E. W. Meijer, R. P. Sijbesma, *Chem. Rev.* **2001**, *101*, 4071.
- [37] T. F. A. De Greef, M. M. J. Smulders, M. Wolffs, A. P. H. J. Schenning, R. P. Sijbesma, E. W. Meijer, *Chem. Rev.* **2009**, *109*, 5687.
- [38] O. Ikkala, G. Brinke, *Science* **2002**, *295*, 2407.
- [39] A. V. Ambade, C. Burd, M. N. Higley, K. P. Nair, M. Weck, *Chem. Eur. J.* **2009**, *15*, 11904.
- [40] S. K. Yang, A. V. Ambade, M. Weck, *Chem. Eur. J.* **2009**, *15*, 6605.
- [41] C. R. South, C. Burd, M. Weck, *Acc. Chem. Res.* **2007**, *40*, 63.
- [42] W. B. Binder, M. J. Kunz, C. Kluger, G. Hayn, R. Saf, *Macromolecules* **2004**, *37*, 1749.
- [43] C. Burd, M. Weck, *Macromolecules* **2005**, *38*, 7225.
- [44] W. H. Binder, S. Bernstorff, C. Kluger, L. Petraru, M. J. Kunz, *Adv. Mater.* **2005**, *17*, 2824.
- [45] D. Lu, Y. Wang, T. Wu, K. Tao, L. An, R. Bai, *J. Polym. Sci. Part A: Polym. Chem.* **2008**, *46*, 5805.
- [46] F. Huang, D. S. Nagvekar, S. Slebodnick, H. W. Gibson, *J. Am. Chem. Soc.* **2005**, *127*, 484.
- [47] A. V. Ambade, S. K. Yang, M. Weck, *Angew. Chem. Int. Ed.* **2009**, *48*, 2894.
- [48] E. B. Berda, J. E. Foster, E. W. Meijer, *Macromolecules* **2010**, *43*, 1430.
- [49] S. H. M. Sontjens, R. A. E. Renken, G. M. L. van Gemert, T. A. P. Engels, A. V. Bosman, H. M. Janssen, L. E. Govaert, F. P. T. Baaijens, *Macromolecules* **2008**, *41*, 5703.

- [50] S. Chen, A. Bertrand, X. Chang, P. Alcouffe, C. Ladaviere, J.-F. Gerard, F. Lortie, J. Bernard, *J. Macromolecules* **2010**, *43*, 5981.
- [51] X. Yang, F. Hua, K. Yamato, E. Ruckenstein, B Gong, W Kim, C. Y. Ryu, *Angew. Chem. Int. Ed.* **2004**, *43*, 6471.
- [52] K. E. Feldman, M. J. Kade, T. F. A. de Greef, E. W. Meijer, E. J. Kramer, C. J.; Hawker, *Macromolecules* **2008**, *41*, 4694.
- [53] A. D. Celiz, O. A. Scherman, *Macromolecules* **2008**, *41*, 4115.
- [54] D. J. M. van Beek, M. A. J. Gillissen, B. A. C. van As, A. R. A. Palmans, R. P. Sijbesma, *Macromolecules* **2007**, *40*, 6340.
- [55] S. K. Yang, A. V. Ambade, M. Weck, *J. Am. Chem. Soc.* **2010**, *132*, 1637.
- [56] B. G. G. Lohmeijer, U. S. Schubert, *Angew. Chem. Int. Ed.* **2002**, *41*, 3825.
- [57] E. M. Todd, S. C. Zimmerman, *J. Am. Chem. Soc.* **2007**, *129*, 14534.
- [58] A. Likhitsup, S. Yu, Y.-H. Ng, C. L. L. Chai, E. K. W. Tam, E. K. W. *Chem. Commun.* **2009**, *45*, 4070.
- [59] Y. Shen, H. Tang, S. Ding, *Prog. Polym. Sci.* **2004**, *29*, 1053.
- [60] J. Bernard, F. Lortie, B. Fenet, *Macromol. Rapid Commun.* **2009**, *30*, 83.
- [61] O. Altintas, P. Gerstel, N. Dingenouts, C. Barner-Kowollik, *Chem. Commun.* **2010**, *46*, 6291.
- [62] H. C. Kolb, M. G. Finn, K. B. Sharpless, *Angew. Chem. Int. Ed.* **2001**, *40*, 2004.
- [63] S. K. Chang, A. D. Hamilton, *J. Am. Chem. Soc.* **1988**, *110*, 1318.
- [64] H. Ihre, A. Hult, J. M. J. Frechet, I. Gitsov, *Macromolecules* 1998, **31**, 4061.
- [65] O. Altintas, B. Yankul, G. Hizal, U. Tunca, *J. Polym. Sci. Part A: Polym. Chem.* 2006, **44**, 6458.
- [66] O. Altintas, G. Hizal, U. Tunca, *J. Polym. Sci. Part A: Polym. Chem.* **2006**, *44*, 5699.
- [67] C. J. Hawker, J. L. Hedrick, *Macromolecules* **1995**, *28*, 2993.
- [68] A.B. Eldrup, C. Christensen, G. Haaima, P.E. Nielsen, *J. Am. Chem. Soc.* **2002**, *124*, 3254.

- [69] O. Plietzsch, C. I. Schilling, M. Tolev, M. Nieger, C. Richert, T. Muller, S. Bräse, *Org. Biomol. Chem.* **2009**, *7*, 4734.
- [70] F. Osswald, E. Vogel, O. Safarowsky, F. Schwanke, F. Vögtle, *Adv. Synth. Catal.* **2001**, *343*, 303.
- [71] S. Chen, B. Song, Z. Wang, X. Zhang, *J. Phys. Chem. C* **2008**, *112*, 3308-3313.
- [72] C. Barner-Kowollik, F. E. Du Prez, P. Espeel, C. J. Hawker, T. Junkers, H. Schlaad, W. Van Camp, *Angew. Chem. Int. Ed.* **2011**, *50*, 60.
- [73] K. Hager, A. Franz, A. Hirsch, *Chem. Eur. J.* **2006**, *12*, 2663.

Concluding Remarks and Outlook

Chapter 6



In the present thesis, initial attempts towards mimicking the structure of natural biomacromolecules via single chain folding of well-defined functional linear synthetic macromolecules are presented. In addition, the design of complex macromolecular structures via (such as stars) supramolecular chemistry is discussed.

6.1 Concluding Remarks

Mimicking the behavior of naturally occurring macromolecules – such as proteins – is one of the key aims of advanced polymer chemistry. Folding of single polymer chains has steadily been growing in popularity, especially for the preparation of covalently tethered polymeric nanoparticles, yet not for mimicking dynamically bound natural macromolecules. The present body of work has shown the applications of self-folding of single polymer chains via multiple hydrogen bonding. The polymer chains are prepared via precision synthesis and are subsequently folded into defined single chain geometries. Moreover, complex macromolecular structures such as supramolecular miktoarm star polymers are additionally prepared through non-covalent interactions via hydrogen bonds.

An effective dynamic or static intramolecular chain collapse of single polymer chain involves the facile and controllable incorporation of appropriate – covalent and non-covalent – cross-linking precursors into an individual polymer chain. To achieve such materials, the polymeric materials have to be prepared with a very high functional group fidelity; often living/controlled radical polymerization can achieve such high fidelities when conducted at low conversions ($< 20\%$) and limited molecular weights (≤ 15000 Da). When considering covalent bond driven single chain collapse, it should be noted that the employed conjugation processes have specific advantages and disadvantages, such as that the formation of e.g. benzocyclobutane only occurs at the high temperatures, the necessity of a catalyst or the presence of an initiator in the free-radical induced cross-linking. In any case, ultra-dilute reaction conditions or a continuous addition technique must be employed to favor intramolecular coupling over intermolecular linking, irrespective of whether the single chain folding is driven by dynamic H-bonding or by covalent linking. To avoid harsh conditions, many synthetic concepts and

strategies have been adopted from small organic molecules based on e.g. free radical reactions, Grubbs' catalyst cross-metathesis, amine-isocyanate reactions, formation of acylhydrazone linkages, photo-induced Bergman cyclization, photodimerization of coumarin or mild modular conjugation chemistries and multiple hydrogen bond formation. The resulting functionalized polymeric nanoparticles have been discussed as versatile building blocks for nano-technologically relevant structures. The preparation of significantly more diversified functional precursors under even milder reaction conditions are the most important challenges in the near future, so that their application in biological systems – e.g. as delivery vectors – can be fully exploited.

6.2 Outlook

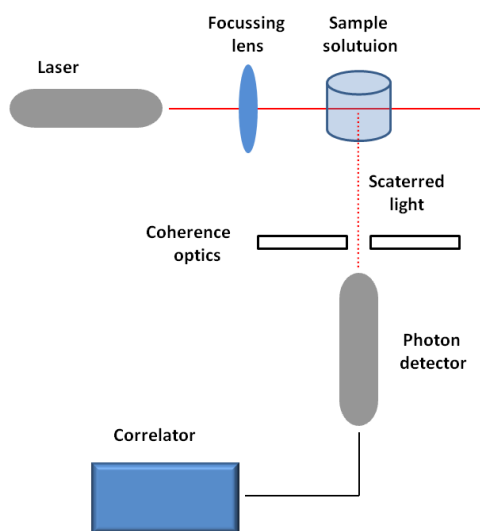
The self-folding of well-defined single polymer chains through non-covalent interactions, aimed at mimicking natural biomacromolecules, is a relatively new field in polymer science. In the current thesis attempts been made to mimic the folding behavior and elements of natural biomacromolecules – such as proteins – on a very simple level, yet on the basis of entirely synthetic polymeric systems. These ‘first-step’ systems should not be viewed as real nature mimics, but rather as first attempts to gain an improved understanding of the scope for reaching true biomimetic protein systems. Efforts in mimicking the protein folding mechanisms, whilst introducing several mutually orthogonal groups into the polymer chains, are a challenging task. The present study has the aim of evaluating the long term possibility of employing single polymer chains in H-bonding driven self-assembly procedures that can fulfill a testable – i.e. in a bioassay – biological function. Whether the ultimate aim of mimicking the functionality as well as secondary and tertiary protein structure coupled with a triggered reversible self-folding

process can be reached remains to be established – first encouraging steps have been taken. It will now require a concerted effort between macromolecular chemists, biophysicists and biologists to progress towards true macromolecular biomimetics. Key questions that need to be addressed include: (i) How does the reversible single chain self-folding process depend on the type of polymer employed (including potential periodic element forming polymer arrays), i.e. flexible vs. inflexible ? (ii) What are the time scales of interchange and the distance dynamics between the orthogonally interacting recognition units ? (iii) Is a block copolymer structure, i.e. segmented arrangement between the individual mutually orthogonal recognition units, desirable and what criteria define 'desirable' ? (iv) How can biologically required functionalities be incorporated during the synthetic approach and how do they affect the self-folding process ? (v) How can bio-signal triggered self-folding be induced and, finally, (iv) does the non-mondisperse nature of the synthetic macromolecular designs presented herein affect their potential biological function ?

Ultimately, true biomimetic synthetic single chain folded polymers carrying biological cues can fulfill a testable biological function – now fulfilled by a natural protein or enzyme – in a bioassay or even a living organism within a timeframe of 10 years. To reach such an ambitious goal a concerted effort is now required between macromolecular chemists, biophysicists and biologists to progress towards true macromolecular biomimetics.

Materials and Characterization Techniques

Chapter 7



In the current these, all small molecules are analyzed by ^1H and ^{13}C nuclear magnetic resonance spectroscopy (NMR) as well as electrospray ionization-mass spectrometry (ESI-MS). The prepared macromolecules are characterized via size exclusion chromatography (SEC), ^1H NMR and attenuated total reflectance-infra red spectroscopy (ATR-IR). Supramolecular interactions are followed by ^1H NMR, static and dynamic light scattering (SLS and DLS).

7.1 Materials

Styrene (Aldrich), methyl methacrylate (MMA, Acros) were passed through a column of basic alumina (Acros) and stored at -18 °C prior to usage. ϵ -Caprolactone (Aldrich) was distilled over calcium hydride and stored over molecular sieves (3 Å). Copper (I) bromide (Fluka) was purified by sequential washing with sulphurous acid, acetic acid and ethanol, followed by drying under reduced pressure.

6-Bromohexanol (97%, ABCR GmbH and Co. KG), 11-bromoundecanol (99%, ABCR GmbH and Co. KG), 6-bromohexanoic acid (99%, ABCR GmbH and Co. KG), 11-bromoundecanoic acid (99%, ABCR GmbH and Co. KG), benzoyl chloride (99%, ABCR GmbH and Co. KG), ethylenediaminetetraacetic acid disodium salt (99%, Acros), thymine (99%, Alfa-Aesar), dimethyl sulfoxide (99%, Acros), 2,2-dimethoxypropane (99%, Acros), *p*-toluenesulfonic acid monohydrate (99%, Aldrich), KOH (99%, Carl Roth GmbH and Co. KG), NaOH (99%, Carl Roth GmbH and Co. KG), Na₂SO₄ (99%, Carl Roth GmbH and Co. KG), MgSO₄ (99%, Carl Roth GmbH and Co. KG), K₂CO₃ (99%, Merck), 5-bromovaleryl chloride (98%, Alfa-Aesar), methyl 4-hydroxybenzoate (99%, Acros), 4-hydroxybenzoic acid (99%, Acros), 5-hydroxyisophthalic acid (99%, Acros), dimethyl 5-hydroxyisophthalate (99%, Acros), 2,2-bis(hydroxymethyl)propionic acid (99%, Aldrich), cyanuric acid (99%, ABCR GmbH and Co. KG), 4-dimethylamino pyridine (DMAP) (99%, Acros), *N,N*-dicyclohexylcarbodiimide (DCC) (99%, Acros), *N,N*-dimethylformamide extra dry (DMF) (99.8%, Acros), tetrahydrofuran extra dry (THF) (99.8%, Acros), sodium azide (99.8%, Acros), α -bromo isobutyric acid (98%, Aldrich), 2-bromo-2-methylpropanoyl bromide (98%, Aldrich), 2-bromo-2-methylpropionyl bromide (98%, Acros), 5-hydroxyisophthalic acid (97%, Aldrich), acetic acid (95%, Carl Roth

GmbH and Co. KG), sulfuric acid (95%, Carl Roth GmbH and Co. KG), propargyl bromide, 80 wt.% solution in toluene (80%, Acros), propargyl alcohol (99%, Acros), succinic anhydride (99%, Acros), 3,3-dimethylbutyryl chloride (99%, Aldrich), 2,6-diaminopyridine (98%, Aldrich), triethylamine (99.7%, ABCR GmbH and Co. KG), *N,N,N',N',N''*-pentamethyldiethyltri-amine (PMDETA) (99.9%, Merck), cupric sulfate pentahydrate (99.5%, Aldrich), (+)-sodium L-ascorbate (98%, Aldrich), oxalyl chloride (98%, Acros), succinic anhydride (99%, Acros), 2,2,6,6-tetramethylpiperidinoxy (TEMPO) (98%, Acros), dibenzoyl peroxide, (75%, remainder water, Acros), benzoyl chloride (99%, Acros) were used as received. Methylene chloride (DCM) was distilled over phosphorus pentoxide and stored over molecular sieves. Toluene, diethyl ether, ethanol, methanol and chloroform were purchased as analytical grade (Aldrich) and used as received.

7.2 Characterization Techniques

7.2.1 Nuclear Magnetic Resonance (NMR) Spectroscopy

The structures of the synthesized compounds in the present thesis were confirmed by ^1H NMR and ^{13}C NMR spectroscopy using a Bruker AM 250 MHz spectrometer or a Bruker AM 400 MHz spectrometer for hydrogen nuclei and 100 MHz for carbon nuclei. All samples were dissolved in CDCl_3 , CD_2Cl_2 or $\text{DMSO}-d_6$. The δ -scale is referenced to tetramethylsilane ($\delta=0.00$) as internal standard. Abbreviations used below in the description of the materials' syntheses include singlet (s), broad singlet (bs), doublet (d), triplet (t), quartet (q), broad multiplet (bm), and unresolved multiplet (m).

7.2.2 Static and Dynamic Light Scattering (SLS and DLS)

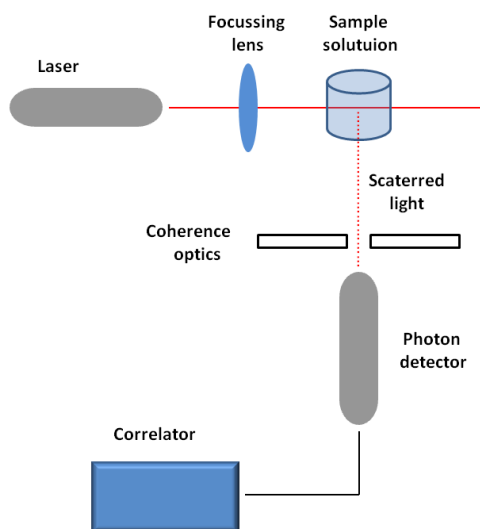


Figure 7.1 Schematic diagram of a conventional 90° dynamic light scattering instrument (DLS). Reproduced with kind permission from Malvern.

The solutions were prepared by dissolving the polymer in CH_2Cl_2 at an appropriate concentration and subsequently taking a part of the stock solution to obtain a series of concentrations by dilution. After allowing time for equilibration close 12h, the solutions were filtered over 0.2 μL filter and analysed by SLS and DLS.

SLS measurements were performed using a MALLS-detector (multi-angle laser light scattering detector) SLD 7000 from Polymer Standard Services (PSS), Mainz, Germany. Various concentrations of the polymers to determine the weight-averaged molecular weight (M_w) and the second virial coefficient (A_2) were employed via a Zim or Debye evaluation as described in the individual chapters. The required dn/dc values were measured in the same solvent with a refractometer Dn/Dc2010 also from PSS, Mainz, Germany. Hydrodynamic diameters were

determined with dynamic light scattering (Nicomp 380 DLS spectrometer from Particle Sizing Systems, Santa Barbara, USA - laser diode: 90 mW, 658 nm). The measurements were performed in automatic mode and evaluated with a standard Gaussian and an advanced evaluation method, the latter using an inverse Laplace algorithm to analyze for multimodal distributions. Numbers given in text are the volume weighted average values. All measurements were determined at 90° to the incident beam.

7.2.3 Size Exclusion Chromatography (SEC)

SEC measurements were performed on a Polymer Laboratories PL-GPC 50 Plus Integrated System, comprising an autosampler, a PLgel 5 μm bead-size guard column (50 × 7.5 mm) followed by three PLgel 5 μm Mixed-C and one PLgel 3 μm Mixed-E columns (300 × 7.5 mm) and a differential refractive index detector using THF as the eluent at 40 °C with a flow rate of 1 mL min⁻¹. The SEC system was calibrated using both linear poly(styrene) (PS) standards ranging from 160 to 6·10⁶ g mol⁻¹ and linear poly(methyl methacrylate) (PMMA) standards ranging from 700 to 6·10⁶ g mol⁻¹. The resulting molecular weight distributions were corrected using the respective Mark-Houwink relationships i.e $K = 14.1 \cdot 10^{-5} \text{ dL} \cdot \text{g}^{-1}$, $\alpha = 0.7$ for PS;¹ $K = 12.8 \cdot 10^{-5} \text{ dL} \cdot \text{g}^{-1}$, $\alpha = 0.69$ for P(MMA);² $K = 12.2 \cdot 10^{-5} \text{ dL} \cdot \text{g}^{-1}$, $\alpha = 0.70$ for P(*n*-BA);³ $K = 13.95 \cdot 10^{-5} \text{ dL} \cdot \text{g}^{-1}$, $\alpha = 0.786$ for PCL⁴ and $K = 5.00 \cdot 10^{-5} \text{ dL} \cdot \text{g}^{-1}$, $\alpha = 0.75$ for poly(isobornyl acrylate).⁵

7.2.4 Electrospray Ionization-Mass Spectrometry (ESI-MS)

Mass spectra were recorded on an LXQ mass spectrometer (ThermoFisher Scientific, San Jose, CA, USA) equipped with an atmospheric pressure ionization source operating in the nebulizer assisted electrospray mode. The instrument was calibrated in the *m/z* range 195-1822 using a

standard containing caffeine, Met-Arg-Phe-Ala acetate (MRFA) and a mixture of fluorinated phosphazenes (Ultramark 1621) (all from Aldrich). A constant spray voltage of 3.5 kV and a dimensionless sheath gas of 8 and a sweep gas flow rate of 2 were applied. The capillary voltage, the tube lens offset voltage, and the capillary temperature, were set to 60 V, 120 V and 275 °C, respectively.

7.2.5 Attenuated Total Reflectance-Infra Red Spectroscopy (ATR-IR)

Solid-state Fourier transform infrared spectra were recorded with an attenuated total reflectance unit (Bruker, *Golden Gate*) coupled to a Bruker Vertex 80 Fourier-transform spectrometer, equipped with a tungsten halogen lamp, a KBr beam splitter and DTGS detector. Each spectrum in the spectroscopic region of 4000-400 cm^{-1} was calculated from the co-added interferograms of 32 scans with resolution of 4 cm^{-1} .

7.3 References

- [1] C. Strazielle, H. O. Benoit, O. Vogl, *Eur. Polym. J.* **1978**, *14*, 331.
- [2] S. Beuermann, D. A. Paquet, J. H. McMinn, R. A. Hutchinson, *Macromolecules* **1996**, *29*, 4206.
- [3] A. Rudin, H. L. W. Hoegy, *J. Polym. Sci., Part A: Polym. Chem.* **1972**, *10*, 217.
- [4] A. Schindler, Y. M. Hibionada, C. G. Pitt, *J. Polym. Sci., Polym. Chem. Ed.* **1982**, *20*, 319.
- [5] B. Dervaux, T. Junkers, M. Schneider-Baumann, F. E. Du Prez, C. Barner-Kowollik, *J. Polym. Sci., Part A: Polym. Chem.* **2009**, *47*, 6641.

Abbreviations

μL	Microliter
AGET	Activators generated by electron transfer
ARGET	Activators regenerated by electron transfer
ATRP	Atom transfer radical polymerization
ATR	Attenuated total reflectance
ATR-IR	Attenuated total reflectance-infra red spectroscopy
C	Carbon
c	Concentration of substance
CA	Cyanuric acid
CD_2Cl_2	Deuterated dichloromethane
CDCl_3	Deuterated chloroform
CH_2Cl_2	Dichloromethane
CRP	Controlled radical polymerization
Cu(I)Br	Copper(I)bromide
$\text{CuSO}_5 \cdot x\text{H}_2\text{O}$	Copper sulfate pentahydrate
CuAAC	Copper catalyzed azide-alkyne coupling
DA	Diels-Alder
DBU	1,8-Diazabicycloundec-7-ene
DCC	N,N' -Dicyclohexylcarbodiimide
D_h	Mean diameter
DMAP	4-Dimethylaminopyridine
DMF	N,N -Dimethyl formamide
DMSO	Dimethyl sulphoxide
$\text{DMSO-}d_6$	Deuterated dimethyl sulphoxide
DLS	Dynamic light scattering
DPTS	4-(Dimethylamino)-pyridinium-4-toluene sulfonate
ESI	Electrospray Ionization
ESI-MS	Electrospray ionization-mass spectrometry
GPC	Gel permeation chromatography
H	Hydrogen
HW	Hamilton Wedge
HDA	Hetero Diels-Alder
IR	Infra red
k_{ad}	Rate constant for addition/activation
k_{d}	Rate constant for decomposition
k_{da}	rate constant for deactivation
K_{eq}	Equilibrium constant
kHz	Kilohertz
k_{i}	Rate constant for initiation
kJ	Kilojoule
k_{p}	Rate constant for propagation
k_{t}	Rate constant for termination

k_{tc}	Rate constant for termination by combination
k_{td}	Rate constant for termination by disproportionation
k_{β}	Rate constant for fragmentation
L	Litre
LRP	Living radical polymerization
mg	Milligram
MgSO ₄	Magnesium sulphate
MHz	Megahertz
mL	Millilitre
mm	Millimeter
MMA	Methyl methacrylate
mmol	Millimole
M_n	Number average molecular weight
mol	Mole
NaH	Sodium hydride
nm	Nanometer
NMP	Nitroxide mediated polymerization
NRC	Nitroxide radical coupling
NMR	Nuclear magnetic resonance
O	Oxygen
<i>PDI</i>	Poly dispersity index
PEG	Poly(ethylene glycol)
PEO	Poly(ethylene oxide)
PMDETA	<i>N,N,N',N'',N'''</i> -pentamethyldiethylenetriamine
PMMA	Poly(methyl methacrylate)
PS	Polystyrene
RAFT	Reversible addition-fragmentation chain transfer
ROP	Ring opening polymerization
R_p	Rate of polymerization
RP	Radical polymerization
S	Styrene
SEC	Size exclusion chromatography
SLS	Static light scattering
TEMPO	2,2,6,6-Tetramethylpiperidinyoxy
THF	Tetrahydrofuran
TIPNO	<i>N</i> -tert-butyl- <i>N</i> -[1-phenyl-2-(methylpropyl)]nitroxide

Curriculum Vitae

Personal Details

Name and Surname: Özcan ALTINTAS

Date of Birth: 15th February 1980

Place of Birth: Sındirgi, Turkey

Permanent Address: Kirmasti Mah. Boyaci Kapi Sk. No: 36, Fatih, Istanbul, Turkey

Nationality: Turkish

Education

1. July 2009–July 2012: **Ph.D in Polymer Chemistry**, from Karlsruhe Institute of Technology (KIT) under the supervision of Prof. Christopher Barner-Kowollik.
2. September 2004–February 2006: **Master of Science in Polymer Science and Technology** from Istanbul Technical University, Istanbul, Turkey a with cumulative GPA of **3.68** on 4 point scale.
3. September 1999–June 2004: **Bachelor of Science in Chemistry** from Istanbul Technical University, Istanbul, Turkey a with cumulative GPA of **3.36** on 4 point scale.

Awards

1. **Bachelor Science (BSc) Honor Award**, (3. Rank), Istanbul Technical University, Istanbul, Turkey, (2004).
2. **Master of Science (MSc) Honor Award**, Turkish Education Foundation (TEV), Istanbul, Turkey, (2006).
3. **Doctorate of Philosophy (PhD) Schlorship**, Merit Scholarship Programme for High Technology of Islamic Development Bank (IDB), Jeddah, Saudi Arabia (2009-2012).

Referred Journal Publication List – Papers originating from the present PhD thesis are marked with an *

1. *Synthesis of PMMA-b-PS containing a Crown Ether Unit at the Junction Point via Combination of ATRP and NMP Routes.* **Altintas, O.**; Yilmaz, I.; Hizal, G.; Tunca, U. **J. Polym. Sci. Polym. Chem.** **2006**, *44*, 3242-3249.
2. *ABC type hetero arm Star Terpolymers through Click Chemistry.* **Altintas, O.**; Hizal, G.; Tunca, U. **J. Polym. Sci. Polym. Chem.** **2006**, *44*, 5699-5707.
3. *A₃ type star Polymers via Click Chemistry.* **Altintas, O.**; Yankul, B.; Hizal, G.; Tunca, U. **J. Polym. Sci. Polym. Chem.** **2006**, *44*, 6458-6465.

4. *One-pot Synthesis of ABC type Triblock Copolymers via in situ Click [3+2] and Diels-Alder [4+2] Reactions.* Durmaz, H.; Dag, A.; **Altintas, O.**; Erdogan, T.; Hizal, G.; Tunca, U. **Macromolecules** **2007**, *40*, 191-198.
5. *One-Pot Preparation of ABC type Hetero-arm Star Polymers via Click [3+2] Reaction* **Altintas, O.**; Yankul, B.; Hizal, G.; Tunca, U. **J. Polym. Sci. Polym. Chem.** **2007**, *45*, 3588-3598.
6. *ABCD 4-Miktoarm Star Quarterpolymers using Click [3+2] Reaction.* **Altintas, O.**; Hizal, G.; Tunca, U. **J. Polym. Sci. Polym. Chem.** **2008**, *46*, 1218-1228.
7. *Dendrimer-like Miktoarm Star Terpolymers: $A_3-(B-C)_3$ via Click Reaction Strategy.* **Altintas, O.**; Demirel, A.L.; Hizal, G.; Tunca U. **J. Polym. Sci. Polym. Chem.** **2008**, *46*, 5916-5928.
8. *Synthesis of an ABCD 4-miktoarm Star Quaterpolymer through a Diels-Alder Click Reaction.* **Altintas, O.**; Hizal G.; Tunca U. **Designed Monomers and Polymers** **2009**, *12*, 83-98.
- 9*. *Single Chain Self-Assembly: Preparation of α,ω -Donor-Acceptor Chains via Living Radical Polymerization and Orthogonal Conjugation.* **Altintas, O.**; Gerstel, P.; Dingenouts, N.; Barner-Kowollik, C. **Chem. Comm.** **2010**, *46*, 6291-6293.
10. *Rapid Bonding/Debonding on Demand: Reversibly Cross-Linked Functional Polymers via Diels-Alder Chemistry.* Inglis, A. J.; Nebhani, L.; **Altintas, O.**; Schmidt, F. G.; Barner-Kowollik, C. **Macromolecules** **2010**, *43*, 5515-5520.
- 11*. *Star and Miktoarm Star Block(Co)polymers via Self-Assembly of ATRP Generated Polymer Segments Featuring Hamilton Wedge and Cyanuric Acid Binding Motifs.* **Altintas, O.**; Tunca, U.; Barner-Kowollik, C. **Polym. Chem.** **2011**, *2*, 1146-1155.
12. *Nitrone-Mediated Radical Coupling (NMRC) Reactions: An Efficient Strategy in Dendrimer Synthesis.* Wong, E. H. H.; **Altintas, O.**; Stenzel, M. H.; Barner-Kowollik, C.; Junkers, T. **Chem. Comm.** **2011**, *47*, 5491-5493.
13. *Synthesis of Terpolymers via Click Reaction.* Altintas, O.; Tunca, U. **Chem. Asian Journal** **2011**, *6*, 2584-2591.
- 14*. *Single Chain Self-Assembly of Well-Defined Heterotelechelic Polymers Generated by ATRP and Click Chemistry Revisited.* **Altintas, O.**; Rudolph, T.; Barner-Kowollik, C. **J. Polym. Sci. Polym. Chem.** **2011**, *49*, 2566-2576.
15. *Microparticles of phosphonate-functionalized copolymers and their composites with CdTe nanocrystals prepared by sonication-precipitation.* Kanelidis, I.; **Altintas, O.**; Gasse, J.-C.; Frahm, R.; Eychmüller, A.; Holder, E.; **Polym. Chem.** **2011**, *2*, 2597-2608.
- 16*. *Constructing Star Polymers via Modular Ligation Strategies.* **Altintas, O.**; Vogt, A. P.; Barner-Kowollik, C.; Tunca, U. **Polym. Chem.** **2012**, *3*, 34-45.
17. *Synthesis of Star and H-Shape Polymers via a Combination of Cobalt-Mediated Radical Polymerization and Nitrone-Mediated Radical Coupling Reactions.* Detrembleur, C.; Debuigne, A.; **Altintas, O.**; Conradi, M.; Wong, E. E. H.; Jérôme, C.; Barner-Kowollik, C.; Junkers, T. **Polym. Chem.** **2012**, *3*, 135-147.

- 18*. *Bioinspired Dual Self-Folding of Single Polymer Chains via Reversible Hydrogen Bonding.* Altintas, O.; Lejeune, E.; Gerstel, P.; Barner-Kowollik, C. *Polym. Chem.* **2012**, *3*, 640-651.
- 19*. *Combining Modular Ligation and Supramolecular Self-Assembly for the Construction of Star-Shaped Macromolecules.* Altintas, O.; Muller, T.; Lejeune, E.; Plietzsch, O.; Bräse, S.; Barner-Kowollik, C. *Macromol. Rapid Commun.* **2012**, DOI: 10.1002/marc.201200019.
- 20*. *Single Chain Folding of Synthetic Polymers via Covalent and Non-Covalent Interactions: Current Status and Future Perspectives.* Altintas, O.; Barner-Kowollik, C. *Macromol. Rapid Commun.* **2012**, DOI: 10.1002/marc.201200049
21. *Selective Dispersion of Single-Walled Carbon Nanotubes via Easily Accessible Conjugated Click-Polymers.* Gerstel, P.; Klumpp, S.; Hennrich, F.; Altintas, O.; Eaton, T. R.; Mayor, M.; Barner-Kowollik, C.; Kappes, M. *Polym. Chem.* **2012**, DOI: 10.1039/C2PY20161E

Patents

1. Funktionsmaterialien mit reversibler Vernetzung. Barner-Kowollik, C.; Inglis, A. J.; Nebhani, L.; Altintas, O.; Schmidt, F.-G.; Fengler, S.; Hilf, S.; Krause, S.; Henning, A. **International Patent PCT**, WO/2011/101176.

Conference Presentations – Papers originating from the present PhD thesis are marked with an *

1. Synthesis of Heterofunctional Initiators. Altintas, O.; Durmaz, H.; Hizal, G.; Tunca, U. **18th National Chemistry Symposia**, 05-09 July 2004, Kars, **Turkey**.
2. Synthesis of PMMA-b-PS Containing a Crown Ether Unit At The Junction Point Via Combination of ATRP and NMP Routes. Altintas, O.; Hizal, G.; Tunca U. **19th National Chemistry Symposia**, 30 September-04 October 2005, Izmir, **Turkey**.
3. Preparation of ABCD Type Hetero-Arm Star Polymers via Diels-Alder Reaction. Altintas, O.; Hizal, G.; Tunca U. **6th International Symposium on Advanced Polymers via Macromolecular Engineering (APME)**, 15-18 August 2005, Istanbul, **Turkey**.
4. Synthesis of unique three-arm star-shaped polymers via atom transfer radical polymerization containing phosphorescent iridium(III) metal centers. Altintas, O.; Shen, J.; Holder, E. **8th International Symposium on Functional π -Electron Systems**, 21-25 July 2008, Graz, **Austria**.
5. Novel Bipolar Light-Emitting Iridium(III) Acetylacetonates. Altintas, O.; Tian, N.; Holder, E. **2nd EuCheMS Chemistry Congress, Chemistry the Global Science**, 16-20 September 2008, Torino, **Italy**.
6. Acrylic Star Block Copolymers as Hydrophobic Drug Carriers. Genc, G.; Batigun, A.; Bayraktar, O.; Altintas, O.; Tunca, U.; Hizal, G. **14th Biomedical Engineering National Meeting**, 20-24 May 2009, Izmir, **Turkey**.

7. Dendrimer-Like Miktoarm Star Terpolymers: A₃-(B-C)₃ via Click Reaction Strategy. Altintas, O.; Demirel, A. L.; Hizal, G.; Tunca U. **Controlled/Living Radical Polymerizations Meeting 2009**, 17-18 September 2009, Houffalize, **Belgium**.
- 8*. Single Chain Self-Assembly: Preparation of α,ω -Donor-Acceptor Chains via Living Radical Polymerization and Orthogonal Conjugation. Altintas, O.; Gerstel, P.; Dingenouts, N.; Barner-Kowollik, C. **2nd International Conference on Multifunctional, Hybrid and Nanomaterials**, 6-10 March 2011, Strasbourg, **France**.
9. With Modular Strategies and Controlled Radical Polymerization to Functional Materials: Surface Design and Bonding on Demand Systems. Barner-Kowollik, C.; Altintas, O.; Barner, L.; Blinco, J.; Bruns, M.; Glassner, M.; Goldmann, A.S.; Hubner, C.; Inglis, A. J.; Nebhani, L.; Schmiedl, D.; Schmidt, F. G.; Tischer, T.; Zydziak, N. **American Chemical Society 242th National Meeting and Exposition**, August 2011, San Francisco, **USA**.

Acknowledgements

I gratefully acknowledge my Ph.D. advisor, Prof. Christopher Barner-Kowollik, for giving me the opportunity to work on this topic in his group as well as his support during the entire time. I am thankful to him for his encouragement and motivation during the entire thesis. His ideas and motivation had a great influence on my work.

I would also like to thank Prof. Ümit Tunca (Istanbul Technical University) for his kind guidance, valuable comments and scientific support throughout my studies.

Thanks must also go to the Islamic Development Bank (IDB) for a Ph.D. scholarship and to Mr. A. S. Huq for the excellent management of all scholarship related matters.

Additional funding from KIT within the context of the *Excellence Initiative* for leading German universities supporting the work is gratefully acknowledged.

For the help with characterization techniques, I am indebted to Dr. Nico Dingenouts (KIT) for the DLS measurements and Dr. Elise Lejeune (KIT) for the SLS measurements. I would also like to thank all additional co-authors of the publications related to my thesis, i.e. Prof. Stefan Bräse, Peter Gerstel, Dr. Thierry Muller, Oliver Plietzsch and Tobias Rudolph.

Dr. Andrew J. Inglis, Dr. Leena Nebhani and Dr. Edgar H. H. Wong are gratefully acknowledged for fruitful and helpful discussions.

Many thanks must go to Dr. Anja S. Goldmann for the careful proof-reading of a substantial amount of my thesis as well as her helpful suggestions. I would additionally like to thank Dr. James Blinco, Dr. Andrew P. Vogt and Dr. Nathalie Guimard for their proof reading of the publications.

Many thanks must go to the entire team – it is a pleasure to work with you !

Last but not the least, I acknowledge my mother for her constant encouragement and support throughout my education.

Finally, I would like to thank my wife Halime Altintas for her patience, understanding as well as for her personal support during my research.

Ich erkläre hiermit, dass ich die vorliegende Doktorarbeit im Rahmen der Betreuung durch Prof. Dr. Christopher Barner-Kowollik, selbständig verfasst und keine anderen als die angegebenen Quellen und Hilfsmittel verwendet habe. Des Weiteren erkläre ich, dass ich mich derzeit in keinem laufenden Promotionsverfahren befinde, und auch keine vorausgegangenen Promotionsversuche unternommen habe.

Karlsruhe, den 23.07.2012